

AD A279638

Report No. A1-161

**EFFICIENT WELDING FABRICATION OF
EXTRUDED ALUMINUM MAT PANELS**

Valdemar Malin, Ph.D.

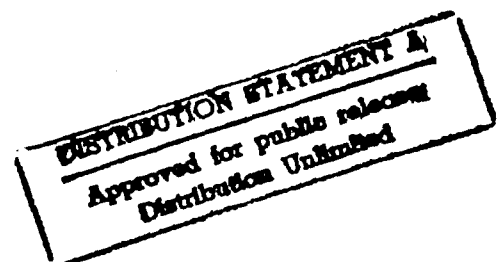
ElectroCom GARD, Ltd.
7449 N. Natchez Avenue
Niles, IL 60648

September, 1991

FINAL REPORT

(May, 1988 - September, 1991)

Contract No. DAAK70-88-C-0024



Prepared for
U.S. Army Belvoir Research, Development and
Engineering Center
Fort Belvoir, VA 22060-5606

REPORT DOCUMENTATION PAGE

Form Approved
OMB No. 0704-0188

1a. REPORT SECURITY CLASSIFICATION Unclassified			1b. RESTRICTIVE MARKINGS		
2a. SECURITY CLASSIFICATION AUTHORITY			3. DISTRIBUTION / AVAILABILITY OF REPORT Approved for public release. Distribution is unlimited.		
2b. DECLASSIFICATION / DOWNGRADING SCHEDULE					
4. PERFORMING ORGANIZATION REPORT NUMBER(S) A1-161			5. MONITORING ORGANIZATION REPORT NUMBER(S)		
6a. NAME OF PERFORMING ORGANIZATION ElectroCom GARD, Ltd.		6b. OFFICE SYMBOL (if applicable)		7a. NAME OF MONITORING ORGANIZATION U.S. Army Belvoir RD & EC	
6c. ADDRESS (City, State, and ZIP Code) 7449 N. Natchez Avenue Niles, IL 60648-3892			7b. ADDRESS (City, State, and ZIP Code) Fort Belvoir, VA 22060-5606		
8a. NAME OF FUNDING / SPONSORING ORGANIZATION		8b. OFFICE SYMBOL (if applicable)		9. PROCUREMENT INSTRUMENT IDENTIFICATION NUMBER DAAK70-88-C-0024	
8c. ADDRESS (City, State, and ZIP Code)			10. SOURCE OF FUNDING NUMBERS		
			PROGRAM ELEMENT NO.	PROJECT NO.	TASK NO.
			WORK UNIT ACCESSION NO.		
11. TITLE (Include Security Classification) Efficient Welding Fabrication of Extruded Aluminum Mat Panels					
12. PERSONAL AUTHOR(S) Malin, Valdemar					
13a. TYPE OF REPORT Final Report		13b. TIME COVERED FROM 5/23/88 TO 9/10/91		14. DATE OF REPORT (Year, Month, Day) 1991 September	
15. PAGE COUNT 366					
16. SUPPLEMENTARY NOTATION					
17. COSATI CODES			18. SUBJECT TERMS (Continue on reverse if necessary and identify by block number)		
FIELD	GROUP	SUB-GROUP			
19. ABSTRACT (Continue on reverse if necessary and identify by block number)					
<p>The program had the following main objectives: to design and procure welded extruded access/egress (A/E) mat panels, to determine feasibility of and to provide means for fabrication of Ribbon Bridge (RB) and Light Assault Bridge (LAB) deck panels using the technology developed under this program, to develop advanced equipment and technology for assembling and welding of A/E mat panels, and to study mechanical and metallurgical properties of welded joints. The existing practice is to design and build roadway mat panels (or bridge deck panels) from wide, single-piece extruded 6061-T6 aluminum components.</p> <p style="text-align: right;"><i>continued on back</i></p>					
20. DISTRIBUTION / AVAILABILITY OF ABSTRACT <input type="checkbox"/> UNCLASSIFIED/UNLIMITED <input type="checkbox"/> SAME AS RPT. <input type="checkbox"/> DTIC USERS			21. ABSTRACT SECURITY CLASSIFICATION Unclassified		
22a. NAME OF RESPONSIBLE INDIVIDUAL			22b. TELEPHONE (Include Area Code)		22c. OFFICE SYMBOL

In order to avoid difficulties associated with procurement of large circle-size extrusions, which are expensive and not readily available, the panel cross-section was constructed from smaller extruded elements using welding. In this respect, various aspects of weldment design were studied, including design of welded joints, and fatigue analysis of their performance since the panels will be subjected to severe environment and heavy load conditions. Also, a procurement base for extruded panels was explored through analysis of data obtained as a result of an industry survey. A state-of-the-art experimental automation fabrication system was developed for assembling and welding of long extruded components. It allows two longitudinal butt welds between three subpanels to be performed simultaneously on each side of the subpanels to form a full-size mat panel up to 28 in. (711 mm.) wide and up to 13 ft. (6,934 mm.) long, with a possible extension up to 28 ft. (8,534 mm.) for fabrication of bridge deck panels. A unique fixture was developed as an integral part of the system to meet the requirements of a welding procedure developed to offset complicated metallurgical reactions typical for welding of age-hardenable aluminum alloys. This allowed strength of the welded joints to be increased by 20% and distortion to be virtually eliminated. A state-of-the-art-double-electrode welding system for pulsed gas metal arc welding (GMAW) was developed. The system features real-time computer control over energy parameters of the welding process, including closed-loop feedback control. Mechanical properties of the welded joints and metallurgical reactions in the heat-affected zone (HAZ) were studied. The study revealed new facts about relationships between welding conditions and strength of the welded joints microhardness and microstructure in the HAZ. The findings were used to achieve maximum possible productivity maintaining the highest quality of the welded joints.

Accession For	
NTIS GRA&I	<input checked="checked" type="checkbox"/>
DTIC TAB	<input type="checkbox"/>
Unannounced	<input type="checkbox"/>
Justification	
By	
Distribution/	
Availability Codes	
Dist	Avail and/or Special
A-1	

SUMMARY

This final report "Efficient Welding Fabrication of Extruded Aluminum Mat Panels" has been prepared by ElectroCom GARD, Ltd. (formerly Chamberlain GARD) for the U.S. Army Belvoir Research, Development and Engineering Center (RD&EC), Fort Belvoir, VA. It describes the work performed under a three-year Manufacturing Methods and Technology (MM&T) program sponsored by the Bridge Division of the Belvoir RD&EC. The program had the following main objectives:

- To design and procure welded extruded access/egress (A/E) mat panels,
- To develop advanced equipment and technology for assembling and welding of A/E mat panels,
- To study mechanical and metallurgical properties of welded joints.

Later in the program, an extra objective was added to determine feasibility of and to provide means for fabrication of Ribbon Bridge (RB) and Light Assault Bridge (LAB) deck panels using the technology developed under this program.

In contrast to a traditional approach in development of welding automation, the most distinguishable feature of GARD's approach was utilization of welding expertise at all stages of welding automation development, especially in analysis of the following issues:

Design of extruded parts and assembly; assembling operations and assembling procedures; welded joint design, location and accessibility; tolerances of extruded parts and the welded assembly; selection of welding process, technique and position; fixture design; means of controlling welding distortion and metallurgical reactions in 6061-T6 age-hardenable aluminum alloy; means of improving microstructure and properties in the heat affected zone (HAZ) of welded joints; and many other issues which might not be addressed at this early stage of welding automation development in the traditional approach. The developed concept for welding automation was based on the optimization of the findings of the analysis described above.

The existing practice is to design and build roadway mat panels (or bridge deck panels) from extruded elements. Selection of extrusions is very beneficial since it provides design flexibility and the highest strength-to-weight ratio. In order to avoid difficulties associated with procurement of large circle-size extrusions, which are expensive and not readily available, the panel cross-section was constructed from smaller extruded elements using welding. In this respect, various aspects of weldment design were studied, including design of welded joints, and fatigue analysis of their performance.

Also, a procurement base for extruded panels was explored through analysis of data obtained as a result of an industry survey.

A state-of-the-art experimental automatic fabrication system was developed for assembling and welding of long extruded components. It allows two longitudinal butt welds between three subpanels to be performed simultaneously on each side of the subpanels to form a full-size mat panel up to 28 in. (711 mm.) wide and up to 13 ft. (6,934 mm.) long. The system was designed in such a manner that the assembling fixture could be further modified in the future to add another module in order to fabricate bridges deck panels up to 28 ft. (8,534 mm.) long. A unique fixture was developed as an integral part of the system to meet the requirements of a welding procedure developed for severe environment and extreme load conditions. The fixture was designed to offset complicated metallurgical reaction typical for welding of age-hardenable aluminum alloys. This allowed strength of the welded joints to be increased by 20% and distortion to be virtually eliminated. A state-of-the-art double-electrode welding system with feedback closed-loop control for pulsed gas metal arc welding (GMAW) was developed. The system features real-time computer control over energy parameters of the welding process, including closed-loop feedback control of such parameters as peak and background current, background voltage, pulse frequency, wire feed rate and electrode extension. The parameters are monitored in real time by special sensors and the information obtained is analyzed in a special microprocessor-based data processing device to compare it with programmed values. If deviation of one parameter occurs, the other parameters are changed in an adaptive mode to keep arc energy input constant. This is accomplished via a special so called "synergic" program. This program establishes the relationships between the interrelated parameters to automatically provide a stable spray-transfer welding process over the wide range of welding conditions required. Also, motion parameters such as torch speed, acceleration, deceleration and travel distance are also controlled using a programmable control mode. Computer capabilities to document and analyze numerous data obtained by monitoring welding parameters were also developed. Thus, total precision control over the all main aspects of the welding process was established to provide consistency and the required quality of the welds.

Mechanical properties of the welded joints and metallurgical reactions in the heat-affected zone (HAZ) were studied. The study revealed new facts about relationships between welding conditions and strength of the welded joints, microhardness and microstructure in the HAZ. The findings were used to achieve maximum possible productivity maintaining the highest quality of the welded joints.

FOREWORD

This report is the documentation of the results of the MM&T program to develop an efficient welding technology for fabrication of extruded access/egress and bridge deck panels made of 6061-T6 aluminum alloy. The program was sponsored and funded by the Bridge Division, the U.S. Army Belvoir Research, Development and Engineering Center (RD&EC), Fort Belvoir, VA under Contract No. DAAK70-88-C-0024.

ACKNOWLEDGEMENT

Close cooperation, administrative and technical guidance on the part of the personnel of the Bridge Division of the Belvoir RD&EC during this 3-year program is greatly appreciated. Special thanks are due to B.K. Hornbeck, G.D. Farmer, J. Kerr, and C. Kominos. Also, GARD recognizes the contribution of CRC-Evans Automatic System, a subsidiary of Pipeline International, Inc., Houston, Texas in supplying welding equipment and parameter control systems for the fabrication system developed at Chamberlain GARD. The author also acknowledges the assistance of GARD's personnel in successful completion of the program. Thanks and appreciation are extended to R.C. Schoon, D.J. Hogan, K.H. Renner, R.E. Sadler, A.N. Henzi, S.F. Fields and P.A. Saigh.

TABLE OF CONTENTS

<u>Section</u>	<u>Page</u>
1 INTRODUCTION	1-1
1.1 BACKGROUND	1-1
1.2 OBJECTIVES AND SCOPE OF THE PROGRAM	1-3
1.3 REPORT ORGANIZATION	1-4
2 DESIGN AND PROCUREMENT OF EXTRUDED MAT PANELS	2-1
2.1 DESIGN OF WELDED ACCESS/EGRESS (AE) MAT PANELS	2-1
2.1.1 Background	2-1
2.1.2 Modification of the Panel Configuration	2-2
2.1.3 Panel Breakdown into Subpanels	2-2
2.1.4 Mating End Design	2-4
2.1.5 Welded Joint Design	2-6
2.2 FATIGUE PERFORMANCE ANALYSIS OF WELDED JOINTS	2-8
2.2.1 GARD's Stress Analysis	2-8
2.2.2 U of I Evaluation of Joint Fatigue Performance	2-9
2.2.3 GARD's Fatigue Evaluation of Type II Joint (Round 1)	2-10
2.2.4 FEM Stress Analysis of Weld Root Tip Area (Round 2)	2-10
2.2.5 GARD's Fatigue Analysis of Type II Joints (Round 3)	2-11
2.3 DESIGN MODIFICATIONS OF AE AND BRIDGE DECK (BD) PANELS	2-12
2.3.1 Implication of Introduction of BD Panels	2-12
2.3.2 Mod. 2 Access/Egress Mat Panel Design	2-12
2.3.3 Evaluation of Bridge Deck Panels	2-13
2.4 PROCUREMENT OF AE PANELS	2-15
2.4.1 Extrudability of Aluminum Alloys	2-16
2.4.2 Metallurgical Aspects of Extrudability of Aluminum Alloys	2-17
2.4.3 Bid Survey Among U.S. Extrusion Manufacturers	2-19
2.4.4 Availability of Extrusion Presses	2-22

TABLE OF CONTENTS (Continued)

<u>Section</u>	<u>Page</u>
3 WELDING METALLURGY OF HEAT-TREATABLE ALUMINUM ALLOYS . .	3-1
3.1 GRAIN STRUCTURES IN THE WELDS OF ALUMINUM ALLOYS	3-1
3.1.1 Types of Grain Structures in the Weld	3-1
3.1.2 Conditions for Grain Structure Formation in the Weld	3-3
3.2 SEGREGATION IN THE WELDS OF ALUMINUM ALLOYS	3-6
3.2.1 Macrosegregation	3-6
3.2.2 Microsegregation	3-6
3.3 SOLIDIFICATION CRACKING (SC) IN THE WELDS OF ALUMINUM ALLOYS	3-8
3.3.1 Role of Temperature Range of Dendrite Coherence in SC	3-8
3.3.2 Role of Liquid Eutectics in SC	3-10
3.3.3 Role of Solidification Rate, Grain Size and Super-heat Temperature in SC	3-10
3.4 PREVENTION OF SOLIDIFICATION CRACKING IN THE WELD METAL	3-11
3.4.1 SC Prevention by Selection of Filler Metals	3-11
3.4.2 SC Prevention by Refining of Grain Structure of the Weld Metal	3-13
3.4.3 Role of Stresses around the Weld Puddle in SC	3-16
3.4.4 SC Prevention by Proper Welding Procedure	3-16
3.5 PROBLEM IN HEAT-AFFECTED ZONE (HAZ)	3-17
3.5.1 Cracking in the HAZ	3-17
3.5.2 Strength Reduction in HAZ	3-19
3.6 EFFECT OF WELDING PROCEDURE ON PROPERTIES OF WELDED JOINTS	3-20
3.6.1 Effect of Welding Parameters	3-21
3.6.2 Effect of Artificial Cooling	3-21
3.6.3 Effect of the Plate Size	3-23

TABLE OF CONTENTS (Continued)

<u>Section</u>		<u>Page</u>
3.7	POROSITY IN ALUMINUM ALLOYS	3-23
3.7.1	General Consideration	3-23
3.7.2	Role of Solidification in Porosity Formation	3-24
3.7.3	Sources of Porosity	3-26
3.7.4	Surface Contamination	3-26
3.7.5	Shielding-gas Contamination	3-31
3.7.6	Effect of Composition on Porosity	3-33
3.7.7	Effect of Welding Variables on Porosity	3-35
4	EXPERIMENTAL WELDING PROGRAM	4-1
4.1	EXPERIMENTAL PROCEDURES	4-1
4.1.1	Objectives and Scope of the Experimental Program	4-1
4.1.2	Requirements for Inspection and Testing of Welded Joints	4-2
4.1.3	Welding Procedure	4-5
4.2	PRELIMINARY INVESTIGATION	4-8
4.2.1	Effect of Edge Cleaning Methods on Weld Porosity (Series K)	4-8
4.2.2	Effect of Weld Storage Period on HAZ Properties (Series D)	4-12
4.2.3	Determination of Usable Ranges of Parameters	4-18
4.3	RESULTS OF EXPERIMENTAL PROGRAM	4-19
4.3.1	Matrix of Welding Experiments	4-19
4.3.2	Methodology	4-23
4.3.3	Results of Inspection	4-24
4.3.4	Analysis of Results of Mechanical Tests	4-27
4.3.5	Effect of Welding Conditions on Tensile Strength	4-28
4.4	RELATIONSHIPS BETWEEN HARDNESS, AND FAILURE LOCATION AND STRENGTH	4-30
4.4.1	Results of Microhardness Tests	4-30
4.4.2	Effect of Hardness on Failure Location	4-32
4.4.3	Effect of Welding Conditions on HAZ Width	4-35
4.4.4	Effect of HAZ Chilling on Tensile Strength	4-35

TABLE OF CONTENTS (Continued)

<u>Section</u>		<u>Page</u>
4.5	RELATIONSHIPS BETWEEN HAZ HARDNESS AND MICROSTRUCTURE	4-38
4.5.1	Precipitation Sequence in 6061 Alloy	4-38
4.5.2	Effect of Precipitates on HAZ Hardness	4-40
4.6	OPTIMIZATION OF WELDING PARAMETERS	4-47
4.6.1	Results of Weld Measurements	4-47
4.6.2	Acceptance Criteria for Weld Geometry	4-47
4.6.3	Analysis of Weld Geometry	4-50
4.6.4	Selection of Optimized Welding Conditions	4-50
4.7	VERIFICATION WELDING	4-52
4.7.1	Verification of Welding Procedure	4-52
4.7.2	Verification of Welding System	4-53
5	DEVELOPMENT OF FABRICATION SYSTEM FOR WELDING ALUMINUM PANELS	5-1
5.1	BACKGROUND	5-1
5.1.1	Objectives and Scope	5-1
5.1.2	Approach	5-2
5.1.3	Scope of Fabrication System	5-4
5.2	THE FIXTURING SYSTEM	5-4
5.2.1	The Rotating Fixture	5-6
5.2.2	The Carriages	5-8
5.2.3	The Parking Mechanism	5-10
5.3	AUXILIARY EQUIPMENT	5-11
5.3.1	The Loading Structure	5-11
5.3.2	The Air Pollution Control System	5-13
5.3.3	The Water Circulating Station	5-14

TABLE OF CONTENTS (Continued)

Section		Page
5.4	CONTROL SYSTEM	5-16
5.4.1	General Description	5-16
5.4.2	The Welding Parameter Control (WPC) System	5-16
5.4.3	The Motion Parameter Control (MPC) System	5-22
5.4.4	The Fixture Control (FC) System	5-24
5.4.5	The Host Computer	5-26
5.4.6	The Joint Tracking (JT) System	5-26
5.5	WELDING AND ASSEMBLING PROCEDURES	5-27
5.5.1	Weld Identification	5-27
5.5.2	Sequence of Welding	5-27
5.5.3	Torch and Wire Positioning Parameters	5-27
5.5.4	Cleaning of Subpanels and Storage of Wire	5-27
5.5.5	Fixture Preparation	5-28
5.5.6	Fixture Loading	5-28
5.5.7	Clamping and Straightening	5-30
5.5.8	Chiller Installation	5-30
5.5.9	Presetting Welding and Motion Parameters	5-30
5.5.10	Torch and Wire Positioning	5-31
5.5.11	Welding of Weld W1 and W2	5-32
5.5.12	Interweld Operations	5-34
5.5.13	Welding of Welds W2 and W4	5-34
5.5.14	Postweld Operations	5-35
6	CONCLUSIONS AND RECOMMENDATIONS	6-1
6.1	DESIGN OF ACCESS/EGRESS MAT PANELS (Conclusions for Section 2)	6-1
6.1.1	Welded Modifications of the AE Panel	6-1
6.1.2	Welded Joint Design	6-1
6.1.3	Bridge Deck Panel Design	6-2
6.1.4	Extrusion Availability	6-2

TABLE OF CONTENTS (Continued)

<u>Section</u>		<u>Page</u>
6.2	EXPERIMENTAL PROGRAM AND FABRICATION SYSTEM (Conclusions for Sections 4 and 5)	6-2
6.2.1	Testing Program	6-2
6.2.2	Preliminary Study	6-3
6.2.3	Inspection	6-3
6.2.4	Mechanical Tests	6-3
6.2.5	Effect of Welding Conditions on Tensile Strength	6-4
6.2.6	Microhardness Profile in the HAZ	6-4
6.2.7	Effect of Hardness on Failure Location	6-5
6.2.8	Effect of HAZ Chilling	6-5
6.2.9	Relationships Between Hardness and Microstructure in the HAZ	6-6
6.2.10	Optimization of Welding Parameters	6-7
6.2.11	Verification Welding	6-7
6.2.12	Fabrication System (<u>Conclusions for Section 5</u>)	6-8
6.3	RECOMMENDATIONS	6-8
6.3.1	Recommendations for Future Panel Design	6-8
6.3.2	Recommendations for Welding Procedure	6-9
6.3.3	Recommendation for Future Design of Fabrication System	6-10

REFERENCES

APPENDICES

APPENDICES A	(Section 2)
APPENDICES B	(Section 4)
APPENDICES C	(Section 5)

LIST OF FIGURES

Figures	Page
Fig. 2-1	Mating end configurations of extruded AE subpanels: Type I (a), Type II (b); schematic representation of a backing bar for welding Type I joint (c) 2-5
Fig. 2-2	Welded joints: Type I (a), Type II (b) 2-7
Fig. 2-3	Type III welded joint 2-14
Fig. 3-1	Typical grain structures in aluminum alloys (Ref. 2) 3-2
Fig. 3-2	Grain structures in alloy 6061 (a) and 7004 (b) as function of welding conditions (Ref. 2) 3-4
Fig. 3-3	Titanium-rich particle (arrow) at the center of a dendrite in alloy 7004 (Ref.2) 3-7
Fig. 3-4	Subgrain structure of a full-penetration weld: (a) at a fusion boundary, (b) at weld centerline (Ref. 7) 3-7
Fig. 3-5	Solidification cracks in Al-Zn-Mg alloys (Ref. 8) 3-9
Fig. 3-6	Incipient solidification crack healed by band of eutectic (Ref. 9) 3-9
Fig. 3-7	Effect of composition on weld solidification crack susceptibility of Al-Mg-Si alloys (Ref. 10) 3-12
Fig. 3-8	Weld solidification cracking in aluminum alloys of 6000 series (Ref. 8) 3-12
Fig. 3-9	Effect of composition on weld solidification crack susceptibility of Al-Zn-Mg alloys (Ref. 8) 3-14
Fig. 3-10	Weld solidification cracking in aluminum alloy of 7000 series (Ref. 8) 3-14
Fig. 3-11	Failed butt joint in alloy 6061 due to cracking in the HAZ (a); cracks in the HAZ (b) (Ref. 19) 3-18
Fig. 3-12	HAZ hardness profiles of a GTA weld of a 3.2 mm-thick sheet in 6061-T6 aluminum (Ref. 12) 3-18

LIST OF FIGURES (continued)

Figures	Page
Fig. 3-13 Effect of heat input parameters EI/Vt on extent of HAZ in aluminum alloys (a) and on 6061-T6 joint strength (b) (Ref. 23)	3-22
Fig. 3-14 Illustration of the morphologies of porosity observed in aluminum alloy welds (Ref. 26)	3-25
Fig. 3-15 Constituents of the topography of a machined surface: (a) general topography which includes the irregularities caused by (b) flexure or slideways, (c) vibration or bad truing, (d) the cutting tool, and (e) chip removal (Ref. 30)	3-30
Fig. 3-16 Contamination concentration levels at which significant changes occur in weld quality (Ref. 28).	3-32
Fig. 3-17 Volume of water available to weldment from saturated air contamination (Ref. 28).	3-34
Fig. 3-18 Measured hydrogen contents of 3003 and 2219 alloy welds deposited by GTAW with contaminated shielding gas (Ref. 26).	3-36
Fig. 3-19 Effect of (a) copper and (b) silicon additions on the solubility of hydrogen in liquid aluminum at 760mm pressure (Ref. 26).	3-36
Fig. 3-20 Effect of welding position and weld pool shape on porosity in (a) uphill, (b) downhill, and (c) overhead welds (Ref. 34).	3-37
Fig. 3-21 Effect of GTAW current on weld porosity and the rate of hydrogen absorption in 1100 aluminum (Ref. 33)	3-37
Fig. 4-1 Test piece cut from a welded panel assembly.	4-3
Fig. 4-2 Layout of test pieces on a welded panel assembly.	4-7
Fig. 4-3 Cross-section areas of a welded joint: Fr - reinforcement, Fg - groove and Fp - arc penetration	4-9
Fig. 4-4 Enlarged photograph of a weld cross-section	4-10

LIST OF FIGURES (continued)

Figures	Page
Fig. 4-5	Strips of temperature indicating liquids on a panel assembly applied prior to welding 4-11
Fig. 4-6	Effect of weld storage period prior to testing on as-welded hardness recovery 4-17
Fig. 4-7	Graphic representation of the matrix of welding experiments 4-22
Fig. 4-8	Suggested modification of Type III welded joint design (dashed lines) 4-26
Fig. 4-9	Effect of linear energy (Q) on tensile strength of the welded joints; Q is varied by travel speed (a) and by arc power (b) 4-29
Fig. 4-10	Microhardness profile of weld B17 4-31
Fig. 4-11	HAZ failure location in weld B16 4-33
Fig. 4-12	HAZ failure location in weld C33 4-34
Fig. 4-13	HAZ failure location in weld B18 4-36
Fig. 4-14	Microhardness profile of weld C30 4-37
Fig. 4-15	Effect of maximum temperature distribution on microhardness and microstructure in the HAZ (weld B16) 4-41
Fig. 4-16	Effect of maximum temperature distribution on microhardness and microstructure in the HAZ (weld B17) 4-42
Fig. 4-17	Effect of maximum temperature distribution on microhardness and microstructure in the HAZ (weld B18) 4-43
Fig. 4-18	Effect of maximum temperature distribution on microhardness and microstructure in the HAZ (weld A5) 4-44
Fig. 4-19	Effect of maximum temperature distribution on microhardness and microstructure in the HAZ (weld B23) 4-45
Fig. 4-20	Effect of maximum temperature distribution on microhardness and microstructure in the HAZ (weld C33) 4-46
Fig. 4-21	Weld geometry 4-48

LIST OF FIGURES (continued)

Figures		Page
Fig. 4-22	Craters in weld B22: at minimum (a) and maximum (b) ramp-down times, and at 1.5 sec. delay plus maximum ramp-down time (c)	4-54
Fig. 4-23	Run-on and run-off tabs on a mock-up of the panel assembly	4-56
Fig. 4-24	Cross-section of weld B22 after removal of the tabs: weld start (a), weld termination (b)	4-57
Fig. 4-25	Copper end chillers (a) and resulting end view of the welded panel assembly after removal of the tabs (b)	4-58
Fig. 4-26	Stacks of short (a) and full-length (b) welded AE mat panels ready for shipment	4-59
Fig. 5-1	Fabrication system for assembling welding of the aluminum AE mat panels	5-5
Fig. 5-2	View of the fixture	5-5
Fig. 5-3	The AE panel assembly clamped in the fixture	5-7
Fig. 5-4	View of the stopper mechanism	5-7
Fig. 5-5	View of the carriage	5-9
Fig. 5-6	View of the parking mechanism	5-9
Fig. 5-7	Views of the loading structure and air pollution control system	5-12
Fig. 5-8	View of the duct support mechanism	5-12
Fig. 5-9	View of the water circulating station and power sources	5-15
Fig. 5-10	View of the main control cabinet	5-15
Fig. 5-11	Views of the welding (a) and motion (b) parameter control pendants	5-23
Fig. 5-12	Schematic representation of Compumotor motion parameter control system	5-23
Fig. 5-13	Front panel of the auxiliary control cabinet of the fixture control system . . .	5-25

LIST OF FIGURES (continued)

<u>Figures</u>		<u>Page</u>
Fig. 5-14	Control cabinets and pendants for joint tracking systems	5-25
Fig. 5-15	Loading of the subpanels (a) and presetting of motion parameters (b)	5-29
Fig. 5-16	Welding of the AE mat panels is in progress	5-33

LIST OF TABLES

Tables

Table 2-1	Extrudability of Al-Mg-Si Alloys	2-18
Table 4-1	Types of Discontinuities Acceptable for Welds on Mat Panel	4-4
Table 4-2	Composition and Properties of Base and Filler Metals	4-5
Table 4-3	Effect of Method of Edge Preparation on Porosity Level in the Weld (Matrix of Experiments, Series K)	4-13
Table 4-4	Effect of Edge Cleaning Methods on Porosity	4-14
Table 4-5	Effect of Natural Aging on HAZ Hardness (Matrix of Experiments, Series D)	4-16
Table 4-6	Effect of Welding Parameters on Weld Joint Properties (Matrix of Experiments, Series A, B & C)	4-20
Table 4-7	Welding Conditions and Dilution (Series A, B & C)	4-21
Table 4-8	Results of Weld Measurements for Welds B22R and C35	4-50
Table 4-9	Selection of Optimal Welding Conditions	4-51

Section 1

INTRODUCTION

1.1 BACKGROUND

Roadway mat panels, deck panels of military bridges, landing mat panels, etc. are presently fabricated from aluminum alloys using extrusion process. Such a panel is made of a one-piece extruded section, usually about or over 24 in. (610 mm) wide. To extrude a panel that large, at least a 14,000 ton press is required. However, today there are only four such presses operating in the country which are owned by two companies. This severely limits availability of this type of extrusion. Therefore, in an effort to improve the situation, in 1988 the U.S. Army Belvoir Research, Development & Engineering Center (RD&EC), Bridge Division, Fort Belvoir, VA established a 3-year Manufacturing Methods and Technology (MM&T) program. The objective of this program was to develop a new technology which allows narrower extruded sections, made on more available smaller presses, to be joined into a wider panel assembly using high quality welding with in-process inspection and efficiency typical for a large-scale production.

To meet these challenging objectives it was necessary:

- 1) To design a welded version of the roadway access/egress (AE) mat panel on the basis of optimization of numerous (sometimes contradictory) requirements.
- 2) To overcome negative metallurgical reactions in heat-treatable 6061-T6 aluminum alloy which deteriorate properties of the heat-affected zone (HAZ) of the welded joints.
- 3) To develop advanced equipment and technology for welding fabrication of the AE panels which provide high productivity and low production cost, without sacrificing high quality of the weld.
- 4) To determine optimal welding conditions which provide the best combination of mechanical and metallurgical properties of the welded joints.

To undertake the efforts described above, the knowledge and expertise in several technical areas were required, including weldment design, metallurgy of heat-treatable aluminum alloys, welding of aluminum alloys and welding automation.

The design of a welded modification of the roadway AE mat panel was associated with certain difficulties. It was necessary to reconcile several contradictory requirements, such as efficient metal utilization and adequate strength of the panels, maximum width of the welded

sections and maximum availability of extrusion, high service performance of the welded joints and ease of panel fabrication, high dimensional precision of the extruded panel and the lowest cost of extrusion, high productivity of welding and adequate strength of welded joints, among others.

Metallurgical problems associated with welding of 6061-T6 and 7005-T53 alloys (the latter was later dropped from the investigation) were also anticipated. There are two categories of aluminum alloys used in structural and plant applications, non-heat-treatable and heat-treatable alloys.

Non-heat treatable alloys are mainly alloyed with Mg. One of the strongest, containing 4.5% Mg and 0.75% Mn, is designated 5083 in American standards. A minimum tensile strength specified by the ASME Boiler and Pressure Vessel Code, Section VIII, Div. 1, for sheets and plates made from 5083 alloy in annealed state are 40 ksi (275 MPa). The same strength is specified for welded 5083 alloy as well.

Heat-treatable alloys are those based on Mg and Si. The most common welded and popular alloy, identified as 6061, contains Mg and Si in amounts up to 1% nominal, often with addition of Cu and Cr. In fully heat-treated (T6) condition (i.e., solution-treated and artificially aged), this alloy should demonstrate, according to the ASME Code, a minimum tensile strength of 38 ksi (262 MPa). However, for welded 6061-T6 alloy, the ASME code allows only 24 ksi (165 MPa). This is due to recognition of a considerable loss of strength typical for this type of alloys as a result of welding.

Weldability of 6061-T6 alloy is mediocre. For example, 6061 alloy composition is such that it is very susceptible to **solidification cracking**. To counter this, a filler metal of much higher alloy content must normally be used, the choice resting between Al-Mg or Al-Si alloys. **HAZ cracking** is another serious problem. And, as mentioned before, a considerable loss of strength in the welded joint occurs because the major effect of the weld thermal cycle is to coarsen the hardening precipitates overaging the alloy in the HAZ. As a consequence, the tensile properties of the welded joints are usually well below not only those of the base metal, but also those of 5083 alloy. An improvement in strength can be obtained by full postweld heat treatment. However, this is not practical for bulky large weldments such as 13-ft. long AE mat panels.

Good extrudability is the main reason why, despite the shortcomings described above, Al-Mg-Si alloys are frequently welded. One reason for this is that these alloys are much easier to form and to produce in complex shapes than Al-Mg alloys with high Mg content. Therefore, it is often easier to obtain Al-Mg-Si alloys, particularly if complex shapes are wanted. Opposite to 6061-T6 alloy, 7005-T53 alloy has better weldability and higher strength after welding. However, the

extrudability of this alloy is very poor and very few manufacturers are willing to produce extruded products from this alloy.

Automatic welding is a very attractive and the only option to efficiently fabricate very long mat panels from narrow extruded sections. However, automatic welding is evidently associated with potential deterioration of properties of the welded joints and weld defects, which depend considerably on welding parameters. That is why control of these parameters is of great importance for quality of welding in aluminum alloy of 6000 and 7000 series. It is obvious that to effectively keep the welding parameters within a specified range, introduction of automatic **real-time monitoring** and **closed-loop control** was needed. However, very few companies in the United States are able to provide this type of welding process control. GARD selected CRC-Evans Automatic Welding, a subsidiary of Pipeline International, Inc., Houston, Texas which was the only company in the U.S. capable of providing a complete package of welding, process monitoring and control equipment as well as an extensive and successful experience in development of welding automation.

1.2 OBJECTIVES AND SCOPE OF THE PROGRAM

General objectives of the program, as stated in Section C of the contract granted to GARD by the U.S. Army Belvoir RD&EC, were the following:

To undertake basic research in the area of automatic welding in order to improve welding and weld quality control of extruded aluminum panels through integration of weld inspection, real-time monitoring of weld parameters and automatic welding equipment into one system with a microprocessor interface. The automatic process shall improve weldments through real-time monitoring and adjusting of parameters during welding. The welding process will eventually become an integral link in the production chain of extruded panels to allow quality control within the best possible environment. Multi-hollow tailored aluminum extruded panels shall be welded from both sides with sufficient strength in all planes to provide an alternative to the wider more costly one-piece extruded aluminum panels.

The scope of the program was formulated according to these general objectives as follows:

1. To design and evaluate a welded multisectional modification of the Access/Egress (AE) roadway mat panel.
2. To procure a batch of the 6061-T6 extruded AE subpanels and to assess the available manufacturing base.
3. To develop an automatic microprocessor-based welding system with real-time monitoring of welding parameters and their adjustment through closed-loop feedback control. This

should be used as an in-process non-destructive inspection tool to improve weld quality.

4. To develop means of operational support which allows both welding of the full-length AE mat panels and verification of the developed system and technology to be made.

5. To establish optimal welding procedure for welding of the AE mat panels using the developed equipment and technology.

6. To weld twelve short (5-ft long) test mat panels for verification of the optimal welding procedure.

7. To fabricate ten full-length (13-ft long) AE mat panels for verification of the developed fabrication system and procedure, and the panel design.

8. To organize the obtained data into a data set package which includes a final report, drawings, experimental data, etc.

1.3 REPORT ORGANIZATION

The final report "Efficient Welding Fabrication of Extruded Mat Panels" consists of five sections and Appendices.

Section 2 "Design and Procurement of Extruded Mat Panels" contains the description of efforts to design multisectional welded Access/Egress (AE) roadway mat panel, including evaluation of fatigue performance of the welded joints and discussion on the applicability of the developed approach to bridge deck panel fabrication. Also, included in this section is the description of the procurement efforts and the discussion on the results of the evaluation of extrusion manufacturing base in the U. S.

Section 3 "Welding Metallurgy of Heat-Treatable Aluminum Alloys" describes the results of an extensive literature search on metallurgical problems which may occur in welding of heat-treatable aluminum alloys of 6000 and 7000 series.

Section 4 "Experimental Welding Program" describes the result of the experimental study to determine an optimal welding procedure to be recommended for welding of the extruded aluminum AE and bridge deck panels. This includes discussion of the results of radiographic inspection, mechanical testing and metallurgical examination of the welded joints.

Section 5 "Development of Fabrication System for Welding Aluminum Panels" describes the main concept, design and operation of the experimental fabrication system developed under this program to efficiently fabricate aluminum AE mat panels. This includes automatic welding system with closed-loop feedback control, fixture mechanism and supporting auxiliary equipment.

The material in the report is not always presented in a chronological order in which this 3-year program advanced but rather in the order which facilitates understanding of the basic concepts and ideas. The report conforms to all the provisions of the military standard MIL-STD-847B "Format Requirements for Scientific and Technical Reports Prepared for the Department of Defense." Each Chapter has its own page, figure and table numbering systems and a corresponding appendix.

Section 2

DESIGN AND PROCUREMENT OF EXTRUDED MAT PANEL

2.1 DESIGN OF WELDED ACCESS/EGRESS (AE) MAT PANELS

2.1.1 Background

Design of the welded multisectional access/egress (AE) mat panel was based on the drawings of the fully extruded single-section AE mat panel furnished by the Belvoir RD&EC. The panel was designed by the U.S. Army Waterways Experiments Station (WES), Corps of Engineers, Vicksburg, Mississippi. The following drawings were provided (see Appendix A1):

- Drawing No. 13227E7062 - Mat, Roadway, Access/Egress - 2 sheets and
- Drawing No. 13227E7065 - Mat, Roadway - 1 sheet.

The drawings describe a hinged access/egress (AE) roadway mat panel extruded from 6061-T6 aluminum alloy. The panels are to be mechanically assembled into a surfacing module which can provide:

- Exit roadways out of rivers for fording/swimming vehicles,
- Access lanes for bridge or raft launching equipment, and
- Roadways to and from a bridgehead.

GARD modified these drawings and designed a welded version of the AE mat panel, based on stress and fatigue analyses of welded joint performance for the traffic loads specified by the Army. This design modification (which will be referred to as Mod. 1) covered the following areas:

- Modification of the original panel configuration,
- Breakdown of the original panel into subpanels,
- Design of the mating ends of the subpanels,
- Welded joint design, and
- Fatigue analysis of welded joints performance.

Later in the program, the Belvoir RD&EC requested that the Ribbon Bridge (RB) and the Light Assault Bridge (LAB) deck panels were included into the program. The requirements were the following:

- To create a universal welded joint design which could be used for both the AE and the bridge deck (BD) panels,
- To redesign the Mod. 1 AE panel in order to include the universal welded joint configuration,

- To evaluate design of the Ribbon Bridge (RB) and the Light Assault Bridge (LAB) deck panels to determine whether the bridge deck panels could be accommodated in the fixture which had already been designed by that time.

In order to distinguish the initial Mod. 1 AE panel design from that with the universal joint, the latter will be referred in the text as Mod. 2 AE panel design.

2.1.2 Modification of the Panel Configuration

Modification of the original AE panel configuration was done to improve the suitability of the panel to possible automation of assembling and welding operations (see Appendix A2). There were some restrictions imposed by the Belvoir RD&EC to be followed. It was not permitted:

- To change the outer envelope dimensions,
- To decrease moment of inertia of the panel cross-section,
- To reduce thickness and number of stiffeners,
- To increase cross-sectional area of the panel,
- To place a tread bar without being supported by a stiffener,
- To offset the center lines of a tread bar and a stiffener.

As a result of the modification, there were the following changes:

- The width of the original mat AE panel was reduced by 0.25 in., (6.4 mm) from 26 in. (660 mm) to 25.75 in. This was needed to turn a round surface of the hinged end connector of the panel into a flat surface to facilitate clamping in the fixture.

- Number and location of the tread bars were changed within the Army limitation requirements to facilitate assembling and welding operations.

- The cross-section area and the moment of inertia of the welded panel were slightly (less than 3%) increased due to introduction of mating design details.

2.1.3 Panel Breakdown into Subpanels

A switch from a single-section extruded mat panel design to a welded multisectional panel design is associated with several potential problems. Severity of these problems increases with an increase in the number of subpanels needed to form a full size panel. The basic problems envisioned were the following:

- Decrease in efficiency of metal utilization,
- Increase in labor for assembling and welding operations,
- Increase in the number of possible weld defects,
- Increase in accuracy requirements for extruded subpanels,

- Decrease in productivity rate, and
- Increase in fabrication cost.

Assessing the optimum design of a welded mat panel, the described above problems were carefully weighed against the extrusion "availability factor". This factor takes into account the number of extrusion presses available nationwide capable to produce the specified extrusion circle size, the cost of the tooling (dies) required and the eventual cost of the extruded subpanels.

Availability of extrusion presses nationwide is one of the important goals of this program. Obviously, splitting the mat panel into two or more sections would substantially increase the available manufacturing base. According to the 1991 Industry Guide published by the Aluminum Extrusion Council (an Association of Captive and Contract Extruders), there are about 195 presses in the U.S., of which only 4 presses owned by 2 companies are capable to extrude panels with circle size above 24 in., while 55 presses owned by 38 companies have the capacity to produce extrusion above 10 in. circle size. There are several reasons for this which will be discussed later.

Analysis of potential fragmentation of mat panels showed that there were not many options available. A two-section mat panel is fabricated from two subpanels. It would be a desirable solution as far as the assembly and welding aspects of the problem are concerned. In comparison with a multisectional panel design, the two-section panel offers the following advantages:

- minimum time (and maximum ease) of assembly,
- minimum number and least total length of welds (2 welds, one from each side of the panel and 26 ft. (7,925 mm) of welds,
- least welding problems, including weld defects, distortion, and
- minimum cost of welding fabrication.

The drawbacks of this design, in comparison with a multisection panel design, are the low availability of presses, higher tooling (dies) cost and higher eventual cost of the extrusion product per pound. According to a 1988 verbal quotation from Alcoa, the cost of the die and extrusion were \$12,000 and \$2.50-3.00 per pound, respectively.

A three-section mat panel consists of three subpanels. This design, in terms of ease and cost of welding fabrication, is inferior to that of the two-section panel because of the greater number (4) and total length (52 ft., 15,880 mm) of welds required to join the subpanels. However, availability of presses is much higher and cost of extrusion and dies are lower for the three-section panel.

A multisectional mat panel consists of more than three subpanels. With further fragmentation of the mat panel, the trend will continue: the number of subsections will increase, and the cost and

the problems of welding fabrication will increase at an accelerated rate. At the same time, the presses will be more available and the cost of extrusion will slowly decrease. For example, a mat panel which is composed of 5 subpanels, requires 8 welds with a total length of 104 ft. (31,700 mm) to join the sections into a mat panel. Application of so many welds is associated with a significant amount of heat transferred into the extruded sections. As a result, a thin and narrow subpanel, may be overheated and the base metal strength may be reduced. Extruding such a long and narrow subpanel is associated with a larger twist and lack of straightness of the extruded section. Also, there is higher probability of weld defects, higher distortion (residual stresses) after welding, higher cost of welding fabrication, and lower productivity.

The analysis described above, showed that three-section panel was the optimal choice. This conclusion was also reinforced by the Army requirement to weld all the joints on the same side of the panel simultaneously. The design providing for more than three sections would require more than two sets of very sophisticated and expensive welding equipment. To implement such a system would be impractical from the technical and economic points of view.

Thus a three-section design was adopted in this program and later was approved by the Belvoir RD&EC.

2.1.4 Mating End Design

Design of mating ends of the sections is interrelated with welded joint design which will be discussed later. Two types of mating end design were analyzed for Mod. 1 AE panels. These are semi-hollow (Type I) and hollow (Type II) mating end configurations shown in Fig. 2-1a and Fig. 2-1b, respectively. The mating end configurations were analyzed in terms of their effect on the overall subpanel design, compatibility with the selected welding process, effect on metallurgical reactions, residual stresses, and other aspects of welding. The most promising configuration was supposed to be integrated into a final panel design.

Type I semi-hollow mating end design, as compared to Type II design, is simpler and easier to extrude. It is obviously associated with slightly lower cost of extrusion due to the fact that there is less bridging required. However, the assembling may be more complicated, in terms of edge alignment and molten weld puddle support since complete penetration for this weld is required. For this design, a special copper water-cooled backing bar was needed similar to the backing bar shown in Fig. 2-1c. This one is made of two identical halves with an air hose in between. When pressurized, the hose would press the bar halves against the back sides of both welds at the same time.

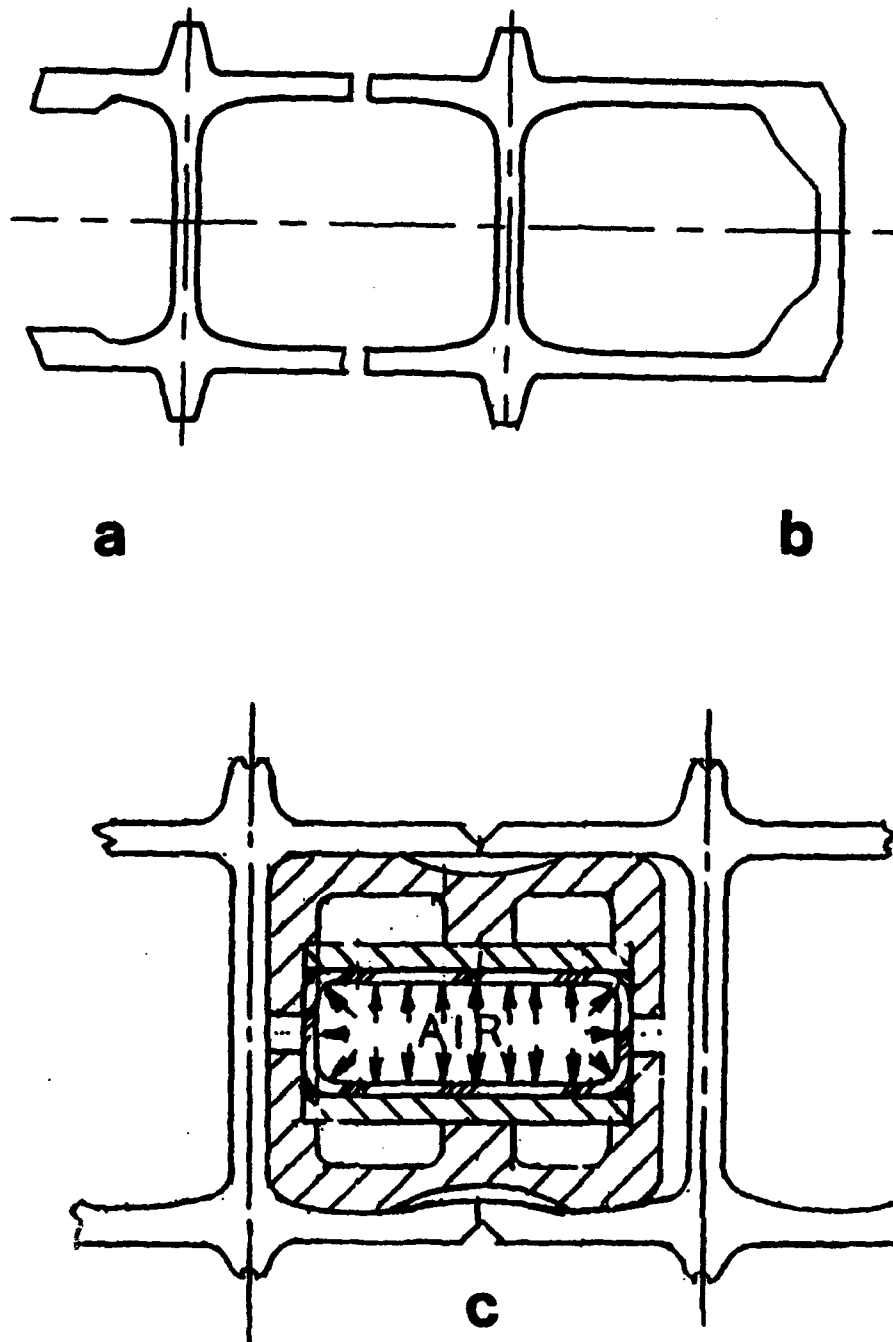


Fig. 2-1. Mating end configurations of extruded AE subpanels: Type I (a), Type II (b); schematic representation of a backing bar for welding Type I joint (c).

Type II mating end design is not that efficient in cost or material utilization. However, it appeals through its simplicity and forgiving behavior with respect to assembling and welding operations.

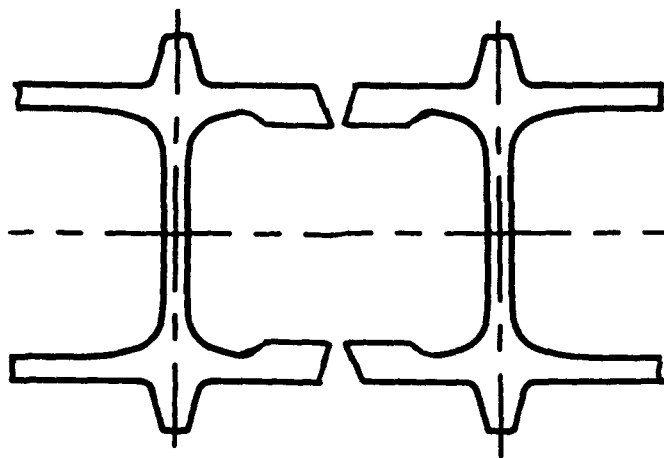
2.1.5 Welded Joint Design

Two welded joints were considered for Mod. 1 AE panels. They are shown schematically in Fig. 2-2 for Type I (a) and Type II (b) mating end configurations. The joints were designed according to the following considerations:

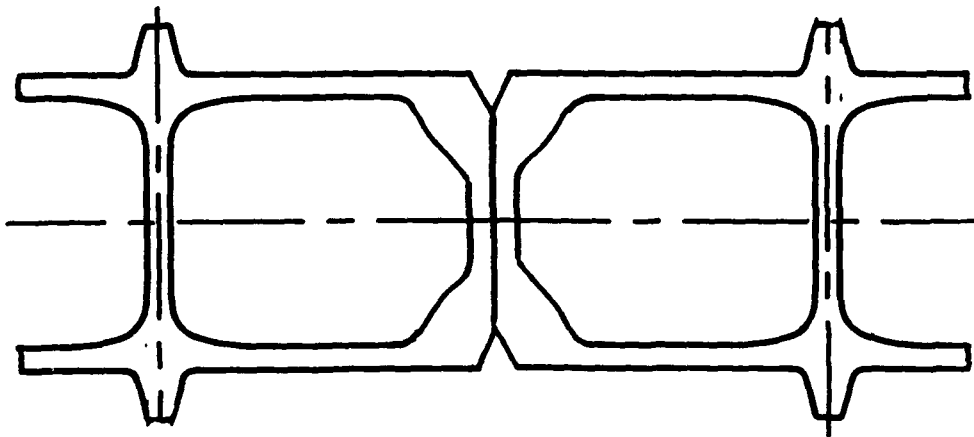
- A 60° V groove was provided to decrease dilution of the crack resistant filler metal with crack susceptible base metal.
- Effective throats of the welds larger than 1/8 in. (3.2 mm) were specified for Types I and II welds (1/8 in. is the thickness of the panel wall) in order to compensate for a weaker filler metal. According to D1.2-90 AWS Structural Code, Aluminum, the thickness of the part for a complete penetration weld (Type I) and the depth of the groove for a partial joint penetration groove weld (Type II) are considered as the effective throats of the weld, respectively. At the same time, for dynamically loaded structures, this code specifies a 0.187-in. (4.8 mm) effective throat as a minimum. Since the access/egress panels were assumed to be subjected to dynamic load, the cross-section areas around the welded joints Type I and Type II joints were increased to allow for a larger effective throat, thus compensating for the reduction in filler metal strength.
- The required groove depth was estimated on the basis of the maximum design stresses allowed by the ASME Pressure Vessel Code, Section VIII, Division 1 for aluminum and aluminum alloy products. This Code specifies 10.5 ksi (72.4 MPa) for 6061-T6 unwelded metal, while for welded metal the design stresses are reduced to 6 ksi (41.4 MPa), yielding a stress safety factor 1.75. To transfer the same force, the effective area (or effective throat for the same effective length) of the weld should be inversely proportional to the safety factor. In other words, the depth of the groove should be about $0.125 \text{ in.} \times 1.75 = 0.22 \text{ in.}$ (5.6 mm) or at least 0.187 in. (4.8 mm) specified by the AWS D1.2-90 Code.

As was mentioned before, Type II welded joint was very attractive from production point of view. However, there was a main concern regarding its fatigue performance under the dynamic load specified by the RD&EC. Type I welded joint was not suitable for automatic production but obviously could perform better than Type II in fatigue environment.

Therefore, GARD decided to conduct theoretical assessment of fatigue performance of Type I and Type II welded joints.



a



b

Fig. 2-2. Welded joints: Type I (a), Type II (b).

2.2 FATIGUE PERFORMANCE ANALYSIS OF WELDED JOINTS

Fatigue analysis of welded joints of Mod. 1 panel design was conducted by GARD's consultant, Professor Frederick V. Lawrence (Department of Metallurgy and Civil Engineering, University of Illinois, Urbana, Illinois).

Researchers at the U of I have had a long history of involvement in problems relating to mechanical behavior of weldments. Prof. Lawrence is well known in the U.S. and abroad for his research in the area of the influence of weld defects on mechanical and, particularly, fatigue properties of weldments made of steel and aluminum alloys. Most recently, he has developed a method for calculating the total fatigue life of weldments using strain-controlled fatigue properties and fatigue crack growth parameters.

Prof. Lawrence was requested to evaluate two types of joints to be welded in terms of their fatigue performance (Fig. 2-2):

- Type I - complete penetration butt joint (semi-hollow mating end panel design), and
- Type II - partial penetration butt joint (hollow mating end panel design).

2.2.1 GARD's Stress Analysis

To provide necessary input information for Prof. Lawrence's evaluation, GARD's Dr. A. Henzi conducted a simplified stress analysis based on a number of conservative assumptions. The main assumptions were the following:

- A. Higher load was considered based on 3,000 passes of Military Load Class MLC70 (5-axle traffic, 15,000 axle/cycles). The loading spectrum specified by the Army was 2,700 passes of MLC24 4-axle traffic + 300 passes of MLC70 5-axle traffic (12,300 axle/cycles total) as per "Trilateral Design and Test Code for Military Bridging and Gap-Crossing Equipment," Jan. 1986.
- B. For Type II joint, stresses were calculated not at the tip of the weld root area (weld centerline) but rather at the edge of the internal web, that is .120 in. (3.0 mm) from the weld centerline. Stresses here are higher than at the weld root.
- C. For Type II joint, the weld depth was assumed to be 1/4 in. (6.4 mm). This predetermined a distance of 0.5 in. between the tip of the weld root area and the neutral axis of the panel, while the tip could have been brought nearer to the neutral axis.
- D. The cell (internal void) shape was taken square rather than the actual shape which has radii. Without radii, stresses are higher at the edge of the web.
- E. Concentrated rather than distributed loads were considered when local (within a cell) stresses were calculated. The former develops higher stresses.

F. Soil strength was assumed to be of an average value of 1.5 CBR, the maximum allowed by the Army. The stronger the soil, the higher the stresses that are developed at the bottom of the panel.

The results of the stress analysis is given in Appendix A3.

2.2.2 U of I Evaluation of Joint Fatigue Performance

Prof. Lawrence has analyzed fatigue performance of Type I and Type II joints using four computer programs. Expected fatigue crack initiation strength (S_a) and crack propagation lives (N_p) were calculated and a corresponding report was submitted to GARD (copy of the report and its attachments are presented as Appendix A4).

The basic conclusions of the report were the following:

- As was expected, Type I joint is superior than Type II joint in terms of fatigue performance.
- The Type I joint estimated fatigue strength for crack initiation, for a given life of 10,000 cycles, exceeds the stresses calculated by GARD by a substantial safety margin.
- The Type II joint estimated fatigue strength for crack initiation, even at 10,000 cycles, was too low for the stresses calculated by GARD. However, fatigue crack propagation life (38,000 cycles for the worst case) was larger than the expected life of the joint by a factor of 2. This means that, despite the fact that the crack may occur in Type II joints at an early stage of the joint service life, it will not propagate through the entire depth (1/4 in., 6.4 mm) of the weld after 3,000 passes of MLC 70 axle traffic.

Based on the results of Prof. Lawrence's report, GARD's conclusions were the following:

- Because of large safety margin and the conservative nature of the stress calculation, there was a strong reason to believe that Type I joint estimated fatigue performance, for the given service conditions, meets the Army requirements. Therefore, it was decided that all further efforts would be concentrated on the analysis of fatigue performance of Type II joint, particularly on crack initiation characteristics.

- Taking into consideration the substantial advantages offered by Type II joints for industrial production (compared to Type I joint), GARD decided to further study fatigue performance of Type II joints moving in two directions:

by assuming more realistic (less conservative) conditions for stress calculations, and
by improving joint design to reduce stresses and stress concentration factors.

2.2.3 GARD's Fatigue Evaluation of Type II Joint (Round 1)

Pursuing this objective, it was decided first to evaluate fatigue crack initiation performance of Type II joints using stresses calculated earlier for MLC 70 (high) and MLC 24 (low, 60% of MLC 70) loads and to apply them for the actual mixed traffic conditions. The latter represent 2700 passes of MLC 24 (10,800 cycles) and 300 passes of MLC 70 (1,500 cycles). In other words, assumption A was eliminated (see 2.2.1).

For analysis of crack initiation performance, it is easier to deal with life (cycles) at a given stress (ksi) than with strength at a given life. Since Prof. Lawrence did not calculate fatigue crack initiation life (N_i) (but rather fatigue strength, S_a), Dr. A. Henzi conducted additional calculations for Type II joint using a corresponding program supplied by Prof. Lawrence (Program ID No.: Ni-Al-Hole is attached in Appendix A4). Stress vs. fatigue crack initiation life (S-N) curves were plotted. This allowed the number of cycles required to initiate a crack to be calculated for high (MLC 70), low (MLC 24) and mixed (actual) loads. The S-N curves and the table summarizing the results are given in Appendix A5.

As shown in the table, N_i values calculated for high loads (under assumption A) were about 10 times more conservative than those for actual mixed loads. Yet, N_i values for Type II joint still remained too low, especially for the internal fibers of the bottom joint (Case #7).

2.2.4 FEM Stress Analysis of Weld Root Tip Area (Round 2)

The next round of the analyses was to eliminate assumption B by conducting a finite element (FEM) analysis to determine stresses at the tip of the weld root area rather than away from the weld. GARD assumed that stress values from this would produce more realistic (higher) N_i values for Type II joint. In addition, joint design has been improved to increase the weld resistance to crack initiation by eliminating assumptions C and D, namely:

- Welds with deeper (5/16 in., 7.9 mm) penetration have been considered in order to bring the tip of the root closer to the neutral axis and to decrease bending moment.
- Internal cell radii of 1/2 in. (12.7 mm) were introduced to reduce stresses in the weld area.

The FEM analysis was conducted by Dr. A. Henzi as described in Appendix A6. As was expected, the stresses at the tip of the weld root appeared to be so low that the lowest N_i values (187,000 cycles) calculated by Dr. A. Henzi exceeded the expected life at mixed load specified by the Army by a factor of 12. This meant that Type II joint was not likely to crack within the expected life of 15,000 cycles.

These results were attributed, to some (unknown) extent, to improvement of the joint design. It was realized that deepening of the groove of the welded joint and beefing up the weld area will be penalized by some sacrifice in welding speed (productivity) and material utilization. However, budget restraints did not allow GARD to refine FEM model further on to obtain optimized results.

2.2.5 GARD's Fatigue Analysis of Type II Joints (Round 3)

GARD continued fatigue analysis of Type II joints. At this, the third round of analysis, Dr. A. Henzi has run Prof. Lawrence's algorithms for straight LOP (lack of penetration) without a crack arresting hole and without gap between the panels. The results are shown in Appendix A7.

The hole was introduced by F. Lawrence to enhance crack initiation life of the joint. However, the hole and the gap, according to F. Lawrence, "did not help much because, by introducing it, large compressive occurrences of stress have become influential and damaging." GARD fully realized that absence of the arresting hole would probably drastically reduce N_i values for Type II joints. Still, due to the large margin in crack initiation life (factor of 12) and GARD's intention to exclude compressive components from the cyclic load by butting the panels against each other without a gap, GARD hoped that the new N_i values would remain greater than required.

As shown in Appendix 7, these expectations were confirmed only for the weld root area at the top of the panel, while the bottom weld root area remained vulnerable to crack initiation. Fortunately, crack propagation life of this weld, calculated by A. Henzi (following F. Lawrence's advice) was so great that a mutual conclusion was made as follows:

Despite the fact that the crack will probably occur in the bottom weld root area as a result of LOP in the early stages of the service life of the panels, due to a significant stress reduction resulting from more reliable joint design at the specified mixed cyclic load, the crack will not propagate into the weld far enough to jeopardize the expected life of the bottom weld. In other words, it will require about 3.8 millions cycles to drive the crack through the bottom weld, while the expected life of the panel is only 11,800 cycles.

Thus, GARD's final conclusion was that, assuming the great technical and cost benefits of Type II joints in mass production of the panel, this type of joint could be accepted for the final design of the panel.

2.3 DESIGN MODIFICATIONS OF AE AND BRIDGE DECK (BD) PANELS

2.3.1 Implication of Introduction of BD Panels

As was mentioned earlier, the bridge deck panels were requested to be included in the program by the Belvoir RD&EC. However, by the time the request was issued, the designs of the AE panel and the fixture had already been completed. Two BD panels were specifically identified, the Ribbon Bridge (RB) panels Light Assault Bridge (LAB) deck panels. The implication of this for the on-going program were the following:

- Type II joint design was not adequate for critical bridge application since it was partial penetration joint.
- A universal (Type III) welded joint design was needed to be applicable for both the AE and BD panels. This was needed to simplify design and fabrication procedure for all the panels to be processed. Another important consideration was to make sure that the knowledge and the data to be obtained during welding experiments with the AE panels could be directly applicable to the bridge panels to avoid or minimize another expensive experimental study in the future.
- Type III joint was required to have a complete penetration. This was necessary to ensure adequate fatigue performance of the BD panels expected from Type I joint.
- Type III joint and the corresponding mating end configuration were required to allow the panels to be assembled and welded in production with the ease expected from Type II joint.
- A new design modification (Mod. 2) of the AE panel was needed to accommodate a new Type III joint design.
- The RB and the LAB deck panel designs had to be evaluated to develop requirements for their modification. This was needed to allow the bridge panels to be processed using the same technology developed for the AE panels. The main concern was greater envelope dimensions of the DB panels, location of their tread bars and obstructive design details. These details had to be accommodated in the fixture design which had already been developed by that time.

2.3.2. Mod. 2 Access/Egress Mat Panel Design

The drawings of the Mod. 2 AE panel are shown in Appendix A8. The main difference between Mod. 1 and Mod. 2 is that the mating ends were modified to utilize a universal (Type III) joint design which can also be used for the RB and LAB deck panels. Also, tolerances were relaxed as will be discussed later.

Type III welded joint is formed as a result of mating of the End and the Middle subpanels. (Fig. 2-3) This is a butt V-grooved joint with 60° included angle. A lip of the End subpanel serves as a backing strip. A small root opening is created by allowing the lip of the Middle subpanel to be shorter than that of the End subpanel.

The mating end design features the following:

a) When assembled, the ends are slid into each other in a male-female fashion similar to that originally used for the LAB deck panels.

b) Tolerances are within the ANSI H35.2 requirements, except for those specifically required by the Army (straightness, flatness and twist). The tolerance system makes emphasis on the consistency of the mating end (male-female) design details in order to provide trouble-free assembling of the subpanels.

c) The tolerances used allow mating to be done with no interference even in the extreme case. This may occur (extremely rarely though) when the male and female ends happen to be the maximum and the minimum, respectively. On the other hand, both subpanels were supposed to be assembled on a flat frame of the fixture. This could result in the situation when an excessive gap may develop between the lips of the subpanels. However, due to proper utilization of tolerances for the mating ends of the subpanels, the possible maximum gap was considerably reduced compared to the LAB panels, from 0.188 in. (4.8 mm) to 0.048 in. (1.2 mm).

d) When assembled, the male lips of the End subpanel rest against the stiffener of the female end of the Middle subpanel. This allows the root opening of the formed joint to be maintained 0.062 - 0.093 in. (1.6 - 2.4 mm) wide. Variation is due to the tolerances allowed by the ANSI Standard. The root opening facilitates arc penetration into the backing strip.

e) The outside stiffener of each of the panel is deliberately placed within 0.250 in. (6.4 mm) from the end tip of the panel to take advantage of tighter tolerances allowed by the ANSI Standard (see footnote 6, page 21 of the Standard). At the same time, when the panels are assembled, a small void formed between the two adjacent stiffeners makes it easier to plug it with a silicon rubber compound. This was considered by GARD as possible environmental protection for the backside of the welded joints.

2.3.3 Evaluation of Bridge Deck Panels

Evaluation of the drawings of the RB and LAB deck panels furnished by the Army showed that fabrication of these panels could be possible in the fixture designed at GARD, provided that the panel design modifications described below are allowed by the Army. These modifications may

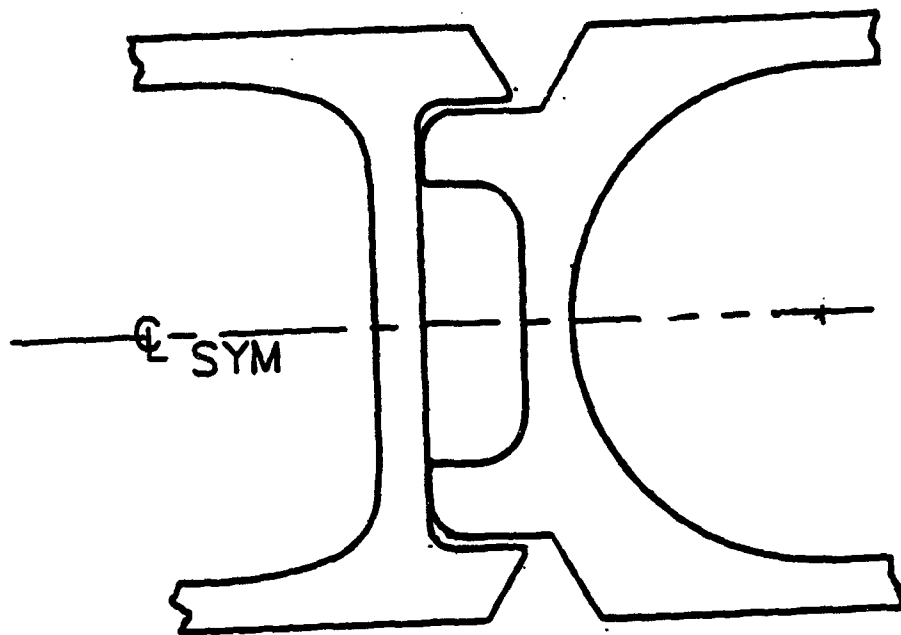


Fig. 2-3. Type III welded joint.

be realized after this project has been completed and the necessity of the fabrication of the BD panels has been established.

The RB deck panel should be redesigned as follows (see Appendix A9):

- The RB panel is currently 80.37 in. (2,041 mm) wide as a result of joining four 20-in. (508 mm) wide (between the centerlines of the joints) sections with three field welds. The new design provides for three sections 26.67 in. (677 mm) wide, each being joined with 2 welds in the field. Each of these sections can be fabricated in the GARD's fixture if it consists of three extruded subpanels about 8.9 in. (226 mm) wide (close to the width of the access/egress Middle subpanel).
- The cell size may be changed within 5% from the original size to relocate tread bars.
- The mating end design of the subpanels will be similar to that of the access/egress subpanels shown in Appendix 8.
- Only one die will be needed to extrude all the subpanels.

The LAB Deck Panel should be redesigned as follows (see Appendix A10):

- The LAB panel is currently 47.5 in. (1,207 mm) wide as a result of joining two sections 13.75 in. wide and two section 10 in. (254 mm) wide. Three welds in the field are required to join the subpanels. The new design provides for two sections 23.75 in. (603 mm) wide each. Each section can be fabricated in the GARD's fixture if it consists of three extruded subpanels. The one in the middle will be 8.5 in. (216 mm) wide (close to the width of the access/egress Middle subpanel) and those on both ends will be 7.625 in. (193.7 mm) wide.
- The existing cell size and support flange location remain the same.
- The mating end design of the subpanels (as well as that of the welded sections) will be similar to that of the access/egress subpanels shown in Appendix 8.
- Four dies will be needed to extrude all the subpanels in this case.

2.4 PROCUREMENT OF AE PANELS

One of the most important objectives of the programs was to increase availability of presses capable of extruding the AE panels. By splitting the AE panel into three subpanels, it was expected to significantly increase the available manufacturing base. However, the size of the subpanels is not the only criteria which affects availability of extrusion. There are many other reasons for which GARD tried to understand and to determine by surveying extrusion fabricators in the U.S. and Canada.

2.4.1. Extrudability of Aluminum Alloys

Specifics of extrusion process are important for understanding of the issue of press availability. The basic process for extrusion of aluminum is carried out by placing a heated aluminum ingot in a special press and forcing it through a shaped opening. The aluminum takes on the shape of a steel die forming the extrusion. The obvious advantage of the extrusion process is that a wide array of voids and opening in the metal can be formed and held to a very accurate tolerance. The resulting product has excellent grain structure, uniform alloying element distribution and characteristics inherent to wrought metal. In order to increase the strength of the extrusion, high-strength aluminum alloys, such as 6061-T6, are usually specified.

An important consideration in design of aluminum extruded component is a **shape factor**, which is a ratio of its perimeter to weight per unit length. Increasing shape factor is a measure of increasing complexity. Designing for minimum shape factor promotes ease of extrusion. The size of the extruded section affects the ease and accuracy of extrusion. As the circumscribing circle size increases, the extrusion process becomes more difficult. There is a tendency of metal to flow faster at the center of the die, thus making it more difficult to design and construct a die that provides uniform metal flow rates to all parts of the shape. Ease of extrusion improves with increasing thickness and favorable size-to-thickness relationship. Wide and thin shapes are more difficult to produce than more balanced and thicker shapes.

Steel die is the main tool of the extrusion process. Hollow shapes are extruded through a so-called bridge die. The term "bridging" refers to a cutload supporting a tapered core which produces a hollow totally enclosed tubular section. Plastic aluminum is forced to flow around the support points and be progressively reduced in sectional thickness to the final die form. The progressive area reduction causes the plastic aluminum to flow beyond the insert support points. Diameter of the die depends on the size of the part selected. The large diameter tapered end is flat and faces the extrusion press ram. The outline pattern of the part is milled into the desk with a generous lead-in radius, connecting a slight tapered section to a straight one at the metal exit point. AISI H Class, air hardening chromium hot work tool steel, is a typical die material. The common choice is AISI H-13 which is free machining, nitridable steel. Despite new computer and programming technology used by die manufacturers, intricate shaped extruded products need sometimes a special craft on the part of a die vendor and an extruder to bring the die and the product to the desired shape and tolerances. This is also dependent on the extruded alloy composition.

2.4.2 Metallurgical Aspects of Extrudability of Aluminum Alloys

A large amount of aluminum alloy used today is formed by extruding to the required product. Each alloy differs in its inherent extrudability. This manifests itself in productivity of the extrusion process, minimum extrudable thickness and other factors which eventually affect the cost of the extrusion. The higher the strength of the alloy, the lower the extrusion rate that can be achieved. Therefore, a premium in strength is usually penalized with lower productivity and, as a result, with higher cost per pound of the extruded product. The actual extrusion rate for a particular product depends on many factors, including pressure, temperature and accuracy of extrusion as well as ingot quality. The materials of interest to the Army for panel fabrication were 6061 and 7005 aluminum alloys. Despite the fact that the latter material was dropped from the experimental investigation by the Army's request, the data for this alloy will be provided in this report also.

Al-Mg-Si alloys of 6000 series are used mainly as hot extruded sections for architectural purposes, road and rail vehicles, general structures and buildings, but also as cold extruded gas cylinders and sheet for auto bodies. In all cases the demand for low cost is considerable because the competing materials (steel, wood, plastics and stone) are themselves cheap.

The metallurgical effort on extrusions now and indeed in the last decade or more, is aimed at rationalizing the many alloys available to the user, reducing the thickness of section which can be produced and increasing the extrusion speed. All of these measures, designed to improve the economics of the product, obviously have to take into account the preservation of necessary properties and surface finish. Also, for maximum economy they should allow the sections to be quenched at the press either in air or in water. Four groups are now available. Their extrudability characteristics are summarized in Table 2-1. According to Ref. 1, extrudability of 6061 alloy is rated as 60% of that of the standard 6063 alloy.

The various combinations of properties and economics of production have been achieved through good understanding of the role of the major (Mg, Si) and minor (Mn, Cu, Cr) elements, the interaction of the extruding metal and the die and the role of thermal treatments applied prior to extrusion.

In the copper free alloys, the strength is achieved by the magnesium (Mg) and silicon (Si) content. Together, they form Mg_2Si . However, the Mg content has a detrimental effect on extrudability and ideally should be at or below the balanced Mg_2Si ratio. Furthermore, Mg in excess of that ratio contributes very little to strength. The Si has far less effect on extrudability

TABLE 2-1. Extrudability of Al-Mg-Si Alloys

A.A. Designation	Grading	Characteristics
6063	Low Strength	Good finish, high extrusion speed. Thin sections. Air quenched. Few distortion problems.
6005, 6106, and 6181	Semi-medium Strength	Adequate strength for some structural applications where stiffness rather than strength is usual concern. Thin sections can be forced air cooled. High extrusion speed.
6061, 6082, and 6351	Medium Strength	Good strength obtained by water quenching. Minimum section thickness greater than Groups 2 & 3. Extrusion speeds less than Group 1 & 2.
6070, 6066	High Medium Strength	10-20% greater strength than Group 3. Water quenched. Corrosion resistance not as good as Group 1, 2 or 3. Alloys contain Cu. Extrusion speed less than Groups Groups 2 & 3.

but, while excess Si adds to the strength, it reduces toughness and can only be compensated for by other alloy additions.

Both manganese (Mn) and chromium (Cr) improve toughness and control grain size but Mn is less detrimental to extrusion speed and surface finish. Increase of either beyond that necessary to achieve adequate toughness adversely affects extrudability. While these additions can also produce a more fibrous and non-recrystalline structure, they result in a coarser structure should recrystallisation occurs.

Additions of copper (Cu) are beneficial in increasing tensile strength by providing better nucleation of the available Mg₂Si. Low levels do not adversely affect extrudability or corrosion resistance but higher copper levels to the excess Si alloys reduce corrosion resistance under certain conditions.

Al-Zn-Mg-Cu alloys of 7000 series is a recent example of the fine tuning of the properties of a well established alloy system to improve the overall performance. Until the introduction of alloys designated 7010 and 7050, the highest strengths obtainable from the Al-Zn-Mg-Cu systems were accompanied by poor stress corrosion resistance and low optimum properties. Careful adjustment of the Zn/Mg/Cu contents, substitution of Cr by Zr and control of Fe and Si to the lowest possible levels consistent with reasonable cost overcame these problems.

However, extrudability of the alloys of the 7000 series still remains far from that desired. For example, according to Ref.1, extrudability of 7005 alloy is rated as 9% of that for the standard 6063 alloy. This limits availability of services to produce extrusion from this alloy, mainly because of faster wear of dies and low productivity.

2.4.3 Bid Survey Among U.S. Extrusion Manufacturers

In August and September 1988, GARD conducted a bid survey among U.S. extrusion manufacturers, members of the Aluminum Extruders Council. Among 150 members listed in the Directory of the Council, only 21 were selected by GARD to participate in the bid by their press capability (circle size of extruded products). The main objectives of the survey were to evaluate the manufacturing base for supplying the extruded AE subpanels, and to determine realistic tolerances and costs.

The survey was viewed by GARD as very important since the results were expected to potentially affect the following aspects of the project:

- Fixture design might be affected and joint tracking devices might become necessary if industry could not meet the accuracy requirements for automatic welding of the extruded subpanels.
- Mat panel design might be affected as a result of industry inability to produce the subpanels technically and/or economically to the specified tolerances.
- Selection of the base material for the subpanels might be reviewed if extrudibility of this material presented a serious problem. This, in turn, might affect that mat panel design as well.

The results of the survey were presented in a special report A1-161-30 (see Appendix A11) and will be discussed below. An introductory letter (see Appendix A11) and a set of the draft drawings were submitted to each of the 21 potential bidders in August, 1988. The drawings (see Appendix A2) were the first draft version of Mod. 1 design featuring Type II joint and tolerances stricter than those required by the ANSI H35.2 Standard to provide adequate conditions for automatic welding.

A feedback from the manufacturers was not as great as GARD had previously expected. It took more than two months for 19 bidders to respond. Among those who did respond, only a few were willing to meet all the requirements specified in the introductory letter. One of the important reasons for reluctance of the manufacturers was a small order size (about 5,000 lbs. needed for the experimental program) and uncertainty in the project follow-up.

A summary of the responses from the manufacturers are given in Appendix A11. Analysis of the results of the survey and post survey inquiries showed that the required panel size, configuration, material and manufacturing tolerances affected both the number of extrusion manufacturers that were capable (or willing) to supply the mat panels and also the cost of the panels.

The size and configuration of the panels appeared to present some technical and economic difficulties for the majority of the bidders. Only eight of them had equipment, skill and willingness to extrude panels of the required circle size (8.67 in., 220 mm) such an intricate and delicate multi-hollow configurations, and ordered in such a small batch.

Some of the reasons for declining to bid were the following:

- Press capacity is not sufficient (most of the bidders).
- Wall thickness (0.120 in. 3 mm) is too thin (Jarl Extrusions).
- Panel is too light and delicate for big presses (Taber Metals).

It turned out that multi-hollow panels require special expertise in addition to a press of sufficient capacity. For example, some manufacturers (Dolton, Cressona Aluminum, among others), which are normally capable of producing extrusions of a larger circle size than the required one, were reluctant to bid because of the delicate panel configuration which could not justify expenses when ordered in such small quantity.

The selected material added also to reluctance of the manufacturers. Selection of 6061-T6 aluminum alloy as a base material for the mat panel reduced the number of the bidders: only four of them were willing to handle this high-strength aluminum alloy.

The main reason for concern were the following:

- The material is too hard to produce it competitively (most of the bidders).
- Difficulties in metal flow (Aluminum Shapes).
- Non-uniformity of properties around the voids due to trapped heat (Mid-America Extrusions).

The desirable substitute for 6061-T6, among the four companies which refused to handle this material, were 6063-T6 and 6005-T6 aluminum alloys.

Tolerances required by GARD played a significant role in reluctance of manufacturers to bid. Even the four companies, which were capable of producing the subpanels from 6061-T6 aluminum alloy, indicated that they would rather produce the extrusion with the tolerances specified by the ANSI H35.2 Standard (Dimensional Tolerances for Aluminum Mill Products).

Panel width tolerances higher than those allowed by the ANSI H35.2 Standard were difficult to achieve technically and justify economically. According to the Standard, for the width of the AE extruded subpanel, a tolerance of ± 0.064 in. (1.6 mm) is allowed. GARD's attempt to reduce the tolerance to ± 0.031 in. (0.8 mm) made two manufacturers drop from the bid. Only two extruders, Mid-America Extrusions Corp. and Magnode Corp., agreed to produce subpanels with ± 0.031 in. (0.8 mm) tolerance. This is still not enough to meet the requirements for automatic welding without guiding devices. However, to extrude the subpanels with even higher accuracy is probably neither technically possible nor economically advisable.

Panel length tolerance affected only cost of extrusion. The panel length tolerance of ± 0.25 in. (9.5 mm), specified originally by the Army could present difficulties in automatic welding. Since the ends of the subpanels are lined up flush at the front end of the panels assembly, the subpanels on the rear end of the assembly may stick out relative to each other by 0.5 in. (12.7 mm) or even by 0.75 in. (19.1 mm) if they are cut to $\pm 3/8$ in. (9.5 mm) per the ANSI standard. This was not

acceptable for automatic welding which would require ± 0.031 in., (0.8 mm) unless a special sensory device is developed to track the locations of the actual ends of the subpanels assembled in the fixture. A tolerance of ± 0.031 in. (0.8 mm) was achievable only by additional cutting as offered by Mid-America Extrusions.

Panel straightness - flatness and twist specified originally by the Army did not raise many complaints. For 13-ft. (6,934 mm) long panels the ANSI Standard allows the following tolerances for straightness, flatness and twist: 0.0125 in./ft. of the width, 0.006 in./ft. of the width and 1/4 deg./ft. (3 deg. max.), respectively. Magnode and Mid-America Extrusions agreed to meet the Army requirement of 1/2 of the ANSI tolerances.

Effect of panel tolerances on cost turned out to be noticeable. Despite GARD's requirement, specified in the introductory letter, to show the cost of extrusions produced with both the ANSI and GARD tolerances, only one manufacturer (Magnode Corp.) responded.

According to Magnode's quotation, stricter tolerances (± 0.031 vs. ± 0.064 in.) for the width (8.67 in., 220 mm) of the extruded subpanel increase the cost of the extrusion by 11% (\$1.90 vs. \$2.11 per lb.). Further tightening of the tolerances to meet the requirement for automatic welding (if technically possible) would increase the cost even more.

The cost of additional cutting of the panels to a specified length with ± 0.031 in. (0.8 mm) tolerance needed for automatic welding (indicated only in Mid-America Extrusions quotation) was negligible, \$1.23 per cut or approximately \$0.006 per lb.

The cost of die charges was not affected by the specified tolerances.

2.4.4 Availability of Extrusion Presses

The short summary and conclusions drawn from the results of GARD's survey discussed above are given below.

GARD contacted the Aluminum Extruders Council for information about availability of the extrusion presses in the U.S. and Canada. According to the 1989 Industry Guide published by the organization, there were 5 presses owned by 3 companies capable to produce extrusion with a circle size above 24 in., three of the presses being owned by ALCOA. The same data for 1991 showed that the number of the presses and the fabricators decreased by 1.

GARD conducted a survey of the extrusion industry considering the importance of the results to the on-going program. According to the 1989 Industry Guide, there were about 200 presses owned by 150 extruders in the U.S. and Canada of which about 60 claimed to be capable of producing extrusion above 10 in. circle size. However, random telephone inquiries showed that

some of them can not handle 6061-T6 alloy or the intricate shape of the AE panel. Others were not interested considering a small batch required for this program. On the basis of the inquiries, a list of 21 fabricators was compiled which expressed interest in the bid and claimed to have the required capability. The responses from the bidders were analyzed and presented in GARD's Report A1-161-30 "Bid Survey Among U.S. Extrusion Manufacturers" submitted for Army consideration in November, 1988 (Appendix A11). The report discussed above showed that the extruded subpanel design (circle size and configuration), selected material (6061-T6) and manufacturing accuracy (stricter than the ANSI Standard H35.2) resulted in a significant reduction of the manufacturing base capable of supplying the subpanels in the U.S. In addition to ALCOA, only two bidders (Magnode and Mid-America Extrusion) were qualified to satisfy all the requirements.

By having relaxed the tolerances to the level specified by the ANSI Standard (which became possible due to the introduction of joint tracking devices), the number of the qualified extruders was increased to five. Additional two companies (Taber and Kaiser Aluminum) could have been added to this list if they had shown interest in bidding for this small job. Also Reynolds Metal was capable of making the subpanels from 6061 but had to upgrade its heat-treating equipment to do this job in temper T6.

As a follow-up of the survey, GARD conducted an additional inquiry to determine whether the relaxation of tolerances to the ANSI level would allow those 4 companies which quoted for 6005 or 6063 aluminum alloys to switch to 6061. Only one company (Indal Aluminum Gulfport) has agreed to bid. The consideration associated with extruding the intricate shape of the panel was the reason for the other three companies to express no interest.

The situation by the time of the survey was conducted, was the following. In addition to very large fabricators, 8 companies were capable of producing the extruded AE subpanels per the ANSI Standard tolerances from 6061-T6 aluminum alloy. GARD has reason to believe that several companies refused to bid for economic rather than technical reasons. Implementation of mass production of the extruded panels would make these companies more competitive. It would also force other companies, which were not willing to bid for technical reasons but are very close in their capabilities to extrude the subpanels, to upgrade their equipment in order to bid for the job.

Finally, considering the fact that there was only two manufacturers left in 1991 capable of producing 26-in. wide extrusion, the idea of constructing the AE panel from the narrow extruded subpanels turned out to be very productive: availability of extrusion was increased at least by a factor of five.

Section 3

WELDING METALLURGY OF HEAT-TREATABLE ALUMINUM ALLOYS

The most common welded heat-treatable aluminum alloys are those based on Mg and Si. The most popular, identified as 6061, contains Mg and Si in amounts up to 1% nominal, often with addition of Cu and Cr. In fully heat-treated (T6) condition (i.e., solution heat-treated, quenched and artificially aged), this alloy should demonstrate, according to the ASME Code, a minimum tensile strength of 38 ksi (262 MPa). However, for welded 6061-T6 alloy, the ASME Code allows only 24 ksi (164 MPa) which reflects a considerable loss of strength typical for this type of alloy. This is a result of negative metallurgical reactions caused by heat of welding in the weld and in the heat-affected zone (HAZ).

The following metallurgical problems were anticipated in welding of 6061-T6 alloy. At first, the composition of alloy 6061 is such that the welds are very susceptible to solidification cracking. HAZ cracking is another serious problem. Tensile strength of the as-welded joint is well below that of the fully heat-treated base metal, because of the major effect of the weld thermal cycle which coarsens the hardening precipitates overaging the alloy in the HAZ. And eventually, porosity in the weld is a concern when gas metal arc welding (GMAW) is used.

Anticipating the metallurgical problems described above in welding of 6061-T6 alloy, GARD conducted a literature search in order to gather pertinent information on metallurgical reactions caused by welding in this alloy. Alloys of 7000 series were also included in that search since these alloys are of interest to the Army as well. The results of this search are presented below.

3.1 GRAIN STRUCTURES IN THE WELDS OF ALUMINUM ALLOYS

The properties of welds performed on aluminum alloys are distinctively related to the weld grain structure. For example, grain growth orientation, with regard to the centerline of the weld, or grain size are known to be associated with hot cracking sensitivity.

3.1.1 Types of Grain Structures in the Weld

According to Ganaha et al. (Ref. 2) there are several types of grain structures observed in aluminum welds, depending on weld chemical composition, heat input and travel speed.

Axial grain structure is characterized by continuous grains in the welding direction at the weld center (Fig. 3-1a). Although occasional new grains could be observed along the axial structures,



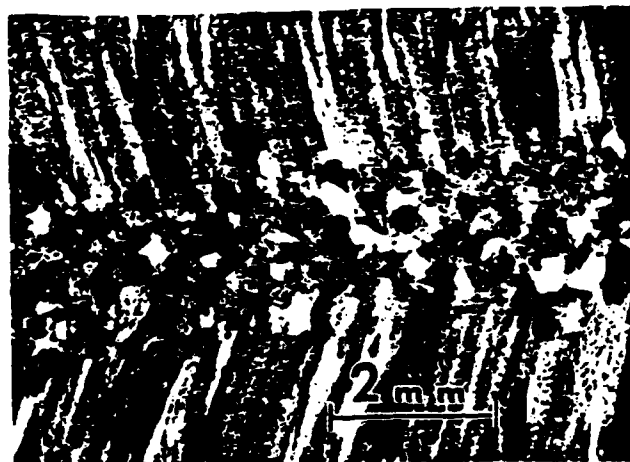
a —Axial structure in alloy 3003 welded at 30 cm/min, 1090 J/s.



b —Centerline structure in alloy 3003 welded at 60 cm/min, 1900 J/s.



c —Stray structure in alloy 5052 welded at 45 cm/min, 1440 J/s.



d —Equiaxed structure in alloy 6061 welded at 75 cm/min, 1900 J/s.



e —Feathery grains along the centerline of alloy 7004 weld.

Fig. 3-1 Typical grain structures in aluminum alloys (Ref. 2).

as illustrated in Fig. 3-1a, most of the axial grains initiated in the original weld bead are continued along the length of the weld.

Centerline grain structure is characterized by grain growth from the fusion boundaries to a distinct centerline (Fig. 3-1b). In the centerline structure occasional large equiaxed grains could be seen near the weld center (Fig. 3-1b).

Stray is a grain structure in which dendrite orientations established near the fusion boundaries are replaced by different dendrite orientations closer to the centerline, as illustrated in Fig. 3-1c. Unlike the axial structure, in the stray structure there is a continual appearance of new grains along the central region of the weld. But since many of these grains grow a considerable distance before they are restricted by the appearance of a new grain, they are not equiaxed. Thus the stray structure resembles the axial structure, in that grains tend to be oriented along the welding direction at the centerline, but in the stray structure each grain has a finite length which is less than the length of the weld.

Equiaxed grain structure is a band of equiaxed grains at the central region of the weld with columnar regions closer to the fusion boundaries (Fig. 3-1d).

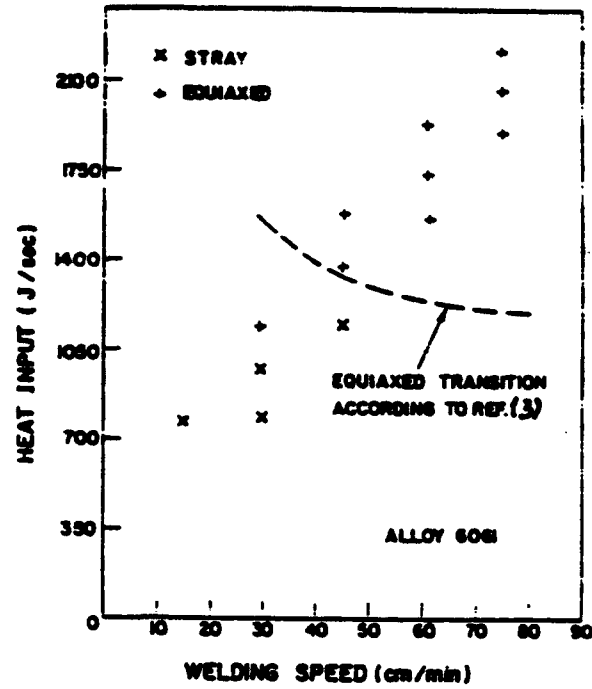
Feathery grain structure is characterized by feather-like completely columnar grains which are developed in some alloys at the region where transition from stray to equiaxed structures occurs (Fig. 3-1e).

3.1.2 Conditions for Grain Structure Formation in the Weld

According to (Ref. 2) formation of the grain structure depends on welding parameters and chemical composition of the weld.

Welding Parameters are of great importance to grain structure formation. **Axial** grain structure is formed in welds at low heat inputs and travel speed (especially in alloys of 3000 and 5000 series). With increasing weld speed the width of the axial region decreases and eventually disappears, leaving the **centerline** structure. Pool shapes were revealed to be associated with this phenomenon (Ref. 2). The decreasing width of the axial region with increased welding speed is due to the gradual change from an elliptical to a teardrop shaped pool, limiting the region over which growth could take place parallel to the welding direction.

In some alloys, such as 6061, **stray** structure appears at low heat input and travel speed. This structure is replaced by the **equiaxed** structure when heat inputs and travel speed exceed some transition level. Fig. 3-2a shows a structure diagram for GTAW of 6061 aluminum alloy (Ref. 2) plotted for wide ranges of heat input (700-2100 J/sec) and travel speed (10-80 cm/min, 3.9 - 31.5



ipm). For comparison the transition line between the two structures, reported by Arata et al. (Ref. 3), is shown also. The diagram shows a good correlation in transition values presented by both authors.

In 7004 aluminum alloy, which is close to 7005 alloy by chemical composition (Fig. 3-2b), however, according to Ref. 2, equiaxial transition occurs at higher heat input (for the same travel speed) or at higher travel speed (for the same heat input). Heat input is identified by the authors as amperage multiplied by voltage. For example, according to Figures 3-2a and b, to convert stray into equiaxed structure at 1,400 J/sec heat input, the travel speed should be maintained at 38 cm/min (15 ipm) for 6061 alloy and at 70 cm/min (27.6 ipm) for 7004 alloy. The same transition occurs for 40 cm/min (15.7 ipm) at 1400 J/sec and 1570 J/sec for 6061 and 7004 alloys, respectively. Another difference between 6061 and 7004 alloys is the presence of feathery grain structure in the transition one of 7004 alloy.

As was shown by Ganaha et al. (Ref. 2), transition from the centerline to the equiaxed structure, like the axial/stray transition, is dependent on the frequency of appearance of new grains. This transition is favored by increased heat input at a given weld speed.

Thus, at low welding speeds and heat input, either axial grains are observed along the weld centerline, or one finds large elongated "stray" grains with columnar grains closer to the fusion boundaries. At high welding speeds the columnar grains either grow all the way to the centerline or are blocked by equiaxed grains.

Chemical Composition of aluminum alloy (and filler metal if used) is essential to grain structure. According to Arata et al. (Ref. 3), various structure transitions in aluminum welds are caused mainly by the changes in growth rate and temperature gradient, with different welding conditions, affecting the amount of constitutional undercooling at the advancing solid-liquid interface. For example, the transition to an equiaxed structure was ascribed to a sufficiently long constitutionally undercooled zone.

However, Ganaha et al. (Ref. 2) showed that the tendency of an aluminum alloy to develop equiaxed structure in the autogenous (without addition of filler metal) weld depends on its chemical composition as well. The probability (P) of equiaxed grain formation, based on regression analysis, was described by the following equation:

$$P(\%) = -24.6 + 2067 \text{ Ti} + 13.9 \text{ Mg} + 53.7 \text{ Si} + 7.2 \text{ Cu}$$

Other elements did not have statistically significant effects. Thus, the probability of finding equiaxed (stray) grains is 60% (100%) for 6061 alloy and 50% (100%) for 7004 alloy, according to this equation.

Hence, in the comparison of stray vs. axial structure, and the transition to equiaxed grains, regression analysis indicates that titanium had the largest effect of all elements. Titanium is widely known to produce second phases which act as nucleating agents in aluminum. This made Ganaha suggest that these transitions are due to heterogeneous nucleation rather than either constitutional undercooling or dendrite arm remelting. The presence of titanium-rich compounds found in the centers of Al-rich dendrites (Fig. 3-3) was used by the author to conclude that the Al-rich phase was nucleated by these compounds. Phases which were not at dendrite centers were also analyzed and were found to contain other elements: Mg and Si in 6061 alloy, and Mg and Zn in 7004 alloy, consistent with Mg_2Si and $MgZn_2$ respectively. In 7004 alloy both zirconium and titanium rich compounds were observed at dendrite centers as well.

3.2 SEGREGATION IN THE WELDS OF ALUMINUM ALLOYS

3.2.1 Macrosegregation

Due to the presence of the electromagnetic force, the impinging force of the arc plasma, the surface tension gradient at the weld pool surface and the momentum of the descending filler metal droplets, strong convection prevails in the weld pool during arc welding. As a result of such a mixing action, the composition of the weld metal is macroscopically uniform in the bulk weld metal even if the composition of the filler metal used is different from that of the base metal. However, in spite of the mixing action which occurs in the weld pool, segregation of alloying elements, macroscopic in scale, can still exist in the weld metal.

Immediately adjacent to the weld pool boundary there exists a very thin boundary layer within which the mixing of alloying elements is suppressed (Ref. 4). As a result, the composition of the weld metal immediately adjacent to the fusion boundary often differs significantly from that of the bulk weld metal. It is likely that the mechanical and corrosion behavior of the weld metal in the region differs significantly from those of the bulk weld metal.

3.2.2 Microsegregation

The subgrain structure is important since it may affect the microsegregation of alloying elements and impurities in the weld metal and HAZ which in turn may affect mechanical properties of the latter. According to Brook (Ref. 5), weld solidification cracking is a direct result of microsegregation of minor alloying elements and impurities which form low melting phases. These liquid phases are segregated along grain boundaries which fissure under the weld related stresses. Also, microsegregation of impurities along boundaries can result in increased corrosion

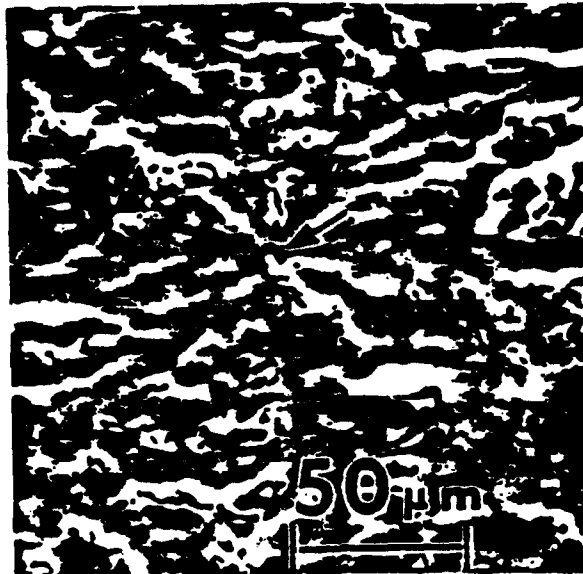


Fig. 3-3 Titanium-rich particle (arrow) at the center of a dendrite in alloy 7004 (Ref. 2).

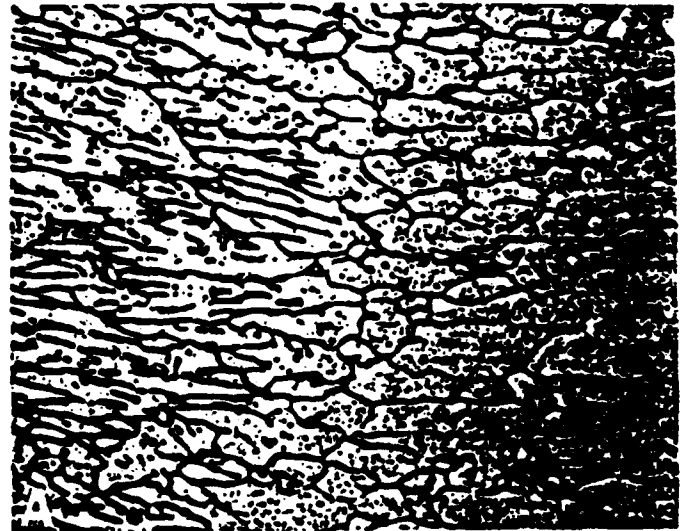
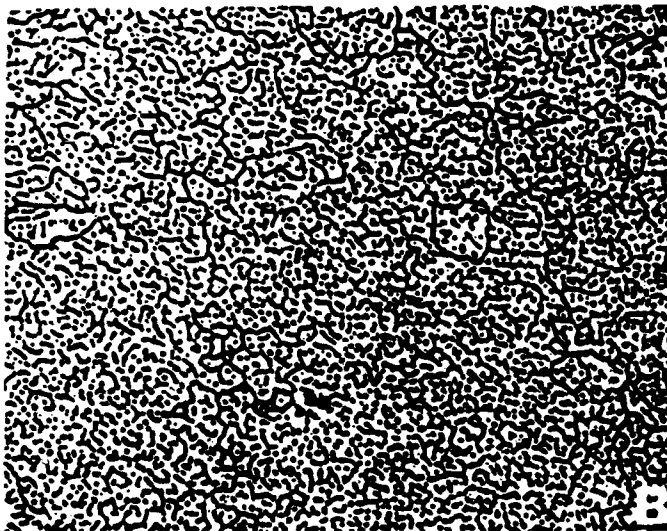


Fig. 3-4 Subgrain structure of a full-penetration weld:
(a) a fusion boundary, (b) at weld centerline (Ref. 7).

rates, low toughness, and accelerated rates of delayed failure. Furthermore, microsegregation can result in non-uniform distribution of critical alloying elements required for alloy strengthening.

As a result of dendritic solidification of the weld metal, microsegregation of alloying elements always exists in the fusion zone.

The subgrain structure of alloy 2014 welds was studied by Lanzafame, et al. (Ref. 6), in which the secondary dendrite arm spacing was found to be proportional to the square root of the heat input per unit length of weld. Apparently, as the heat input per unit length of weld is increased, the cooling rate of the weld metal through its freezing range is reduced. As a result, more time is available for the coarsening of dendrite arms and the dendrite arm spacing is increased.

Lanzafame, et al. (Ref. 6) also observed that dendrite arm spacing varies significantly in the same weld, i.e., coarser at the fusion line and finer at the weld centerline. Similar trends (Fig. 3-4) were also observed in alloy 6061 by Kou, et al. (Ref. 7). It was demonstrated in this study that the cooling rate of the weld metal through the freezing range is slower at the fusion line than at the weld centerline. Consequently, dendrites are coarser at the fusion line.

As mentioned previously, the dendritic structure is finer with a lower heat input per unit length of weld. Alloying elements and nonequilibrium interdendritic second phases, if there are any, tend to be more uniformly distributed in such a structure. As a result, better mechanical properties of the weld metal can be obtained in welds with fine dendritic structure.

3.3 SOLIDIFICATION CRACKING (SC) IN THE WELDS OF ALUMINUM ALLOYS

Solidification cracking (SC), sometimes called hot cracking, is a metallurgical phenomenon which has negative effects on weldability of high-strength aluminum alloys (Fig. 3-5). According to Dudas and Collins (Ref. 8), it is mainly associated with two factors:

- a) the temperature range of dendrite coherence and
- b) the time and amount of liquid available during freezing.

3.3.1 Role of Temperature Range of Dendrite Coherence in SC

For binary alloys the coherent interlocking dendrites are first formed within the temperature coherence range, which is the temperature difference between the coherence line (the highest temperature of dendrite coherence) and the solidus, plotted on an Al-alloy binary diagram. Unfortunately, metal has very low strength and practically no ductility in the coherent ("mushy")

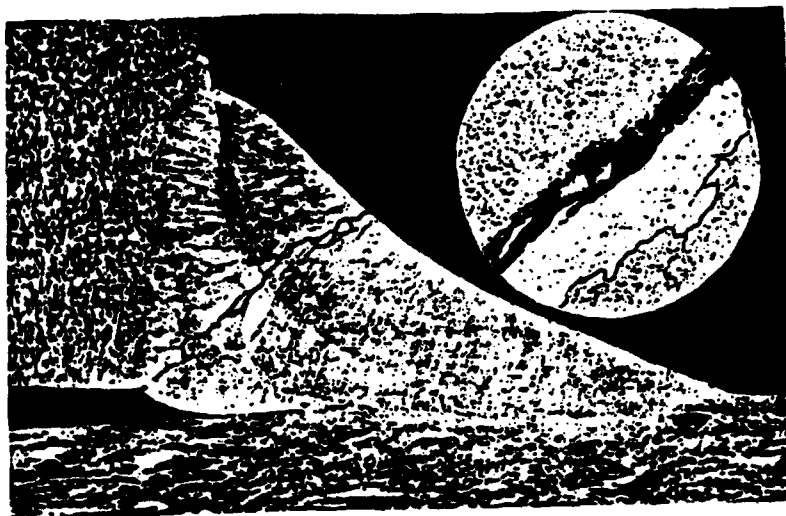


Fig. 3-5 Solidification cracks in Al-Zn-Mg alloys (Ref. 8).

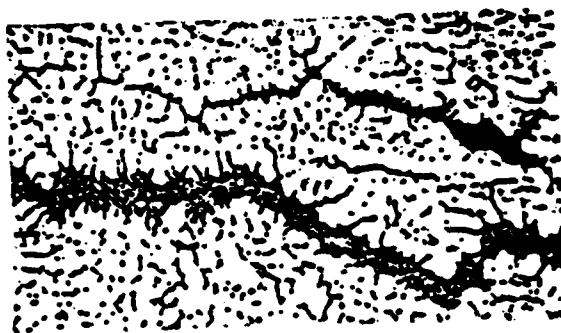


Fig. 3-6 Incipient solidification crack healed by band of eutectic (Ref. 9).

temperature range (the terminal stage of solidification) when the stresses developed across the adjacent grains may exceed the strength of the almost solidified weld metal. Such stresses can be induced by the following factors:

- a) solidification shrinkage of the weld metal and
- b) thermal contraction of the workpiece.

Both factors are significant with aluminum alloys.

Solidification shrinkage strains are proportional to the temperature interval over which solidification occurs (Ref. 8). Therefore, the wider the coherence range, the greater the tendency to solidification cracking. The severity of thermal contraction stresses in the workpieces increases with both the degree of constraint and the thickness of the workpiece. They depend on joint type and location, bead contour and, particularly, welding parameters.

3.3.2 Role of Liquid Eutectics in SC

The coherent interlocking solid network separated by essentially continuous thin liquid films may rupture from the developed stresses. If a sufficient amount of liquid metal is present near the cracks, it can "backfill" or "heal" the incipient cracks, as was shown by Lees in Ref. 9 (Fig. 3-6). Otherwise, the cracks appear as open tears.

Liquid eutectic is most helpful for preventing cracks because it freezes at a constant temperature. The amount of eutectic necessary to prevent cracking varies with composition and freezing rate. Less than a critical amount of eutectic may actually aggravate cracking by forming interdendritic films, which create zones of weakness in the already coherent metal.

3.3.3 Role of Solidification Rate, Grain Size and Super-heat Temperature in SC

These factors can also affect solidification cracking but only to the extent that they influence the coherence range or amount of available liquid during freezing.

Solidification rate of welds, in comparison with casting, is much too rapid to follow equilibrium. Undercooling occurs, which tends to suppress both the temperature of coherence and the solidus, and generates increasing quantities of eutectic. As a result, maximum cracking of welds occurs at a much lower composition level than that predicted for equilibrium. For example, Al-Si welds develop peak cracking at 0.8% Si rather than the equilibrium value of 1.65% Si (Ref. 8). However, it should be mentioned that for ternary alloys, particularly for Al-Mg-Si (including 6061), the presence of the Mg_2Si phase may play a complicating role compared to binary Al-Si systems, as noted by Jennings et al. (Ref. 10).

Fine-grained structures crack less than coarse-grained structures because a coherent

network of dendrites is formed at a later stage in freezing and thus the coherence range is decreased (Ref. 9). Also, fine crystals have greater ability to move and relieve the local contraction stresses that develop during freezing. For example, according to Ref. 11, fine equiaxed grains can deform to accommodate contraction strains more easily.

Super-heating of aluminum alloy above the liquidus increases the tendency to crack during freezing because more grain-forming nuclei are lost by dissolving at these high temperatures and thus grain refining is reduced. According to Ganaha et al. (Ref. 2), at lower temperature gradients (which may be created by super-heating), nucleation may occur further ahead of the columnar interface, so that the new grains can grow larger before the columnar grains catch up to them.

3.4 PREVENTION OF SOLIDIFICATION CRACKING IN THE WELD METAL

3.4.1 SC Prevention by Selection of Filler Metals

The solidification cracking susceptibility of high strength aluminum alloys, as in other alloys, is strongly affected by the composition of the weld metal.

Aluminum Alloys of 6000 Series. Solidification cracking phenomenon in Al-Mg-Si and Al-Cu-Si alloys was studied by Jennings et al. (Ref. 10) in the late 40's. Using a ring-casting and restrained weld tests, the authors developed a solidification cracking diagram which has still been recommended as a reference (Ref. 12) to predict solidification crack sensitivity of aluminum alloys of the 6000 series.

According to Jennings et al. (Ref. 10), maximum sensitivity to solidification cracking in Al-Mg-Si alloys occurs at a total alloy content of between 0.5 to 1.0%. The maximum in this respect occurs when the alloying elements (Mg and Si) are present in the proportion (2 to 1) corresponding approximately to the compound Mg_2Si . The results of weld-restrained test are shown on a diagram in Fig. 3-7, where maximum tendency to cracking occurs at about 1% Mg_2Si , followed by a decrease which is particularly rapid between 1.5 and 2%. According to this diagram an autogenous weld in 6061 alloy may display rather high sensitivity to solidification cracking since it contains close to 1% Mg_2Si . The same refers to the weld metal formed with the aid of the 6061 filler metal or filler metal of different composition but severely diluted with the base metal.

Therefore, the easiest way to avoid weld cracking in 6000 series alloys is to create a favorable (in terms of crack sensitivity) composition of the weld metal, by selecting proper filler metal and by controlling dilution.

According to a diagram presented by Dudas and Collins in Ref. 8 (Fig. 3-8), it is obvious that welding of 6061 alloy with the filler metal of the same (6061) or similar (6063) compositions

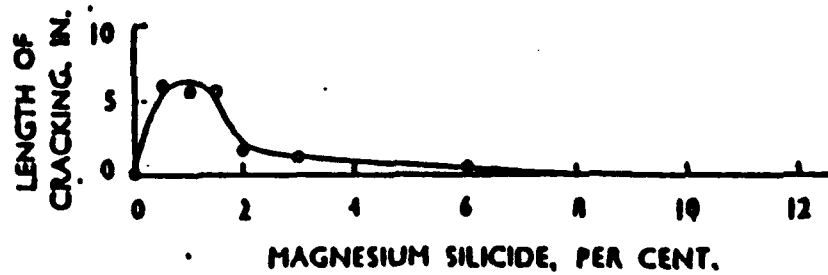


Fig. 3-7 Effect of composition on weld solidification crack susceptibility of Al-Mg-Si alloys (Ref. 10).

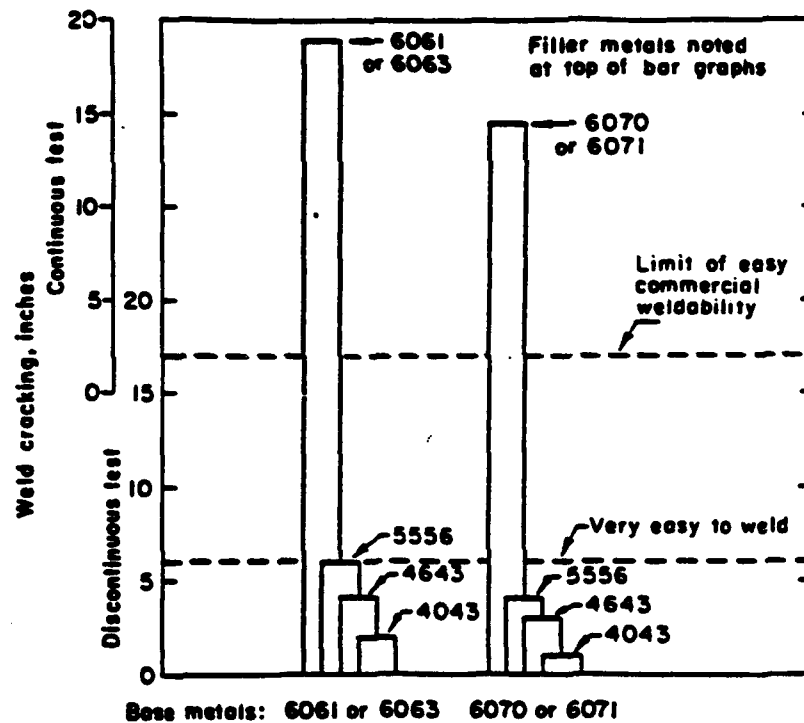


Fig. 3-8 Weld solidification cracking in aluminum alloys of 6000 series (Ref. 8).

are not desirable because of extremely high crack propensity of the weld metal. Cracking is decreased, however, by dilution of the weld with excess magnesium (Al-Mg filler metals) or excess silicon (Al-Si filler metals). With 5556 filler metal (5.2% Mg), cracking of fillet welds is reduced to a "very-easy-to-weld" category. 4643 and 4043 (used in this study) filler metals (5 and 4.1% Si) provide even higher resistance to cracking but usually at some sacrifice in weld strength and ductility. 4643 filler metal contains some Mg (0.2%) in addition to Si for improved weld strength.

7000 Series Aluminum Alloys. According to a study (Ref. 8), Zn in the range of 3.5-6% exhibits no marked influence on cracking in Al-Zn-Mg alloys of 7000-series. The sensitivity to cracking varies principally with Mg content, as shown on a diagram in Fig. 3-9, where maximum cracking occurs at about 1.2% Mg. According to this, 7005-alloy (1.4% Mg) falls into the lowest crack resistance category if welded with filler metal of the composition close to the base metal (Fig. 3-10). Addition of Zr reduces cracking by refining the coarse grains.

However, the most effective action for reducing cracks to the lowest level is the use of Al-Mg filler wires (5556, 5356) with about 5% Mg. This is accompanied, though, by sacrifice of some weld strength. Artificial post-weld aging is not recommended as well because of possible susceptibility to stress corrosion cracking. The 5180 filler metal, which contains about 2% Zn, provides stronger welds but with more cracks.

Filler metal 4043 is recommended for welding 7005 - alloy only where ease of welding far outweighs considerations of high strength and ductility.

3.4.2 SC Prevention by Refining of Grain Structure of the Weld Metal

One of the ways to reduce solidification cracking is to refine the grain structure of the weld metal. It has been reported that coarse columnar grains are often more susceptible to solidification cracking than equiaxed grains (Ref. 9). This can be due to the fact that fine equiaxed grains can deform to accommodate contraction strains more easily (Ref. 30). Liquid feeding and, therefore, healing of incipient cracks can also be more effective in fine-grained materials.

Several different techniques have been used to grain refine welds of high strength aluminum alloys.

Modification of the Weld Metal by Ti or Zr. Using inoculants, such as Ti and Zr, due to heterogeneous nucleation, fine grains can be produced and the resistance to solidification cracking can be enhanced. Fig. 3-10 shows the reduction in the total crack length of 7005 alloy by grain refining with Zr (Ref. 8). In fact, alloy 7005 and filler metals 5356, 5556 and 5183 all contain small amounts of Ti or Zr in order to improve weldability through grain refinement.

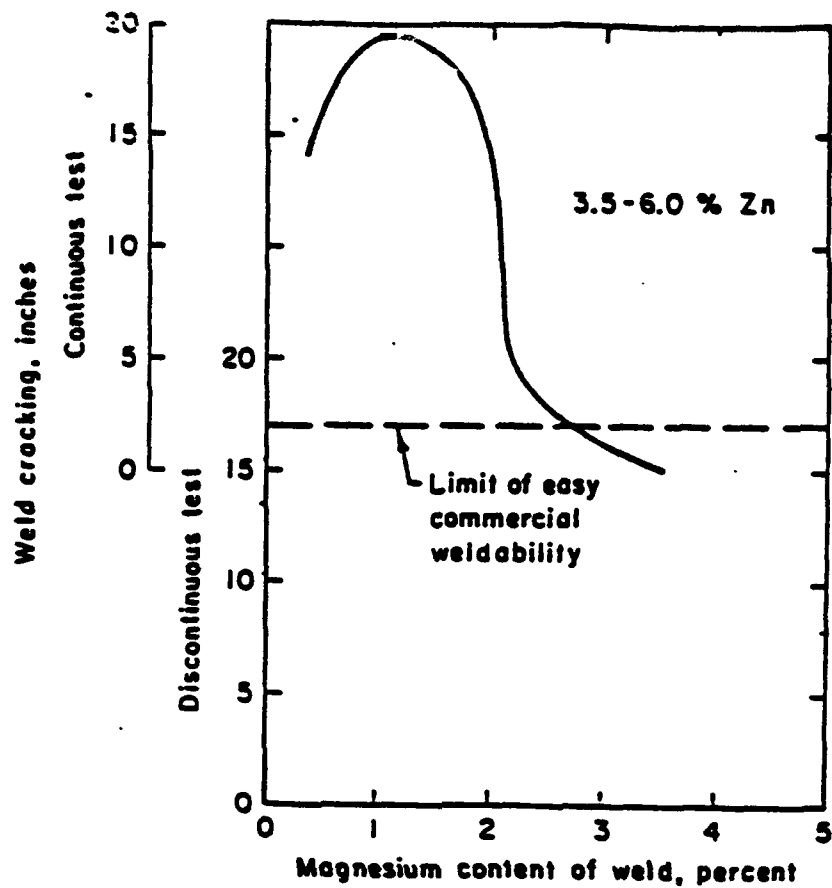


Fig. 3-9 Effect of composition on weld solidification crack susceptibility of Al-Zn-Mg alloys (Ref. 8.).

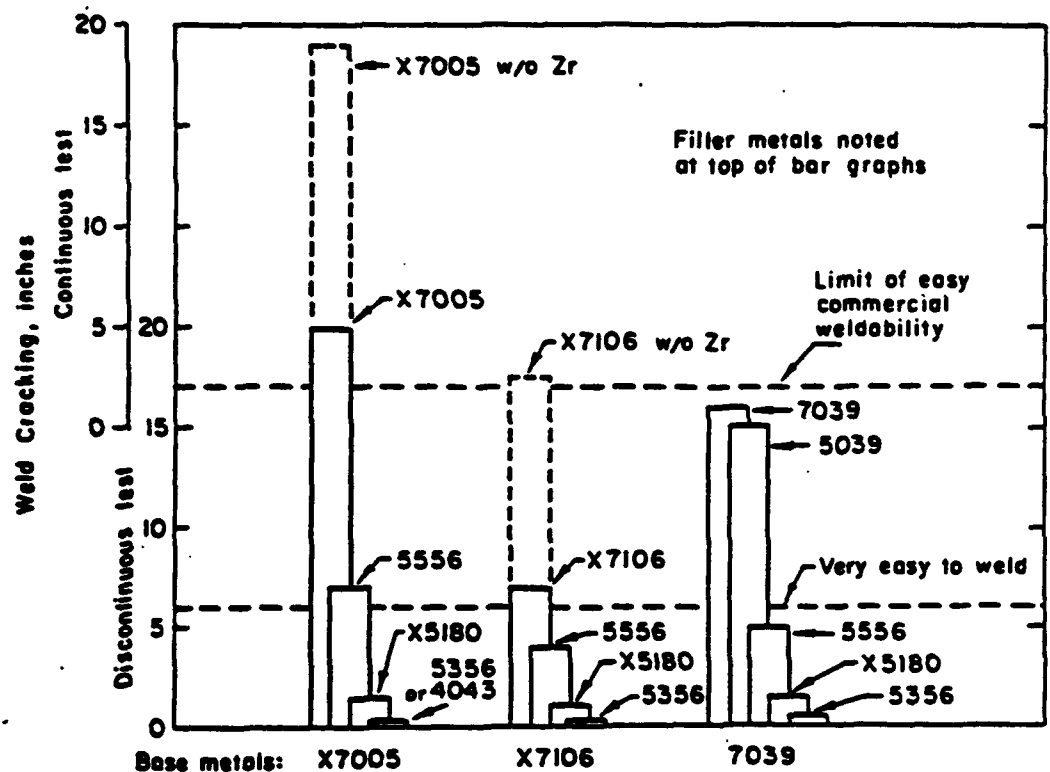


Fig. 3-10 Weld solidification cracking in aluminum alloy of 7000 series (Ref. 8).

Stirring of the Weld Metal Stirring of the weld metal is a technique used to affect hydrodynamics of the molten weld pool with the main objective to refine grain structure. In Ref. 13, Matsuda et al. refer to different methods of stirring, including mechanical, electromagnetic and ultrasonic vibrations, mostly for GTAW.

The mechanism of refinement by stirring is described by Matsuda et al. (Ref. 14) as dendrite fragmentation, while in recent study Pearce and Kerr (Ref. 15) explained it as detachment of grains from the partially molten zone ahead of the advancing solidification interface.

Electromagnetic stirring is carried out by application of an external alternating magnetic field parallel to the electrode. It results in rapid circular motion of the welding arc which in turn causes rotary motion of the liquid metal of the welding pool. If polarity is reversed, the direction of liquid motion is reversed too, resulting in crystal multiplication. According to Matsuda et al. (Ref. 13), in GTAW the refining action is effective at an optimum frequency of magnetic field which is proportional to travel speed. Therefore, at high travel speed, where equiaxed zone is formed, the magnetic stirring is not effective. It is not applicable for thin sheet metal and it is effective only for those alloys which are modified by Ti.

This was confirmed by Pearce and Kerr (Ref. 15), who found for GTA welds that insufficient content of Ti makes magnetic stirring ineffective. Again, magnetic stirring was found to be restricted only to alloys with a relatively wide partially molten zone. Of all alloys studied, only 7004 met this requirement.

Stirring by arc pulsation (used in this project) is carried out by forced thermal fluctuations produced by the pulsed arc. Matsuda, et al. (Ref. 14) found that effective weld grain refinement of alloys of 5000-series occurs only over a limited range of pulsing in GTAW: pulsation frequency less than 10Hz and pulsed current peak over background current greater than 80A. It was noticed that a steep front of the pulse is essential in order to generate vigorous movement of the molten metal.

Reduction of microsegregation of Zn and Mg in the GTA weld metal of Al-Zn-Mg alloy in pulsed arc welding, compared to steady arc welding, was reported by Mironenko, et al. (Ref. 16).

Stirring by arc oscillation is carried out by reciprocative movement of the arc across the weld joint. Grain refinement by arc oscillation was reported by many investigators. Kou, et al. (Ref. 17), in a recent study of arc oscillation induced by a magnetic probe, found that alternating columnar grains, produced by transverse arc oscillation at low frequencies (e.g., 1 Hz), tends to force the crack path to wind around and, hence, reduces solidification cracking. The effect was observed for autogenous GTA welds of 6061 alloy.

3.4.3 Role of Stresses Around the Weld Puddle in SC

Solidification cracking occurs when solidifying weld metal is stressed in the temperature range immediately above the solidus temperature. In this range, according to Chihoski (Ref. 18) aluminum alloy "has the strength and consistency of cottage cheese" and cannot resist tensile stress at all.

The strain pattern produced during fusion welding around the weld puddle varies in a similar manner with the heated metal. Immediately ahead of the arc it is subjected to compression since the cooler surrounding metal hinders its free expansion. The region behind the arc is subjected to tension caused by reaction to solidification shrinkage and contraction of the heated metal.

Many techniques employed to prevent solidification cracking rely on modification of the strain distribution, including the use of hold down clamps, tack welds, local spot heating or cooling, weld sequence, etc.

As was found by Chihoski (Ref. 18), travel speed has a profound effect on the character of the forces applied to the behind-the-arc region of solidified metal: tensile at slow speed (6 ipm, 2.54 mm/s) and compressive at high speed (20 ipm, 8.47 mm/s). This may play an important role in controlling solidification cracks by selecting a travel speed which shifts the tensile strain peak off the solidified zone.

3.4.4 SC Prevention by Proper Welding Procedure

Proper welding procedure may play an important role in prevention of solidification cracking.

Filler metal selection is the easiest method to avoid cracks in high strength aluminum alloys. For example, selection of 4043 filler metal for 6061 alloy reduces solidification cracking in the weld metal. However, this is only possible, if the relatively lower strength of the weld metal is allowed or compensated by corresponding joint design.

Joint geometry affects the rate of dilution of the crack resistant filler metal with the base (crack sensitive) metal. V-groove provides less dilution than does square groove. This improves crack susceptibility by involving more crack resistant filler metal.

Welding Process is important because of the necessity to use rapid travel speed and more concentrated heat source. In this respect, GMAW has advantages over GTAW due to its ability to deposit larger amounts of filler metal at higher travel speed, and to provide a more concentrated arc.

Bead Geometry affects the ability of the weld to feed the void created by the considerable shrinkage typical for aluminum alloys. A convex bead is less susceptible to cracking one which is concave, due to its ability to heal incipient cracks.

Electrode angle may be used to provide favorable bead geometry. Back-hand technique (electrode inclination in the direction opposite to weld progress tends to "dam up" the metal behind the arc and facilitates formation of the more desirable convex bead.

Clamping is important to maintain compressive stresses on the parts being welded. A properly designed fixture provides sufficient clamping force and allows the hot metal adjacent to the weld to be plastically deformed to relieve nearby shrinkage stresses.

3.5 PROBLEMS IN HEAT-AFFECTED ZONE (HAZ)

The principal feature distinguishing heat-treatable from non-heat treatable alloys is the formation of second phase precipitates during heat treatment of the former, which improves mechanical properties of the alloys. However, the temperature variations during welding may considerably affect the precipitation sequence and/or cause dissolution of the strengthening precipitates in the heat-affected zone (HAZ), leading to a local structure and properties very different from those of the original.

3.5.1 Cracking in the HAZ

According to Gittos and Scott's study published in 1981 (Ref. 19), HAZ cracking is the most severe problem in 6061 alloy (Fig. 3-11). It manifests itself in the appearance of surface or subsurface cracks of various lengths and depths located at or near the fusion boundary. Surface cracks are often initiated at the weld toe but may propagate away from the fusion line maintaining intergranular pattern. The extent of the problem is often difficult to assess, regardless of the postweld inspection method applied, until a number of sections of the welded joint are completed. Cracking is usually associated with the use of Al-Mg rather than Al-Si filler metal, regardless of welding process (GTAW or GMAW), type of welded joint (butt or fillet), or form of the base metal (plate, sheet, or extrusion shapes).

Metzger (Ref. 20) reported HAZ cracks in 1967 in GTAW of 6061 alloy using Al-Mg (up to 1.9% Mg) filler metal. Called "base metal" cracks by the author, the cracks were described as "very fine multidirectional surface crazing" confined to the face side between weld toe and clamping fingers. Metzger suggested that this phenomenon occurs if the solidus temperature of the weld metal is higher than the temperature range of solidification cracking in the base metal or if the weld metal has a relatively high yield strength at this range. The HAZ cracking made some of Metzger's



Fig. 3-11 Failed butt joint in alloy 6061 due to cracking in the HAZ (a), cracks in the HAZ (b) (Ref.19).

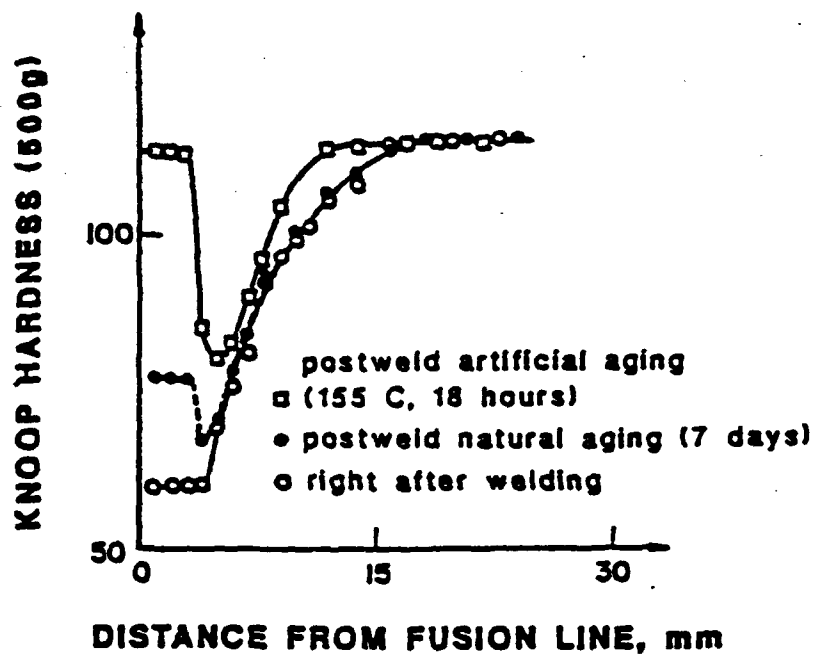


Fig. 3-12 HAZ hardness profiles of a GTA weld of a 3.2 mm-thick sheet in 6061-T6 aluminum (Ref. 12).

test results invalid due to drastic reduction in tensile strength and fracture toughness of transverse-weld specimens.

A later explanation of HAZ cracking mechanism, given by Gittos and Scott (Ref. 19), was similar to that given by Metzger. During welding, grain boundary melting occurs in the HAZ and with certain weld metal compositions, it is possible for the weld metal solidus to be higher than the base metal solidus. Thus, when the tensile strains, arising from the weld metal solidification, are imposed on the HAZ, cracking occurs at such boundaries.

No information on HAZ cracking in 7005-alloy was available.

The methods to prevent HAZ cracking in 6061 alloy could be reduced to the following recommendations (Ref. 19):

- 1) Specify 6061 alloy of the lowest (if possible) allowable alloy content to increase the solidus temperature of the alloy,
- 2) Lower the solidus temperature of the filler metal by using Al-Si filler metal with high (5%) silicon content, 4043 for example.
- 3) Increase dilution of the weld metal with base metal using Al-Si filler metal. (However, this may increase risk of solidification cracking in the weld)
- 4) Apply fixturing to ensure that the HAZ is in compression since tensile strains are necessary to cause cracking.

3.5.2 Strength Reduction in the HAZ

When welds are made on heated-treated aluminum alloys the heat of welding reduces mechanical properties of the HAZ. It is generally recognized that the rates of heat input and removal affect the HAZ width and the strength of the welded joint. This is reflected as hardness change in the HAZ.

HAZ Strength Reduction in 6000 Series Alloys. Fig. 3-12 shows the hardness profiles in the HAZ of a 6061-T6 sheet (Ref. 12). The high hardness level in the base metal is due to artificial aging before welding. The low hardness at the fusion-zone side of the HAZ, on the other hand, is due to the solution (complete reversion) of the precipitate phases during heating. Reprecipitation from the solid solution is not possible during subsequent cooling, since the cooling rate in this area is rather high. (The hardness level in this area, though, can be increased slightly by postweld natural aging and much more significantly by postweld artificial aging). The minimum hardness between this area and the base metal, after postweld artificial aging, is due to overaging. As a result of this, the loss of strength in the HAZ is permanent, unless the entire workpiece is

resolutionized, quenched and aged. This, however, may not be possible with large welded structures. Also, distortion of the weldment may be unacceptable in some cases.

According to Metzger (Ref. 20), the effect of the preweld and postweld heat treatments on the strength of alloy 6061 was studied by Burch who showed that welding in the natural aged (T4) condition is preferred to that in the artificially aged condition (T6), due to the greater tendency (lower HAZ hardness) to overage in the latter case.

However, results obtained by Metzger (Ref. 20) showed that hardness of the HAZ in welded 6061-T6 alloy can reach the same level as that of the T6 base material unaffected by welding, provided solution-quenching and artificial-aging heat treatment was applied after welding.

HAZ Strength Reduction in 7000 Series Alloys. The age hardening of Al-Zn-Mg alloys is quite different from that of 6000 series aluminum alloys. In general, Al-Zn-Mg alloys tend to age more slowly than 6000-series alloys. This results in less severe overaging of the HAZ, if it occurs. Furthermore, unlike 6000 series alloys, Al-Zn-Mg alloys can gain significant strength by natural aging. For these reasons Al-Zn-Mg alloys are attractive, especially when postweld heat treatment is not feasible.

According to Kelsey (Ref. 21), properties of 7039 alloy base material are not affected in locations where temperature during welding does not exceed 400°F. HAZ metal heated in the 400-600°F range undergoes hardness reduction which cannot be restored by natural or artificial postweld aging. HAZ metal heated to 600°F and above shows greater reduction in hardness immediately after welding, however its hardness can be almost fully restored by postweld natural or artificial aging.

Effect of natural aging on restoration of properties in the HAZ of the welded joint made on 01915 aluminum alloy (the USSR equivalent of the 7005 alloy) was studied by Makarov (Ref. 22). It was shown that the most extensive increase of tensile and yield strength of the 01915 alloy (up to 95% of that of the base metal) is observed within the first 15 days after welding, the strength of the butt welded joint being defined by the HAZ properties. After 30 days the strength of the welded joint is not practically changed and is defined by that of the weld metal.

3.6 EFFECT OF WELDING PROCEDURE ON PROPERTIES OF WELDED JOINTS

Heat of welding produces changes in the properties of the weld metal and HAZ. These changes are significantly affected by the welding procedure employed, particularly for welding aluminum alloys of 6000 and 7000 series.

3.6.1 Effect of Welding Parameters

Metzger (Ref. 20) noticed an increase in HAZ hardness in 6061-T6 alloy when low energy (360A, 20ipm, (8.46 mm/s) 13,000 watt-sec/in.) welds were performed, although the weld metal hardness was not appreciably changed. Fracture toughness was considerably improved due to finer dendritic structure of low energy welds. By comparing his data with those reported by Burch, Metzger found that travel speed affects transverse tensile strength of the over-aged zone of a welded joint more effectively than power input. For example, Burch reported that welding at 5 ipm (2.11 mm/s) and 25.6 kwatt-sec/in. resulted in tensile strength of 32.7 ksi, while Metzger obtained 41 ksi at 10 ipm and (4.22 mm/s) 24.5 kwatt-sec/in.

Brungraber (Ref. 23) found that for GMAW of 6061-T6 alloy the width of HAZ (Fig. 3-13a) and weld strength (Fig. 3-13b) in as-welded conditions depend on the heat input parameter defined as power (EI) divided by travel speed (V) and plate thickness (t). By using a large number (11) of passes (for 3/8 in. (9.5mm) thick plate with 60° V-bevel), each resulting in low high input parameter (220A, 22.1V, 48.6 ipm, (20.56 mm/s), 268 watt-min/in.²), the strength of welded joints close to that of unaffected base metal can be obtained. The strength decreases nearly linearly with increasing values of heat input parameters (Fig. 3-13b). 7000 series aluminum alloy, similarly to 6000 series alloys, are sensitive to heat input. According to Kelsey (Ref.21), in GMAW of 7039-T63 alloy, hardness in the HAZ drops and the HAZ width grows with increase of heat input (or decrease of number of passes). The same effect was reported for continuous welding compared to that with interpass cooling down to 150°F.

3.6.2 Effect of Artificial Cooling

By plotting the data reported by Burch on that of tensile strength of 6061-T6 GTA welds made with 4043 filler metal and artificially aged to the T6 temper after welding, Brungraber (Ref. 23) came to a conclusion that artificial cooling of the aluminum sheet during welding (water-cooled backing bar) has an affect on weld strength similar to that of a reduction of the heat input parameter.

Effect of local cooling of the butt weld and the base metals 2mm (.080 in) thick in GMAW of aluminum alloys was studied by Birman et al. (Ref. 24). Water was sprayed on the solidified weld at the tail of the weld puddle and on both sides of the latter. This increased cooling rate in the temperature range of 300 - 500°C (572-932°F), from 60°C/sec/(140°F) to 200°C/sec (392°F). It also drastically decreased (halved) the width of the HAZ. In addition, density of the joint

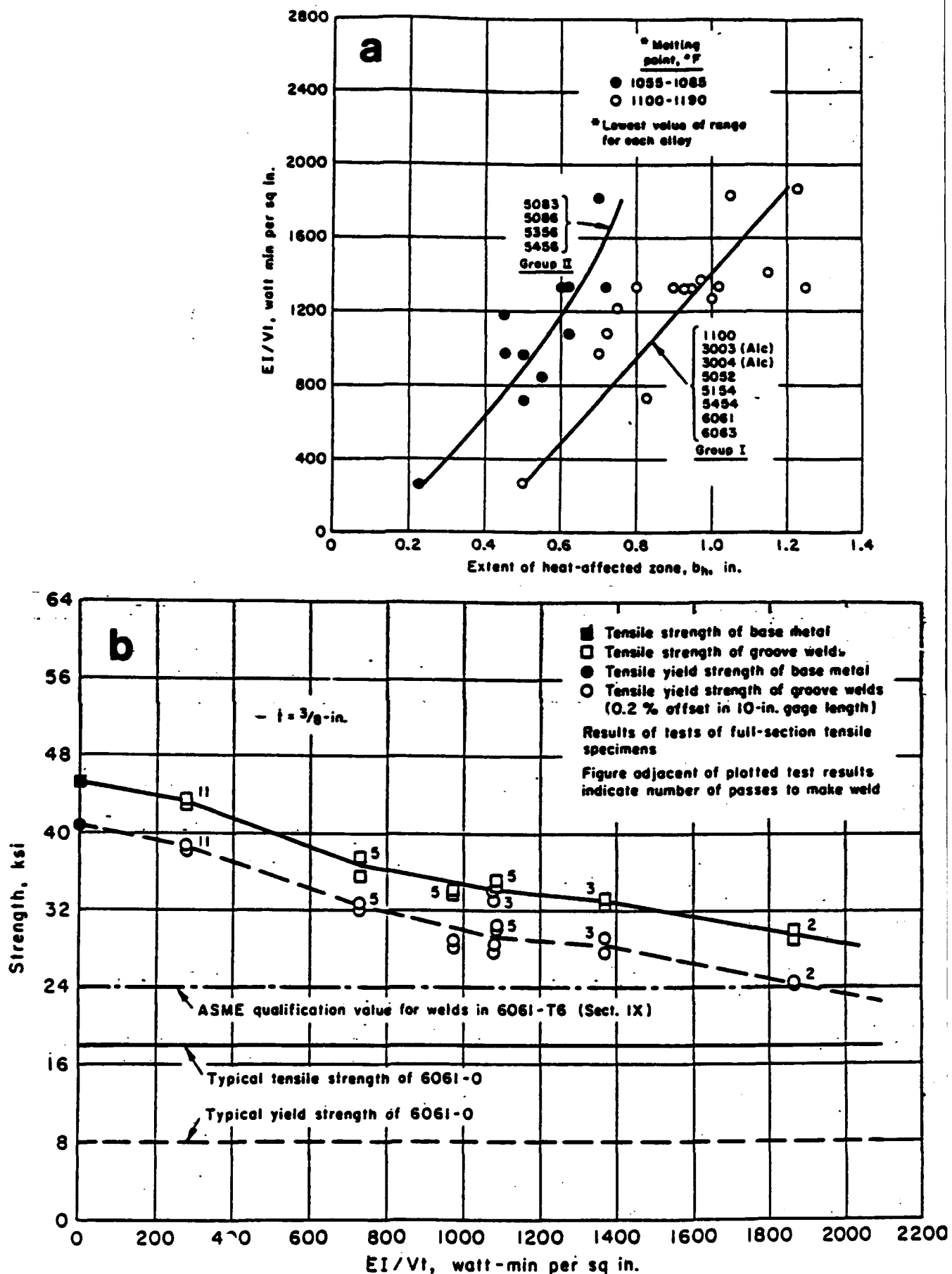


Fig. 3-13 Effect of heat input parameters EI/Vt on extent of HAZ in aluminum alloys (a) and on 6061-T6 joint strength (b) (Ref. 23).

increased by 1.5-2 times at almost unchanged tensile strength due to grain refinement, reduction of segregation of Mg and Si and more uniform distribution of precipitates.

3.6.3 Effect of the Plate Size

As was reported by Kelsey (Ref. 21), in welding of long thick panels, the width of the panel may affect the properties of the welded joint, including the width and hardness of the HAZ and tensile strength of the joint. Narrow plate provides less metal to act as a heat sink and generally may have a wider, softer and weaker HAZ than do wider plates. For example 4 pass continuous welding of a panel made of 7039 alloy 6 in. (127 mm) wide and 1-1/4 in. (32mm) thick, increased the temperature (to 400°F, 204°C)) and decreased hardness of the whole panel, while HAZ reached the edge of the panel.

3.7 POROSITY IN ALUMINUM ALLOYS

3.7.1 General Consideration

Hydrogen is the dominant cause of porosity in aluminum alloy welds. The sources of hydrogen most commonly encountered in commercial welding practice are hydrocarbons (grease, oils, etc.) and moisture contaminants on surfaces of the filler metal and plate. These contaminants are immediately converted to atomic hydrogen by the arc and are subsequently transferred into the molten weld pool. Both primary porosity (forming from the liquid) and secondary porosity (precipitating from the solid) may occur in welds. However, the more voluminous primary porosity is the major cause for rejection of aluminum welds by various non-destructive codes such as NAVSHIPS-0900-003-9000, ASME Boiler and Pressure Vessel Code, Sec. III Div. 1 Sub. NA and AWS D1.2-83 Structural Welding Code, Aluminum, Section 8-10.

Aluminum alloys are far more susceptible to porosity formation than all other structural metals because merely trace levels of hydrogen usually exceed the threshold concentration needed to nucleate bubbles in the molten weld pool. Alloying elements, such as Cu, Mg, and Si, significantly alter this threshold concentration. The size, shape, distribution and amount of hydrogen pores generated in the weld are dependent upon the solidification mode, cooling rate, degree of convective fluid flow, welding parameters, bead shape, shielding gas mixture and external pressure. "Getters" such as cobalt and freon are effective in reducing porosity.

Though a great deal has been reported on the causes and effects of porosity, little is known about the mechanism of pore formation relative to solidification mechanics, nucleation, growth and transport of gas bubbles in the weld pool.

3.7.2 Role of Solidification in Porosity Formation

The solubility of hydrogen in solid aluminum is very low, about 0.036 cc/100 g or 8.1×10^{-6} atomic percent just below the melting point. At 660°C (1220°F), the solubility of hydrogen in molten aluminum increases 60 times to about 0.7 cc/100 g or 1.55×10^{-6} atomic percent. The solubility further increases with increasing temperatures.

As the molten weld metal solidifies, excess hydrogen, above the solubility limit, is rejected as tiny pores of hydrogen gas scattered through the aluminum.

The role of solidification in the formation of hydrogen porosity in aluminum welds has only recently received considerable attention, particularly in the Soviet Union. It is generally agreed that during solidification of aluminum alloy welds, hydrogen in the melt will be rejected at the solid-liquid interface (on the liquid side) in the same manner in which solute is rejected from the solid in alloys having an equilibrium partition ratio, K , less than unity or

$$K = C_s/C_L < 1$$

where C_s and C_L are alloy concentrations in solid and liquid phases, respectively.

Nikiforov et al. (Ref. 24) determined $K = 0.052$. Many investigators agree that K is approximately 0.05. This means that hydrogen has 20 times higher solubility in the liquid phase than in the solid phase. For comparison, sulphur, the most mobile alloy in steels, has $K = 0.05$.

According to Grigorenko (Ref. 25), if the hydrogen content of the weld pool liquid is less than the maximum solubility of hydrogen in solid aluminum at the freezing temperature, no bubbles will form and the weld will solidify without porosity.

According to Ref. 26, primary porosity in solidified weld metal is observed in two morphologies: (a) interdendritic at low to moderate levels of supersaturation of liquid, and (b) large spherical pores for highly supersaturated liquids (Fig. 3-14).

The interdendritic pores are growth-substructure controlled whereas spherical pores are surface tension controlled. Since interdendritic porosity is dependent upon the solidification mechanics of a given aluminum alloy, variations in cellular dendrite shape, size and growth rate will determine the shape, size, and growth rate of the interdendritic pore.

At fast weld cooling rates, the presence of numerous tightly spaced cellular dendrites severely restricts the detachment and growth of large bubbles while slow cooling rates produce wide spacings between cellular-dendritic arms. The relative rate of cellular growth compared to bubble growth is an important factor in determining the shape of a pore. If the welding rate is fast and small intercellular bubbles cannot grow as fast as the advancing cells, isolated pores remain

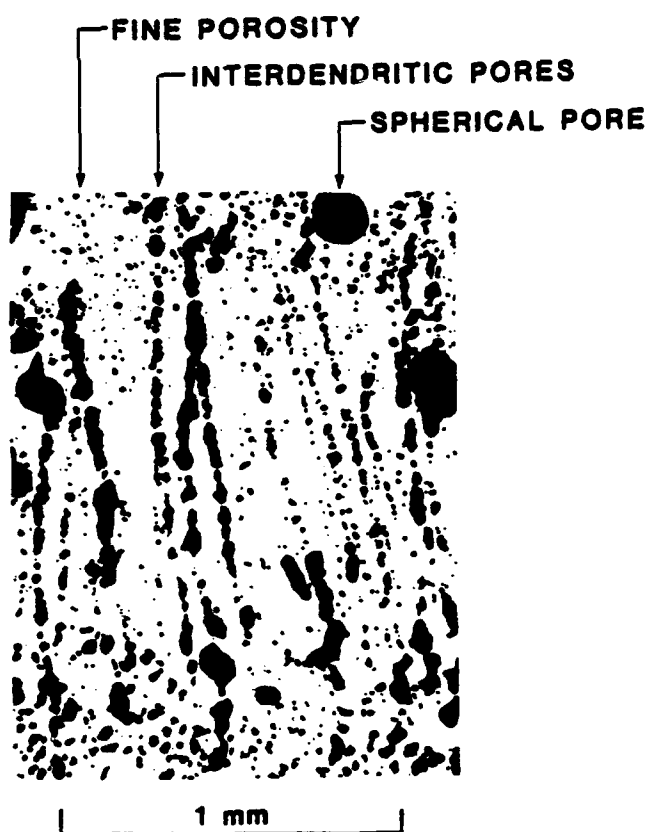
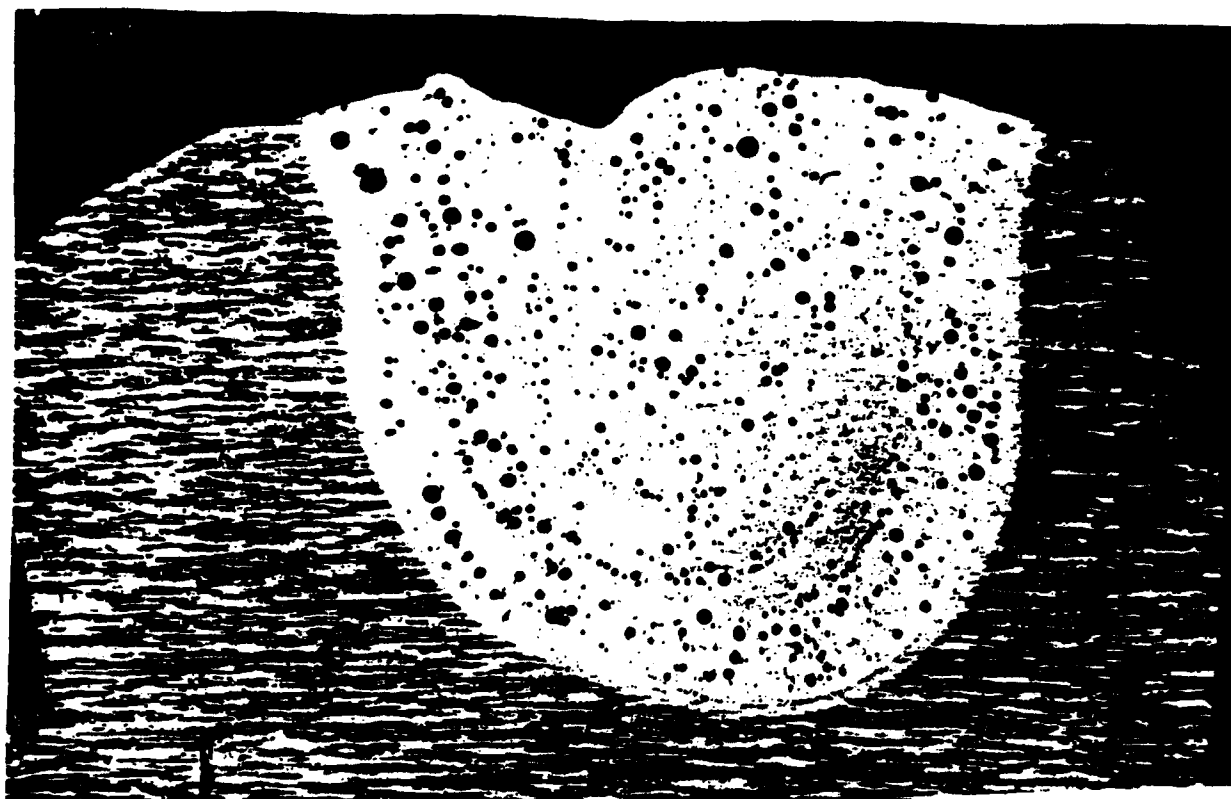


Fig. 3-14 Illustration of the morphologies of porosity observed in aluminum alloy welds (Ref

entrapped between adjacent cells. At very slow cooling rates, bubbles may grow at a rate greater than the advancing cells. These bubbles, grow to large diameters and may detach and float into the liquid ahead of the solidification front. However, at intermediate rates of cooling where bubble expansion approximately matches that of the growth of cells, the bubble may not be able to detach itself from the intercellular space but still grows in length in a direction parallel to the cell axis. This type of "wormhole" porosity is intercellular but can also form between cellular dendrites, as illustrated in Fig. 3-14, provided the length and growth rate of secondary arms are insufficient to block the lengthening growth of the bubble.

According to Matsuda, et al. (Ref. 13) turbulent convective fluid flow during solidification has been shown to produce a substantial reduction in porosity and grain size in 5083 and 5052 aluminum welds deposited by the GTAW process. This appears to be due to convection which is vital in accelerating the nucleation, growth and ultimate escape of bubbles from the molten weld pool.

3.7.3 Sources of Porosity

The most serious problem encountered in welding aluminum alloys is that of porosity due to hydrogen contamination from a variety of sources. Aluminum alloys are the most susceptible to porosity and small concentrations of hydrogen contamination in aluminum welds can cause severe porosity while similarly contaminated welds deposited on steel would be sound. For example, according to Boeing investigators (Ref. 27), a single fingerprint could cause three times the minimum level of hydrogen necessary to cause porosity.

Hydrogen can enter the welds from a variety of sources which include:

- a) hydrogen bearing contamination or hydrated oxide films on the surfaces of the filler and base metals.
- b) hydrogen or water vapor in the shielding gas, and
- c) hydrogen contained within the filler and base metals.

3.7.4 Surface Contamination

Many investigators believe that the surface condition of the base plate and welding wire is the most important factor contributing to porosity. Aluminum oxidizes rapidly and may contain water in the adsorbed or the chemically combined forms.

Sources of Surface Contamination. From a practical standpoint, all surfaces which are prepared for welding are "contaminated" to some degree. The extent of contamination will be dependent upon a number of factors which include but are not necessarily limited to the following:

- (a) initial as-received surface condition,
- (b) machining variables,
- (c) environmental conditions,
- (d) chemical treatments,
- (e) solvent treatments,
- (f) storage durations.

The effects of these factors may be generalized in terms of more directly measurable surface factors which include the following:

- (a) surface topography,
- (b) surface plastic deformation,
- (c) oxide thickness,
- (d) oxide crystalline structure,
- (e) adsorbed gases, vapors, or liquids (particularly hydrogen-bearing substances such as water organic solvents, lubricants, etc.),
- (f) miscellaneous residuals (i.e., F, Cl, Na, etc., in combined or free form resulting from various preparation treatments).

The problem that confronts the aluminum welding fabricator is that of establishing surface preparation specifications which, despite the contamination, will not degrade weld quality to some unacceptable level.

An ideally clean surface is virtually impossible to achieve for normal welding fabrication. It is possible to produce a perfectly clean metallic surface by cleaving or fracturing a metal within an ultra high vacuum (10^{-10} torr or better). However, surface adsorption of gases occurs on the freshly fractured surfaces almost immediately after fracture. At a pressure of 10^{-6} torr, a monolayer of gas will form within 1 second (Ref. 28). It is obvious that to weld only freshly cleaned surfaces in a shop environment is a virtual impossibility. However, it would appear necessary to approach this condition so as to minimize defect potential.

Basic Contaminants. All aluminum surfaces involved in the welding process are to some degree contaminated. According to Ref. 29, three classes of contaminants may be present:

- 1) Substances derived from the base metal, comprising generally oxides of the metal, but also including various compounds formed by corrosion or other surface reactions.
- 2) Substances not chemically associated with the base metal, such as water, oils, greases, solvents, drawing compounds, buffing and polishing compounds, and miscellaneous dirt

picked up in manufacturing, handling, or shipping. Such substances may be attached very loosely or in either a physical or chemically adsorbed state. The latter condition may be most difficult to remedy.

3) Substances due to an altered base-metal surface layer. The surface of the base metal itself may be physically unsound because it consists of a film of stressed, distorted, broken, or disordered base metal. Alternatively, such metal may be readily converted to oxides, hydroxides, or other oxidation products of the altered metal.

Mechanisms of Surface Contamination. The surface chemistry and physics of aluminum immediately after the preparation of the surface for welding may have significant effects on formation of the oxide film which forms at room temperature. The degree of moisture adsorption, or hydration, is also sensitive to variations in methods of surface preparation for welding.

Surface adsorption is probably the most detrimental surface condition, with respect to weld-defect potential. Adsorbed hydrogen-bearing contaminants would be expected to be the principal cause of porosity-type defects. The preparation of a "good" weld joint surface should be one that is relatively free of adsorbed hydrogen-bearing contaminants.

According to Ref. 28, two types of surface adsorption are distinguished: physical adsorption and activated adsorption (generally termed chemisorption).

Physical adsorption is characterized by the concentration of molecules on the surface of the metal at comparatively low temperatures. It is essentially a rapid and reversible process because very low activation energy is required for this phenomenon. The surface concentration of the adsorbate decreases with increasing temperature, and increases with increasing partial pressure. Considering the surface preparation of aluminum for welding, physical adsorption could conceivably have an important effect on subsequent weld quality. For example, if a thick fragmented oxide were produced as a result of joint preparation, considerable water adsorption may occur during exposure in the ambient atmosphere. Moisture from the atmosphere could be "sponged" up by the porous oxide.

Chemisorption is a potentially more damaging type of adsorption. In chemisorption the adsorbed molecule or molecular fragment is held to the surface or surface oxide by strong bonds characteristic of covalent, ionic, or metallic bonding. As a result specific chemical changes take place between the surface adsorbent and the specific adsorbate. The rate of adsorption may be slow, but once adsorption has taken place, it is not easily reversed, and the application of comparatively high temperatures may be needed before desorption can occur.

Water absorbtion is the most damaging. The simple desorption of physically adsorbed water can be rapidly achieved at approximately 212°F (100°C) at ambient pressures, whereas much higher (up to 760°F, 404°C) temperatures are required to desorb chemically adsorbed water.

Absorbtion of constituents other than water (such as solvents, lubricants, etc.) may also take place on aluminum/aluminum oxide surfaces, and they may be equally or more important than water. Irreversible adsorption can occur with a large number of simple organic molecules (including benzene, ethyl alcohol, and carbon tetrachloride) on various oxide surfaces (CuO, NiO, ZnO, and MgO). It is usually assumed that a final solvent cleaning or degreasing of a surface is satisfactory, provided that a sufficiently pure or volatile solvent is used. According to Ref. 28, this supposition is incorrect. Where complete freedom from adsorbed organic material is desired, it is better to avoid using any organic solvent in the last stage of cleaning the solid surface. The implications of this conclusion as related to the surface preparation for welding are quite obvious.

Gaseous constituents of air (oxygen, nitrogen, carbon dioxide, etc.) can be absorbed as well. Oxygen, of course, is abundant in the oxide form. The other gases may be adsorbed to the detriment of weld quality. However, the adsorption of nitrogen, carbon dioxide, etc., is of negligible importance compared to the adsorption of hydrogen-bearing constituents.

Surface topography conditions of the aluminum/aluminum oxide surface may have important effects on weld-defect formation (Ref. 30). Although a majority of surfaces appear to have random topographies and consist of many irregular, jagged protrusions, there are definite patterns which can generally be classified according to their respective wave lengths. Fig. 3-15 shows constituents of the topography of a machined surface, which, when combined together, characterize the surface profile. In many cases, these characteristics are broadly classified.

Roughness takes into account the finer irregularities caused by the cutting tool and the machine tool feed.

Waviness is the wider spaced irregularity resulting from machine or work deflections, vibrations or heat treatments.

Flaws is a class of random irregularities which occur at one place or at relatively infrequent intervals in a surface. Scratches, tears, ridges, holes, peaks, cracks, or checks are examples of flaws.

In general, the character of a surface depends upon the degree to which a machine is properly set up and used, the particular machine cutting apparatus, the direction of the cut, the feed and tool shape, the structure of the material, etc.

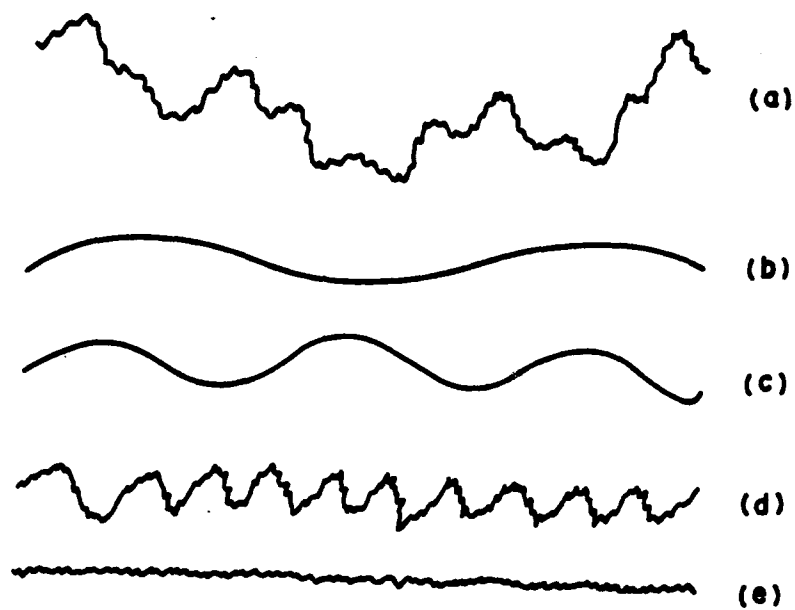


Fig. 3-15 Constituents of the topography of a machined surface; (a) general topography which includes the irregularities caused by (b) flexure or slideways, (c) vibration or bad truing, (d) the cutting tool, and (e) chip removal (Ref. 30).

At least two possible effects of surface roughness are immediately evident. The actual area, rather than the apparent area, of a surface increases in direct proportion to its roughness. The potential amount of surface oxide and/or adsorbed contaminants would, therefore, be expected to be directly proportional to surface roughness. Consequently, surface roughness could potentially affect weld soundness by providing more or less actual surface area for adsorption of damaging contaminants.

The second possible effect of surface topography is that related to the mechanical entrapment of harmful contaminants. Folds, tears, scratches, crevices, and other such irregularities may promote the mechanical entrapment of cutting tool debris, lint, lubricants, solvents, water, and even humid air on the surface of a weld joint preparation. This type of entrapment could cause subsequent weld defects. One very important attribute of this type of mechanical entrapment is its statistically random nature.

3.7.5 Shielding-gas Contamination

Moisture in the shielding gas is a major cause of porosity. Saperstien (Ref. 31) showed that welds deposited using shielding gas with dew points below -40°F (-40°C) were virtually free from porosity, while porosity concentration increased exponentially with increasing dew-point temperature above -40°F (-40°C).

In a NASA-sponsored study (Ref. 27), effect of shielding-gas contamination on porosity was found to be much more significant than effects of the other factors investigated.

The effects of individual gas contaminants were studied by Boeing investigators (Ref. 27) by making welds in an atmospheric-control chamber containing various levels of gas contamination.

The following results were obtained:

- 1) Increasing hydrogen concentration increased porosity.
- 2) Increasing water vapor increased porosity.
- 3) Increasing oxygen did not increase porosity; in some cases, a slight decrease in porosity was observed.
- 4) Increasing nitrogen had little effect on porosity.

The Boeing investigators presented Fig. 3-16 as a guide for controlling shielding-gas contamination. The contamination levels shown indicate where occurrence of a weld-quality change is initially observed. The figure indicates that 250 ppm of either hydrogen or water vapor was necessary before significant quality changes were observed. As shown in Fig. 3-16, shielding-gas contamination caused various effects, including surface discoloration, undercut, and reduction in

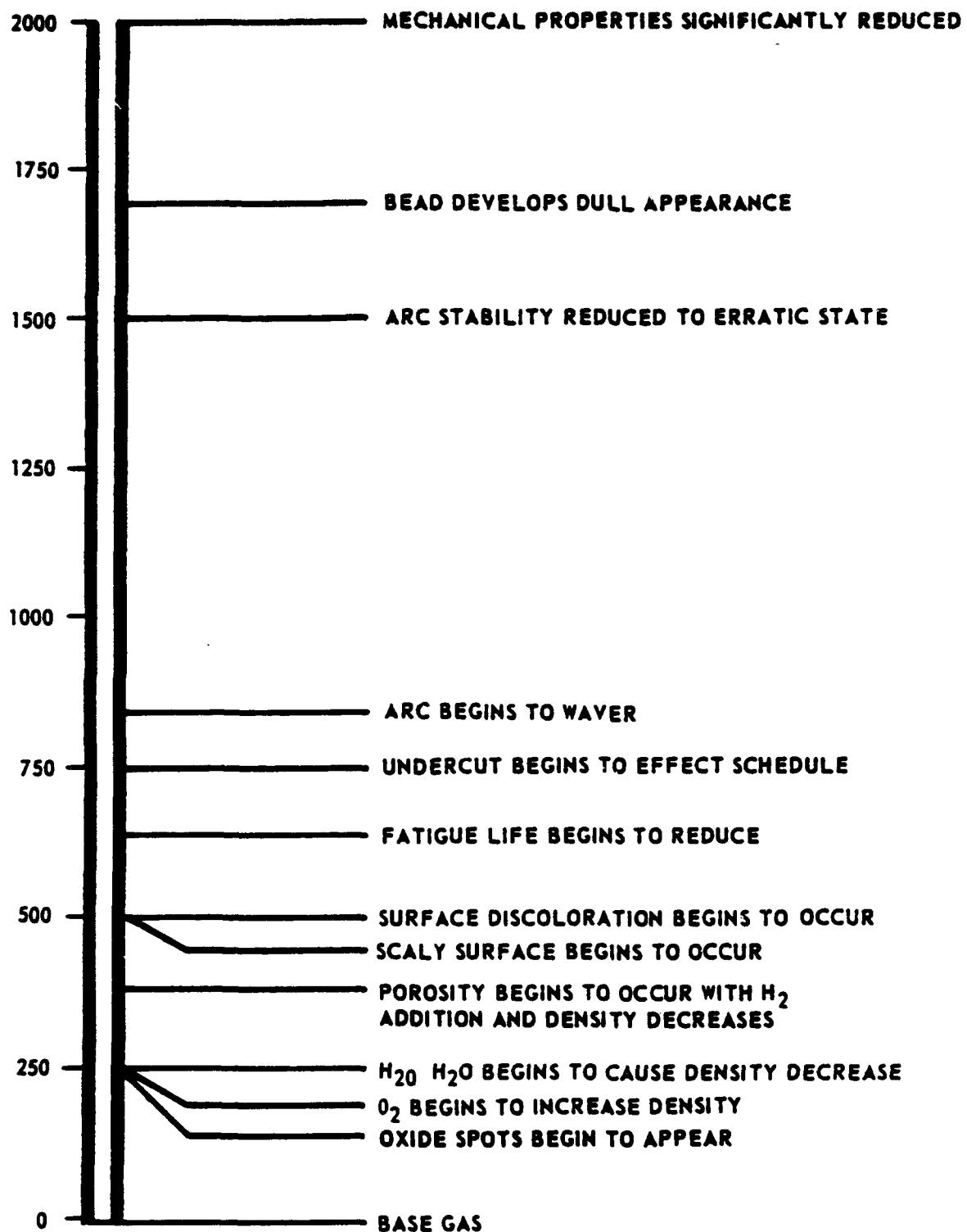


Fig. 3-16 Contamination concentration levels at which significant changes occur in weld quality (Ref. 28).

arc stability.

Fig. 3-17 gives the calculated relationship, as determined by the Boeing investigators, between percent of water-saturated air in the base gas and resulting hydrogen concentration. The figure indicates that at 70°F (21°C), for example, an addition of 0.6 percent saturated air to pure helium would result in 250 ppm hydrogen in the shielding gas.

On the basis of experience gained in the Boeing program, it was concluded that commercial gases which meet NASA specification (MSFC-364A) are believed to have sufficient purity.

However, gas contamination can occur within the bottle, or sometimes between the bottle and the torch nozzle. Contamination could occur in a partially empty bottle, for instance. Or, it could occur due to defective connections in the tubing system.

Another source of gas contamination is hydrogen available by decomposition of hydrocarbon on the weld groove.

According to the Boeing investigators calculation, it requires less than 1 mg of hydrocarbon per inch of weld to continuously generate 250 ppm hydrogen in the shielding gas. It is estimated that a single fingerprint would result in a 750-ppm hydrogen increase in the area contaminated. This may cause a significant increase in porosity.

3.7.6 Effect of Composition On Porosity

In terms of relative importance, the influence of aluminum alloy composition is second to that of partial pressure of hydrogen in the arc atmosphere. However, it is evident that welding certain aluminum alloys tend to result in higher concentration of porosity than the other.

More recent studies have conclusively shown that the dominant influence of alloy additions is due to the influence of alloy content on the solubility of hydrogen in aluminum. For example, additions of 3% copper markedly reduce hydrogen solubility, whereas a 6% magnesium content nearly doubles the hydrogen solubility in aluminum (Ref. 26). The alloy additions may also alter the solidification range and modify the solidification mode which may further contribute either positively or negatively to the formation of porosity.

While the rate of hydrogen absorption may be influenced by the alloy concentration, the dominant factor affecting porosity in welds is in the influence of alloy content on solid solubility. For the aluminum/magnesium alloys, the addition of 1% and 6-1/2% magnesium substantially reduced weld metal hydrogen content compared to commercially pure 1100 aluminum according to Ref. (26).

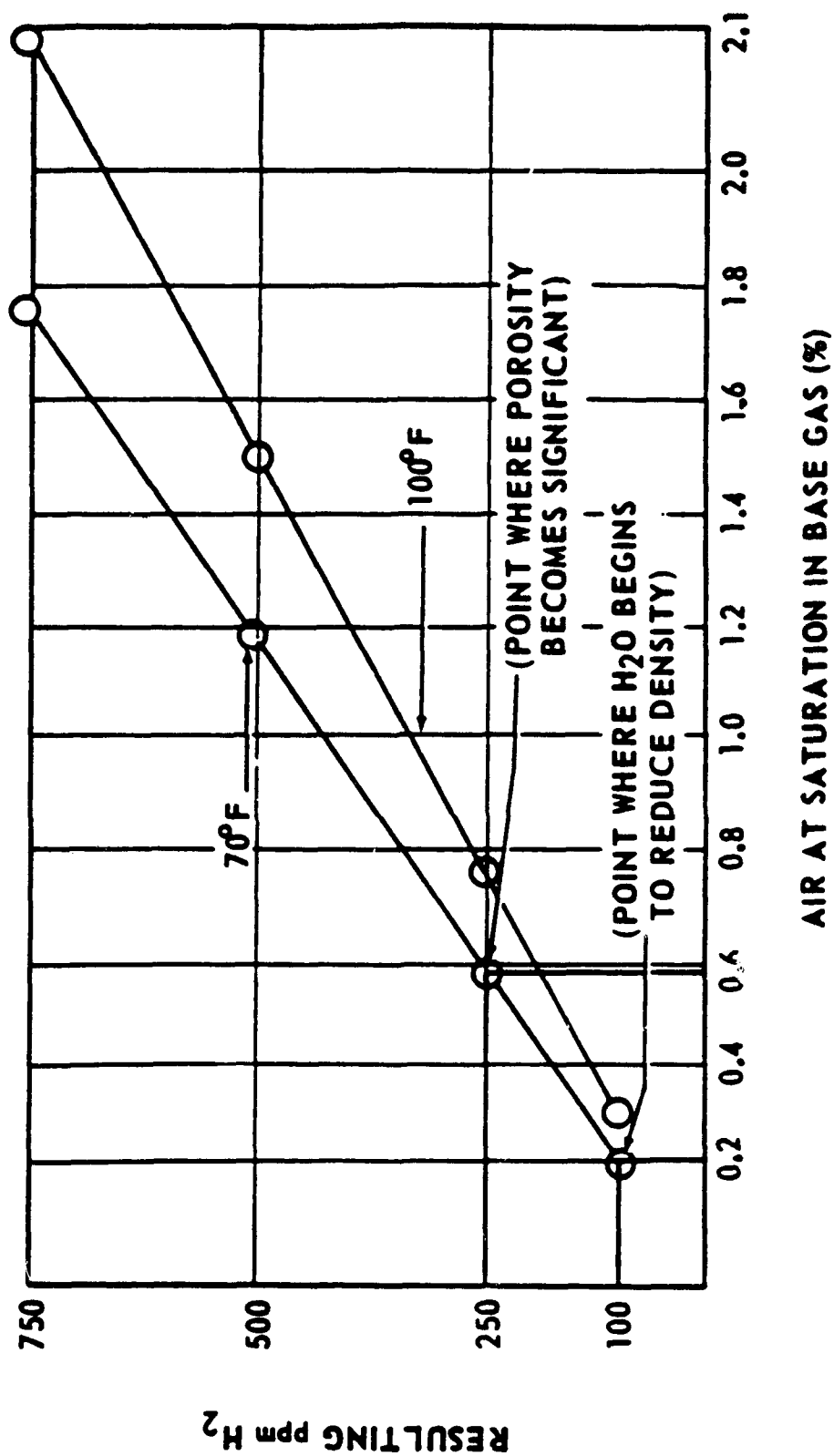


Fig. 3-17 Volume of water available to weldment from saturated air contamination (Ref. 28).

The influence of zinc is somewhat more complex than that of magnesium (Fig. 3-18). Relative to 1100 aluminum, a slight addition of zinc, i.e., 1%, actually increases the absorption rate of hydrogen whereas the 6-1/2% zinc level produced significantly-reduced porosity, primarily due to a much lower rate of hydrogen absorption. In the case of the commercial alloy 7039, which contains 3.8% zinc and 2.5% magnesium, a high rate of absorption is offset by a high solid solution capacity. Therefore porosity thresholds required relatively high arc contents of hydrogen, but once a threshold was achieved, the rate of porosity increase was very rapid.

While magnesium dramatically increases the solubility of hydrogen in aluminum, copper and silicon additions both decrease the hydrogen solubility. The results of copper and silicon additions are shown in Fig. 3-19. The influence of copper is significantly greater than that of silicon with respect to the influence on hydrogen solubility.

This information may serve as a guideline to define the relative tendency for porosity formation and, hence, the relative amount of precautions and care that must be taken to prevent porosity or at least limit the porosity level in welding alloys of 6000 and 7000 series.

In this respect, modification of the aluminum alloy with some elements may play important role in reducing porosity. This could be the elements that increase the amount of nuclei in the molten weld pool, like cobalt, which reduce the size distribution of porosity (Ref. 32).

"Getters", which are certain reactive elements, may scavenge hydrogen preferentially in aluminum alloy welds. Although in principle this technique is feasible in aluminum alloys, no successful commercial use of "getters" of hydrogen has been reported except chlorine and freon gases introduced into the shielding gas (Ref. 26). Chlorine has been used as a getter in the aluminum foundry industry, but has not been commercially utilized in welds, though substantial porosity reductions are reported. Similarly, freon, which is less toxic than chlorine, has also been shown to improve the soundness of aluminum weldments.

3.7.7 Effect of Welding Variables on Porosity

Weld bead shape is perhaps one of the most significant variables controlling the amount of porosity resulting in aluminum welds. Welds that are narrow and have a high crown tend to trap porosity since individual pores must rise a long distance before escaping to the surface (Ref. 34). Fig. 3-20 illustrates the manner in which a 25%-35% downhill GMA weld pool traps hydrogen bubbles due to a long escape path. As a result, nondestructive inspection indicates that fewer surface and internal pores are produced welding uphill than welding downhill.

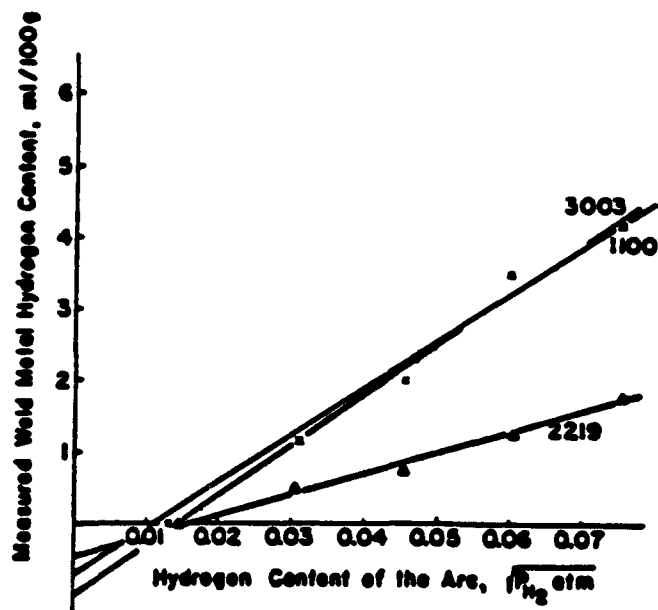


Fig. 3-18 Measured hydrogen contents of 3003 and 2219 alloy welds deposited by GTAW with contaminated shielding gas (Ref. 26).

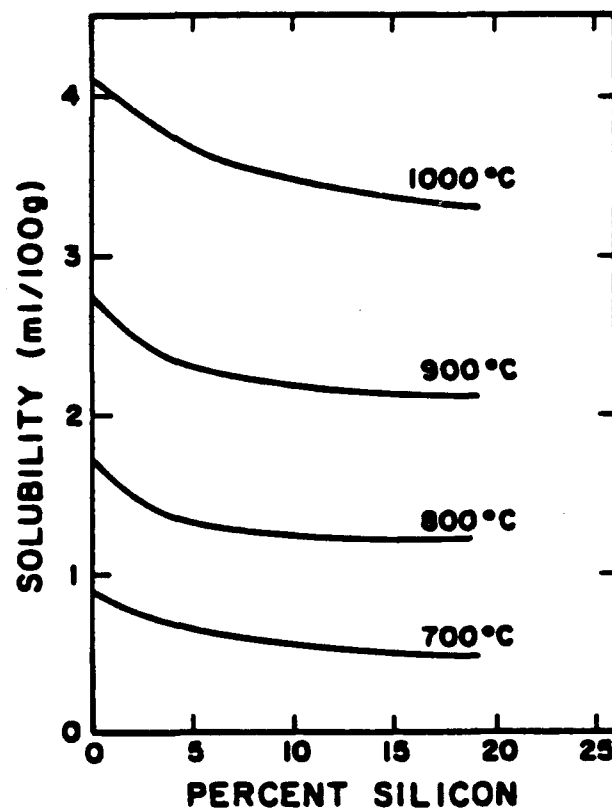
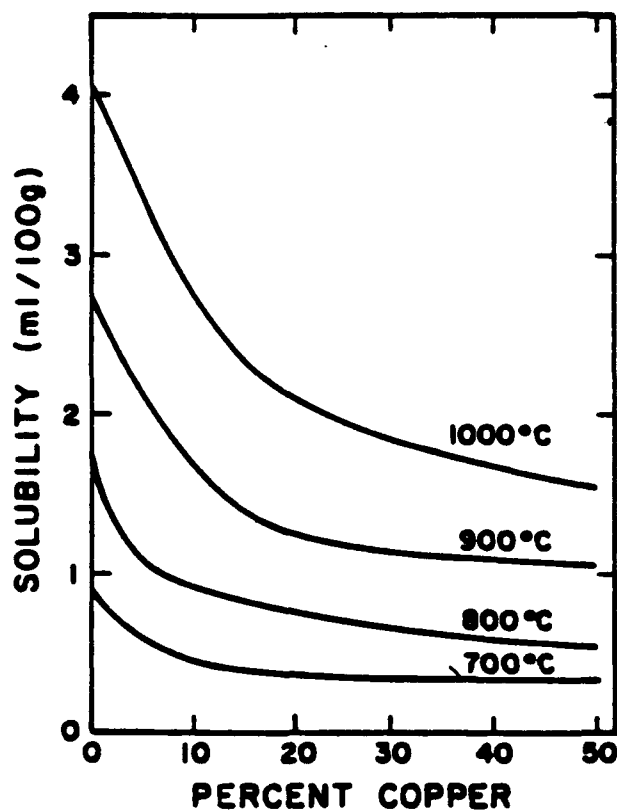


Fig. 3-19 Effect of (a) copper, and (b) silicon additions on the solubility of hydrogen in liquid aluminum at 760-mm pressure (Ref. 26).

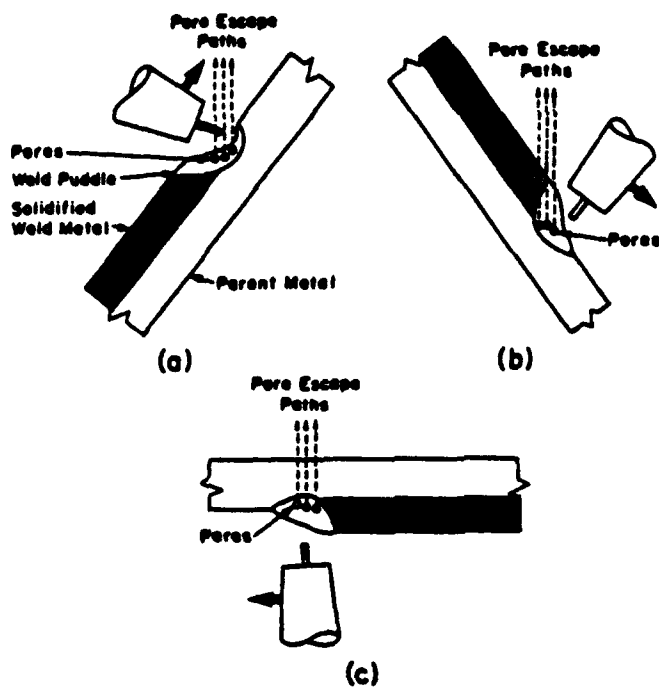


Fig. 3-20 Effect of welding position and weld pool shape on porosity in (a) uphill, (b) downhill, and (c) overhead welds (Ref. 34).

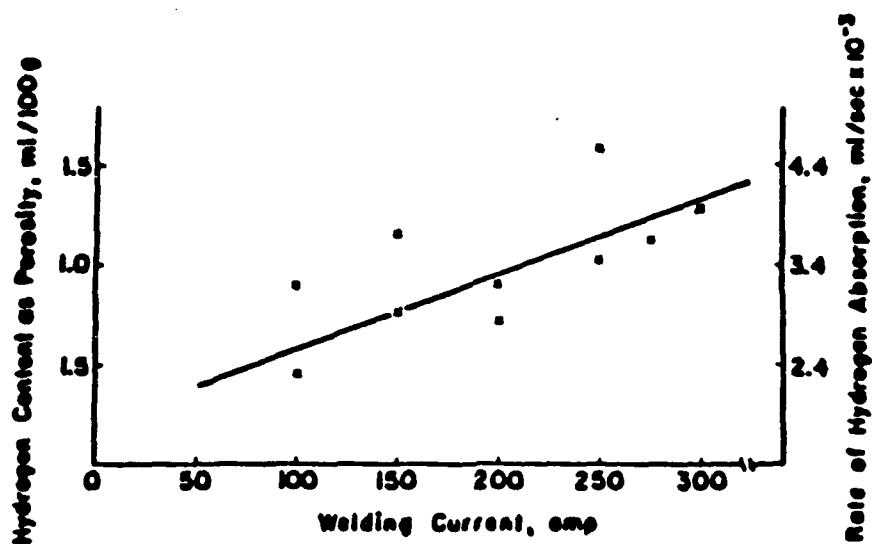


Fig. 3-21 Effect of GTAW current on weld porosity and the rate of hydrogen absorption in 1100 aluminum (Ref.33).

Welding process affects porosity as well. In comparing the GTAW and GMAW processes, welds deposited by GMAW are more susceptible to porosity for two primary reasons. First, the large surface area associated with small diameter wires required for GMAW provide ample opportunity for surface contamination by moisture, lubricants and other hydrocarbons. Second, the higher droplet temperature in GMAW increases the amount of hydrogen absorption during metal transfer across the arc.

Welding parameters effect the degree of porosity in an aluminum alloys.

Welding current increase raises porosity level in aluminum alloy weld because both the volume of molten metal and rate of hydrogen adsorption from the external source increase. Woods (Ref. 33) proposes that increasing current raises the average surface temperature of the molten weld pool and also enlarges the hot annular zone through which hydrogen absorption is believed to be funneled into the weld. As a result, hydrogen porosity increases with increasing current in GTAW as shown in Fig. 3-21.

Fast cooling rates produce only a minimal volume of many fine pores, while very slowly cooled welds contain very few but large pores. It is at the moderate levels of weld cooling rate of heat input that produce the maximum total volume of porosity that have a medium average pore size.

Travel speed affects porosity in a more complex way. High welding speeds and low heat inputs correspond to fast weld cooling rates which suppress porosity formation. Similarly, slow welding speeds and high heat inputs reduce weld metal porosity by providing sufficiently slow cooling rates for bubbles to escape from the weld. Even when the value of heat input is either maintained constant or increasing with increasing travel speed, the volume of weld metal porosity always decreases at high welding speeds. In other words, fast welding speeds suppress the formation and growth of pores in aluminum welds.

The shielding gas mixture for GTAW and GMAW process was found to affect the degree of porosity. A 65% helium-35% argon mixture produces sound welds over a greater current and voltage range than both pure argon and pure helium.

Section 4

EXPERIMENTAL WELDING PROGRAM

4.1 EXPERIMENTAL PROCEDURES

4.1.1 Objectives and Scope of the Experimental Program

The main objectives of the experimental welding program were to determine and to verify optimal welding procedures to be recommended for welding of the extruded AE aluminum mat panels and to test new equipment and technology developed under this contract.

The scope of the experimental program was the following:

- Development of Requirements for Welding, Inspection and Testing Procedures. The basic requirements for welding procedure, visual and radiographic (x-ray) inspections, mechanical testing and metallurgical examination of weld and welded joints were developed and specified for the experimental program.
- Assessment of Edge Cleaning Methods. The task was performed to determine a practical method of cleaning of the base metal prior to welding.
- Assessment of Effect of Natural Aging. This task was performed to determine and minimize the effect of weld storage period prior to testing on the results of the testing program.
- Determination of Usable Ranges of Parameters. A number of trial welds were performed to establish usable ranges of two main parameters, wire feed rate and travel speed. The usable range was supposed to provide welds usable for testing.
- Development of Matrix of Experiments. A matrix was developed which specified a set of welding parameters for each experimental weld selected within the usable range of parameters determined earlier.
- Experimental Welding and Testing. A number of 5-ft long subpanels were welded according to the matrix described earlier to study the effect of welding conditions on properties of the welded joints. The welds were subjected to inspection and testing according to the procedures described earlier.
- Analysis of Experimental Data. The data obtained as a result of inspection and testing were analyzed and optimal welding parameters were selected. The criteria was based on quality (weld geometry, integrity and properties) and production considerations (ease of implementation and productivity).

1

- **Verification Welding.** Using the optimal and non-optimal welding parameters requested by the Army, twelve 5-ft. long panels were welded and shipped to the Belvoir RD & EC for verification tests. Each panel consisted of three 5-ft long subpanels welded together.

- **Determination of Transient Welding Parameters.** Experimental welding was conducted to determine optimal transient (start and termination) welding conditions for the selected optimal welding parameters.

- **Preproduction Welding.** Using optimal welding parameters, ten full-length (13-ft long) AE panels were welded and shipped to the Belvoir RD & EC for fatigue performance test under actual military traffic conditions.

4.1.2 Requirements for Inspection and Testing of Welded Joints.

Main requirements for inspection and testing of the welded joints obtained in the experimental program were specified in "GARD's Specification for Inspection and Testing of Welded Mat Panels" (see Appendix B1). This was developed to meet the requirements in the Army's Statement of Work. The specification was submitted to and approved by the Belvoir RD & EC. According to the requirements of this specification all welded experimental panels were cut into test pieces. Each test piece (Fig. 4-1) represented an individual set of welding conditions and was subjected to visual and radiographic (x-ray) inspections, and testing procedures as described below.

Visual Inspection. Each test piece was subjected to visual inspection to detect flaws such as cracks, blow holes, undercuts, lack of fill, etc. The results of the inspection will be discussed later.

Radiographic Inspection. A 17-in. long portion of the weld was radiographed to include one inch from both sides of the centerline of the weld upon completion of the visual examination. Radiographic inspection was performed in accordance with the AWS D1.2, Structural Welding Code, Aluminum, and the ASTM Standards, E94 and E142, latest editions. The results of the inspection are reported in Appendix B2 and will be discussed later. The radiographs were evaluated against applicable referenced radiographs in the ASTM E390 Standard. The referenced radiographs were graded according to the severity levels, 1 through 5, in order of increasing severity as indicated in Table 4-1 below. The remainder of the discontinuities listed in Table 2 of ASTM E390 were ungraded and treated as unacceptable. The acceptable radiographs of the test piece were interpreted as showing equal or less severity in a nine inch long test weld than those indicated in Table 4-1.

TABLE 4-1. Types of Discontinuities Acceptable for Welds on Mat Panel

Discontinuity Type	Severity Level Grading
Scattered Porosity	3
Fine Scattered Porosity	3
Coarse Scattered Porosity	2
Clustered Porosity	2
Linear Porosity	2
Slag Inclusions	2

Mechanical Testing. Mechanical tests of the welded joints were conducted according to the AWS D1.2-83 Structural Welding Code, Aluminum and the ASME Boiler and Pressure Vessel Code, Section IX. The test specimens were machined to remove the stiffeners, tread bars, weld reinforcement and lock design details of the joint. Mechanical testing included tensile and bend tests.

Tensile tests were performed on two transverse reduced-section specimens cut from a test piece transverse to the weld. Minimal tensile strength of 24 ksi (165 MPa) was taken as an acceptance criterion in accordance with the AWS D1.2 and the ASME Codes. Tensile strength and failure location were documented in Appendix B3.

Bend tests were performed on four transverse specimens. Two root-bend and two face-bend specimens were tested. The results were reported in Appendix B3.

Metallographic Examination. Metallographic examination was conducted on two specimens.

Macroexamination was conducted on a transverse specimen with weld reinforcement intact. The cross-section of the specimen was prepared for macroexamination and photographed. The enlarged photographs were used for determination of rate of dilution and weld geometry, including depth of penetration, width and height of reinforcement.

Microexamination was conducted on a transverse specimen which was prepared for microstructure and microhardness evaluations.

Microhardness tests (Knoop, 100g) were performed to determine hardness distribution measured across the HAZ. The Knoop imprints were made with increments of 0.125 in. (3.2 mm) in the area away from the fusion line (FL). The increments were reduced to 0.062 in. (1.6 mm) and then to 0.031 in. (0.8 mm) with the FL approaching. A relatively small (100g) load was selected in

order to increase resolution of the hardness test. This was instrumental in the areas immediately adjacent to the FL where imprints were taken with an increment of 0.005 in. (0.127mm).

4.1.3 Welding Procedure

The extruded subpanels were made from commercial 6061 aluminum-silicon-magnesium alloy. The alloy's actual composition and properties determined by the corresponding chemical analyses and tensile tests at GARD are given in Table 4-2.

TABLE 4-2. Composition and Properties of Base and Filler Metals

Metal	Element (wt - %)									Strength (avg.)		Elongation
										Tensile	Yield	in 2 in. max.
	Si	Mg	Cu	Fe	Mn	Zn	Cr	Ti	Al	ksi	MPa	%
Base 6061	0.68	0.85	0.22	0.32	0.07	0.05	0.06	0.02	Bal	<u>44.35</u> 305.8	<u>41.9</u> 288.9	9
Filler 4043	4.80	0.05	0.17	0.24	0.05	0.05	0.05	0.05	Bal	-	-	-

Heat treatment of the panels were delivered heat treated to T6- temper. This includes solution heat treatment at 990°F (532°C), quenching and artificial aging at 350°F (177°C) for 8 hours.

The fixture (described in Section 5) was used to assemble and clamp three 60 in. (1,524 mm) long mating subpanels into a panel assembly prior to welding as shown in Fig 5-3.

Pulsed "synergic" GMAW (gas metal arc welding) process operating on direct current reverse polarity was used for joining.

The welding system used is described in Section 5. It features computerized closed-loop feedback control over welding and motion parameters.

Mean values for current, voltage and travel speed were determined through a computerized statistical analysis of the parameters values sampled by the sensors of the system 100 times per second. The data were recorded in tabulated and graphic formats (See Appendix C2. Section 5).

The welding wire used was 0.045 in. (1.2 mm) in diameter. It has AWS designation of ER4043. Chemical composition of the wire is shown in Table 4-2. When it was not in use, the wire was stored in a hermetically sealed container filled with argon under pressure up to 6 ksi.

The shielding gas was argon of welding grade quality. Gas flow rate was 32-45 cf/hr (0.25-0.35 l/s).

The welded joints formed between the subpanels were V-groove butt joints with 60° included angle and groove depths slightly above 3/16 in. (4.8 mm).

The copper chiller bars (shown in Fig 5-3, item 12) ran along both sides of each welded joint in close proximity to the groove edges.

A layout of the test welds on the experimental panel assembly is shown in Fig. 4-2. As was mentioned earlier, the experimental panel assembly consisted of three 60-in. (1,524 mm) long AE subpanels. Both face and back sides of the panel assembly were welded. Each side contained two welded joints. Each joint was divided into three 20-in. (508 mm) long sections to represent three individual sets of welding conditions. The three right-hand (looking from the start) test welds performed with torch #2 on the face side of the panel were considered the **main test welds** intended for the following testing. In Fig. 4-2, which schematically describes layout of Series A, the main welds are identified as 3, 4, and 5. Their counterpart left-hand welds performed simultaneously with torch #1 (also on the face side of the panel) using the same welding conditions were the **duplicate test welds**. They are numbered as 1, 2, and 3. The duplicate weld was supposed to replace the corresponding main weld if the latter was not acceptable. The same layout was arranged on the back side of the assembly. There the main and duplicate welds were identified as 10, 11, 12 and 7, 8, 9, respectively (Fig. 4-2b). Thus a panel assembly provided up to six main and six duplicate test welds representing up to six different sets of welding conditions.

HAZ chilling was utilized for all the welds, with the exception of three control test welds. These were performed without chilling for comparison with their chilled counterpart welds performed using the same welding conditions. The distance between the chiller bar and the weld edge (Dch) appeared to influence metallurgical processes in the HAZ of the welded joint. However, the fixture utilized for welding experiments had fixed locations of the chiller bars relative to the center of the corresponding joint. Therefore Dch values were not equal for all the welds performed on various welding conditions. In fact, Dch varied from 0 to 0.24 in. (6.1mm) because of the weld width variations. Fortunately, this influenced Dch in one direction: the wider the weld, the closer was the weld edge to the chiller. This means that the wider welds performed on higher

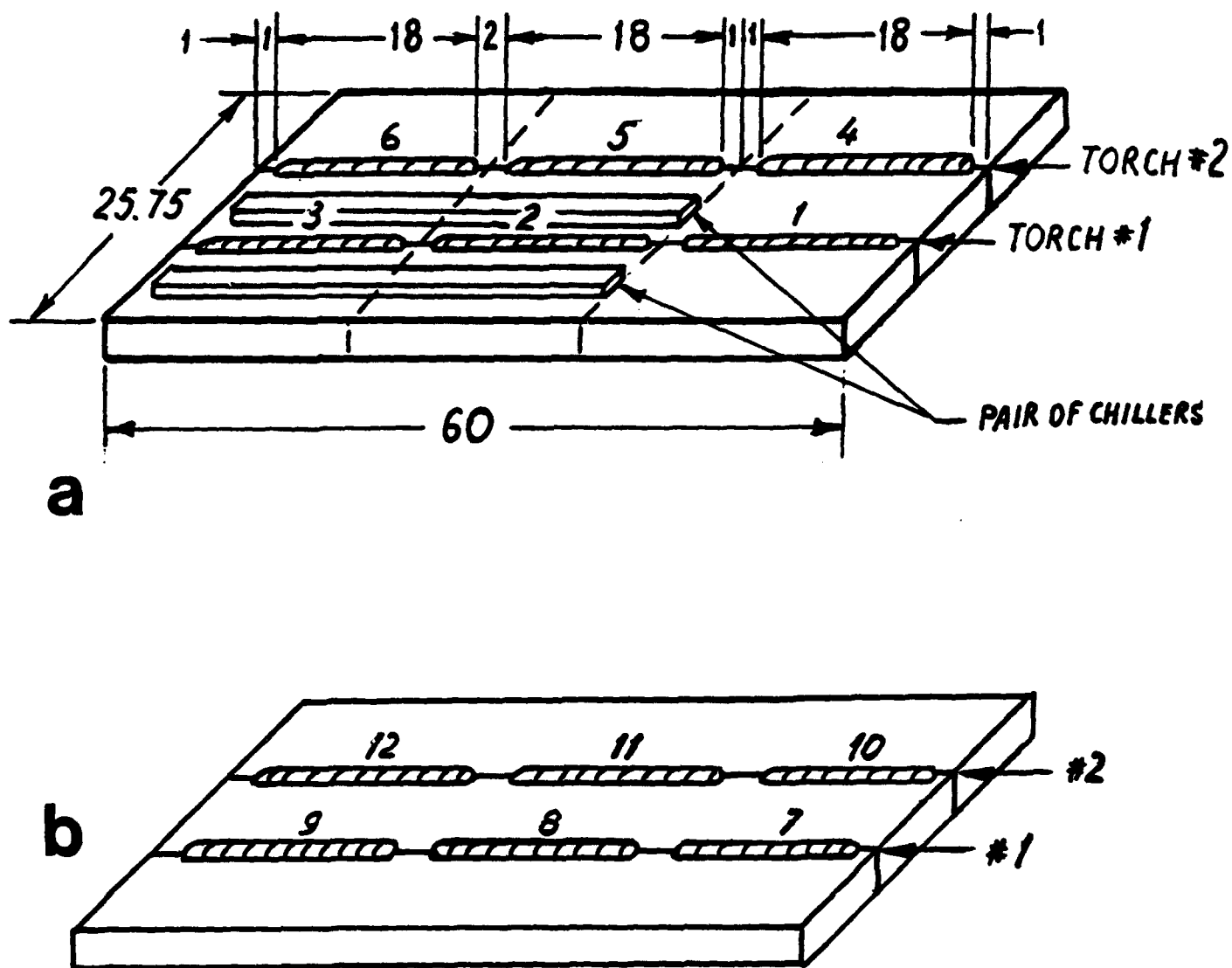


Fig. 4-2. Layout of test pieces on a welded panel assembly.

linear energy (Q) compared to those performed on lower Q, were chilled relatively better and demonstrated slightly better properties that they could have shown if Dch had been equal for both welds. Nevertheless, this did not effect the trends of relationships between welding conditions and properties of the welded joints revealed by the experiments.

Dilution rate was determined from a transverse specimen with weld reinforcement intact. The cross-section of the welded joint was photographed and the rate of dilution and weld geometry were determined from the photographs on which the weld area was enlarged by a factor of 10. The factor varied within 0.5%. Dilution rate (DR) was calculated using the following formula:

$$DR = F_p / (F_g + F_r + F_p) \times 100\%$$

where F_p , F_g and F_r - cross-section areas (Fig 4.3) of arc penetration, groove and weld reinforcement, respectively, measured from the enlarged photographs (Fig. 4-4) with the aid of a polar planimeter. The accuracy of the measurement was within 3%.

Peak temperature distribution across the HAZ was measured with the aids of temperature indicating liquids. Prior to welding, narrow strips of the liquids rated from 200° F(93.3°C) to 900° F(482.2°C) were applied by brush to the surface of the panels perpendicular to the joint to be welded and dried as shown in Fig. 4-5. After welding, the distance was measured from the edge of the weld to the end of the melted portion of the strip where the rated temperature has been reached. Unfortunately, the temperatures above 700°F (371.1°C) could not be reliably determined and therefore were extrapolated up to the solidus temperature. The solidus was determined from Ref. 35 for known 4043-type weld metal composition and the calculated rate of dilution.

4.2 PRELIMINARY INVESTIGATION

A preliminary investigation was conducted to support the main experimental program. The objectives of this investigation were the following:

- To select a realistic method of edge cleaning to reduce porosity in the welds,
- To assess effect of variations in weld storage period prior to testing on possible variations in HAZ strength, and
- To determine usable ranges of welding parameters to limit the scope of experimentation.

4.2.1 Effect of Edge Cleaning Methods on Weld Porosity (Series K)

Information on this issue was obtained from the experiments of **Series K**. The objective was to assess effect of various methods of edge cleaning on level of porosity in the welds. In fact, as was discussed in Section 3, porosity represents a very wide subject by itself for a single study to

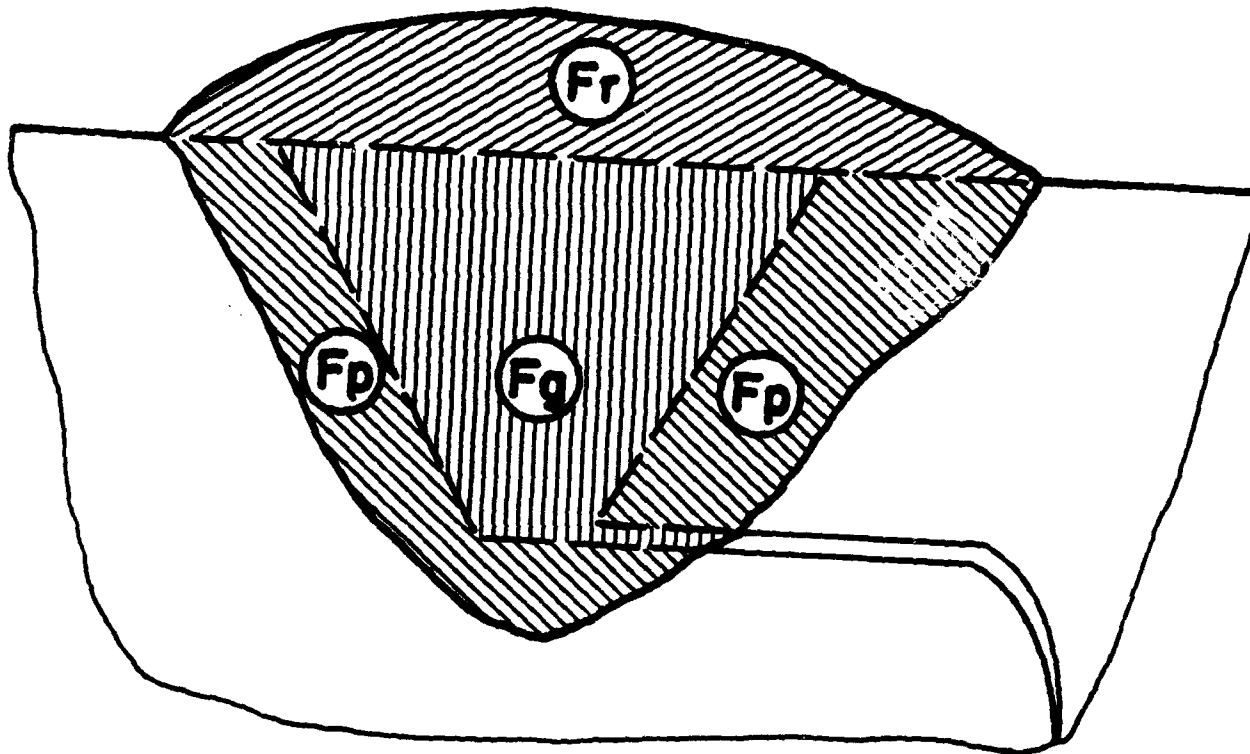


Fig. 4-3. Cross-section areas of a welded joint:
Fr- reinforcement, Fg - groove and Fp - arc penetration.



Fig. 4-4. Enlarged photograph of a weld cross-section.



Fig. 4-5. Strips of temperature indicating liquids on a panel assembly applied prior to welding.

cover. There are so many variables which may affect the results of the experiments, including cleaning methods, surface conditions of wire, purity of gas, welding parameters, atmospheric conditions, among others. That is why, experiments of Series K were limited to a pragmatic evaluation of several cleaning methods.

Experiments of Series K were conducted according to the matrix shown in Table 4-3. Several welds were performed over the edges prepared by three methods: **brushing (BR)**, **grinding (GR)** and **machining (M)**. Degreasing of the edges was performed with two types of solvents, **isopropyl alcohol (A)** and **methyl ethyl ketone (K)**. Freon 113, recognized as the best solvent for aluminum alloys, according to NACA experience (Ref. 36), was not used in these experiments because of environmental considerations. The welds were sectioned, polished and examined under an optical microscope with magnification up to 600. Pores of various sizes larger than 0.0016 in. (0.04 mm) were counted and presented in Table 4-4.

The results showed the following:

- When degreased in isopropyl alcohol, machine edged (method M/A) caused less porosity than brushed edges (method BR/A).
- Methyl ethyl ketone degreases edges better than isopropyl alcohol but is more toxic. Welding over brushed edges cleaned with ketone (BR/K) produced much less porosity than welding over the brushed edges cleaned with isopropyl alcohol (BR/A).
- Grinding (GR/K) is an inferior method compared to brushing (BR/K). It also introduces a great number of inclusions (probably sand particles). The disk is quickly soiled and has to be frequently replaced.
- Considering that there are 24 edges per mat panel assembly to be cleaned, high cost of machining makes this method of edge preparation in production a very remote possibility. Technical feasibility of milling 13-ft. long edges, which are not ideally straight, is also questionable.
- As far as economics and safety are concerned, degreasing in alcohol and brushing would be a desirable production combination, however, an acceptable level of porosity is difficult to achieve. Therefore, degreasing in ketone followed by brushing was considered as a realistic production edge preparation method. This method was used for the experimental welding program as well.

4.2.2 Effect of Weld Storage Period on HAZ Properties (Series D)

It is known (Ref. 12) that in heat treatable alloys a significant reduction in hardness (and strength) occurs in the so-called overaged zone of the HAZ in as-welded conditions. It is also

TABLE 4-3. Effect of Method of Edge Preparation on Porosity Level in the Weld
(Matrix of Experiments, Series K)

Operating Conditions	Test Piece/Sample #	Wire Feed Rate ipm	Amperage (Approx.) A	Voltage (Approx.) V	Travel Speed ipm	Scope of Testing	Cleaning Method
Wire - 4043 Wire dia. -.045 in. Gas - Argon Chilling-CH	39/1	350	195	21	19.5	MI	BR/A
	39/2					MI	M/A
	40/1	350	195	21	19.5	MI	BR/K
	40/2					MI	GR/K

LEGEND:

- MI - Test pieces subjected to metallographic examination only.
- CH - Copper chilling of the heat affected zones on both sides of the weld.
- A - Degreasing with isopropyl alcohol.
- K - Degreasing with methyl ethyl keton.
- BR - Edge preparation with fine stainless pneumatic brush.
- M - Edge milling on a milling machine.
- GR - Edge grinding with flexible sand disk grinder.

TABLE 4-4. Effect of Edge Cleaning Methods on Porosity

Pore Diameter, in.	Number of Pores			
	BR/A	M/A	GR/K	BR/K
0.0016 - 0.0032	57	27	40	16
0.0033 - 0.0048	10	3	9	6
0.0049 - 0.0080	3	-	8	6
0.0081 - 0.0160	1	-	-	-
0.0161 - 0.0240	-	1	1	-
0.0241 - 0.0320	-	-	1	-
TOTAL	71	31	59	28

LEGEND:

- A - Degreasing with isopropyl alcohol.
- K - Degreasing with methyl ethyl ketone.
- BR - Edge preparation with fine stainless pneumatic brush.
- M - Edge milling on milling machine.
- GR - Edge grinding with flexible sand disk grinder.

known (Ref. 12) that natural aging (storing at room temperature) is likely to restore hardness to a certain degree. The specifics of GARD's experimental program did not allow testing of the weld to be performed immediately after welding. The time period between welding and testing (storage time) could vary due to the schedules of the radiographic and metallurgical laboratories. That is why it was important to determine how these variations in storage time could possibly affect HAZ properties. This information was obtained through measuring microhardness across the HAZ in a series of experimental welds identified as Series D.

The matrix of the experiments is shown in Table 4-5. According to the matrix, two welds were performed (test pieces D37 and D38) using the low and the high linear energies (Q), respectively. ($Q = I \times U/S$, where I = current, U = voltage and S = travel speed). Four samples adjacent to each other were cut from each test piece. The samples were tested for microhardness distribution across the HAZ according to a special schedule which covered aging periods of 4 hours (as-welded condition), 7, 14 and 28 days. The results are summarized below:

- Welding reduces hardness in the HAZ dramatically, when measured in as-welded condition.
- The most significant reduction in hardness is observed in the area of the HAZ called the overaged zone (OAZ). The lowest hardness in the OAZ may reach about 60% of that of the base metal.
- Weld storage restores hardness in the OAZ to some degree due to natural aging. This is evident for low Q conditions (#37), where storage for 1, 2 and 4 weeks recovered 16, 21 and 28% of as-welded hardness in the OAZ, respectively. As shown in Fig. 4-6, the most strong hardness recovery occurs in the first week of storage, with an average recovery rate of 2.3% per day. After that, the recovery rate is close to linear and hardness increases at a much lower rate. For example, after two weeks of storage hardness recovers at an average rate of 0.5% per day.
- However, this trend was not that evident for high Q conditions (#38). In this case, there is no recovery after the first week of storage and finally hardness increased by 8% total after four weeks of storage.

Conclusions. Judging by the results of Series D, it was concluded the following:

- Since hardness can be considered as a qualitative indicator of strength of the HAZ, considerable loss of hardness may turn OAZ into the weakest area of the welded joint and a potential failure location for tensile test specimens.

**TABLE 4-5. Effect of Natural Aging on HAZ Hardness
(Matrix of Experiments, Series D)**

Operating Conditions	Test Piece/Sample #	Wire Feed Rate ipm	Amperage (Approx.) A	Voltage (Approx.) V	Travel Speed ipm	Scope of Testing	Storage Period
Wire - 4043 Wire dia. - .045 in. Gas - Argon Chilling-CH	37/1	260	140	19	19.5	H	As Welded (4 hrs)
	37/2					H	7 days
	37/3					H	14 days
	37/4					H	28 days
	38/1	430	240	22.5	9.75	H	As Welded (4 hrs)
	38/2					H	7 days
	38/3					H	14 days
	38/4					H	28 days

LEGEND:

- H - Test pieces subjected to microhardness test only.
CH - Copper chilling of the heat-affected zones on both sides of the weld.

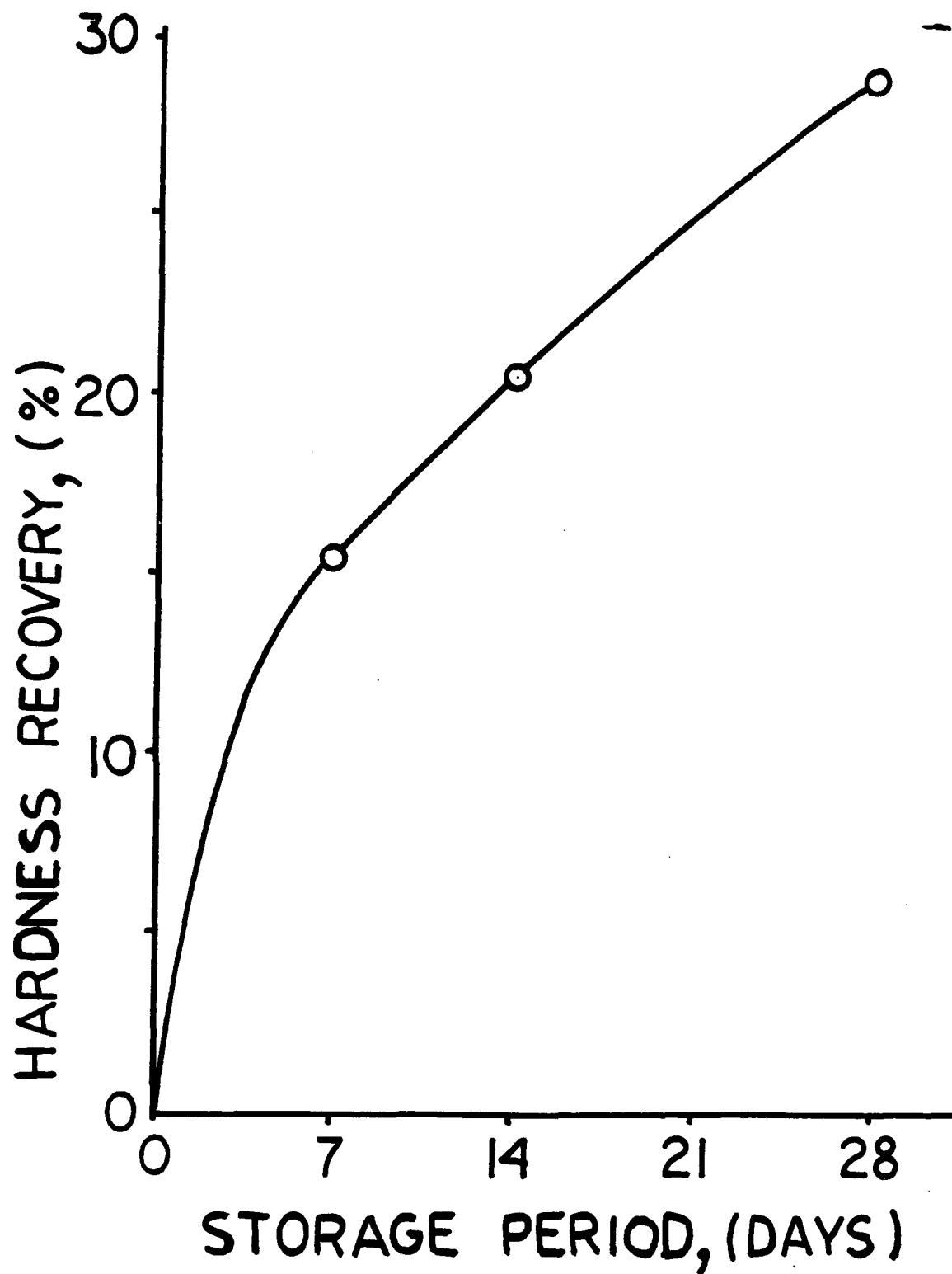


Fig 4-6. Effect of weld storage period prior to testing on as-welded hardness recovery.

- Strength of the tensile specimens failed through the OAZ may be affected depending on how long this specimen was stored prior to testing.
- In order to compare the test results of the welded joints on equal basis, the testing of the specimens (hardness and mechanical tests) should not be performed during the first several days after welding.
- During the first week, the rate of hardness (strength) recovery is still high and varies considerably with storage (natural aging) time.
- In order to minimize effect of natural aging on comparative test results, the testing should be done after two weeks of storage, when an average rate of hardness recovery is slowed down to about 0.5% per day. This makes it easier to maintain test result accuracy. For example, to maintain 5% accuracy, testing may be conducted any time within 10 days after the 2-week storage period has been over.

4.2.3 Determination of Usable Ranges of Parameters

In order to minimize the number of experiments needed to meet the main objective of the experimental program, determination of optimal welding conditions, usable ranges of welding parameters had to be experimentally established for each wire feed rate. The parameters within the limits of a usable range are expected to produce welds of quality and geometry required for the following testing.

An intricate, thin-wall design of the extruded AE subpanels did not allow application of maximum welding current ($I = 350A$) available from the power source. If welding current (I) was too high, it created **melt-through** conditions in which the arc burns through the wall or the backing lip of the End subpanel. On the other hand, if I was too low, it created **underfill** (the groove is not filled to the top) or **incomplete penetration** conditions. The welds were not acceptable for mechanical and/or metallurgical testings if they were performed under the extreme conditions described.

In order to establish the widest possible parameter range usable for testing, a number of trial welds were performed on the panel assembly. Various wire feed rate (WFR) (WFR controls welding current) and travel speed (S) values were used. The obtained welds were inspected visually and weld width (Ww) and height of reinforcement (Hr) were measured.

The results of the experiments showed that a practical WFR range is within 260-430 ipm (110-182 mm/s) (corresponds to $I = 140-240A$), while the overall range of travel speed S should be within 7-26 ipm (3-11 mm/s). For example, at $WFR > 260$ ipm, the groove can be completely filled

at S not exceeding 14 ipm (5.9 mm/s), while at $S < 7$ ipm, incomplete penetration and/or excessive reinforcement are likely to occur. At $WFR > 430$ ipm, melt-through conditions are likely to occur, especially at the start and termination (transient) portions of the weld. The groove is filled, when S does not exceed 27 ipm (11.4 mm/s). The data obtained through these trials were used to develop a matrix for the experimental program.

4.3 RESULTS OF EXPERIMENTAL PROGRAM

4.3.1 Matrix of welding experiments

The matrix is shown in Table 4-6. It was designed to study effect of welding parameters on mechanical and metallurgical properties of the welded joints. Table 4-7 shows actual welding parameters (as recorded during welding) and corresponding calculated dilution rates DR.

Arc power P was calculated as follows:

$$P = I \times U \text{ (watt)}$$

where I and U - mean values of current (amperes) and arc voltage (volts).

Power P of low, medium and high levels are represented by A, B, and C series of experiments, respectively, as shown in Table 4-7. Values of average power (P_{ave}) for each level were 2,777, 4,133 and 5,530 watt, respectively. Maximum deviation from P_{ave} within each level was 4%.

Linear arc energy Q was calculated as follows:

$$Q = P/S \times 60 \text{ (kJ/in.)}$$

or

$$Q = P/S \times 2.36 \text{ (kJ/mm)}$$

where P - arc power (watt) and

S - travel speed (ipm or mm/s, respectively).

Among various levels of linear arc energy Q, values of low, medium and high levels were achieved in each series (A, B and C), with Q values within the same level being equal. Values of average linear energy (Q_{ave}) for the low, medium and high Q levels were 12.86 kJ/in. (0.506 kJ/mm), 17.16 kJ/in. (0.676 kJ/mm) and 25.21 kJ/in. (0.992 kJ/mm), respectively. Maximum deviation from Q_{ave} within each level did not exceed 1.5%.

Since Q can be varied by varying P and/or S, the matrix of the welding experiments was designed in such a way that the effect of Q on properties of welded joints could be analyzed for three different modes as shown in Fig. 4-7.

- **S-mode:** $Q_s = \text{var}$, $P = \text{const}$ and $S = \text{var}$.

Here, Q_s mean that Q is varied by keeping P constant and varying S. These conditions are represented by solid curved lines. For example, welds identified as C30, C29, C28, C35 and C33

TABLE 4-6. Effect of Welding Parameters on Weld Joint Properties
(Matrix of Experiments, Series A, B & C)

Experiment Series #	Test Piece #	Wire Feed Rate ipm	Amperage (Approx.) A	Voltage (Approx.) V	Travel Speed ipm	Scope of Testing	Commentary
A Wire - 4043 Wire dia. -.045 in. Gas - Argon	4	260	140	19	9.75	AT	NC
	5				6.50	AT	CH
	6				9.75	AT	CH
	10				13.00	AT	CH
	11				14.60	-	CH
	12				19.50	H	CH
B Wire - 4043 Wire dia. -.045 in. Gas - Argon	16	350	190	21	9.75	AT	NC
	17				9.75	AT	CH
	18				13.00	AT	CH
	22				14.60	AT	CH
	23				19.50	H	CH
	24				26.00	H	CH
C Wire - 4043 Wire dia. -.045 in. Gas - Argon	28*	430	240	22.5	9.75	AT	NC
	29				9.75	AT	CH
	30				13.00	AT	CH
	34				14.60	-	CH
	35				19.50	AT	CH
	36**				26.00	H	CH

LEGEND:

- AT - Test pieces subjected to all tests according to GARD's Specification.
- H - Test pieces subjected to microhardness test only.
- CH - Copper chilling of the heat affected zones on both sides of the weld.
- NC - No chilling.
- * - Downgraded to H-scope of testing later on.
- ** - Upgraded to AT scope of testing later on.

**TABLE 4-7. Welding Conditions and Dilution
(Series A, B & C)**

Weld ID	Current I	Voltage U	Power P = IxU	Travel speed S		Linear Energy Q = P/S		Dilution Rate	
				(ipm)	(mm/s)	(kJ/in.)	(kJ/mm)		(level)
A4*	145.68	19.27	2,807	13.0	5.5	12.95	0.510	L	39.37
A5	142.11	19.63	2,790	13.0	5.5	12.88	0.507	L	22.22
A6	136.62	20.22	2,763	9.75	4.12	17.00	0.669	M	18.36
A10	134.35	20.39	2,739	6.5	2.75	25.29	0.996	H	16.60
A9	144.82	19.24	2,786	19.5	8.25	8.57	0.337	EL	43.14
Low Pave = 2,777									
B16*	197.10	21.16	4,171	13.0	5.5	19.25	0.758	MH	62.00
B17	184.71	22.39	4,136	13.0	5.5	19.09	0.752	MH	36.00
B18	185.78	21.36	3,968	9.75	4.12	24.42	0.961	H	34.50
B22	191.59	21.97	4,209	14.6	6.18	17.30	0.681	M	37.22
B23	202.04	20.60	4,162	19.5	8.25	12.81	0.504	L	54.65
B24	202.03	20.55	4,152	26.0	11.0	9.58	0.377	EL	53.30
Medium Pave = 4,133									
C28*	241.92	23.03	5,571	13.0	5.5	25.71	1.012	H	63.70
C29	249.30	22.10	5,510	13.0	5.5	25.43	1.001	H	44.46
C30	228.61	23.87	5,457	9.75	4.12	33.58	1.322	EH	37.38
C35	246.04	22.71	5,588	19.5	8.25	17.19	0.676	M	59.93
C33	251.70	21.95	5,525	26.0	11.0	12.75	0.502	L	54.92
High Pave = 5,530									

Legend: *HAZ is not chilled; Q levels: L - low, M - Medium,
M - high, EL - extra low, EH - extra high, MH - medium high

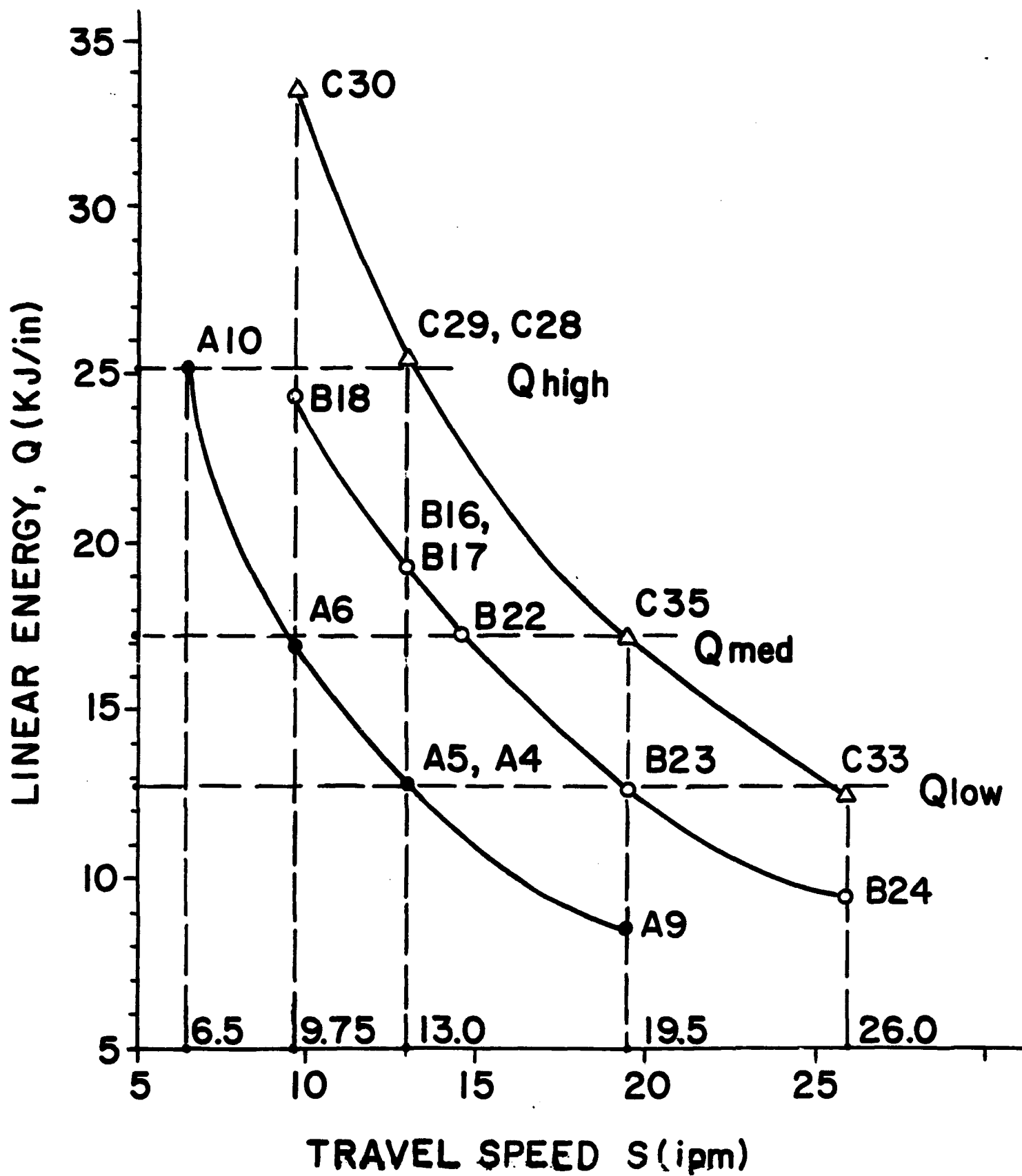


Fig. 4-7. Graphic representation of the matrix of welding experiments.

were performed on high P level ($P_{ave} = 5,530$ watt) and travel speeds S varying from 6.5 ipm (2.75 mm/s) to 26 ipm (11.0 mm/s).

- **P - mode:** $Q_p = \text{var}$, $P = \text{var}$ and $S = \text{const}$.

Q_p means that Q is varied by varying P and keeping S constant. These conditions are represented by the vertical dashed lines. For example, welds identified as A6, B18 and C30 were performed on low, medium and high arc power P, respectively, and constant speed $S = 9.75$ ipm (4.12 mm/s).

- **PS-mode:** $Q_{ps} = \text{const}$, $P = \text{var}$ and $S = \text{var}$.

Q_{ps} means that Q is kept constant by varying both P and S. These conditions are represented by the horizontal dashed lines. For example, welds identified as A6, B22 and C35 were performed on medium Q level ($Q_{ave} = 17.16$ kJ/in, 0.676 kJ/mm) achieved by the corresponding changes of both P and S.

4.3.2 Methodology

Experimental welding program was designed to study effect of welding parameters on properties of welded joints. Welding of three series of experiments (A, B and C) were conducted according to the matrix described earlier (Table 4-6). The schedule was maintained to provide (natural aging) periods prior to testing longer than two weeks and possibly equal for each series. Actual storage periods varied within 19-20 days prior to microhardness tests and 20-26 days prior to mechanical tests. Each weld within each series was performed using the same arc power P. Each series consisted of 5-6 main welds (18 in. long) performed under various travel speeds. Simultaneously with each main weld to be tested, a duplicate one was performed under the same conditions. If, as a result of visual or x-ray examinations, the main weld (or its portion) was not accepted, this weld was replaced with its duplicate (or its portion). If both (main and duplicate) welds were not accepted, a new weld was performed under the same conditions.

Random sectioning of the welds performed previously showed some level of porosity. Acceptance of porosity level was verified by radiographic inspection which was done according to the AWS D1.2 Code and the ASTM E390 Standard. Grading of defects was done according to the ASTM E390 as required by the Belvoir RD & EC. The acceptance criteria (Table 4-1) was also based on the Army requirements.

Testing of the welded joints was done according to the requirements described earlier in 4.1.2.

Microhardness was measured across the HAZ using Knoop 100g method described in 4.1.2. Weld measurements were done from the photographs of the weld cross-sections.

4.3.3 Results of Inspection

The results of radiographic (x-ray) inspection are presented in Appendix B2.

Welds of Series A. The welds of this series were performed under the low linear energy (Q) level (see Table 4-7). The series consisted of 6 main welds to be subjected to testing (Fig. 4-2) identified on the face side as A4, A5, A6 and on the back side -- A10, A11, and A12. Simultaneously with each main weld, its duplicate was welded under the same conditions, identified as A1, A2, A3, and A7, A8, A9, respectively.

As a result of x-ray inspection, an end portion of main weld A5 was not accepted because of a small incomplete fusion (lack of fusion) indication. As far as porosity is concerned, A5 was acceptable. Since its duplicate (A2) was also rejected by x-ray inspection (Class 3 coarse porosity), it was decided to mark the unacceptable portion of weld A5 and allow the remaining portion of it to be tested.

Weld A10 and its duplicate A7 had interruptions in the first half of the weld and were also rejected by x-ray inspection because of Class 3 coarse porosity. Therefore later on, a new weld A10REP was produced (along with B-Series) to replace A10. This weld was accepted by x-ray inspection.

Welds A4 and A6 were accepted by visual and x-ray inspections.

Weld A12 was rejected by visual inspection (lack of fill due to malfunction of the joint tracking system). It was replaced by its duplicate A9 for microhardness tests.

Welds of Series B. The series represents the medium linear energy (Q) level. Main welds were designated as B16, B17, B18, and B22, B23, B24. Duplicate welds were designated as B1, B2, B3, and B19, B20, B21, respectively.

The first half of B16 was rejected because of a small lack of fusion indication. This area was marked on the test plate to prevent it from being used for mechanical or other tests. Then the test piece was accepted for testing.

Weld B22 and its duplicate B19 were not accepted by visual inspection due to process interruptions. A replacement weld B22REP was performed instead of B22.

Test pieces B17, B18 and B22REP were rejected because of Class 2+ and 3 coarse porosity. Since this kind and level of porosity may become a main obstacle in mass production of the mat panels, it was decided to subject these test pieces to mechanical testing. The objective was to assess detrimental effect of this type and level of porosity on properties of the welded joints. As will be shown later, all the samples cut from these test pieces passed tensile and bend test

requirements of the AWS D1.2. Moreover, they demonstrated tensile strength higher than those (of Series A) which showed acceptable level of porosity. This is an indication that welding conditions play a greater role in defining strength of the welded joints than coarse porosity of unacceptable Class 3 level.

Welds of Series C. The series represents the high linear energy (Q) level. Main welds were designated as C28, C29, C30, and C34, C35, C36. Duplicate welds were designated as C25, C26, C27 and C31, C32, C33, respectively.

Weld C28 and its duplicate C25 could not be continued further than 2-3 in. from the start because they were not chilled and the arc penetrated through the curved wall of the End subpanel causing melt-through condition. Therefore, C28, which was originally intended to be fully tested (scope AT according to Table 4-6) had to be downgraded to scope H (microhardness test only).

C29 and C30 were rejected because of Class 2+ coarse porosity. Based on experience of Series B, these test pieces were allowed to be tested as well.

Weld C34 and its duplicate C31 were not welded since they were not scheduled for testing.

C35 and C36 showed the lowest level of porosity (fine, Class 1) compared to other welds. However, a portion of C36 (about 4 in. long) had melt-through conditions and was rejected. Since there was not enough weld left for testing, the duplicate C33 was radiographed and accepted. Also, it was decided to upgrade C36 and C33 (originally under scope H, Table 4-6) to scope AT since lack of fill expected for this welding conditions turned out to be very small. This made it acceptable for mechanical testing.

Example with Series C showed that, in fact, welding conditions have a profound effect on porosity. Welds C29 and C30 were cleaned the same way and welded using the same arc power P as C35 and C36, except that travel speeds were different: 13 ipm for C29 and C30 vs. 19.5 and 26 ipm for C35 and C36, respectively. Higher speed drastically reduced weld susceptibility to porosity. As far as porosity is concerned, it seems that higher energy levels along with higher travel speeds are preferable.

In this respect, the joint design of the existing panel may require some slight modification to prevent melt-through conditions at high energy level. Namely, it may be needed to increase the area of the panel cross-section area around the joint to be welded as shown in Fig 4-8 (dashed lines). This modification will require a slight modification of the existing die rather than procurement of a new die.

Summary of the results of inspection are given below:

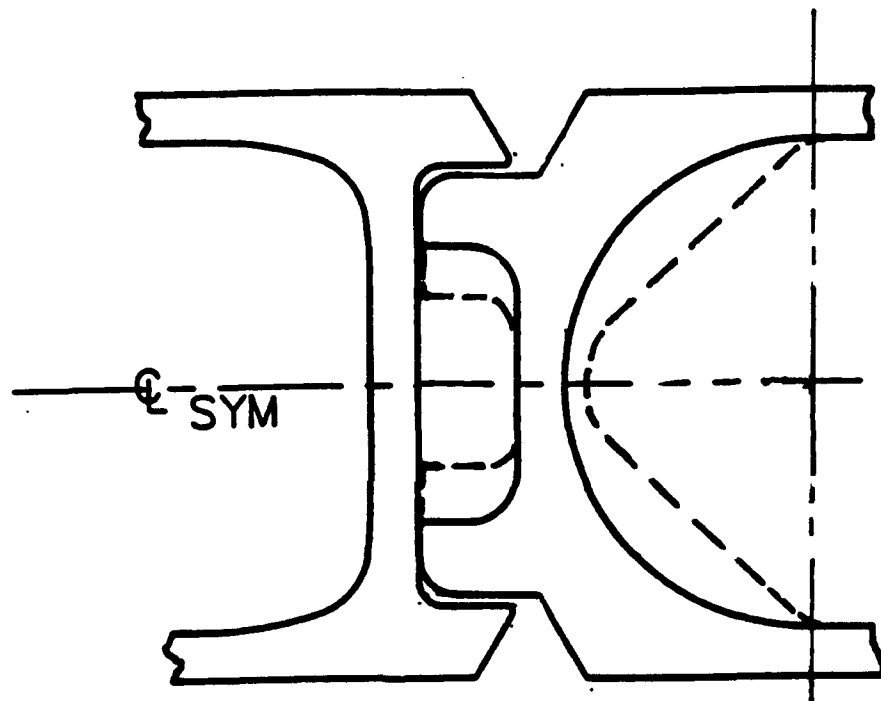


Fig. 4-8. Suggested modification of Type III welded joint design (dashed lines).

- No cracks were observed in any of the welded joints examined.
- Occasional rare spots of incomplete penetration (lack of fusion) were observed under unfavorable (too low or too fast) travel speeds.
- The main defect which caused most of rejections was Grades 2+ and 3 coarse porosity.
- It was found that under equal circumstances, porosity was very sensitive to welding conditions (energy and speed). Higher energy levels in combination with higher travel speed seems to cause less porosity.
- Also, switch from isopropyl alcohol to methyl ethyl ketone decreased porosity for some welding conditions.
- It may be necessary to elevate the acceptance level of coarse porosity to Grade 3 since this type and level of porosity do not compromise properties of the welded joints. This may help to maintain efficient mass production of the mat panels.
- Since higher energy levels and higher travel speeds seem to reduce sensitivity to porosity, the existing joint design of the AE mat panel may require some slight modification to withstand higher energy conditions without melt-through.

4.3.4 Analysis of Results of Mechanical Tests

The test results of Series A, B and C are given in Appendix B3.

The results of the mechanical tests are the following:

- All the welded joints met the 24 ksi minimum tensile strength requirement called for by the ASME/AWS Codes,
- Copper chillers proved to be effective means to strengthen the welded joints, (up to 20%) compared to non-chilled welds,
- Series B showed the highest values of tensile strength (29.7 - 31.8 ksi) compared to Series A (29.3 - 30.3 ksi) and Series C (27.5 - 30.6 ksi).
- Despite the rejection of some welds (B17, B18, B22 REP, C29 and C30) by x-ray inspection (coarse porosity, Grade 2 and 3), tensile strength of the samples cut from these test plates showed acceptable values of tensile strength (27.5 - 31.8 ksi), higher than the 24 ksi minimum tensile strength requirement called for by the ASME/AWS Codes.
- Among the test pieces of Series B and C, B22REP and C35 showed the highest values of tensile strength (31.8 ksi - 30.6 ksi), B22 REP being the strongest weld among all the series tested.

The results of bend tests are the following:

- Root bend tests were successful for all the specimens tested, except C 30 and C 33.
- Face bend tests were successful for all the specimens tested, except A5 and A6.

4.3.5 Effect of Welding Conditions on Tensile Strength

Deterioration of mechanical properties of welded joints typical for heat-treatable aluminum alloys is the fact widely recognized and confirmed by many investigators. As was shown by Kelsey (Ref. 21) for 7039 aluminum alloy, increase in linear energy $Q = P/S$ (where P =arc power ($I \times U$), I =current, U =voltage and S =travel speed) is associated with decrease in tensile strength of multipass welded joints. However, it has long been suspected that linear energy-strength relationship is more complicated than that. For example, it was noticed by Metzger (Ref. 20) that welding using the same linear energy could produce welded joints of different strengths, with higher strength being at higher travel speed. No explanation of the fact has been given in literature.

In this study, as was described in 4.3.1, in order to better understand the effect of Q on tensile strength, Q (identified as Q_s or Q_p) was varied by varying only S or P , respectively. Also, Q (identified as Q_{ps}) was kept constant by varying correspondingly both P and S . Effect of chilling of the HAZ on tensile strength was studied also.

The results of the experiments are presented in Fig. 4-9. Here, tensile strength of the specimens of Series A, B and C is plotted against linear energies Q_s (Fig. 4-9a) and Q_p (Fig. 4-9b). Weld ID numbers displayed on the graph correspond to those presented in Tables 4-6 and 4-7. The data on both graphs presented in both U.S. customary units (bottom and left side, kJ/in. and ksi) and metric units (top and right side, kJ/mm and MPa). The data for the chilled and non-chilled specimens are presented with the solid and dashed lines, respectively.

The conclusions derived from the results of the experiments are the following:

- Tensile strength has more complicated relationship with linear energy Q than was previously thought.
- The relationship is not linear and tensile strength reaches maximum at some optimal Q value (Q_{opt}). This is true regardless of a variable parameter (S or P) used to control Q as shown in Fig. 4-9a or b, respectively.
- It also explains the fact noticed by Metzger (Ref. 20) as follows. Tensile strength as function of travel speed S (Fig. 4-9a), for welds performed on high arc power (P high), for example, reaches a maximum at $Q_{opt} = 17 \text{ kJ/in. (0.669 kJ/mm)}$. It means that further decrease or increase in Q (increase or decrease in travel speed S) results in tensile strength reduction.

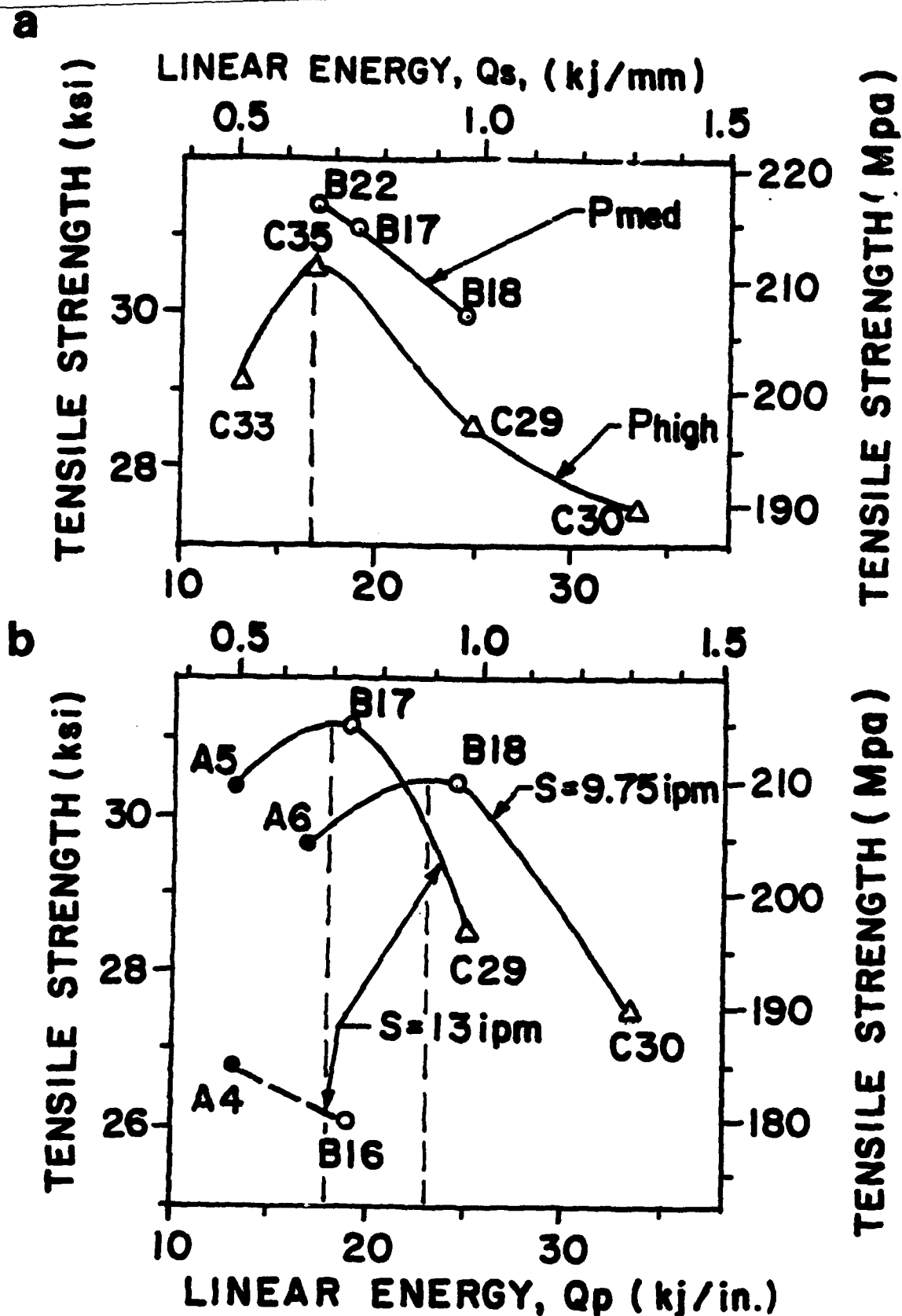


Fig. 4-9. Effect of linear energy (Q) on tensile strength of the welded joints; Q is varied by travel speed (a) and by arc power (b).

- However, the magnitude of Q_{opt} does depend on the parameter controlling Q . For example, Q_{opt} (maximum strength) is achieved at higher Q values when Q is controlled by P (Fig. 4-9b), compared to that when Q is controlled by S (Fig. 4-9a).

- Artificial HAZ chilling has a significant effect on tensile strength. For example, according to Fig. 4-9b, HAZ chilling increased strength of chilled welds A5 and B17, compared to non-chilled welds A4 and B16 performed using the same welding conditions, by 14% and 21%, respectively.

- Thus under the explored conditions, the objective of obtaining the maximum tensile strength can be achieved only at some optimum values of arc power P , travel speed S and their derivative, linear energy Q . Knowledge of the interrelationships between these parameters makes this task easier.

4.4 RELATIONSHIPS BETWEEN HARDNESS, AND FAILURE LOCATION AND STRENGTH

4.4.1 Results of Microhardness Tests

As was discussed earlier, a transverse specimen was cut from each of the test pieces of Series A, B and C. The specimens were prepared for microexamination and tested for microhardness distribution across the HAZ according to GARD's Specification for Inspection and Testing of Welded Mat Panels described in 4.1.2. Originally, Knoop 500g was the method specified for microhardness testing. However, preliminary trials showed that 500 g load produces imprints too large for testing some small areas of interest in the heat-affected zone (HAZ). Therefore the load was reduced to 100 g. This load was applied throughout the entire testing program. All the measurements were taken across the FL along the straight line parallel to and 0.062 in. (1.6mm) below the weld face surface of the specimen. The measurements were taken across the fusion line on the side of the middle subpanel (M-end) and on the side of the End subpanel (E-end). The extent of the measurements away from the FL was up toward the HAZ to 0.875 in. (22.2 mm) and toward the weld up to its centerline. The increments were progressively smaller as the FL approached, from 0.125 in. and down to 0.005 in (0.127mm) in the area 0.031 in. (1.2 mm) wide immediately adjacent to the FL.

The results showed the following:

Welding dramatically changes hardness in the HAZ and in the weld. There are three typical areas observed as far as hardness distribution is concerned. This is illustrated in Fig. 4-10 where microhardness profile across the FL is plotted over the cross-section of weld B17.

Following the base metal (BM), not affected by heat of welding, and moving toward the FL,

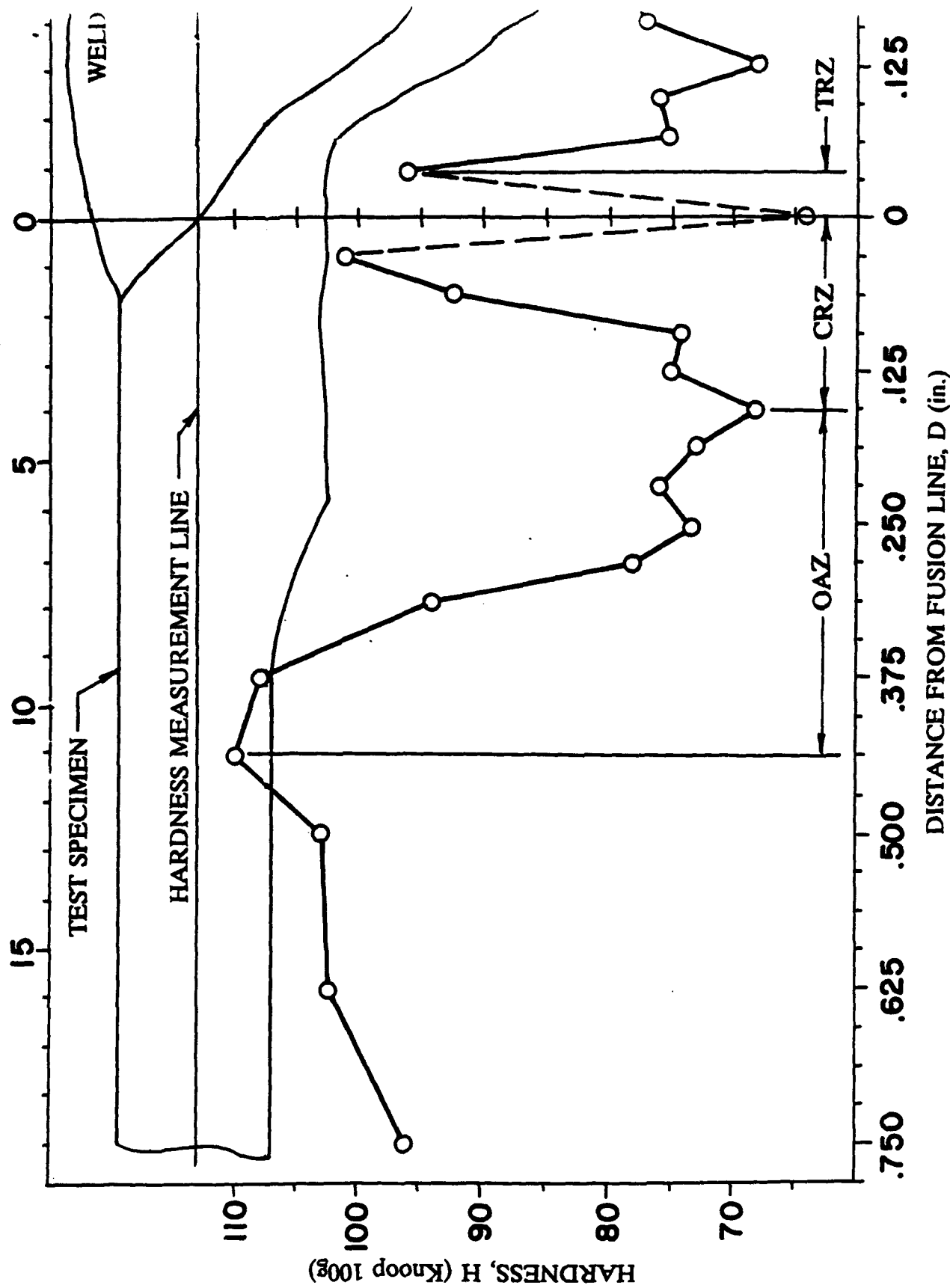


Fig. 4-10. Microhardness profile of weld B17.

a relatively wide area, sometimes called **overaged zone (OAZ)**, is encountered. A significant reduction in hardness is observed in the overaged zone (OAZ). The lowest hardness at the "bottom" of the OAZ may drop down to 60% of that of the base metal. The fact that the most of the tested specimens failed in the OAZ indicates that this zone is the weakest zone of the welded joint. This fact is fairly surprising since the weld was expected to be the weakest area of the joint because of the use of relatively soft (4043) wire. The OAZ typically occupies a larger portion of the HAZ. The width of this zone (W_{OAZ}) depends on welding conditions. The higher heat input, the wider W_{OAZ} and therefore W_{HAZ} .

The next area of the HAZ adjacent to the fusion line is sometimes called in literature the **complete reversion zone (CRZ)**. The zone is characterized by a continuous sometimes significant hardness recovery, up to 80% of that of the base metal. The CRZ, which occupies the rest of the HAZ, is narrower than the overaged zone (OAZ). The CRZ is a relatively heat sensitive area. Its width (W_{CRZ}) seems to be affected by welding conditions. Also, an unknown zone was revealed in this investigation. The portion of CRZ in the area 0.010-0.031 in. (0.3 - 1.2mm) wide immediately adjacent to the FL is characterized by a sudden sharp hardness drop sometimes to a very low level. The nature of this zone was not established.

Another very narrow zone adjacent to the fusion line (also not reported in literature) was observed in the weld which was named **transition zone (TRZ)**. Here, hardness again dramatically recovers. The width (W_{TRZ}) and the nature of the TRZ were not established. Since hardness may be considered as a qualitative indicator of strength of materials, local softness in the TRZ under some unfavorable circumstances, like presence of porosity, for example, may turn TRZ into the weakest zone of the welded joint. In fact, during tensile tests, some test specimens failed along the fusion line in the area where the TRZ and CRZ were found.

4.4.2 Effect of Hardness on Failure Location

Failure location appeared to be related to hardness distribution in the HAZ. Most of the failures of the specimens during tensile tests occurred in the HAZ. It was found that when HAZ failure occurred, the failure location was always at the lowest hardness point ("bottom") between the overaged zone OAZ and complete reversion zone CRZ. This is illustrated in Fig. 4-11. Here, the hardness profile (hardness H plotted against the distance from the fusion line D) of weld B16 is superimposed on the cross-section of this weld using the same scale. Weld B16 was performed on medium levels of arc power P and linear energy Q , and without HAZ chilling. It is evident that the specimen failed right through the "bottom" of the OAZ.

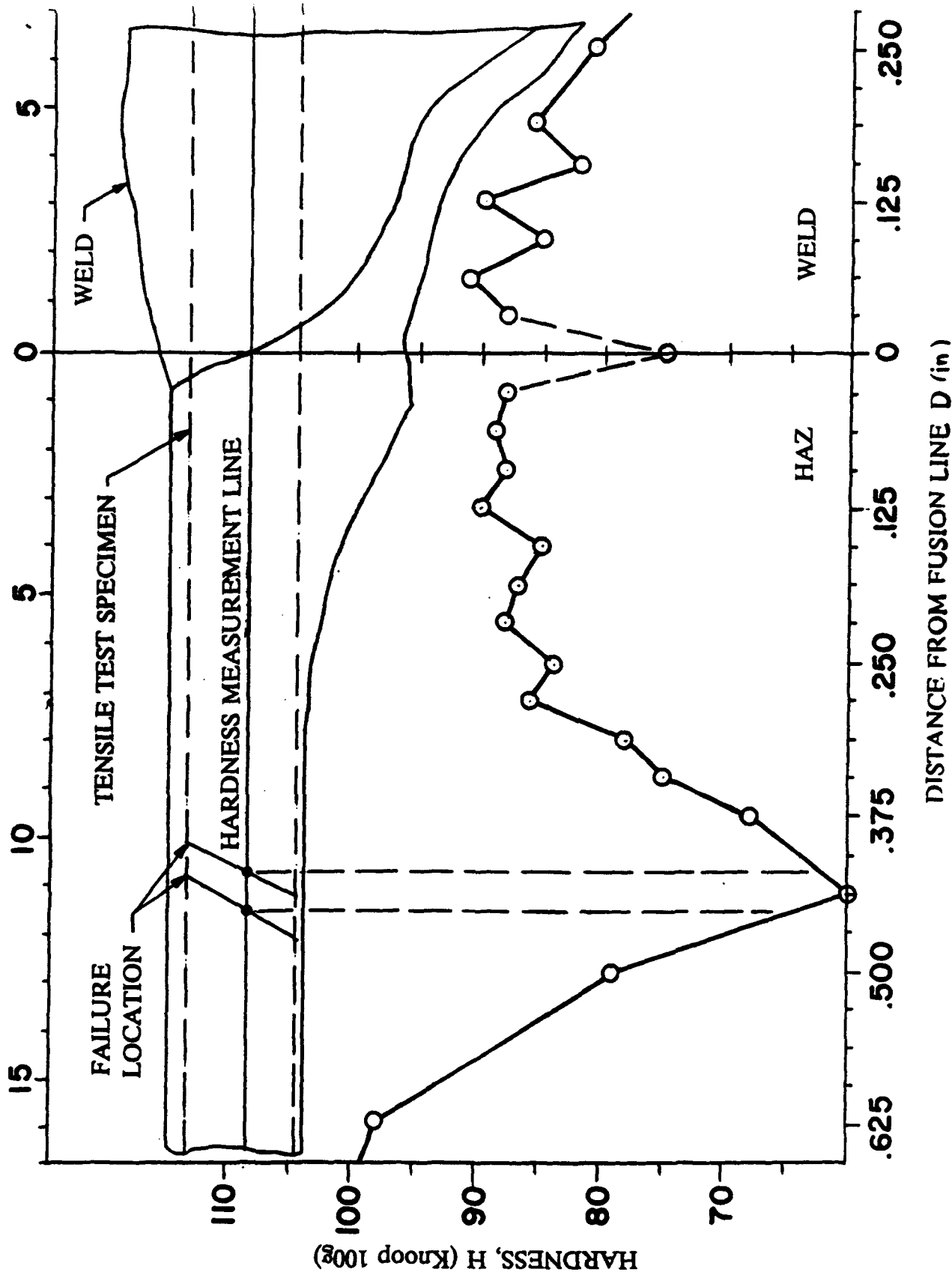


Fig. 4-11. HAZ failure location in weld B16.

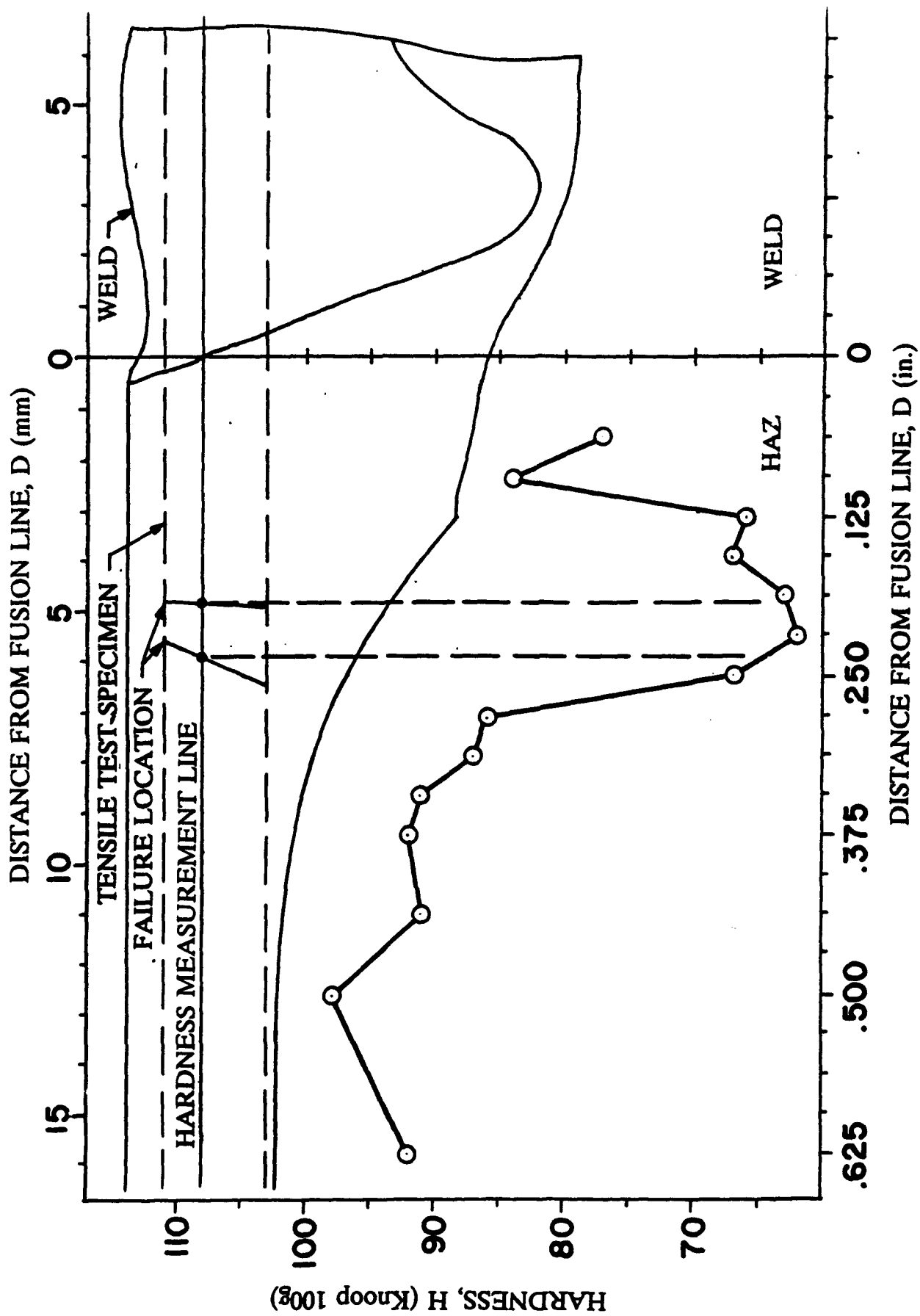


Fig. 4-12. HAZ failure location in weld C33.

The described phenomenon was observed for all tested specimens regardless of welding conditions. For example, as shown in Fig. 4-12, the same result was obtained for chilled weld C33 which, contrary to B16, was chilled and performed under quite different conditions, namely, high P and low Q. In another example, switch to medium P and high Q did not change the result for chilled weld B18 also, as shown in Fig. 4-13.

4.4.3 Effect of Welding Conditions on HAZ Width

Width of the HAZ can be presented as follows:

$$W_{HAZ} = W_{OAZ} + W_{CRZ}$$

where W_{OAZ} and W_{CRZ} are the widths of the overaged and complete reversion zones.

It was found that in presence of HAZ chilling, W_{OAZ} showed higher sensitivity to welding conditions. For example, Fig. 4-14 shows the microhardness profile for chilled weld C30 (33.58 kJ/in., 1,322 kJ/mm). Comparing it with that for chilled weld C33 (12.75 kJ/in., 0.502 kJ/mm) shown in Fig. 4-12, it is evident that an increase in Q resulted in a significant (56%) W_{OAZ} increase, from 0.281 in. (7.1mm) to 0.437 in. (11.1mm). At the same time, W_{CRZ} remained practically the same, about 0.187 in. (4.8mm). As other examples for chilled welds showed, W_{CRZ} is much less sensitive to welding thermal cycle compared to W_{OAZ} . Thus, width of the HAZ (W_{HAZ}) sensitivity to heat of welding is largely determined by that of the OAZ.

Effect of HAZ Chilling on HAZ Width . HAZ chilling dramatically reduces the widths of the CRZ, OAZ, and HAZ. For example, Fig. 4-10 shows the microhardness profile of chilled weld B17. Comparing it with that for its non-chilled counterpart weld B16 (Fig. 4-11) performed under the same conditions, it is evident that chilling significantly reduced the widths of the CRZ, OAZ and, eventually, HAZ as follows:

- W_{CRZ} - by 57%, from 0.437 in. (11.1mm) to about 0.187 in. (4.8mm),
- W_{OAZ} - by 20%, from 0.312 in. (7.9mm) to 0.250 in. (6.3mm), and
- W_{HAZ} - by 41%, from 0.750 in. (19.0mm) to 0.437 in. (11.1mm).

4.4.4 Effect of HAZ Chilling on Tensile Strength

HAZ chilling effectively suppresses metallurgical reactions, especially in the CRZ. This may positively affect HAZ microstructure and properties. For example, chilled weld B22R represents conditions relatively close to those described above for non-chilled weld B16 (shown in Fig. 4-10), except that Q is lower by 10.5% (17.3 and 19.25 kJ/in. respectively). However, due to presence of chilling, the results of mechanical tests were dramatically different: average tensile strength increased by 21%, from 26.0 ksi (179MPa) to 31.4 ksi (215 MPa).

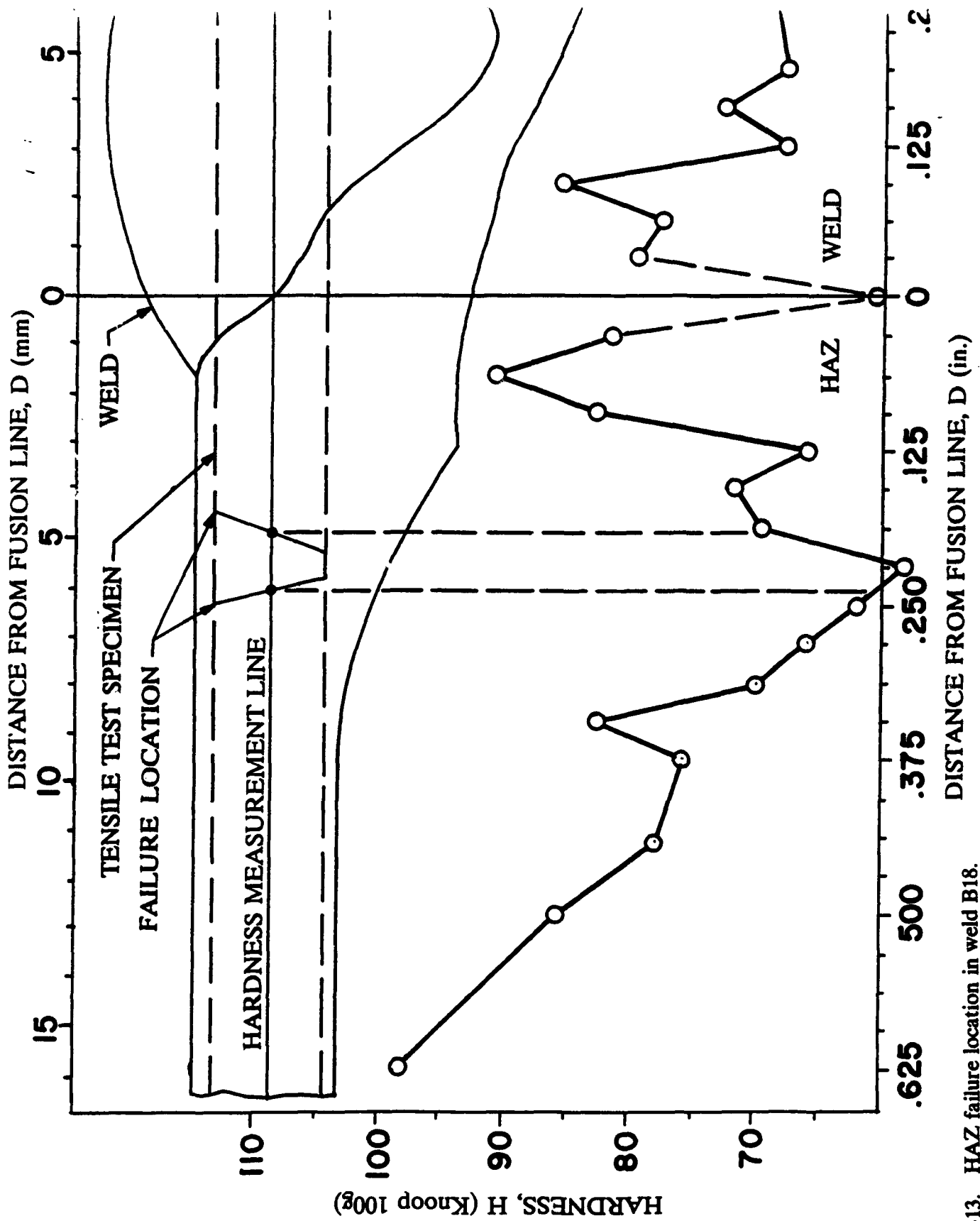


Fig. 4-13. HAZ failure location in weld B18.

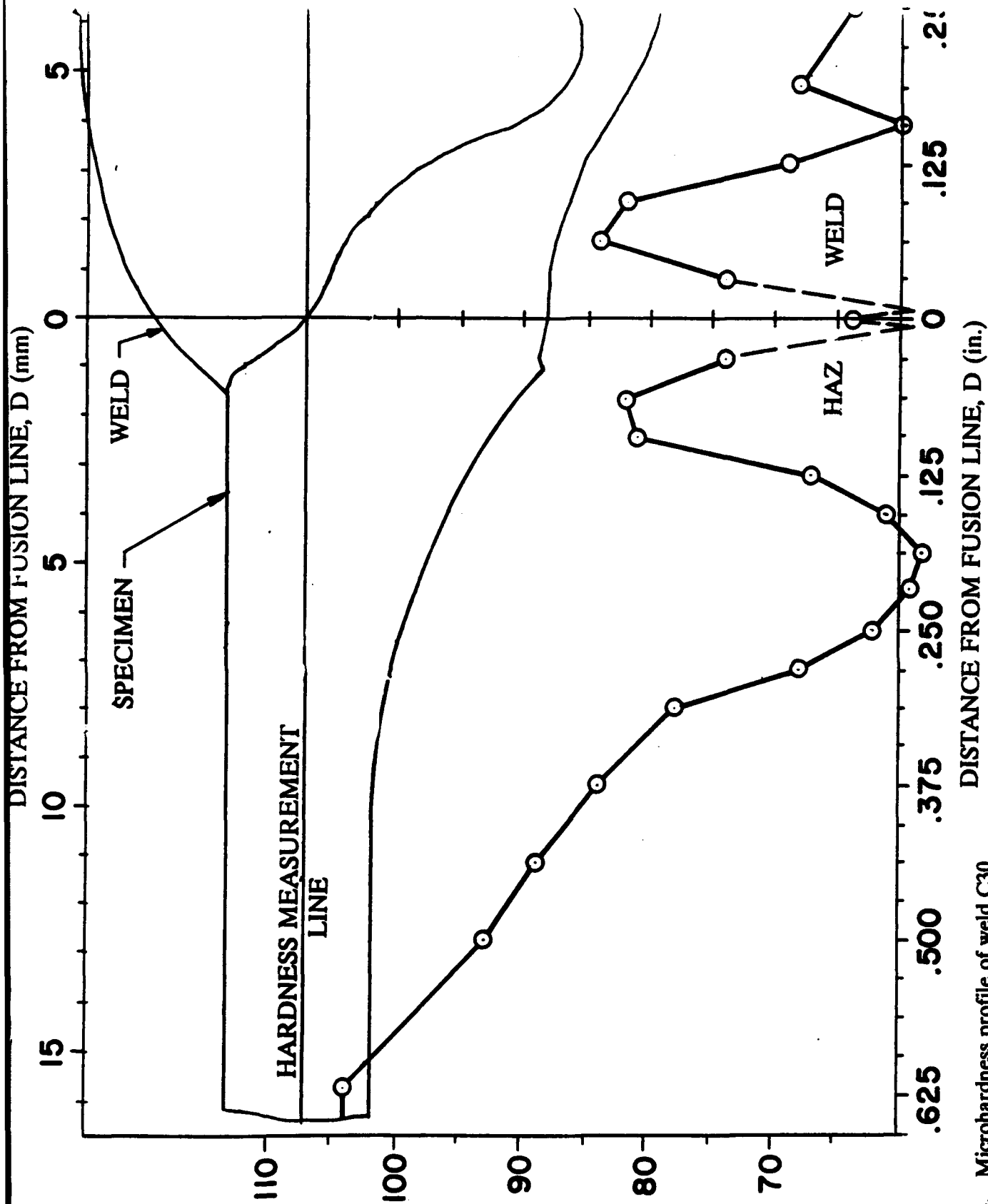


Fig 4-14. Microhardness profile of weld C30.

This increase in strength became possible due to significant positive changes in HAZ microstructures which are obviously associated with the size of the specific zones in the HAZ. In fact, in this case, the widths of the zones were reduced even more dramatically than for previously described weld B17:

- W_{CRZ} - by 71%, from 0.437 in. (11.1mm) to .125 (3.2mm),
- W_{OAZ} - by 50%, from 0.312 in. (8.7mm) to 0.156 in. (4.0 mm), and finally
- W_{HAZ} - by 62%, from 0.750 in. (19mm) to 0.281 in. (7.1mm).

4.5 RELATIONSHIPS BETWEEN HAZ HARDNESS AND MICROSTRUCTURE

4.5.1 Precipitation sequence in 6061 alloy.

The precipitation sequence in 6061 alloy is well established in literature. Despite some ambiguity concerning structure and morphology of some precipitates, generally recognized (Ref. 37) sequence of metastable phases produced by ternary (Al-Mg-Si) alloys along the pseudo-binary (Al-Mg₂Si) line during solution heat treatment is the following:

$$\alpha' = GP + B'' + B' + B$$

In this study, letter B is used instead of β , frequently used in literature to describe the precipitates developed in pseudo-binary alloys, to reflect some structural differences in the precipitates found in 6061 commercial alloy by Dumolt (Ref. 38). In order to distinguish these precipitates from those described for pure pseudo-binary alloys, Dumolt identified the precipitates by letter B. This rule will be followed in this study as well. The description of these precipitates is given below.

Supersaturated solid solution (α') is a structure produced by solutioning and quenching. Solutioning is a heat treatment in which an alloy is heated and held at a temperature close to eutectic until equilibrium solid solubility limit is attained. The purpose is to put maximum practical amount of hardening solutes (Mg and Si) into solid solution in the aluminum matrix. As a result of quenching (rapid cooling to room temperature), the solid solution becomes supersaturated. The resulting structure (α') is very soft but has a tendency to precipitate the solute which is in excess over the amount actually soluble at room temperature. This increases hardness.

Gunnier - Preston (G.P.) zones are the first product of decomposition of supersaturated solution. As all the other precipitates, G.P. zones are beyond resolution of an optical metallograph. According to Panceri, et al. (Ref. 39), formation of G.P. zones are observed at the temperature, below 160°C (320°F). That is why Lutts (Ref. 40) referred to G.P. formation as "pre-precipitation" (or clustering) meaning that actual precipitation follows. G.P. zones have not yet been observed via transmission electron microscopy (TEM) but their presence was detected by resistivity

measurements by Panceri, et al. (Ref. 39) in Al-1.4% Mg₂Si alloy. Being the smallest in size compared to other precipitates, G.P. zones are able to make only modest contribution to the mechanical properties of the material, according to Panceri, et al. (Ref. 39). This was also confirmed by Enjo and Kuroda (Ref. 41). The morphology of the G.P. zones are thought to be spherical or needle-like, according to Mondolfo (Ref. 37).

B" phase is the next phase in the precipitation sequence. It is the first phase visible via TEM and precipitates as needles. It can grow (coarsen) significantly upon continued aging or temperature rise up to 220°C (428°F) as reported by Thomas (Ref. 42) or 240°C (464°F) as reported by Miyauchi et al. (Ref. 43). Thomas (Ref. 42) showed that the maximum hardening in pure Al-0.97% Mg-0.61%Si alloy (Mg₂Si equivalent of 6061) occurs when it is aged to produce the needle structure. This is confirmed by Enjo (Ref. 41) for 6063-T5 alloy. However, as was shown by Dumolt (Ref. 38), increase in aging temperature leads to considerable softening of the alloy due to coarsening of the B" precipitate. Therefore, the standard T6-temper specified by the Aluminum Association recommends aging at modest 350°F (177°C) for 8 hours after a solution treatment with the objective to precipitate B" phase in the matrix.

B' phase precipitates are next in the sequence. They are described by Thomas (Ref. 42) as rod-shaped particles with a structure corresponding to highly ordered unit cell of Mg₂Si. Formation of the rods occurs from the needles by an increase both in their length and diameter. The aging temperature range of rod existence is 240-380°C (464-716°F) according to Miyauchi, et al. (Ref. 43). However, according to Dumolt (Ref. 38) this range is much wider, 350-460°C (662-860°F). Transformation of B" phase into B' phase is associated with softening of the alloy since the needles (B") contribute more to hardening of the alloy than the rods (B') according to Enjo and Kuroda (Ref. 41).

The equilibrium B phase (Mg₂Si) is developed at the final stage of the precipitation sequence. It exists as platelets which grow out of the intermediate rod structure or nucleate independently (Ref. 42). According to Enjo and Kuroda (Ref. 41), Mg₂Si contribution to hardness of the alloy is very small.

Insoluble compound may also be present in commercial 6061 alloy. These particles were found in the structure at all the stages of the precipitation sequence. However, their effect on hardness of the alloy is negligible according to Enjo and Kuroda (Ref. 41).

Conclusion: B" phase produces the strongest effect on hardness of alloy 6061, while contribution of B' phase is moderate. All the other particles affect hardness very little.

4.5.2 Effect of Precipitates on HAZ Hardness

Based on the results of the studies of Dumolt (Ref. 38), and Enjo and Kuroda (Ref. 41), and the comprehensive analysis of hardness (H) distribution discussed earlier in the present study, probable metallurgical reactions in the HAZ of 6061-T6 alloy are described below using Fig. 4-15 as an illustration. Here, for weld B16, H and T max profiles across the HAZ are superimposed on each other. Experimental and extrapolated points are connected with solid and dashed lines, respectively. Solvus temperatures of the start (Ts1) and the end (Ts2) of B" phase formation, and of the end of B' phase formation (Ts3) are indicated by horizontal lines. The values of Ts1, Ts2 and Ts3 are taken from Ref. 41.

As it is seen in Fig. 4-15, the hardness area identified as the OAZ specially coincides with the temperature interval (ΔT_B) of B' phase existence. The solvus temperature (Ts3) of this interval falls right into the "bottom" (the softest point) of the OAZ fairly accurately. Analysis of H-T-max relationships for many chilled and non-chilled welds in this study confirmed this conclusion no matter what welding conditions were used. For example, Fig. 4-15 described above was plotted for non-chilled weld B16 performed on medium power P and medium linear energy Q. The same results were obtained for weld B17 (Fig. 4-16), the chilled counterpart of weld B16, performed using the same conditions. Figure 4-17 shows similar results obtained for chilled weld B18 (medium P and high Q), while Figures 4-18, 4-19 and 4-20 show the same phenomenon for welds A5, B23 and C33 performed on low Q level and low, medium and high P levels, respectively.

Thus it is evident that the OAZ hardness area accurately represents the location of a structural zone where **coarsening of B" phase and its transformation into B' phase** occur in the HAZ of 6061-T6 alloy. The fact is rather important since hardness test is more available and less expensive tool than TEM in practical applications. Knowledge of the profile and location of the OAZ is very important since most of the failure in this study during the tensile tests occurred through the "bottom" of this zone.

The hardness area identified as the CRZ may be called **solution-hardening zone** since in this area dissolution of B" and B' phases occurs. This happens during the heating and cooling periods of the welding thermal cycle since this area is held at temperatures higher than B' solvus temperature (Ts3). Dissolution of precipitates B" and B', enriches solid solution of the aluminum matrix with Si and especially with Mg. This increases hardness of the CRZ. The closer the metal to the FL, the higher the temperature, the higher amount of precipitates is dissolved, the higher hardness and strength of the metal.

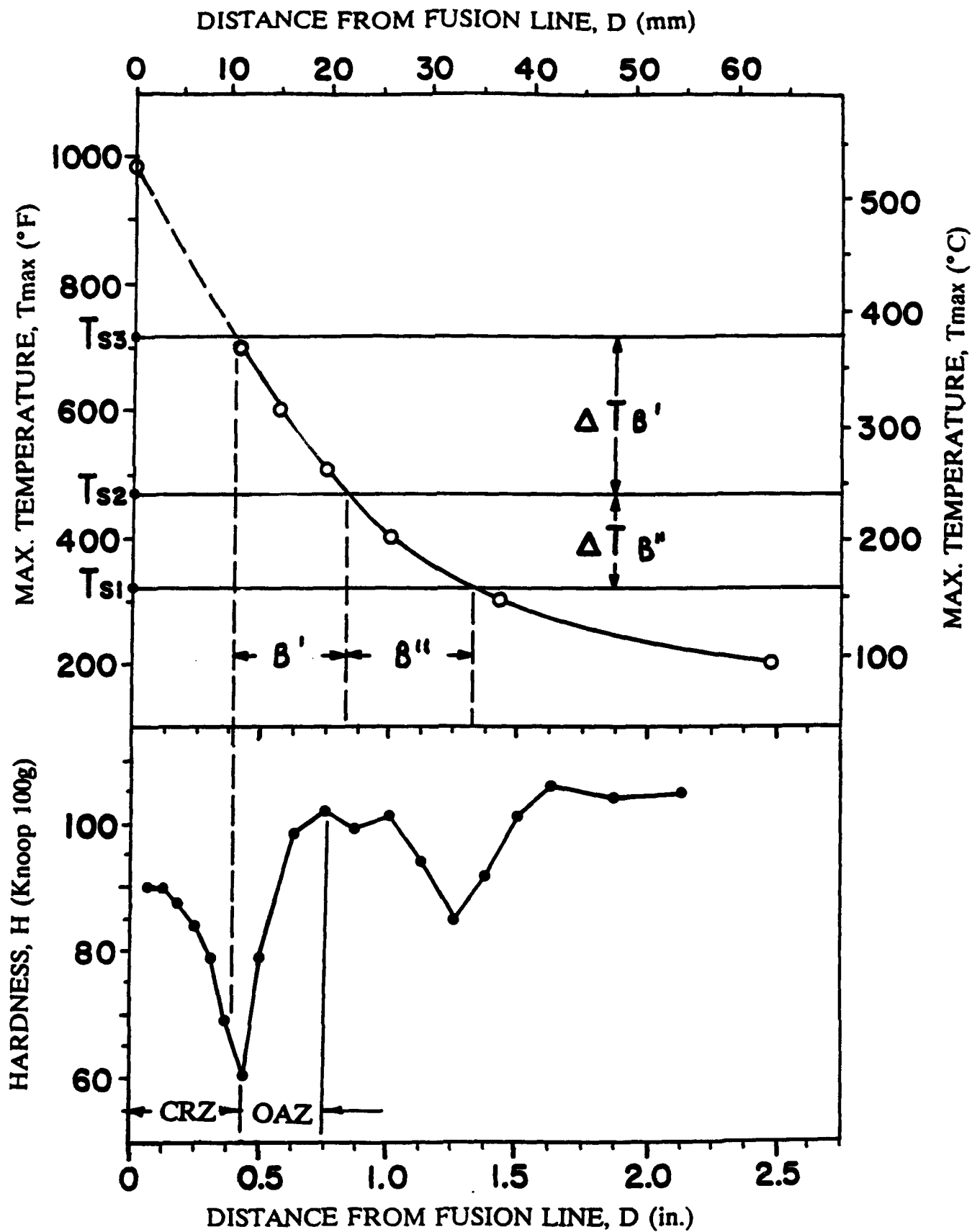


Fig. 4-15. Effect of maximum temperature distribution on microhardness and microstructure in the HAZ (weld B16).

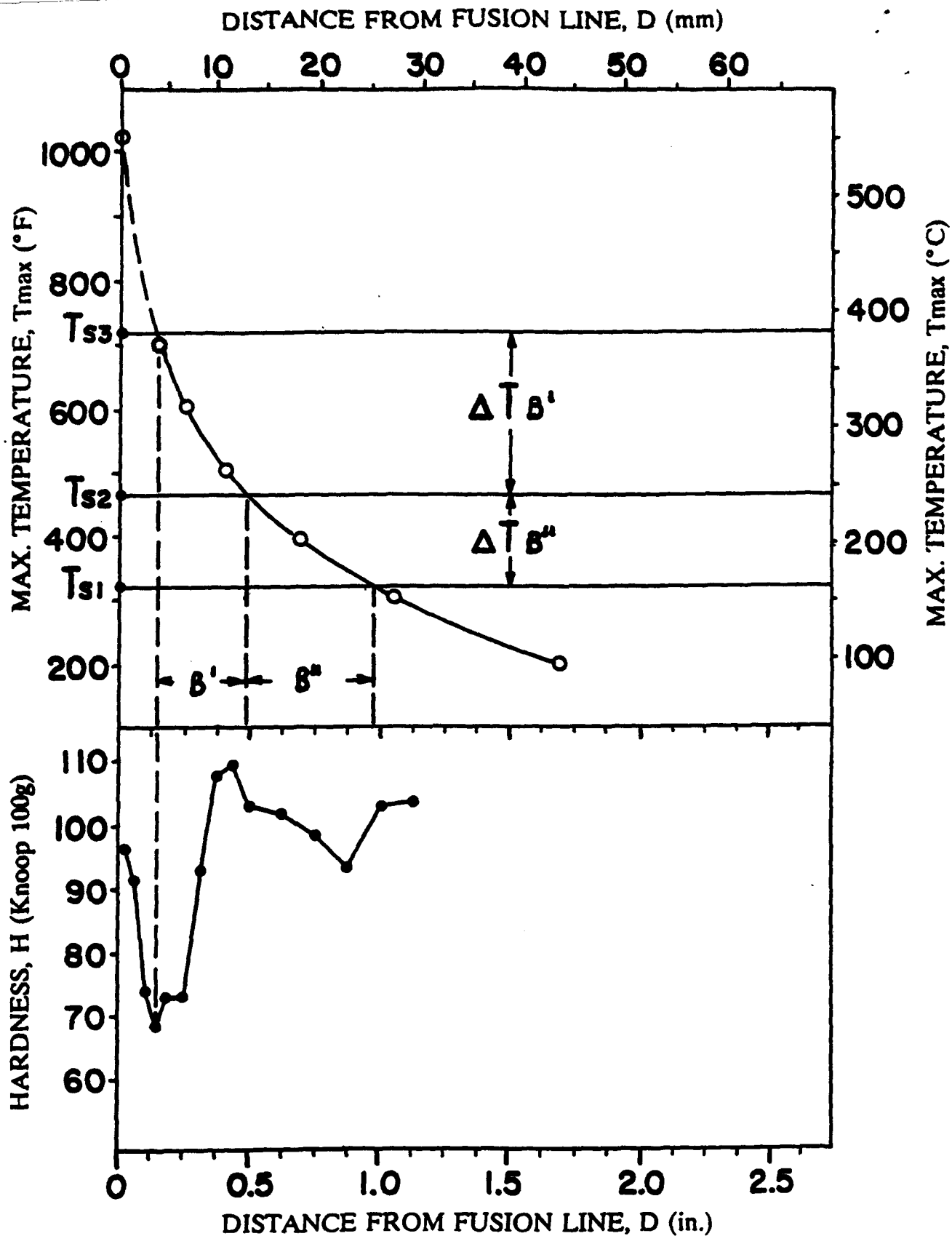


Fig. 4-16. Effect of maximum temperature distribution on microhardness and microstructure in the HAZ (weld B17).

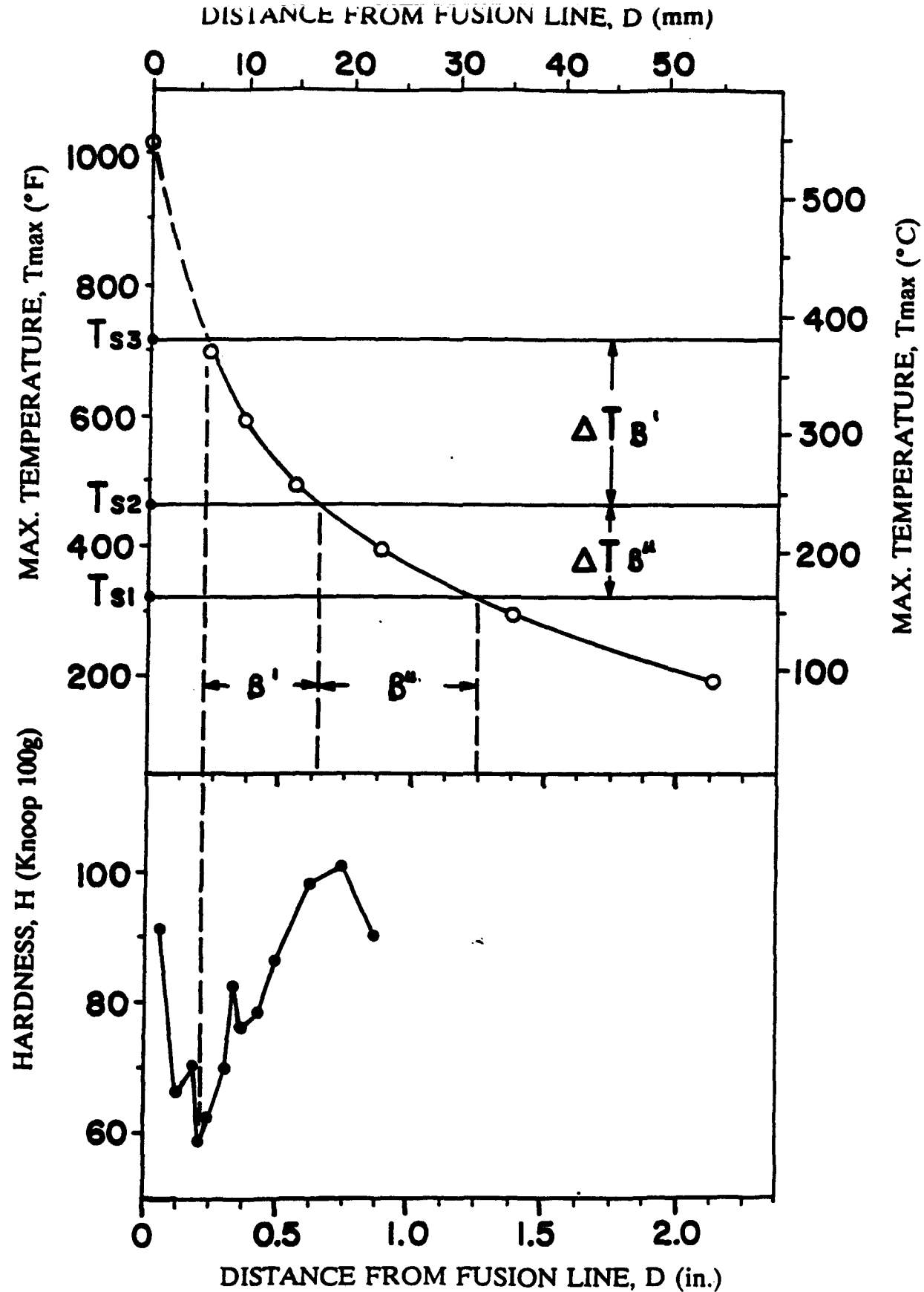


Fig. 4-17. Effect of maximum temperature distribution on microhardness and microstructure in the HAZ (weld B18).

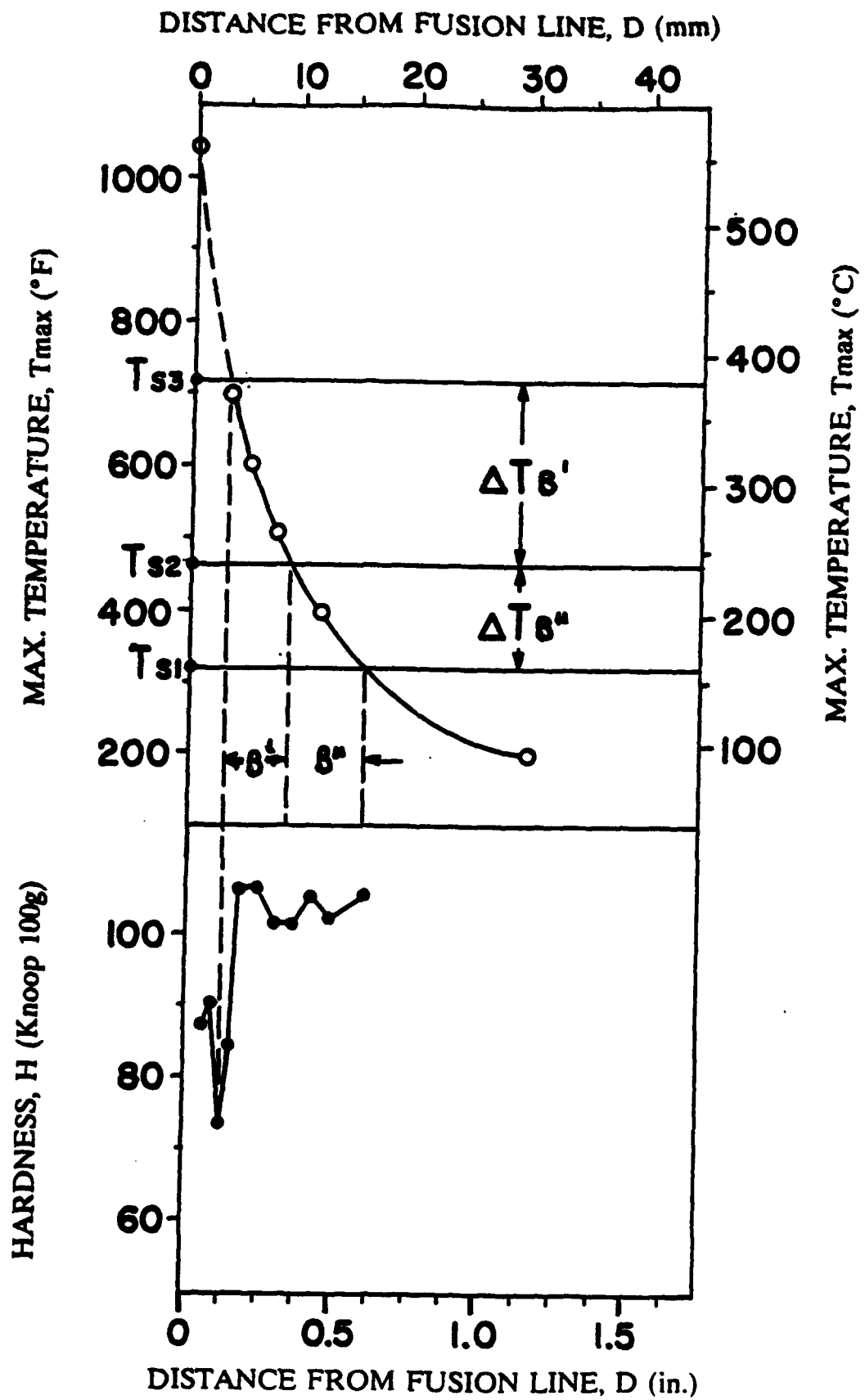


Fig. 4-18. Effect of maximum temperature distribution on microhardness and microstructure in the HAZ (weld A5).

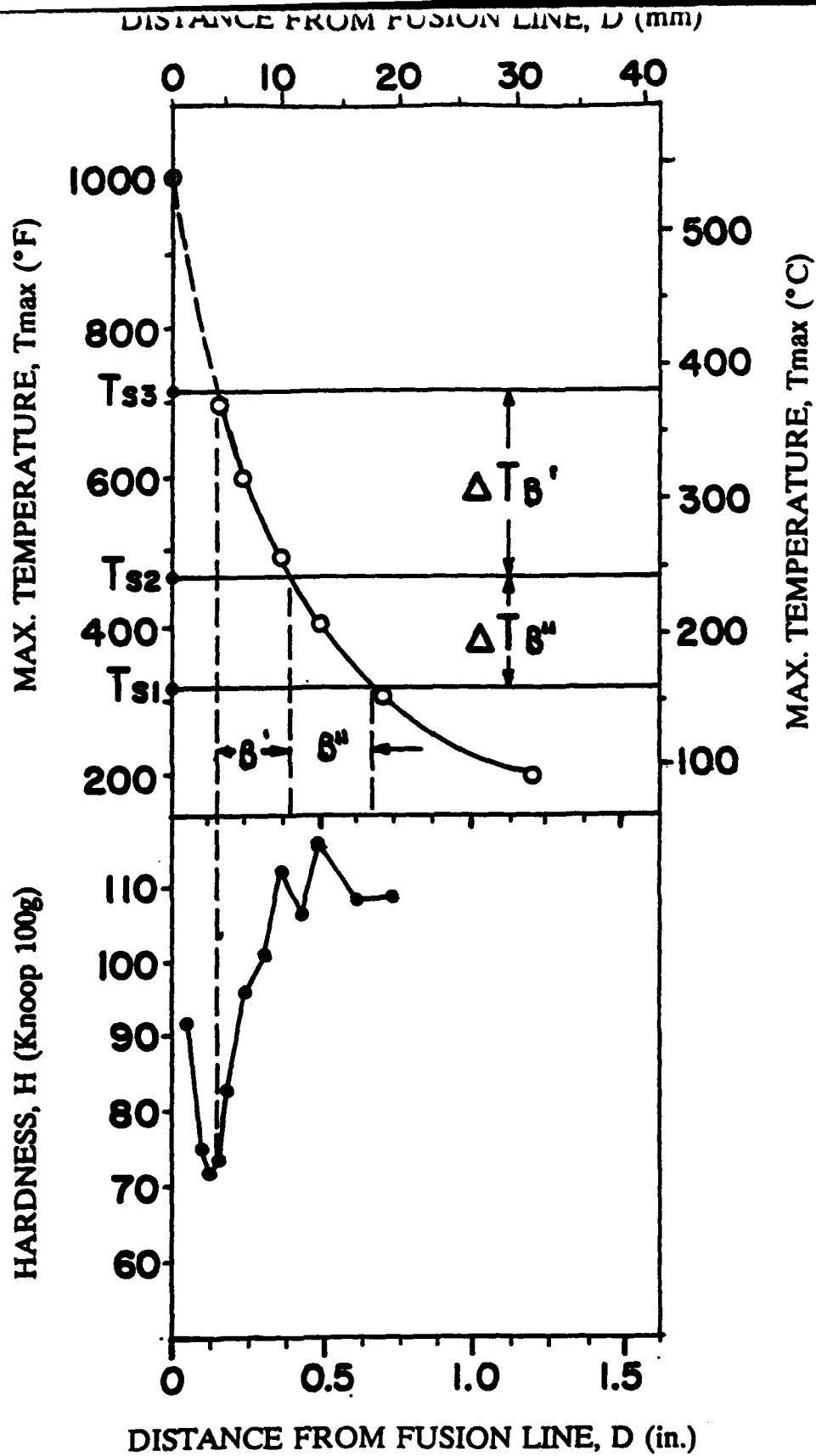


Fig. 4-19. Effect of maximum temperature distribution on microhardness and microstructure in the HAZ (weld B23).

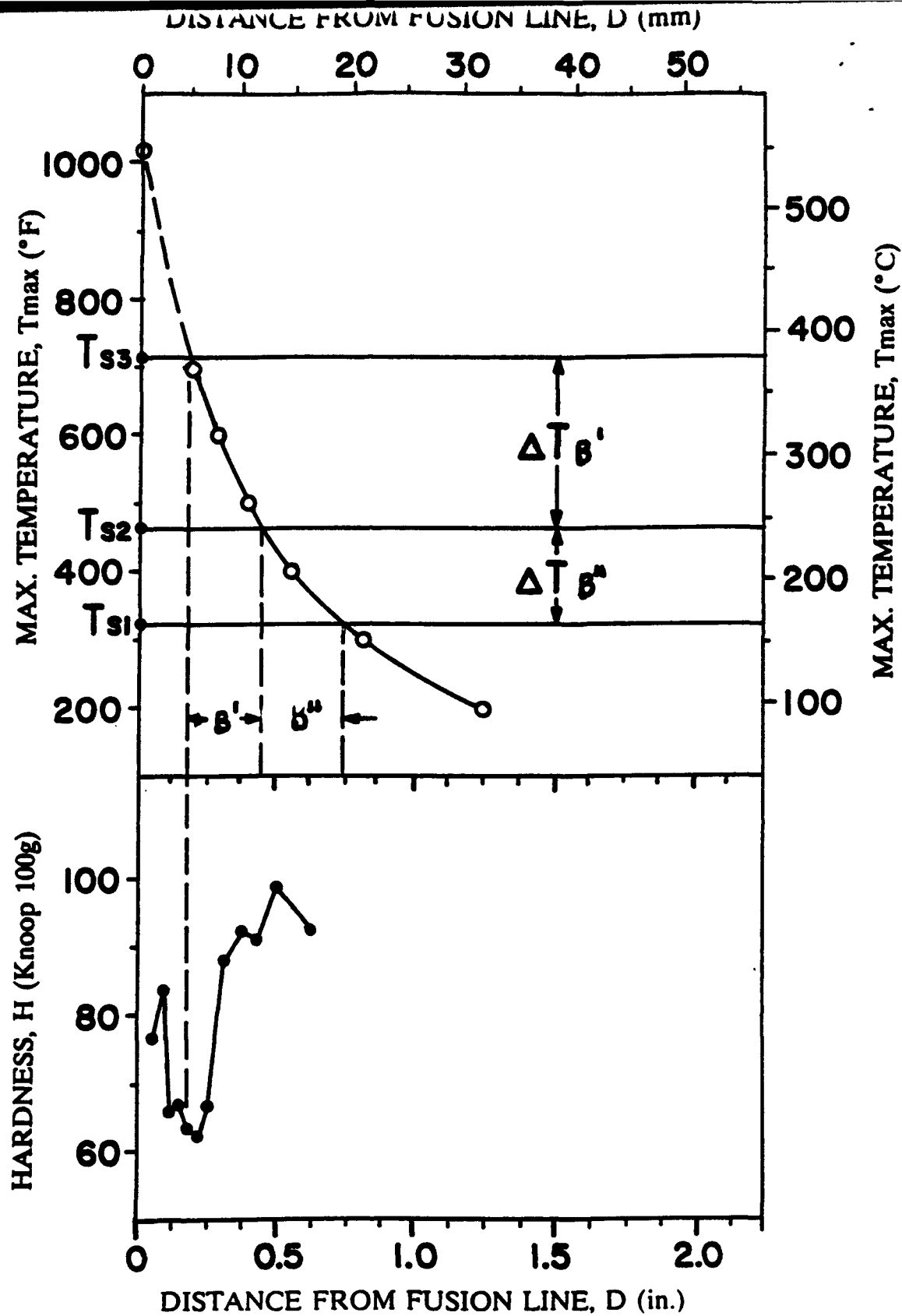


Fig. 4-20. Effect of maximum temperature distribution on microhardness and microstructure in the HAZ (weld C33).

4.6 OPTIMIZATION OF WELDING PARAMETERS

4.6.1 Results of Weld Measurements

Measurements and Calculations. A cross-section of a welded joint on each test piece was prepared for a macroexamination. The cross-sections were photographed with magnification of 10:1. As it is seen in Fig. 4-21 asymmetry of the existing welded joint design resulted in corresponding asymmetry of the weld about the groove centerline. Lack of heat sink on the side of the Middle subpanel resulted in a larger weld overlap and deeper penetration through the groove sidewall compared to those on the side of the End subpanel. This was taken into consideration when measurements of the weld profile were taken.

The following dimensions were measured (Fig. 4-21):

- weld width (Ww),
- width of the top of the groove (Wg),
- weld overlap on the Middle subpanel (Wom),
- the same on the End subpanel (Woe),
- height of reinforcement (Hr),
- minimum depth of penetration through the groove sidewall on the Middle subpanel (Hm),
- the same on the End subpanel (He), and
- max. penetration through the bottom of the groove (Hb).

Also, using a polar planimeter, the following weld cross-section areas on the photographs were measured (Fig 4-3):

- reinforcement (Fr),
- groove (Fg) and
- the entire weld (Fw).

The results of measurements were used to calculate the cross-section areas of penetration through the sidewalls and the bottom of the groove (Fp) and dilution rate of the filler metal with the base metal (DR) as follows:

$$Fp = Fw - (Fr + Fg)$$

$$DR = Fp/Fw \times 100 \%$$

4.6.2 Acceptance Criteria for Weld Geometry.

Analysis of the measurement data was performed to develop acceptance criteria for the parameters shown in Fig. 4-21.

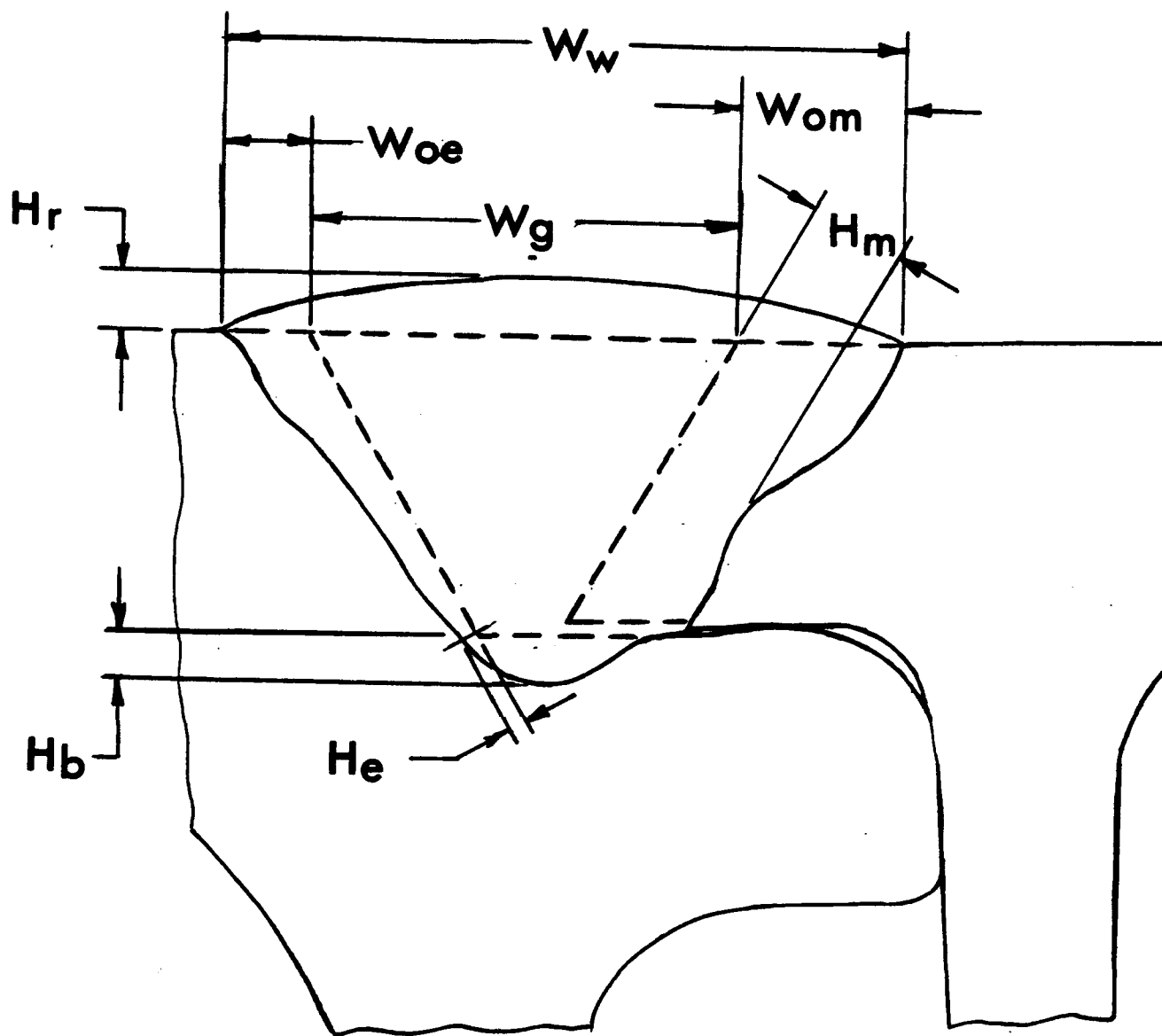


Fig. 4-21. Weld geometry.

Width of weld overlap (Wo) is an indicator of completeness of groove fill on the side of the Middle (Wom) and the End (Woe) subpanels.

Woe is always smaller than Wom due to a great heat sink on the side of the End Subpanel. If Woe is too small, this may result in a situation in which the groove may be partially filled (lack of fill condition) at a small variation of operating conditions, such as groove cross-section area or torch position relative to the center of the groove. To provide minimum margin of safety against lack of fill on the side of the End subpanel, the following conditions should be observed:

$$\mathbf{Woe\ min. = 0.031\ in.\ (1.2mm)}$$

At the same time, the weld overlap on the side of the Middle panel (Wom), which is always much greater than that for the End subpanel, should not be too wide. From the practical standpoint, the following condition should be observed:

$$\mathbf{Wom\ max = 0.187\ in.\ (4.8mm)}$$

Weld width (Ww) can be assessed based on the values of groove width (Wg) and weld overlap (Wo). Taking into consideration relatively small variations in groove width ($Wg = 0.260 - 0.275\ in.$), the criteria of acceptance for the width of the weld should be:

$$\mathbf{Ww\ min = Wg + 2\ Woe\ min}$$

$$\mathbf{Ww\ max = Wg + 2\ Wom\ max}$$

Using the values of the members in the formulae above, the limits for Ww can be calculated as follows:

$$\mathbf{Ww\ min = 0.265 + 2 \times 0.031 = 0.327\ in.\ (8.3mm)}$$

$$\mathbf{Ww\ max = 0.275 + 2 \times 0.187 = 0.650\ in.\ (16.5mm)}$$

Thus the criteria of acceptance for the width of the weld are the following:

$$\mathbf{0.327\ in.\ \leq Ww \leq 0.650\ in.}$$

Height of reinforcement (Hr) is specified by the AWS D1.2 Structural Welding Code, Aluminum (page 55). The maximum acceptable $Hr = 3/32\ in.\ (2.4mm)$. The minimum acceptable Hr from the practical standpoint was considered to be $0.030\ in.\ (1.2mm)$. Thus the criteria of acceptance for Hr was assumed to be:

$$\mathbf{0.030\ in.\ (1.2mm) \leq Hr \leq 0.093\ in.\ (24mm)}$$

Depths of penetration through the groove sidewalls (Hm, He) and the bottom (Hb) are usually associated with the possibility of incomplete fusion of the groove. At the same time, deep penetration may cause melt-through conditions and unfavorable metallurgical reactions. The acceptance criterion for the depth of penetration Hp (through the groove sidewalls or the bottom)

from the practical standpoint was assumed to be as follows:

$$0.010 \text{ in. (0.3mm)} \leq H_p \leq 0.125 \text{ in. (3.2mm)}$$

Dilution rate (DR) of the filler metal with the base metal is an indicator of potential weld susceptibility to solidification cracking in welding 6061 aluminum alloy. The higher dilution, the lower resistance of the weld metal to cracking. Since there is no data available in literature on acceptable dilution level, lower dilution was favored in comparison of competitive welds.

4.6.3 Analysis of Weld Geometry. Analysis of the results of weld measurements showed that only the welds of Series B and C can be considered as candidates for selection of optimized welding conditions. The welds of Series A are prone to develop incomplete fusion because of low power level of the arc.

Among the welds of Series B and C, two potential candidates were accepted to satisfy the criteria described above, namely B22R and C35. The measurements for these two specimens are given in Table 4-8.

TABLE 4-8. Results of Weld Measurements for Weld B22R and C35

CRITERIA	B22R		C35	
	in.	mm	in.	mm
Ww	0.446	11.3	0.475	12.1
Woe	0.056	1.4	0.050	1.3
Wom	0.106	2.7	0.150	3.8
Hr	0.040	1.0	0.040	1.0
Hm	0.070	1.8	0.085	2.0
He	0.011	0.3	0.052	1.3
DR	37.2%		59.9%	

4.6.4. Selection of Optimized Welding Conditions.

Optimized welding conditions were selected taking into consideration the following factors listed in order of their importance in Table 4-9. Two sets of welding conditions, represented by welds C35 and B22R, were selected as satisfying most of the acceptance criteria discussed above.

According to Table 4-9, C35 conditions produce more favorable results in comparison with

TABLE 4-9. Selection of Optimal Welding Conditions

#	Acceptance Criteria	Weld ID			
		C35		B22R	
		A/R	Value	A/R	Value
1.	Visual Inspection	A	No defects ^a	A*	No defects ^a
2.	X-ray Inspection	A*	PF, Gr. 1 ^b	R	PC, Gr. 2-3 ^b
3.	Mechanical Properties				
	Tensile Strength (ksi)	A	30.6	A*	31.4
	Root bend	A	No cracks	A*	No cracks
	Face bend	A	No cracks	A*	No cracks
4.	Productivity (welding speed, lpm)	A*	19.5	A	14.6
5.	Metallurgical Characteristics				
	Width of overaged zone W_{OAZ} , (in.)	A	0.156	A*	0.156
	Width of the HAZ, W_{HAZ} , (in.)	A	0.562	A*	0.281
	Dilution, D (%)	A	59.9	A*	37.2
6.	Susceptibility to melt-through conditions	A		A*	
7.	Weld Geometry				
	Weld width, W_w , (in.)	A	0.48	A*	0.45
	Weld reinforcement, H_r , (in.)	A	0.02-0.040	A*	0.040
	Depth of penetration into groove bottom, H_b , (in.)	A*	0.14	A	0.03
	sidewall, H_m , (in.)	A*	0.08	A	0.07
	sidewall, H_e , (in.)	A*	0.05	A	0.01

Legend: A - accepted; R - rejected; P - porosity;
F - fine; C - coarse; Gr - Grade.

Notes: (a) - Absence of cracks, undercuts, lack of fill, etc.
(b) - According to Table 1 of GARD's Specification
* - Preferred value

those to B22R if judged by criteria of productivity and porosity level. Namely, they

- Produce the least of porosity and
- Provide higher productivity.

However, these conditions are inferior judging by other criteria, namely:

- the shape of weld reinforcement is not symmetrical,
- tensile strength is slightly (2.5%) lower,
- metallurgical reactions in the HAZ are more detrimental (the widths of OAZ and HAZ are wider, dilution is higher) and
- melt-through condition is more probable for the existing joint design.

Improvement in joint design, similar to that recommended earlier in Section 2 to avoid melt-through conditions, may improve weld C35 profile and metallurgical reactions in its HAZ as well. This will make C35 welding conditions a definite choice for future mass production of the mat panels.

For the existing joint design, a modification of C35 conditions through reduction of travel speed was one of the options. In fact, 25% reduction in travel speed is allowed by the AWS D1.2 Code without requiring welding procedure requalification. Another option was to utilize B22 conditions.

4.7 VERIFICATION WELDING

4.7.1 Verification of Welding Procedure

Twelve 5-ft. long AE panels were welded and shipped to the Belvoir RD & EC for the Government-performed test in order to verify developed welding procedures and weld quality. Eight panels were welded using welding conditions requested by the Army. The conditions used were the following: A5 - 2 panels, B18 - 2 panels, B22 - 4 panels. The rest of the panels (4) were requested to be welded using C35 conditions. However, during preliminary trials it was realized that it was difficult to use C35 without a risk of melt-through conditions for the existing joint design. In order to improve the situation, GARD tried milder conditions C40 and C45. In the latter mildest set, current and travel speed were reduced, compared to C35, from 250A and 19.5 ipm to 220A and 16 ipm, respectively. However, melt-through occasionally occurred depending on the location of the joint with regard to the copper chillers. This location is varied due to variation of the width of the panels allowed by the Aluminum Association Standard ANSI H35.2. Despite this, four short panels were welded using C45 conditions. One of them was damaged by a melthrough and was redone.

The following **conclusion** was made with regard to the results of the verification of the welding procedure. Since C45 conditions were close to B22 conditions (200A, 14.6 ipm), GARD requested the Army's consent to weld full-size (long) mat panels using B22 conditions. This was necessary to avoid the risk of damaging the long panels since GARD had a limited number of extra panels available. As a reminder, B22 and C35 were the two optimal sets of welding conditions, which met the requirements of the AWS D1.2 Structural Welding Code, Aluminum. They also satisfied other requirements better than the rest of the conditions explored. The difference between C35 and B22 was that C35 is more productive. Also, typical for C-series of welds, C35 developed less porosity.

4.7.2 Verification of Welding System

Optimization of Transient Welding Conditions. This task started with the effort to determine optimal welding conditions for transient (start and termination) portions of the weld for B22 conditions.

The first trials using the existing technique (variation in ramp-down time Trd) were unsuccessful since the crater could not be completely filled when Trd was minimum (Fig. 4-22a). It turned out that the maximum ramp-down time provided by the SPC of the existing welding parameter control system was not sufficient to fill the crater (Fig. 4-22b). After consultations with CRC, GARD realized that the maximum ramp-down time could not be increased any further. That is why GARD implemented a modification of the control circuitry, namely, added a timer for each welding system in order to delay the signal for start of the termination cycle. This allowed the weld crater to be filled by the arc for additional several seconds after the carriage has been stopped and the command to start ramp-down sequence has been initiated. Experimental welding on a solid plate using a new technique showed a certain improvement in crater appearance (Fig. 4-22c) in comparison with the existing technique (Fig. 4-22b). However, in the groove on a real panel, the best crater filling conditions explored were not satisfactory.

Considering importance of the transient weld areas for future panel performance under the load of military traffic, it was decided to try **run-on** and **run-off** tabs. A normal welding practice requires that the tabs were reliably welded to the workpieces to avoid solidification cracks. However, this would probably impose a serious penalty on productivity of panel fabrication. That is why the tabs were tried without welding them to the panels but rather clamping them with the clamps of the fixture. In order to do this, each tab was cut from the full width of the corresponding

a



b



c



Fig. 4-22 Craters in weld B22: at minimum (a) and maximum (b) ramp-down times, and at 1.5 sec. delay plus maximum ramp-down time (c)

extruded subpanel. Three run-on tabs were used at one end of the panel assembly and three run-off tabs were used at the other end of the assembly as demonstrated on a 10-in. long trial panel assembly shown in Fig. 4-23. All the tabs were of the same length (1-1/2 in., 38.1mm). When these tabs are clamped in the fixture they look like a 1-1/2 in. (38.1mm) extension on both ends of the panel assembly to be welded. The results were excellent for the weld starts. Fig. 4-24a shows cross-section of the weld start after removal of the run-on tab. However, for the weld terminations, the results were not stable. Sometimes the results were relatively good as shown in Fig. 4-24b, and sometimes melt-through conditions occurred at the junctions between the panels and the run-off tabs. Heat saturation at the end of the panels and poor contact in this junction were the reasons for this to happen.

To improve the situation, an improvement in heat sink at the end of the panels was needed. GARD designed special copper chillers to increase heat dissipation. Each start and termination of each joint was chilled with a separate set of end chillers. The set consists of two chillers (Fig. 4-25a). One of them has a rectangular cross-section and is split in two tapered halves. It is inserted into the void under the joint. The other has a semi-circular cross-section and fits into the circular void in the End subpanel. This solved the problem. Fig. 4-25b shows the resulting cross-section of the end of the panel after the run-off tab has been removed.

Welding of Full-Length Mat Panels. Prior to prefabrication of the full-length (13 ft. long) panels, GARD welded several long mat panels to test the machine. The results were generally successful. However several problems were identified. There were clearance problems between the carriage #2 and the fixture. This caused interruptions in the weld and short circuiting of the wire feeder. As a result, a moderate damage to the torch #2 was done. The problems were rectified. The torch was repaired. Also, Omni-guides of the joint tracking devices turned out to be overheated by the arc. This was not evident problem when short welds were welded. However, a longer exposure in welding of the long panels damaged a plastic insulator inside the Omni-guide #2. New parts were ordered and the guide was repaired. Protective covers were installed over the guides also. There were also human errors associated with learning process of operating such a complicated system.

Ten mat panels were welded using B22 conditions and shipped to the Belvoir RD & EC. Fig. 4-26 shows stacks of the short (a) and full-length (b) panels ready for shipment.

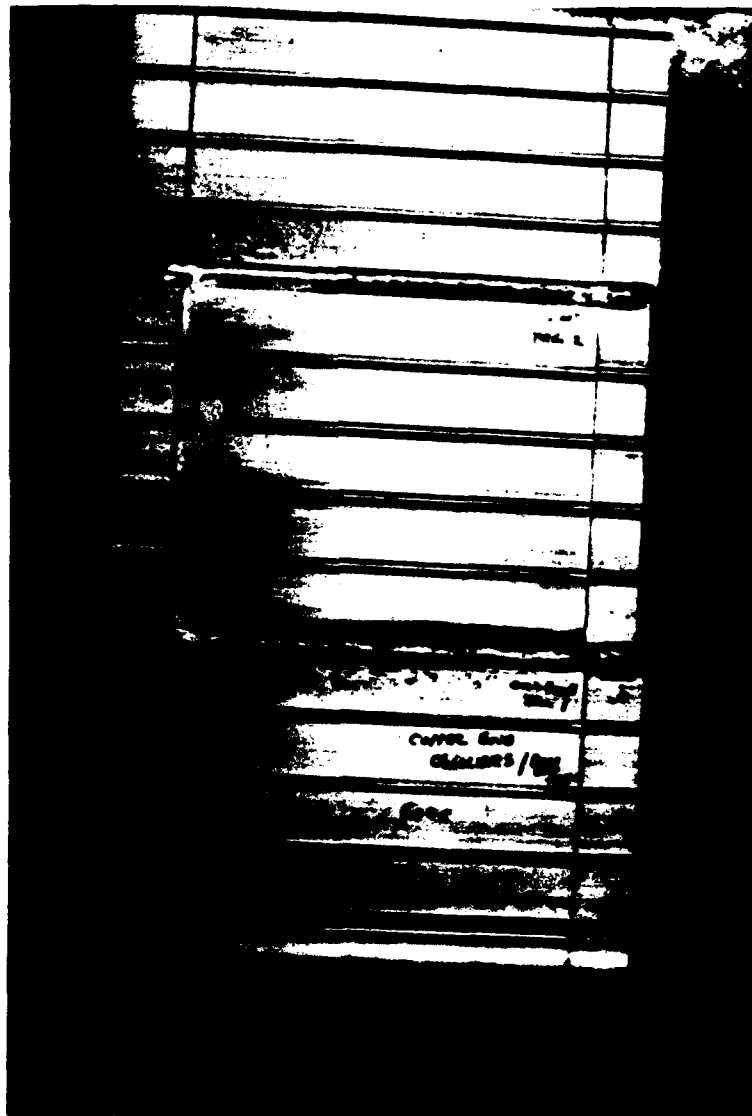


Fig. 4-23. Run-on and run-off tabs on a mock-up of the panel assembly.

a



b

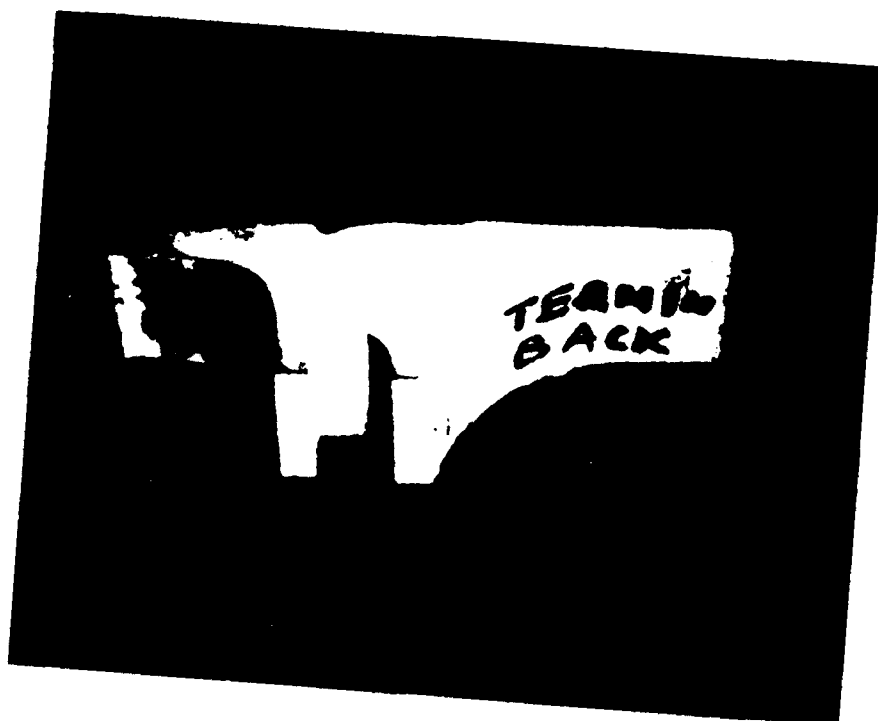


Fig 4-24 Cross-section of weld B22 after removal of the tabs: weld start (a), weld termination (b)

a



b



Fig 4-25 Copper end chillers (a) and resulting end view of the welded panel assembly after removal of the tabs (b)

a



b



Fig. 4-26. Stacks of short (a) and full-length (b) welded AE mat panels ready for shipment.

Section 5

DEVELOPMENT OF FABRICATION SYSTEM FOR WELDING ALUMINUM PANELS

5.1 BACKGROUND

5.1.1 Objectives and Scope

According to the Belvoir RD&EC requirements, the main **objective** of this task was to undertake a basic research to improve the welding process and weld quality control for aluminum extruded panels. This was required to be done through integration of means for real-time monitoring of welding parameters with welding equipment into a welding system with closed-loop feedback control and microprocessor-based interface.

The **scope** of this task was outlined by GARD according to these objectives. A unique fabrication system developed by GARD was the result of the following efforts:

- 1) Conducting basic research on welding automation, GARD created an automatic welding system with computerized closed-loop feedback control of welding and motion parameters operating in an adaptive mode.

- 2) GARD developed a unique experimental multifunctional fixturing system. The complexity and uniqueness of the system was dictated by the size, configuration, and allowed tolerances of the AE subpanels to be processed. The system design was also influenced by the Army's strict requirements for distortion of welded panel assemblies, and for weld integrity and quality. The fixturing system provides means for mechanized assembling and straightening of the panels, positioning of the welding torches and welded joints with relation to each other, joint tracking, and controlling welding distortion and adverse metallurgical reactions in the welded joints. The system can be transformed into a production prototype after some modifications. It can also be modified to process bridge deck panels.

3) Also, GARD created mock-ups of auxiliary equipment, including a panel loading structure, support and guiding mechanisms for communications lines, an original pollution control system and a water circulating station. Without this auxiliary equipment the experimental program could not be carried out. Reliable performance of the equipment proved GARD's conceptual ideas which may become a solid basis for designing similar equipment for production purposes.

All the systems and equipment developed and purchased by GARD were integrated into a unique experimental fabrication system which may facilitate dramatically creation of an efficient production line for fabrication of roadway and bridge deck panels and possibly other components in bridge and non-bridge applications.

5.1.2 Approach

In contrast to a traditional approach in development of welding automation, GARD's approach was based on a preliminary comprehensive analysis of the future fabrication environment targeted for automation, and optimization of weldment design and fabrication procedure to improve their suitability to welding automation. The most distinguishable feature of GARD's approach to welding automation was the utilization of welding expertise at all the stages of this analysis and of welding automation development later on. The most important areas of application of welding expertise were the following:

Optimization of parts and weldment design; sequence of assembling operations and assembling procedures; welded joint design, location and accessibility; tolerances of extruded parts and the welded assembly; selection of welding process, technique and position; fixture design; measures to minimize welding distortion; control of metallurgical reactions in age-hardenable 6061-T6 aluminum alloys in order to minimize their negative effect on microstructure and properties in the heat-affected zone (HAZ) of welded joints; and many other issues which might not be addressed in the traditional approach at this early stage of welding automation development.

The developed concept for welding automation was based on the optimization of the findings and results of the analysis described above. To illustrate this philosophy, there are several examples below showing interrelationships of various aspects of welding automation taken into consideration. To avoid cracks in the weld, the following measures were utilized: dilution of filler metal with the base metal was minimized through corresponding joint design (adequate cross-section area of the groove), weldment design (configuration of the mating ends), selection of welding technique (pulsed arc) and selection of electrode wire composition (crack resistant AWS ER 4043). Measures specified to prevent cracking in the HAZ influenced fixture design (introduction of special powerful clamping devices to put the HAZ in compression and the rotating capability to the fixture to keep welded parts clamped until welding on both sides has been completed). Danger of excessive loss of strength in the HAZ affected fixture design (introduction of HAZ chillers), welding parameter control system (limitation on parameter range) and carriage design (selection of a drive mechanism according to the parameter range). Requirement to control distortion influenced fixture design (straightening and rotating capabilities of the fixture), welding technique (double-electrode welding) and weldment design (joint locations symmetrical to the neutral axis of the cross-section). All these and other interrelated requirements were implemented in such a way that, when combined, they resulted in optimum final results in terms of weld geometry, integrity and properties, ease of implementation and operation, as well as the highest possible productivity. For example, it was found during implementation that the combination of the clamping arrangement scheme, fixture chilling capability and optimum welding schedule was responsible for a significant improvement in properties of the HAZ, resulting in up to 21% increase in strength of the welded joints compared to what could be obtained without these features. Welding expertise allowed all these measures to be specified on early design stages of the project.

5.1.3 Scope of Fabrication System

A general view of the fabrication system for mat panels is shown in Fig. 5-1. The system contains the following subsystems and main components:

The Fixturing System contains the following components:

- The Rotating Fixture (1),
- Two Carriages (2) and
- The Carriage Parking Mechanism (3).

The Auxiliary Equipment contains the following components:

- The Loading Structure (4),
- The Air Pollution Control System (5) and
- The Water Circulation Station (6).

The Control System consists of the following components:

- Two Power Sources (7),
- The Computerized Welding and Motion Control System (8),
- The Fixture Control System (not seen) and
- Two Joint Tracking Systems (not seen).

5.2 THE FIXTURING SYSTEM

The fixturing system is designated to perform the following tasks:

- To straighten subpanels prior to assembling, if necessary,
- To assemble subpanels into a panel assembly,
- To reliably clamp and hold subpanels in a predetermined position,
- To accurately position welded joints relative to torch travel trajectories,

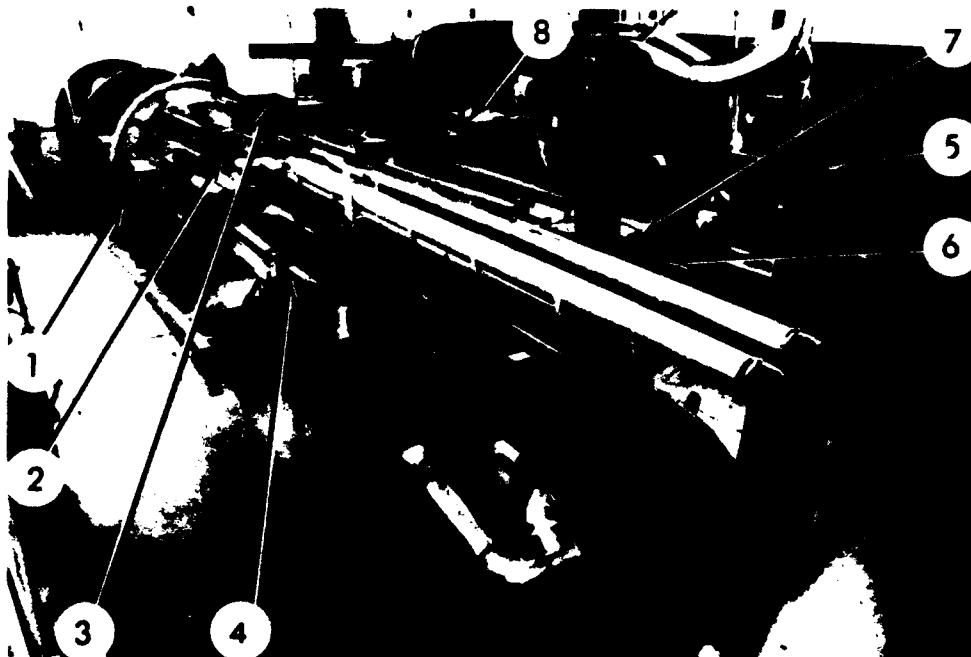


Fig. 5-1. Fabrication system for assembling and welding of the aluminum AE mat panels.

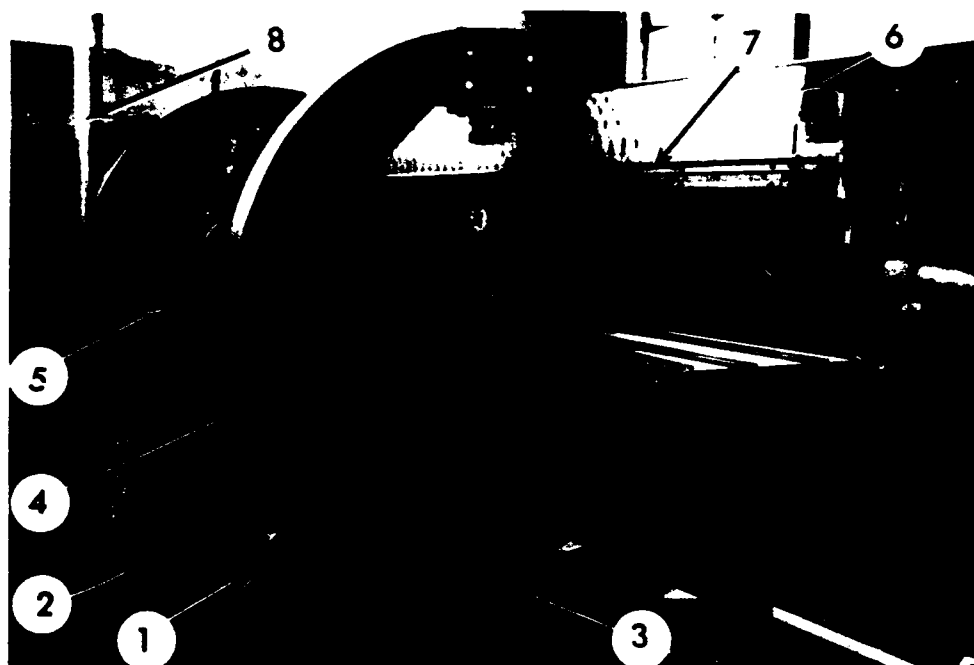


Fig. 5-2. View of the fixture.

- To provide guiding tracks for travel of two carriages along the welded joints,
- To carry welding accessories, sensors and joint tracking devices,
- To provide torch access to both sides of the panel assembly by rotation of the assembly,
- To provide flat position for welding joints on both sides of the panel assembly,
- To prevent movement of subpanels relative to each other during rotation of the panel assembly, and
- To provide artificial continuous cooling of the heat-affected zones on both sides of the welds.

5.2.1 The Rotating Fixture

The rotating fixture is shown in Fig. 5-2. It is supported by four rollers (1) mounted on the base (2). One of the rollers is driven by the fixture drive (3). The fixture has three rigid rings (4) held together by two longitudinal (left-hand and right-hand) support beams (5) and two vertical (top and bottom) support plates (6).

A pair of the guide rails (7) is mounted on both sides and along the entire length of the support plate. One pair is on the top and another is on the bottom of the support plates (6). Each guide rail contains a rack (not seen) to be engaged with the pinion (not seen) of the carriage to provide carriage travel.

The beams (5) and plates (6) support four pneumatically operated clamps for assembling mat panels, shown in Fig. 5-3. They are capable of developing a clamping force up to 250 lbs. per linear inch. Looking from the fixture drive end, the following clamps are shown in Fig. 5-3:

- the vertical clamp L.H. (1) which clamps the End subpanel (5),
- the vertical clamp Middle (2) which clamps the Middle subpanel (6),
- the vertical clamp R.H. (3) which clamps another End subpanel (5) and

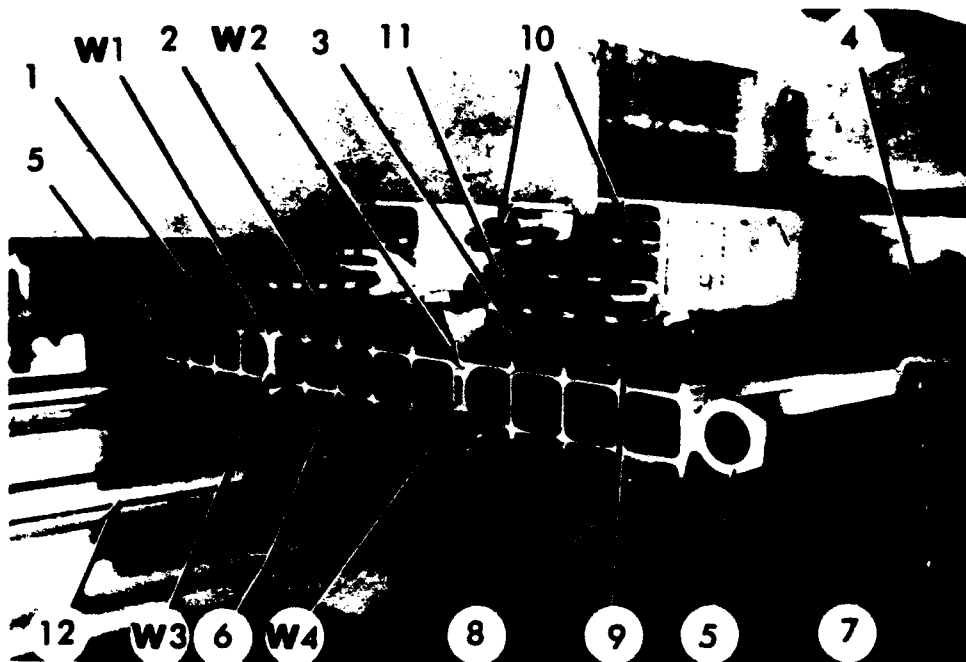


Fig. 5-3. The AE panel assembly clamped in the fixture.

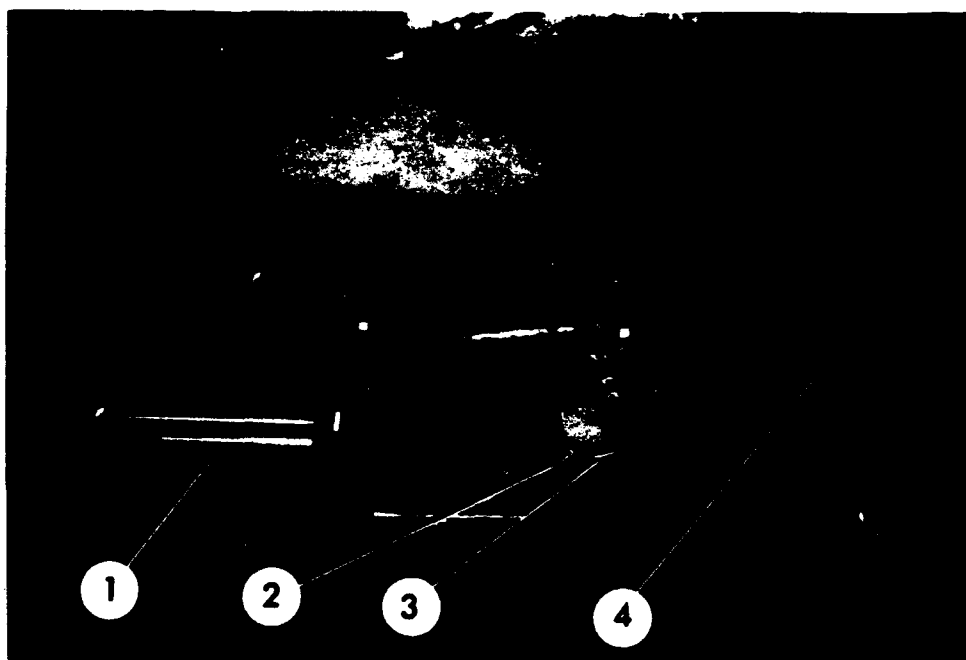


Fig. 5-4. View of the stopper mechanism.

the horizontal clamp (4) which assembles all three subpanels into a panel assembly prior to clamping.

The horizontal clamp (4) is mounted on the right-hand support beam. It can push the subpanels across the fixture against the opposite support beam with the aid of the pneumatic (inflatable air hose) actuator (7). Similarly, two smaller actuators (not seen) return the horizontal clamp to the initial position. Each vertical clamp consists of the immovable bottom base plate (8) permanently fixed to the fixture and movable top plate (9) moving with the aid of the pneumatic actuators (10) and (11), up and down, respectively. The chiller bars (12), made of continuous copper strips, are attached to the edges of the bottom (8) and top (9) plates of each vertical clamp.

The stopper, shown in Fig. 5-4, is a pneumatically operated mechanism designated to accurately bring and fix the fixture into a predetermined position after the fixture drive mechanism has stopped its rotation. This is done with the aid of the pneumatic cylinder (1) by engaging the stopper plate (2) with the stopper roller (hidden) which is mounted on the bracket (3). Two brackets are mounted 180° apart on the front ring (4) to provide two accurate fixture positions: the initial position (0°) and the reverse position (180°). Looking from the fixture drive end, the reverse position is achieved by rotating the fixture 180° clockwise (CW). Return to the initial position is achieved by the fixture rotation 180° counter clockwise (CCW).

5.2.2 The Carriages

The carriage (Fig. 5-5) is a self-propelled mechanism designated to carry:

- Welding accessories,
- Joint tracking (JT) devices and
- Sensors of welding process control system.

Two carriages roll on the guide rails (1) on both sides of the top support plate (2). After 180° rotation of the fixture, the carriages can run again on the guide rails located on the bottom

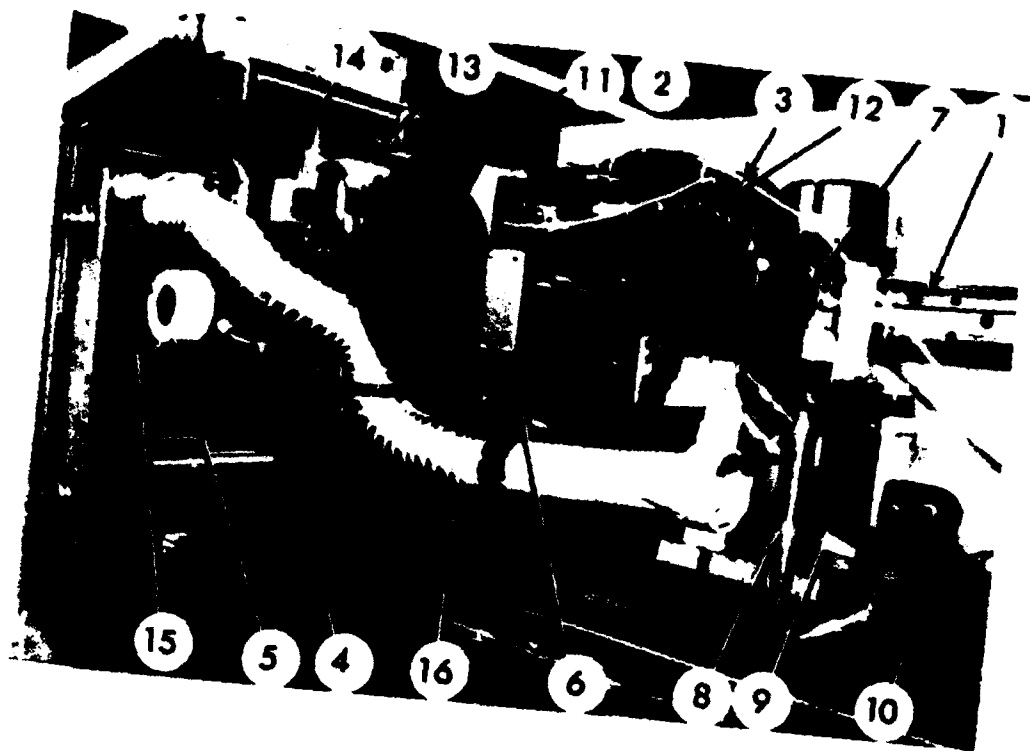


Fig. 5-5. View of the carriage.

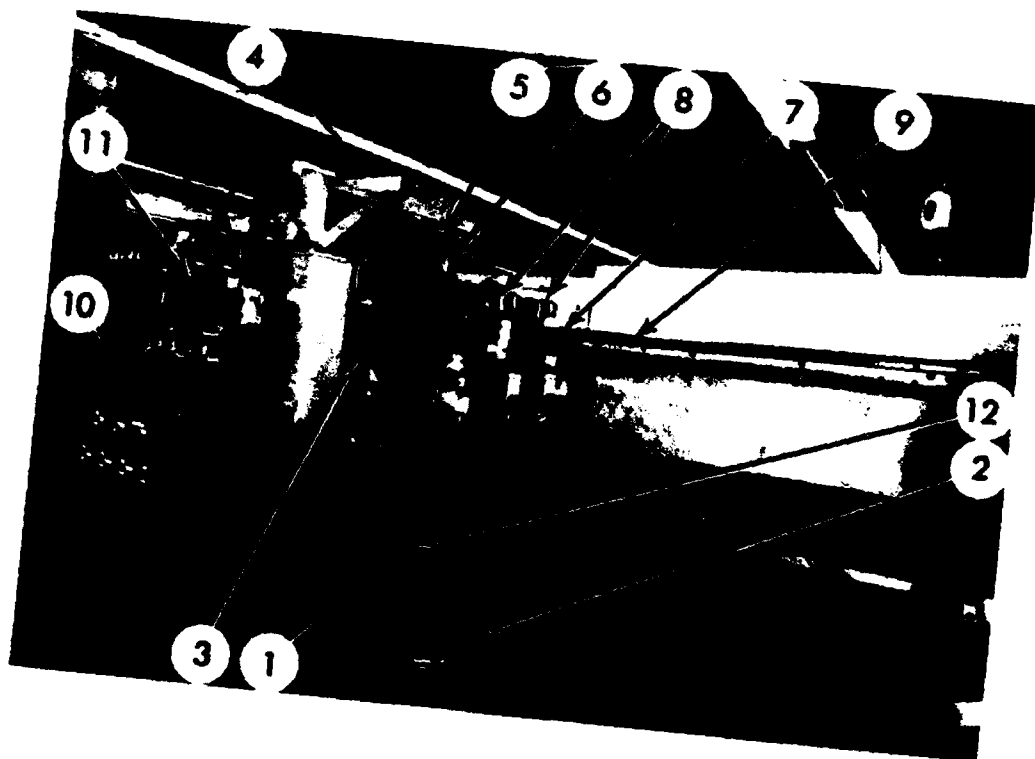


Fig. 5-6. View of the parking mechanism.

support plate (not seen). The carriage is a plate (3) equipped with a pair of the top and a pair of the bottom adjustable rollers (not seen) which are tightened to the guide rail (1). The carriage pinion is engaged with the rack of the guide rail (1). Each carriage is driven by the microstepping motor (4) with encoder (5) for feedback control of travel parameters. The carriage carries the motor-driven 2-axis JT cross-slide assembly (6) of the joint tracking (JT) system on which the capstan wire feeder (7) is installed. The capstan wire feeder provides extreme accuracy and reliable wire feeding under all welding conditions. The capstan drive, as opposed to conventional wire feeders, uses approximately 3 in. of surface contact area to transmit rotary motion to the electrode thus increasing the tractive force between the wire feed drive wheel and the electrode. This provides an extremely accurate and consistent wire feed rate. The wire feeder (7) holds the torch (8) and the manual 5-axis JT adjustment mount (9) on which the JT Omni-guide sensor (10) of the joint tracking system is mounted. The wire spool (11) is mounted on the carriage as well as four sensors: wire feed rate sensor (12), voltage sensor (13), gas flow sensor (14) and travel speed sensor (15). Current sensor (not seen) is installed separately on the parking mechanism.

5.2.3 The Parking Mechanism

The parking mechanism (Fig. 5-6) is a pneumatically operated mechanism designated for:

- Parking of the carriages outside of the fixture in "home" position initially and during the fixture rotation and
- Accurate aligning of the short guide rails of the parking mechanism with those mounted on the top and bottom support plates of the fixture.

The parking mechanism consists of the rigid stand (1) mounted on the base (2) of the fixture. The vertical slide (3) can move up and down along the stand (1). It carries the lateral slide (4) which can move transversely. The lateral slide (4) in its turn carries the longitudinal slide (5) which moves longitudinally back and forth. The vertical plate (6), welded to the longitudinal slide

(5), supports a pair of short guide rails (7) on which a pair of carriages (8) park in the "home" positions on both sides of the vertical plate (6). The racks (not seen) and the short guide rails (7) of the parking mechanism are automatically positioned in strict alignment with those (9) of the fixture when the vertical (3) and lateral (4) slides are pushed against their corresponding stops by their air cylinders (not seen). The air cylinder of the longitudinal slide (5) brings the short guide rails (7) in contact with those of the fixture (9) so that they become continuous tracks for travel of the carriages. A control cabinet of the fixture control system (10) is mounted on the stand (1). It controls the pneumatic valves (11) of the air cylinders. Two control units (12) of two joint tracking systems are also installed on the stand (1) of the parking mechanism.

5.3 AUXILIARY EQUIPMENT

Auxiliary equipment was added to the fixture to meet the needs of the experimental program, such as loading/unloading of heavy panels, support and guidance of numerous and extremely long communication lines and exhaust ducts, evacuation of toxic fume created as a result of welding and cooling of both welding torches. Therefore, the auxiliary equipment was built as mock-ups using mostly GARD's available lumber, scrapped metal parts and laboratory equipment. The auxiliary equipment was modified during testing and experimentation.

5.3.1 The Loading Structure

The loading structure (Fig. 5-7) is designated to perform the following tasks:

- To facilitate loading of the subpanels into the fixture,
- To facilitate unloading of the welded panel assembly from the fixture and
- To provide support and guidance for metal flexible conduits and exhaust ducts.

The loading structure represents a rigid table (1) on which multi-level support structure is built. On the top of the table (1) (first level of the structure), the roller conveyor (2) is mounted



Fig. 5-7. Views of the loading structure and air pollution control system.



Fig. 5-8. View of the duct support mechanism.

to facilitate loading/unloading operations. On the second level (3), two guide channels (4) are mounted to support and guide two flexible metal conduits containing control wires, welding cables, and gas and water hoses. Each conduit is folded forming the lower branch (5) moving in the guide channel (4). The upper branch (6) is supported by the roller assemblies (7). The roller assemblies (7) are moving along the guide (8) suspended from the beams (9) on the third level of the loading structure. An open end of the lower branch (5) of the conduit is permanently attached to the structure of the second level, while that of the upper branch (6) is attached to and driven by the carriage. The metal portion (10) of each exhaust duct line of the pollution control system is attached to and rides on the corresponding conduit. The third level also supports immovable cables, hoses and ducts.

5.3.2 The Air Pollution Control System

The air pollution control system (Fig. 5-7) provides:

- Efficient removal of air pollutants generated in the welding area,
- Transportation of the pollutants to the air filtering unit,
- Return of purified air into the shop and
- Support and guiding of flexible exhaust ducts.

The air pollution control system consists of the electrostatic precipitator (borrowed from GARD for this program), an industrial two-stage air filtering unit (11), two continuous exhaust duct lines (12) and two duct support mechanisms (13).

Each exhaust duct line consists of the following components. A 3-in. diameter flexible metal duct (shown in Fig.5-5, item 16) is attached to the carriage. Through this duct welding fume is sucked into the line. As shown in Fig. 5-7, fume moves further on through a 5-in. diameter non-flexible metal (10) and flexible non-metal (14) ducts, which both ride on top of the conduit. The end portion of the line, a 8-in. diameter immovable flexible non-metal duct (12), is connected to the

precipitator (11).

Each duct support mechanism (Fig. 5-8) consists of the frame (1) bolted to the table (2) of the loading structure and the rotating take-up drum (3). A 5-in. diameter flexible duct (4) is wound around the drum. During welding, the carriage drags the conduit along with the metal duct. As a result, the flexible duct is unwound off the drum. When the carriage is returned, the flexible duct (4) is wound around the drum with the aid of the dead weight (not seen) attached to the drum by means of the cables (5) and the pulleys (6). The 8-in. diameter immovable portion of the flexible duct (7) is connected to the movable 5-in. diameter flexible duct (4) (wound around the drum) through the metal ducts (8) and the rotating sleeve (9) mounted in the center of rotation of the drum.

5.3.3 The Water Circulating Station

- The water circulating station (Fig.5-9) is designated:
- To supply water for cooling two welding torches,
- To provide close loop water circulation,
- To dissipate heat accumulated during welding,
- To generate a warning signal if water stops flowing through the lines, and
- To measure water temperature.

The water circulating station (borrowed from GARD) is shown in Fig. 5-9. It consists of the pump (1) which supplies water for both welding torches under pressure of 60 psi, heat exchanger (not seen) and the aluminum tank (2) containing three gallons of water. The pump (1), the tank (2), the heat exchanger and two welding torches (connected in parallel) are connected with rubber hoses (3) to provide a close loop water circulation. Two water sensors (4) sense water flow in each torch

line. The sensor generates an electric signal to block welding start or abort welding if there is no

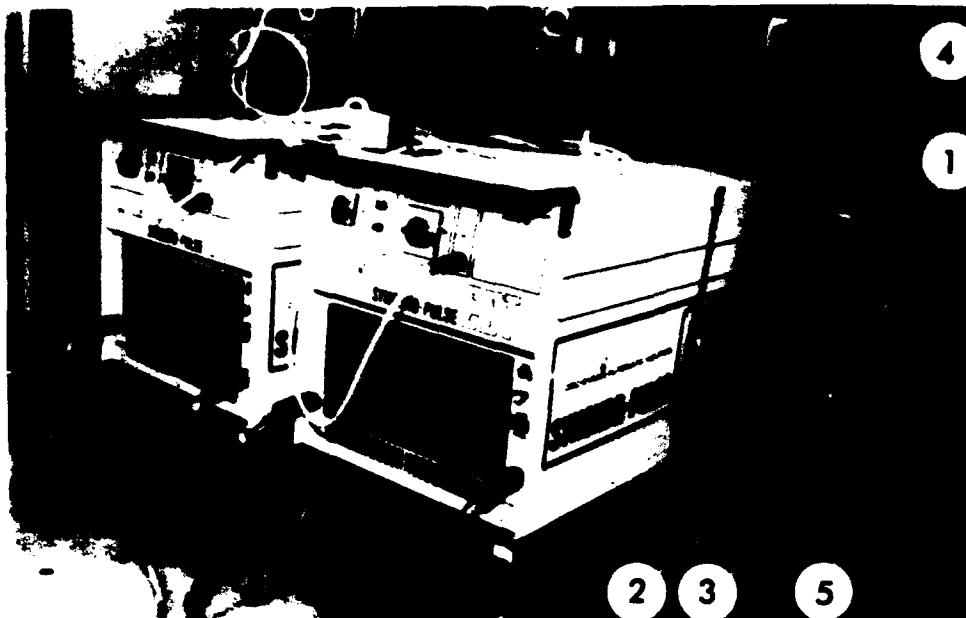


Fig. 5-9. View of water circulating station and power sources.

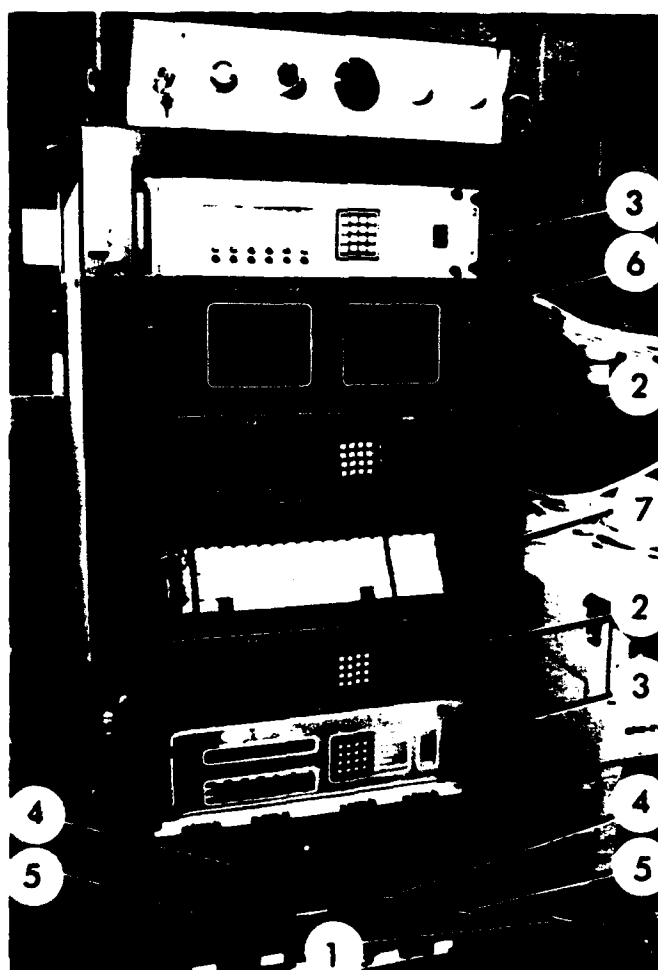


Fig. 5-10. View of the main control cabinet.

water flowing through the torch. Water temperature is measured by the thermometer (5).

5.4 CONTROL SYSTEM

5.4.1 General Description

The Fabrication Control System consists of the following major subsystems integrated under a common control:

- Two Welding Parameter Control (WPC) Systems,
- Two Motion Parameter Control (MPC) Systems,
- The Fixture Control (FC) System,
- The Host Computer, and
- Two Joint Tracking Control Systems.

The Fabrication Control System was developed by GARD. CRC-Evans Automatic Welding, a division of CRC-Evans Pipeline International, Inc., provided off-the-shelf components for the WPC systems integrated under a common control. GARD developed the MPC system (based on off-the-shelf components provided by Compumotor Corp., a division of Parker Corp.) and the FC System. Also, GARD was responsible for integration of all the control components into the fabrication system control. Although GARD's proposal did not intend to provide computer but rather "IBM PC compatibility", the fabrication system developed under this contract does include a host computer in order to expand flexibility and analytical capability of the developed system. Cyclomatic Industry, Inc. provided joint tracking systems.

5.4.2 The Welding Parameter Control (WPC) System.

The WPC system controls welding (arc energy) parameters of pulsed gas metal arc welding (GMAW) process operating in a synergic programmable mode. The objects of control are pulsed parameters, such as arc time, current, voltage, electrode extension and wire feed rate.

Initially, temperature of the HAZ of the welded joints was among the parameters to be

measured and controlled according to the Army requirements. However, as a result of an analysis of the requirements for welding process control of the automatic welding system, GARD has concluded that from a technical standpoint, temperature control is not necessary and offers little benefit for fabrication of aluminum mat panels. The reasons for this conclusion was summarized in the report "Analysis of Temperature Control Requirements for Automatic Welding System" submitted and approved by the Belvoir RD&EC. The report is presented in Appendix C1.

Each WPC system consist of the following components located in the main control cabinet shown in Fig. 5-10:

- The Synchro-Pulse CDT Synergic Power Supply (1),
- The Arc Data Monitor ADM (2), including sensors (shown in Fig. 5-5) and
- The Synergic Programmable Controller SPC (3).

Detailed description of operation and installation of the WPC system can be found in the corresponding CRC manuals provided as part of the Data Set package.

The Synchro-Pulse CDT Synergic Pulse-Power Supply is shown in Fig. 5-10, item 1 and Fig. 5-9. The term "synergic" when applied to a pulse-arc welding power supply, simply means "a single knob control", which automatically tunes the power supply to provide the proper pulse parameters for a given wirefeed setting. The parameters that should be adjusted via this single knob, in a truly synergic power supply, are as follows:

- Pulse frequency or duty cycle,
- Background current,
- Background voltage, and
- Wirefeed speed.

All of the aforementioned parameters must be adjusted with an appropriate change in wirefeed speed in order to ensure proper pulse conditions.

The primary reason for using a pulse-arc process is to provide a means for stable weld metal transfer, while reducing the average voltage and current input to the weld material. In the pulse-arc process, the weld material is transferred in a spray transfer mode. To reduce the amount of energy supplied to the work piece, the pulse parameters must be accurately controlled. By

evaluating the arc physics involved in material transfer through a plasma column, it can be seen that the primary heating elements available for melting and transferring the weld material from the filler wire to the weld pool are as follows: anode heating potential, electrode extension and resistivity of filler wire.

The anode heating potential is a function of the ionization potential of the shielding gas. The resistivity for a given filler wire can be determined by the electrode extension, the diameter of the wire and the composition of the wire. The electrode extension however, in a semi-automatic process, becomes operator dependent. Even in a mechanized operation the electrode extension may not be specifically defined. By knowing the aforementioned items, an optimum pulse current level can be determined that will provide sufficient energy to melt a single droplet of weld material approximately equal to the wire diameter. It is important to note that the amount of pulse current required for a specific wire type, will be affected by the type of shielding gas used. It is therefore important that the pulse parameter be determined for a specific type of shielding gas.

Two individual parameters affect the actual pulse energy available for melting and detaching a droplet of welding material. They are the Peak Pulse Current and the Pulse "On Time". In evaluating high speed photography of metal transfer in a pulse arc, it has been determined that the optimum transfer of the welding droplet occurs during the falling edge of the pulse. During this period, the energy in the plasma column is decreasing and the droplet is not overheated, while being transmitted from the welding wire to the weld pool. Both the pulse peak and the pulse "On Time" must be carefully selected for a given weld material and shielding gas. This is needed to ensure that the droplet is detached at the falling edge of the current pulse.

In conjunction with the pulse "On Time" and pulse current, the synergistic type of control must also maintain the background voltage and current levels. The background current is used to sustain the plasma column during the off period of the pulsing process. This "keep alive" current must be varied as the wirefeed speed is increased. The amount of current required in the background period is related to the impingement velocity of the welding wire and the physical arc length, the arc length being a function of the pulse peak current and voltage at the time the droplet is detached. If an insufficient amount of background current is supplied, the welding arc will extinguish at the fall of the current pulse. This will result in an increase in spatter due to the short circuiting. As the wirefeed speed is increased, the background current must also increase.

As stated previously, another contributing factor to the melting of the weld material is the electrode extension. In semi-automatic welding, this is an extremely difficult parameter to control. With small diameter wire, the electrode extension may be the major contributing heating element to the melting of the filler wire. In order to accurately control a pulse welding synergic power supply, a method was devised to accurately monitor changes in electrode extension. These changes must then result in appropriate modification of the pulse frequency or duty cycle. If this parameter is not measured, then unstable operation indicated by increased spatter or poor material transfer through the arc will occur. By sensing the impedance across the welding arc during the background period, a control algorithm was developed which allowed for compensation of the electrode extension. This control provides proper operation and selection of pulse parameters under varying electrode extension conditions.

In order to implement a truly synergic pulse power supply the following parameters must be controlled: Pulse Peak Current, Pulse "On Time", Background Current, Background Voltage and Pulse Frequency. All of these parameters are programmed into a synergic power supply to enable single knob control of pulse parameters. The single knob control controls the main welding parameter, wirefeed speed. The wirefeed speed then determines the actual pulse welding parameters required for that wirefeed speed. Each weld program must be derived for specific conditions, which include type and diameter of filler wire and the shielding gas used. Only if any of the above conditions change, then a new program must be generated.

The CDT (Control Drop Transfer) pulse-power supply is a secondary SCR switching power supply and which provides an approximate square wave output pulse. The CDT has capabilities of storing up to 12 different weld programs in an internal E-PROM. Each weld schedule is dedicated to a specific wire material, diameter and shielding gas combination. For combinations not included in the memory of the CDT, new programs can be ordered from CRC-Evans. The power supply incorporates a patented arc sensing control method for compensation of the electrode extensions. This compensation circuitry allows semi-automatic welding with optimum pulse conditions impervious to changes in electrode extension. The use of the SCR secondary switching circuitry allows optimization of pulse shape, while allowing minimum power dissipation in the weld pool. By having individual programs defined by wire type, wire diameter and gas, the CDT can optimize the synergic control algorithms for the broadest dynamic range of welding conditions.

The CDT incorporates a microprocessor which is used to implement the synergic control algorithms. It also implements the closed-loop control functions necessary to assure optimum pulse parameters under all welding conditions. By using closed-loop adaptive feed-back control methodology, the CDT can provide optimum pulse conditions and material transfer, while minimizing the heat input into the work piece; thereby reducing weld spatter and thermal distortion.

The Arc Data Monitor (ADM) is shown in Fig. 5-10, item 2. The ADM is a data logging system designed for monitoring arc welding. The ADM has the capability of monitoring arc voltage, welding current, travel speed, elapsed time, wirefeed speed, and shielding gas flow rate through real-time sensing. An extra channel is reserved for other parameters like surface temperatures. The ADM provides information regarding the primary welding parameters and their calculated derivatives (heat input, elapsed time, travel distance, etc.) to the Host Computer. Also, the ADM provides a fault analysis capability which characterizes the overall stability of the arc welding process.

The ADM is a microprocessor-controlled system which provides diagnostic testing capabilities of the welding arc. The ADM monitoring configurations are programmed through a 16-key keypad on the front panel. The ADM also has the Host Computer link which can be used to program, analyze and monitor the welding arc. The ADM also provides a hard copy printout of welding data in a tabular or graphic formats and fault analysis via an external printer as shown in Appendix C2. The analysis is done through a special software package "ADMSTAT Arc Data Monitor Statistical Analysis Program." The operational manuals of the ADM and the "ADMSTAT" are provided as part of the Data Set package. The print format and type of print are programmable through the ADM keypad and the Host Computer interface.

The ADM is connected to the wirefeed drive system and the gas-flow lines. Arc voltage is sensed between the welding torch and the work piece. The welding current sensor is mounted on the parking mechanism. The voltage and current signals are connected to the analog signal processor within the ADM. The wirefeed speed, travel speed, and gas flow are all coupled to the digital-transducer I/O within the ADM. As an outside feedback link, a fault signal is connected from the internal I/O section of the ADM to the outside weld controller. This signal provides fault indication or out-of-bound conditions for any of the predetermined welding parameters. This ADM capability can be used for indirect in-process non-destructive inspection of weld quality. In fact, the fault output signals can be utilized to provide the following:

1) Warning information to the operator through audio and/or video signals about abnormal conditions detected by the system control. The operator can mark the defective areas of the weld manually. The welding parameter responsible for this can be determined by plotting the time of accident (calculated by dividing the distance between the defective area and the weld start by travel speed) against the data on a tabular or a graphic printout recorded by the computer.

2) Passive intrusion into the process by activating a paint-marking mechanism to mark defective portions of the weld.

3) Active intrusion into the process by interrupting the welding process automatically.

The Synergic Programmable Controller (SPC) is shown in Fig. 5-10, item 3. The SPC is a microprocessor-based, programmable controller that provides necessary control and interface circuitries for operating the Synchro Pulse CDT Power Supply and Capstan Wire-Feed System.

The major components of the SPC are as follows:

1) Precision wire feed controller which provides a wire feed speed regulation of 0.05 percent of set point. This controller is a microprocessor-based phased-loop control (PLL) which provides precise speed regulation required for synergistic operation of the Synchro Pulse CDT. Wire-feed speeds, ramp-up and ramp-down times, crater fill and burn-back times are programmed using the SPC.

2) The microprocessor-based CPU provides the necessary operator and control software interfaces for operating the SPC. The CPU consists of an 8-bit microprocessor, a 40 character LCD alphanumeric display and a 16-key key-pad used for data entry. This provides the operator interface to the controller and allows the user to program the parameters like wire feed speed, ramp up, ramp down routines, crater fill and burn back times, and to select the desired Synchro Pulse CDT welding schedules.

In addition to these standard items, an additional RS-232C communication port and a 0-10 volt analog output channel were included. The RS-232C port is used to communicate with the Arc Data Monitor (ADM) to provide control input information to the wire feed speed control system and to the Synchro Pulse CDT. The additional 0-10 volt analog channel can be used to interface the complete control system to an external travel-speed controller. The actual travel speed is monitored by the ADM, which in turn, can communicate corrective measures to the SPC. The SPC then can provide changes in the speed reference output analog channel.

The WPC Pendant is shown in Fig. 5-11a. It is suspended from the support stand (See Fig. 5-2, item 8). The front panel of the pendant is divided into three sections.

The "**Systems Control**" (top section) is designated for controlling both WPC systems simultaneously. It contains pushbuttons which exercise the following functions for both WPC systems.

- "**E (emergency). Stop**" pushbutton stops welding in emergency situations without initiating proper termination schedules (sequence of operations).

- "**Start. Weld**" pushbutton starts welding by initiating starting welding schedules.

- "**Stop. Weld**" pushbutton stops welding by initiating termination welding schedules.

"Torch I" (middle section) and Torch II (bottom section) are designated for controlling each of the WPC systems separately. Each section contains similar pushbuttons and switches which exercise the following functions for each of the corresponding WPC systems:

"**E. Stop**", "**Start, Weld**" and "**Stop, Weld**" pushbuttons have the same functions as described above for the top section.

"**Purge**" two-position switch allows shielding gas flow rate to be checked prior to welding.

"**Wire**" three-position switch allows forward and reverse manipulation of welding wire to be performed prior to welding.

"**Volt**" and "**Amp**" two-position switches allow fine adjustment of voltage and amperage to be made during welding.

5.4.3 The Motion Parameter Control (MPC) System

The MPC system is shown in Fig. 5-10, items 4 and 5. It controls motion parameters of the welding torch which rides on the carriage. The system is based on the Compumotor Microstepped System which controls travel speed, acceleration/deceleration and distance of the carriage. Each system consists of the following main components (Fig. 5-10):

- Indexer (4),

- Drive (5), and

- Microstepping motor (located on the carriage, Fig. 5, item 4).

A detailed information about the MPC system can be found in the Compumotor manual provided as part of the Data Set package.

The MPC system is schematically shown in Fig. 5-12. **The Indexer** is a microprocessor-based device designated to generate pulse rates according to commands provided by the computer. The

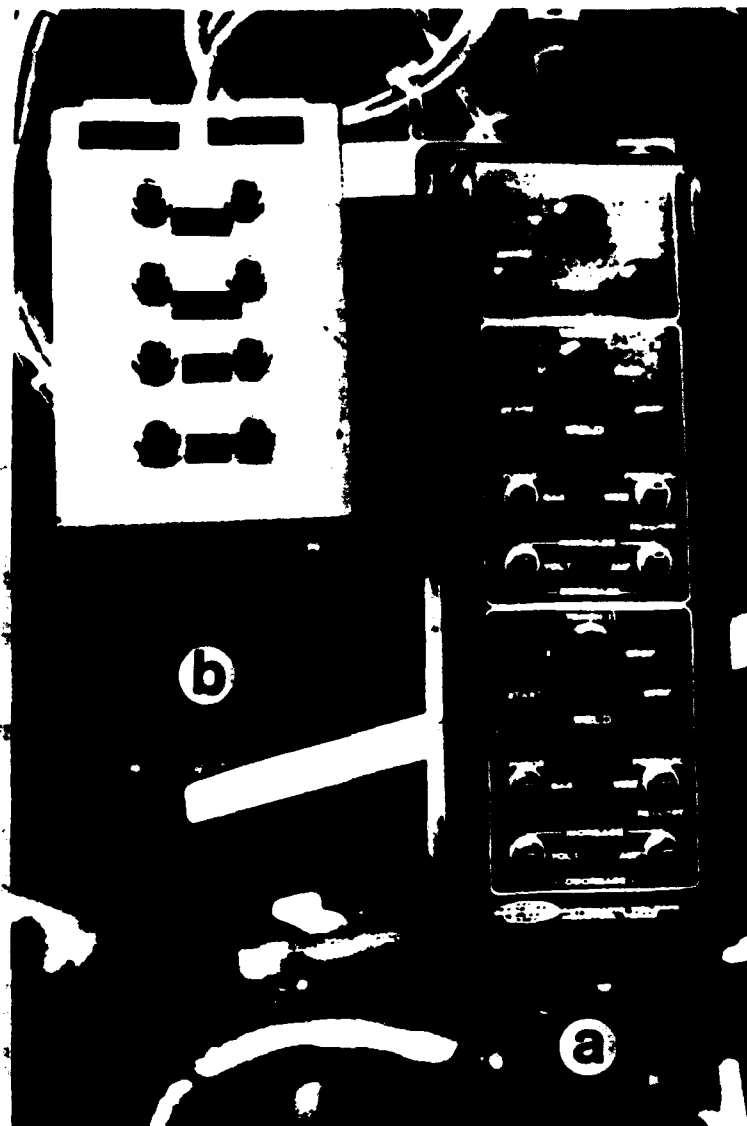


Fig. 5-11. Views of the welding (a) and motion (b) parameter control pendants.

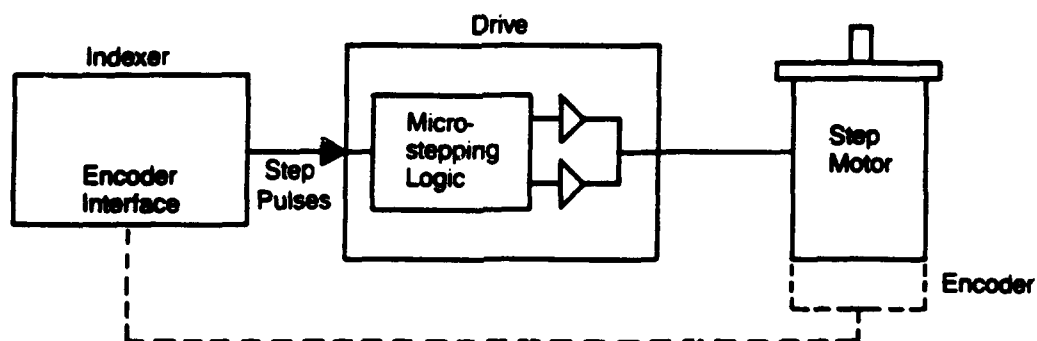


Fig. 5-12. Schematic representation of Compumotor motion parameter control system.

C3). The drive receives step pulses and a direction signal from the indexer. Microstepping logic determines the correct current level for each phase of the microstepping motor. The power amplifiers generate and maintain these levels. The power supply provides the necessary voltages from an AC source. The result is discrete incremental motion that is effectively continuous at any speed. Position is determined by counting pulses and verified by the Encoder. MPC system utilizes CYMO CMA 41:11-E CYMO gearmotor with Encoder, Compumotor Model AH Motor Drive System and Model 372 Indexer.

The schematic of the interface between the WPC and MPC systems is given in Appendix C4.

The MPC pendant (shown in Fig. 5-11b) is also suspended from the support stand (see Fig. 5-2, item 8). The front panel of the pendant is divided into two sections, namely "No. 1" (left) and "No. 2" (right) sections.

Each section is designated for controlling the corresponding MPC systems autonomously and contains pushbuttons which exercise the following functions.

"Start" and "Stop" pushbuttons initiate and terminate carriage movement. They are used for prepositioning of the carriages prior to welding or for returning them into the "home" positions after welding.

"FWD" and "REV" pushbuttons establish forward and reverse directions of carriage travel, respectively.

5.4.4 The Fixture Control (FC) System

The FC system is designated to control air cylinders and actuators of the fixture and the parking mechanism, and the electric drive of the fixture. All the elements of the FC system are located in the auxiliary control cabinet shown in Fig. 5-6, item 10. The pertinent documentation on FC System is given in Appendix C5. The control is carried manually with the aid of the switches located on the door of the cabinet. As shown in Fig. 5-13, switches "Fixture" and "Park Area" control the group of pneumatic valves located on the top of the FC cabinet (See Fig. 5-6, item 11). The valves operate the air cylinder of the stopper of the fixture, (See Fig. 5-4, item 1) and three air cylinders of the vertical, lateral and longitudinal slides of the parking mechanism (See Fig. 5-6, items 3,4 and 5). The top switch "ROTATE" controls the electric drive which rotates the fixture. The bottom switches control another group of the valves (located on the base of the fixture next to the rear support ring). They operate three vertical and one horizontal clamps of the fixture. Several

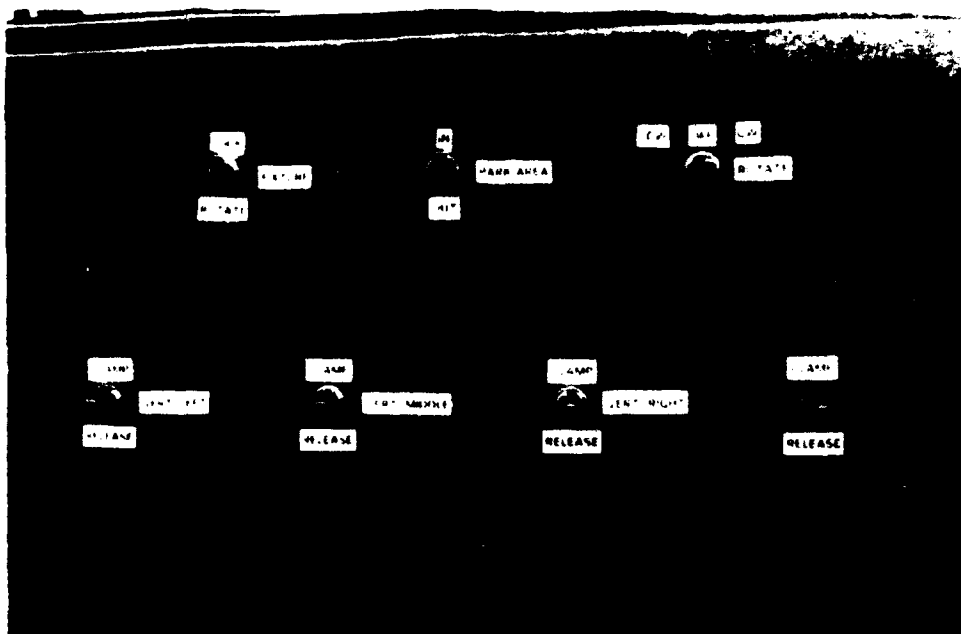


Fig. 5-13. Front panel of the auxiliary control cabinet of the fixture control system.



Fig. 5-14. Control cabinets and pendants for joint tracking systems.

limit switches are also a part of the FC system.

5.4.5 The Host Computer

The host computer, shown in Fig. 10, item 6, is primarily utilized to generate commands for the motion parameter control (MPC) system via special program developed by GARD. It is also used to record and analyze data obtained by the sensors on welding parameters via special software package "ADMSTAT" provided by the CRC-Evans. The commands to the MPC system are given using the keyboard (Fig. 10, item 7).

5.4.6. The Joint Tracking (JT) System

Each welding torch is equipped with a joint tracking system provided by Cyclomatic Industries, Inc. This is needed to offset the variations in the location of the welded joint with respect to the carriage travel trajectory. Each system is operated and controlled autonomously. The JT control system consists of the following main components:

- The JT Control Unit (Fig. 5-14, item 1),
- The JT Cross-slide assembly (Fig. 5-5, item 6),
- The JT Omni-guide sensor (Fig. 5-5, item 10) and
- The JT pendant (Fig. 5-14, item 2).

The JT system is an automatic torch positioning system. The main principles of operation of the JT system are as follows (see Fig. 5-5). The welding torch (8) is mounted on the cross-slide assembly (6) providing two-axis (lateral and vertical) positioning of the torch. The Omni-guide sensor (10) is mounted on the torch through the 5-axis mount (9). A spring-loaded pivoted tip of the sensor contacts the groove of the joint and senses any lateral and vertical deflections of the welded joint with respect to the moving torch. The control unit, located on the stand of the parking mechanism (see Fig. 5-14, item 1) contains electronic circuitry used in the system. The JT pendant (shown in Fig. 5-14, item 2) has four switches for hand-held operations:

- "**MODE**" (Manual/Automatic),
- "**SIDETRACK**" (Left/Off/Right) providing joint tracking capability when the Omni-guide sensor tip is not guided by the welded joint and
- "**MANUAL**" (Up/Down and Left/Right) providing manual torch movements in lateral and vertical directions.

More detailed description of the joint tracking system can be found in the Cyclomatic Users Manual provided as part of the Data Set package.

5.5 WELDING AND ASSEMBLING PROCEDURES

5.5.1 Weld Identification

The access/egress mat panel assembly, shown in Fig. 5-3, contains four welds, joining the following subpanels:

- End subpanel, L. H. (item 5) to Middle subpanel (item 6) - top weld #1 (W1) and bottom weld #3 (W3),
- Middle subpanel (Item 6) to End subpanel, R. H. (item 5) - top weld #2 (W2) and bottom weld #4 (W4).

5.5.2 Sequence of Welding

The sequence of welding of the subpanels should be as follows (Fig. 5-3):

- 1) Joining of the subpanels with top welds W1 and W2,
- 2) Rotation of the panel assembly 180°, and
- 3) Joining the subpanels with bottom welds W3 and W4.

5.5.3 Torch and Wire Positioning Parameters

The following positioning parameters of the torch and the wire relative to the welded joint are to be checked prior to welding:

- Torch angle (a) - an inclination of the torch centerline to the horizontal in the vertical plane,
- Wire angle (b) - an inclination of the wire centerline to the horizontal in the vertical plane,
- Nozzle extension (c) - a torch contact tip extension outside of the nozzle,
- Wire extension (d) - a distance from the top of the subpanel to the contact tip of the torch,
- Wire displacement (e) - the max. allowed lateral displacement of the wire from the centerline of the joint.

5.5.4 Cleaning of Subpanels and Storage of Wire

Cleaning of the subpanels is needed prior to welding to remove surface contaminants such as paint, oil, grease, moisture, dirt, oxides, etc.

- Clean the surfaces to be welded upon and adjacent surfaces about 3/8 in. wide from the top of the groove and bevel edges.
- Clean the surfaces four hours or earlier prior to welding by degreasing in methyl ethyl ketone and then brushing with a fine stainless wire brush to bright metal.

- Do not soil cleaned surfaces with fingerprints, dirty gloves, etc.
- Degrease the brush every day.

Storage of the wire should be done using the following precautions:

- Store the aluminum wire and rods used for repair in a special hermetically sealed container filled with argon under higher than atmosphere pressure in a dry place at relatively uniform room temperature.
- Return the wire (or rods) to the container if it is not used for welding for eight hours or more. The container should be pressurized and tightly sealed again whenever pressure is close to zero.

5.5.5 Fixture Preparation

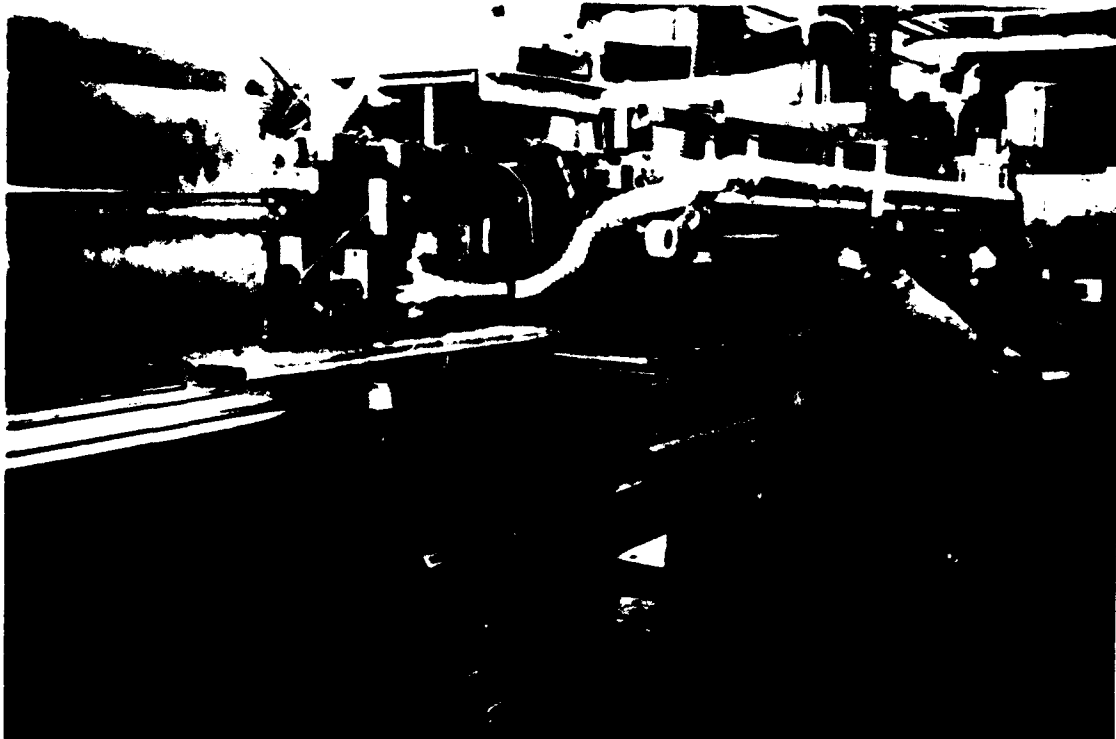
- Turn on the shop electric and compressed air lines. Pressure shown on the gages should be 70-80 psi for the high pressure line (clamping) and 30-40 psi for the low pressure line (clamp release).
- Make sure that:
 - Fixture is in the initial (0°) position (Fig. 5-2),
 - Fixture stopper is engaged with the roller of the front ring (Fig. 5-4),
 - All the clamps (Fig. 5-3) are released,
 - The carriages are in the "home" positions on the parking area (Fig. 5-6),
 - The guide rails of the parking area are engaged with those of the fixture (Fig.

5-6).

5.5.6 Fixture Loading

- Bring the subpanels to the welding machine and place them on the roller conveyor (Fig. 5-15a). Align the subpanels transversely with the corresponding vertical clamps.
- Push each subpanel inside the fixture until the subpanels are completely inserted into the fixture and lie under the corresponding vertical clamps (Fig. 5-3). Allow 1-1/2 in. from the edge of the clamps for the run-on tabs.
- Make sure that the center of each welded joint is located approximately in the middle between the copper chillers. Edges of the subpanels should be aligned evenly.
- Install run-on and run-off tabs and align them with the subpanels. Each tab is a 1-1/2 in. long piece of the corresponding subpanel. Three tabs are installed on each end of the panel assembly. Fig. 4-23 shows the location of the tabs on an experimental mock-up of the panel assembly.

a



b



Fig. 5-15. Loading of the subpanels (a) and presetting of motion parameters (b).

- Make sure that the groove formed between the tabs is a continuation of that formed between the corresponding subpanels.

5.5.7 Clamping and Straightening

Clamping is performed as follows:

- Turn on switch "Horizontal, Clamp" and all three subpanels will be pressed against the opposite wall of the fixture. Wait for 5-10 seconds until full pressure is applied.
- Turn on other three switches "Vertical Left, Clamp", "Vertical Middle, Clamp" and "Vertical Right, Clamp." All three subpanels will be clamped as shown in Fig. 5-3.

Straightening of the subpanels is sometimes needed when one or more subpanels are out of straightness or flatness limits. In this case, straightening is performed as follows:

- Repeat the clamping operations once or twice prior to actual clamping.

5.5.8 Chiller Installation

- Insert a set of copper end chillers in the openings inside the tabs and subpanels. Each set is designated for each of four welded joints as shown in Fig. 4-25a. This is needed to avoid melt-through conditions at the junction between the tabs and the subpanels.
- Move two tapered halves of the rectangular chiller into the opening under the groove until they wedge themselves. Tap slightly with a hammer.
- The chiller should be inserted far enough to provide heat sink to both the end portion of the panel assembly and the tab.
- Move the round chiller into the opening and wedge it with a piece of wood.

5.5.9 Presetting Welding and Motion Parameters

For the operating conditions described below, welding parameter settings should be as follows:

1. Operating Conditions

Station (Torch) #		1 or 2
Weld #		W1,W3 or W2,W4
Number of passes per weld		1
Shielding gases		Weld grade argon,100%
Wire diameter	(in.)	0.045
Nozzle diameter	(in.)	0.75

2. Welding Parameters *

Wire feed speed	(ipm)	350
Wire run-in speed	(ipm)	100
Current (approx.)	(amp)	190 ^a
CDT schedule #		2 ^b
Prepurge time	(sec)	3
Postpurge time	(sec)	5
Wire feed ramp up	(SPC setting)	1 (100 ipm/sec)
Wire feed ramp down	(SPC setting)	1 (100 ipm/sec)
Arc voltage, static	(SPC setting)	151 ^c
Arc voltage (approx.)	(volt)	22 ^a
Gas flow rate	(cf/hr)	32

3. **Motion Parameters***

Travel Speed	(computer setting)	0.40 (14.6 ipm)
Travel start delay	(timer setting)	2.0 (2.0 sec)
Travel stop delay	(timer setting)	1.5 (1.5 sec)

Notes: * Welding and motion parameter settings are based on B22 conditions described in Section 4 and applied to Access/Egress Mod. 2 mat panels only.

^a This parameter is not directly controlled and is given for reference purpose only.

^b The CDT schedule numbers for various wire compositions and diameters and shielding gases are given in Appendix C6.

^c This parameter may be slightly changed if spatter occurs during welding.

Welding parameters (except gas flow rate) are preset on the SPC board (Fig. 5-15b) for each station (torch) as described in the CRC-Evans SPC Operation/Installation Manual provided as part of the Data Set package. Illustration of this procedure for wire feed rate is given in Appendix C7. Gas flow rate is preset on the gas flow sensor located on the carriage.

Motion parameters (travel speed) are preset on the computer keyboard as described in Appendix C7. Travel start and stop delay times are preset on the corresponding time relays located at the bottom of the main control cabinet.

5.5.10 Torch and Wire Positioning

- Bring each carriage to the "start" position, (approximately in the middle of the run-on tabs). This is done by pushing the corresponding buttons "FWD, No. 1" and "FWD No. 2" on the MPC (motion parameter control) pendant (see Figure 5-11b).

- Initiate joint-search operations. Push the button "Down" on each JT (joint tracking) pendant. Each torch goes down until the Omni-guide of the joint tracking device is in a close proximity to the joint. Push the buttons "Auto" and "Start Cycle" on each of the JT pendant. Each Omni-guide sensor tip will automatically establish its position in the center of the corresponding groove.

- Check whether the tip of the wire is in the center of the groove. If not, correct wire position using manual cross slide of the 5-axis mount (see Fig. 5-5, item 9).

- Check wire positioning parameters (described in 5.5.3.). The parameters for each torch should be as follows:

• Torch angle (a)	(deg.)	$90 \pm 2^\circ$
• Wire angle (b), approx.	(deg.)	$5^\circ *$
• Nozzle extension (c)	(in.)	$.030 \pm 0.15$
• Wire extension (d)	(in.)	$.625 \pm .015$
• Wire displacement (e)	(in.)	$0 \pm .010$

Note: * The value is given for reference only. The wire angle is a result of prebending the wire inside the wire feeder to form a uniform annular cast opposite to direction of welding.

5.5.11 Welding of Weld W1 and W2

- Welds W1 and W2 are performed on the face side of the panel assembly with torches #1 and #2, respectively.

- Push button "START, "SYSTEM CONTROL" on the WPC (welding parameter control) pendant (see Fig. 5-11a). The start welding schedule (a programmed starting sequence of welding operations) will be performed automatically for both welds simultaneously according to the preset welding parameters (described in 5.5.9).



Fig. 5-16. Welding of the AE mat panels is in progress.

- The operator duty is to periodically watch welding process (Fig. 5-16).
- The end welding schedule begins separately for each weld after each carriage has reached the corresponding limit switch at the end of its travel. If the operator pushes button "STOP, SYSTEM CONTROL," the end schedule for both welds will be initiated simultaneously at any moment during welding.

5.5.12 Interweld Operations

The interweld operations are performed to make preparations for welding of the back side of the panel assembly.

- Raise the tips of each Omni-guide sensor above the weld by pushing the corresponding buttons "UP" on the JT pendants.
- Return the carriages to their "home" positions by pushing the buttons "REV, No. 1" and "REV, No. 2." The carriages will stop automatically by the corresponding limit switches.
- Disengage the guide rails on the parking area and the fixture by turning switch "PARKING AREA" in "OUT" position.
- Release the fixture stopper by turning the switch "FIXTURE" in "ROTATE" position.
- Rotate the fixture 180° by turning switch "ROTATION" in "CW" position. This will turn the fixture 180° in a clockwise direction. The fixture will be stopped automatically close to the 180° position by a limit switch.
- Engage the fixture stopper by turning the switch "FIXTURE" in "LOCK" position. This will bring the fixture accurately into the 180° position.
- Engage the guide rails of the parking area and the fixture by turning switch "PARKING AREA" in "IN" position.

5.5.13 Welding of Welds W2 and W4

- Repeat operations described in 5.5.10 and 5.5.11 to position the torches and the wires, and to perform welding of welds W3 and W4.

5.5.14 Postweld Operations

- Repeat operations described in 5.5.12 to return the carriages to the "home" positions. To bring the fixture in the initial (0°) position, turn switch 'ROTATION' in 'CCW' position.

- Release all four clamps by turning the corresponding switches in "RELEASE" positions.

The welded assembly will be released.

- Remove the welded panel assembly from the fixture onto the roller conveyor.
- Clean the shields on the tips of the Omni-Guides of joint tracking devices from spatter regularly (after each welding cycle).
- Clean copper/steel edges of the clamps facing the weld from accumulation of dust, spatter, etc. with a rag regularly (once a week).
- Check the size of the opening of the exhaust pipe at each torch. Normal opening should be covered over approximately 75% of its square area and not produce draft down at the nozzle area.

SECTION 6

CONCLUSIONS AND RECOMMENDATIONS

6.1 DESIGN OF ACCESS/EGRESS MAT PANELS (Conclusions for Section 2)

The following conclusions can be made with regard to efforts to design welded modifications of the aluminum panels made of extruded 6061-T6 aluminum alloy.

6.1.1 Welded Modifications of the AE Panel

The access/egress (AE) roadway mat panel designed by the U.S. Army Waterways Experiments Station (WES), Corps of Engineers, Vicksburg, MS was modified by Chamberlain GARD.

A welded version of the WES AE multisectional panel design is an attractive alternative to a one-piece extruded AE mat panel currently used by the Army.

A three-section (sub-panel) design is an optimal concept judging by many considerations, including extrusion cost and availability, product cost and ease of fabrication, amount of welding and weld quality.

Two modifications were designed for the welded AE mat panels. Mod. 1 incorporates Types I or II end configurations/welded joint designs, while Mod. 2 features Type III end configuration/joint design.

6.1.2 Welded Joint Design

According to GARD's stress analysis, and U of I and GARD's fatigue performance analyses, Type I (complete penetration) welded joint is adequate for both roadway and bridge applications.

Under the traffic load specified by the Army, a very high service life (crack initiation and propagation lives) was estimated for Type I joint. However, application of this joint design in production is associated with a number of difficulties.

Type II (partial penetration) welded joint design is considered inadequate for bridge application due to its low crack initiation life. However, its very high crack propagation life combined with ease of fabrication makes it a realistic candidate for roadway application.

Type III V-groove butt joint with an integrated backing lip is an optimal welded joint design which can be universally applicable to both access/egress and bridge deck panels. It combines the advantages of both Type I and Type II joints from production and performance points of view.

Type III joint design needs some minor modification judging by the results of the welding experimental program. The cross-section of the end subpanel should be enlarged to withstand higher current without melt-through.

6.1.3 Bridge Deck Panel Design

Fabrication of the Ribbon Bridge (RB) and Light Assault Bridge (LAB) deck panels is possible using the fabrication method developed by GARD for the AE roadway mat panels.

However, the design of the bridge panels should be modified according to the corresponding concepts developed by GARD.

6.1.4 Extrusion Availability

Availability of extrusion in the U.S. and Canada was evaluated by GARD using a bid-survey methodology.

Availability of one-piece extrusion for the AE mat panel is presently extremely low.

Presently, out of 195 presses owned by the extruders in the U.S. and Canada, only 4 presses have capacity (above 14,000 ton) to produce extrusion larger than 24 in. (610 mm) circle size. They are owned by only 2 companies.

The situation even worsened since 1988 when there were 5 presses owned by 3 companies.

The idea of fabricating the AE mat panels from narrow (less than 9 in., 225mm circle size) extruded sections proved to be a very fruitful one. It considerably increased (up to 8 companies) the manufacturing base capable of producing the AE mat panels.

6.2 EXPERIMENTAL PROGRAM AND FABRICATION SYSTEM

(Conclusions for Sections 4 and 5)

An experimental program was conducted by GARD to determine and verify optimal welding conditions using the fabrication system for welding of the AE mat panels. The following conclusions were made with regard to the results of the experimental program and the performance of the fabrication system.

6.2.1 Testing Program

A number of welds were performed according to a special matrix which allowed various welding conditions to be tested under controlled requirements.

A comprehensive test program was conducted to determine weld integrity and geometry, and mechanical and metallurgical properties of the welded joints.

The test program included visual and radiographic inspections, tensile and bend tests, macro-examination of weld geometry (penetration and resulting dilution rate), determination of micro-

hardness and maximum temperature distributions in the HAZ.

6.2.2 Preliminary Study

As a result of a preliminary study, a realistic production method of edge cleaning was determined.

The method includes degreasing in methyl ethyl ketone followed by brushing with a fine stainless steel brush.

Effect of weld storage period prior to testing on weld properties was determined.

As-welded hardness in the HAZ was found to recover to various degree depending on weld storage period.

The most strong average recovery rate (2.3% per day) was observed during the first week of storage, while it was reduced to 0.5% per day after two weeks of storage.

It is not recommended to conduct testing during the first week after welding to avoid an excessive scatter of results.

6.2.3 Inspection

As a result of visual and radiographic inspections the following conclusions were made:

No cracks were observed in any of the welded joints examined.

Occasional rare spots of incomplete penetration (lack of fusion) were observed under unfavorable (too low or too fast) travel speeds.

The main defect which caused most of rejections was Grades 2+ and 3 coarse porosity.

Under equal circumstances, porosity was very sensitive to welding conditions (linear energy and speed). Higher arc power level in combination with higher travel speed seems to cause less porosity.

Switch from isopropyl alcohol to methyl ethyl ketone decreased porosity for some welding conditions.

6.2.4 Mechanical Tests

The results of tensile tests showed the following:

All the welded joints met the 24 ksi minimum tensile strength requirement called for by the ASME/AWS Codes.

Series B showed the highest values of tensile strength (29.7 - 31.8 ksi) compared to Series A (29.3 - 30.3 ksi) and Series C (27.5 - 30.6 ksi).

Among the test pieces of Series B and C, B22REP and C35 showed the highest values of tensile strength (31.8 and 30.6 ksi), respectively, B22 REP being the strongest weld among all the

series tested.

Despite the rejection of some welds (B17, B18, B22 REP, C29 and C30) by radiographic inspection (coarse porosity, Grade 2+ and 3), tensile strength of the samples cut from these test plates showed acceptable values of tensile strength (27.5 - 31.8 ksi).

Copper chillers proved to be effective means to strengthen the welded joints, (up to 20%) compared to non-chilled welds.

The results of bend tests showed that welded joints cracked only in specimens performed on low (Series A) and high (Series C) values of arc power/linear energy.

6.2.5 Effect of Welding Conditions on Tensile Strength

Effect of welding conditions on tensile strength of welded joints was analyzed. Linear energy $Q = P/S$ was varied by varying travel speed (S) or arc power (P). As a result of this analysis, the following conclusions were made:

Tensile strength has more complicated relationship with linear energy Q than was previously thought.

The relationship is not linear and tensile strength reaches maximum at some optimal Q value (Q_{opt}). It means that further decrease or increase in Q (increase or decrease in travel speed (S), if Q is controlled by S), results in tensile strength reduction.

This is true regardless of a variable parameter (S or P) used to control Q. However the magnitude of Q_{opt} does depend on the parameter controlling Q.

Artificial HAZ chilling has a significant effect on tensile strength. For example, HAZ chilling increased strength of chilled specimens A5 and B17, compared to non-chilled welds A4 and B16 performed using the same welding conditions, by 14% and 21%, respectively.

Thus under the explored conditions, the objective of obtaining the maximum tensile strength can be achieved using chilling and only at some optimum values of arc power P, travel speed S and their derivative, linear energy Q. Knowledge of the interrelationships between these parameters makes this task easier.

6.2.6 Microhardness Profile in the Haz

Microhardness profiles were determined in the HAZ of the welded joints. The results were analyzed and the following conclusions were made.

Welding dramatically changes hardness in the HAZ and in the weld. There are three typical areas observed in the HAZ as far as hardness distribution is concerned.

Following the base metal, not affected by heat of welding, and moving toward the fusion line,

a relatively wide area, sometimes called overaged zone (OAZ), is encountered.

A significant reduction in hardness is observed in the overaged zone (OAZ). Hardness at the "bottom" of the OAZ may drop down to 60% of that of the base metal.

The fact that most of the tested specimens failed in the OAZ indicates that this zone is the weakest zone of the welded joint.

The next area of the HAZ adjacent to the fusion line is sometimes called in literature the complete reversion zone (CRZ). The zone is characterized by a continuous, sometimes significant, hardness recovery, up to 80% of that of the base metal.

An unknown zone was also revealed in this investigation. The portion of CRZ in the area 0.010-0.031 in. (0.3 - 1.2mm) wide immediately adjacent to the fusion line is characterized by a sudden sharp hardness drop sometimes to a very low level. The nature of this zone was not established.

Another very narrow zone adjacent to the fusion line (also not reported in literature) was observed in the weld. In this zone, named transition zone (TRZ), hardness dramatically recovers again.

Since hardness may be considered as a qualitative indicator of strength of materials, local softness in the TRZ under some unfavorable circumstances, like presence of porosity, for example, may turn this zone into the weakest zone of the welded joint. In fact, during tensile tests, some test specimens failed along the fusion line in the area where the TRZ and CRZ were found.

6.2.7 Effect of Hardness on Failure Location

Failure location appeared to be related to hardness distribution in the HAZ, the area where most of the failures of the specimens occurred during tensile tests.

HAZ failure location is always at the lowest hardness point ("bottom") between the overaged zone OAZ and complete reversion zone CRZ.

The described phenomenon was observed for all tested specimens regardless of welding conditions.

6.2.8 Effect of HAZ Chilling

HAZ chilling dramatically decreases the widths of the OAZ, CRZ and HAZ.

In the presence of HAZ chilling, the width of the OAZ is more sensitive to welding conditions than that of the CRZ.

HAZ chilling effectively suppresses metallurgical reactions, especially in the CRZ.

This positively affects HAZ properties and manifests itself in increasing tensile strength of

the welded joint.

The increase in strength became possible due to significant positive changes in the HAZ microstructures which are obviously associated with the size and location of the specific zones in the HAZ.

6.2.9 Relationships Between Hardness and Microstructures in the HAZ

Relationships between hardness and microstructure in the HAZ were established by studying the effect of welding thermal cycle on precipitation process.

Literature search showed that a generally recognized sequence of metastable phases produced by ternary Al-Mg-Si alloys along the pseudo-binary (Al-Mg₂Si) line during solution heat treatment is the following:

$$\alpha' = \text{G.P.} + B'' + B' + B$$

where α' is supersaturated solid solution, and G.P., B'' , B' and B are precipitates produced by decomposition of α' . It is also known that among these precipitates, B'' produces the strongest effect on hardness of alloy 6061, while contribution of B' is moderate. All the other precipitates affect hardness very little.

Comparing hardness (H) and maximum temperature (T_{max}) profiles in the HAZ, it was found that the hardness area identified as the OAZ spatially coincides with the temperature interval of B' phase existence.

The solvus temperature of this interval falls right into the "bottom" (the softest point) of the OAZ fairly accurately. Analysis of H-T max relationships for many chilled and non-chilled welds in this study confirmed this conclusion no matter what welding conditions were used.

The analysis showed that the OAZ hardness area accurately represents the location of a structural zone where coarsening of B'' phase and its transformation into B' phase occur in the HAZ of 6061-T6 alloy.

Knowledge of the profile and location of the OAZ is very important since they are associated with strength of the welded joint. In fact, most of the failure in this study during the tensile tests occurred through the "bottom" of this zone.

The hardness area identified as the CRZ may be called solution-hardening zone since in this area dissolution of B'' and B' phases occur, while this area is held at a temperature higher than B' solvus temperature.

Dissolution of precipitates B'' and B' enriches solid solution of the aluminum matrix with Si and especially with Mg which increase hardness in the CRZ.

6.2.10 Optimization of Welding Parameters

Analysis of the results of the experimental program allowed the following conclusions to be made:

Selection of optimal welding conditions was based on the analysis of the results of inspection, mechanical tests, metallurgical and weld geometry evaluations, and production considerations.

Two sets of welding conditions, represented by welds C35 and B22R, were selected as satisfying most of the acceptance criteria.

C35 set of conditions produces more favorable results in comparison with those produced by B22R, if judged by criteria of productivity and porosity level. Namely, it produces the least of porosity and provides higher productivity.

However, these conditions are inferior judging by other criteria, namely: the shape of weld reinforcement is not symmetrical, tensile strength is slightly lower, metallurgical reactions in the HAZ are more detrimental (the widths of OAZ and HAZ are wider, dilution is higher) and melt-through condition is more probable for the existing joint design.

Improvement in joint design, similar to that recommended earlier in Section 2 to avoid melt-through conditions, may improve weld C35 profile and metallurgical reactions in its HAZ as well. This will make C35 welding conditions a definite choice for future mass production of the mat panels.

6.2.11 Verification Welding

Verification welding of the AE mat panel was conducted to verify welding procedure, equipment and control systems developed by GARD.

Twelve short (5-ft. long) AE panels were welded for the Government-performed test in order to verify developed welding procedures and weld quality. Panels were welded using welding conditions requested by the Army, namely, A5, B18, B22 and C45.

C45 conditions were introduced instead of C35 conditions to reduce risk of melt-through by reducing current and travel speed. However, melt-through occasionally occurred even using C45 conditions.

B22 conditions, which are close to C45 conditions but do not produce melt-through, are recommended for production welding of the AE Mod. 2 mat panels.

Transient welding conditions were determined for start and end portions of weld B22.

Several methods were tried to provide acceptable quality of the weld starts and terminations,

including variation in ramp-down time, extra time delay and the use of run-on and run-off tabs with and without special copper end chillers.

The method using the tabs and end chillers produces excellent quality of the start and end portions of the weld.

Ten full-length (13-ft. long) AE mat panels were successfully welded using B22 conditions to verify performance of the fabrication system developed by GARD.

6.2.12 Fabrication System (Conclusions for Section 5)

According to the Army objectives, the fabrication system was developed by GARD for assembling and welding of the AE mat panels.

An automatic double-electrode welding system with computerized closed-loop feedback control was developed.

The system features real-time monitoring of parameters of pulsed GMA welding and operates in a "synergic" adaptive mode.

The system has also analytical capabilities to analyze and record information obtained through sensing of welding process parameters and fault detection capabilities as well.

An experimental multifunctional fixturing system was developed to assemble the AE mat panels.

The fixturing system provides means for straightening and assembling of the panels, weld torch positioning and travel, joint tracking, and controlling distortion and adverse metallurgical reactions in the weld.

Auxiliary equipment was also developed to support the experimental program, including loading structure, support and guiding mechanism for communication lines, pollution control and water circulating systems.

All GARD's concepts were successfully implemented and proved to be reliable and productive.

All equipment and systems were integrated into an efficient fabrication system capable of producing high quality AE mat panels.

After certain modifications, the fabrication system developed by GARD can be turned into a production system capable of handling both the access/egress and bridge deck panels.

6.3 RECOMMENDATIONS

6.3.1 Recommendations for Future Panel Design

Since higher energy levels and higher travel speeds seem to reduce sensitivity to porosity,

the existing joint design of the AE mat panel may require some slight modification to withstand more productive higher energy conditions without melt-through. This may be achieved by enlarging the cross-section area around the groove to be welded.

As an alternative to the use of run-on and run-off tabs, it is recommended to increase length of the AE panel by at least 2 in. (51mm) to allow for start and termination of the weld. The extra inch on both sides of the welded panel assembly can be cut off after welding has been completed.

It is recommended to conduct theoretical evaluation of fatigue performance of Type III welded joint similar to what was already done for Types I and II joints.

It is recommended that the Ribbon Bridge and Light Assault Bridge deck panel are redesigned according to the corresponding concepts developed by GARD. This allows the bridge panels to be fabricated using the advanced technology developed by GARD.

6.3.2 Recommendations for Welding Procedure

It may be necessary to elevate the acceptance level of coarse porosity to Grade 3 since this type and level of porosity do not compromise tensile properties of the welded joints. This may help to maintain efficient mass production of the mat panels using B22 welding conditions.

If C35 conditions are used, the existing acceptance criteria are quite adequate since C35 produces little porosity.

It is recommended for mass production of the mat panels to use C35 conditions which are more productive. This, of course, is possible only after the area around the welded joint has been modified to increase its cross-section. This allows the joint area to withstand higher current without melt-through.

It is recommended that welding wire is ordered from vendors rather than from distributors. This allows the period of time of adverse exposure of the wire to be reduced. If not in use, the wire should be stored in a hermetically sealed and pressurized container filled with argon.

HAZ chilling is greatly recommended since it increases tensile strength of the welded joint. It is recommended that in the future fixture modification the distance between the copper chiller bars and the edge of the selected optimal weld be maintained as minimum as possible. The distance of about 3/16 in. (4.8mm) seems to be close enough to produce adequate chilling effect. At the same time, it is far enough not to interfere with welding process due to width variations of the subpanels allowed by the ANSI H35.2 Standard.

It is recommended that in large-scale production, mechanized methods of multiedge preparation (degreasing and especially brushing) are used to reduce preparation time. Presently,

labor is relatively high using manual method of edge preparation.

If tensile tests are used for selective inspection of welded joints and the schedule of mass production does not allow the weld storage period to be consistent for all the panels, it is recommended that the storage period of at least a week is observed to avoid excessive scatter of the results due to natural aging. The least of scatter is obtained when the tests are conducted after 2 weeks of storage after which effect of natural aging is minimal.

It is recommended that the study of the HAZ of the welded joints is expanded to explain some of the metallurgical phenomena revealed during this experimental program.

6.3.3 Recommendation for Future Design of Fabrication System

It is recommended that all the support rings of the fixture are machined together around the outer circumference to provide an equal diameter (within ± 0.015 in.) and an even, circular configuration. The ring outer surface should be machined since it may be slightly distorted as a result of welding. This may exert unnecessary stresses on some bolted connections during fixture rotation and may cause dislocation of some components relative to each other after some period of service.

Inside openings in the rings should be machined in corresponding areas to provide accurate basic flat surfaces for assembling of the longitudinal components (beams, angles, brackets, etc.). This will facilitate assembling and adjustment of the fixture.

The number of bolted connections should be reduced, where necessary. They should be replaced by welding and subsequent machining, if needed. The rest of the bolted connections should be dowel-pinned to avoid periodical readjustment of the fixture.

Slightly larger clearance is needed for carriage travel inside the fixture. Presently wire-feed motor is rather close to the guide rails.

Right-hand and left-hand wirefeed motor arrangements should be used for the carriage to avoid clearance problems. Presently left-hand motors only are installed on both carriages because the right-hand motor was not available at that time from CRC-Evans.

The microstepping motor for the carriages should be ordered with 29:1 gear ratio rather than 11:1 ratio to avoid the main peak of mechanical resonance. Unfortunately, the main peak of resonance in present system fell into the operating range of welding travel speeds, causing some vibration at some travel speeds.

An alternative to a microstepping motor can be a servo-motor which is more expensive but does not experience resonance.

REFERENCES

1. Metal handbook, Properties and Selection: Nonferrous Alloys and Pure Metals. ASM, 9th Edition, Vol. 2, p. 54, 1979.
2. Ganaha, T., Pearce, B. P. and Kerr, H. W. Grain Structures in Aluminum Alloy GTA Welds. ASME, Metallurgical Transactions, Vol. 11A, pp. 1351-1359, August 1980.
3. Arata Y., et al. Trans. Japanese Research Welding Institute, Vol. 3, pp. 89-97, 1974.
4. Malin, V. Processes at the Base/Weld Metal Interface of Dissimilar Metal Welds During Welding and Post Weld Elevated Temperature Exposure. Presented at Dissimilar Metal Weld Task Group Meeting, Joint ASTM-ASME-MPC Committee, Chattanooga, TN, September 1983.
5. Brooks, J. A. and Allen, R. M. Microsegregation in Al-Cu Welds. Abstract of the paper, 1983 AWS Convention, Philadelphia, PA., p. 24.
6. Lanzafame, J. N. and Kattamis, T. Z. Solidification Structure and Tensile Properties of 2014 Aluminum Alloy Welds. Welding Journal, Vol. 52, pp. 226-232, May 1973.
7. Kou, S. and Le, Y. Three-Dimensional Heat Flow and Solidification during the Autogenous GTA Welding of Aluminum Plates. ASME, Metallurgical Transactions, Vol. 14A, pp. 2245-2253, November 1983.
8. Dudas, J. M. and Collins, F. R. Preventing Weld Cracks in High-Strength Aluminum Alloys. Welding Journal, Vol. 45, pp. 241-249, June 1986.
9. Lees, D. C. G. The Hot-Tearing Tendencies of Aluminum Casting Alloys. Journal of Institute of Metals, Vol. 72, p. 343, 1946.
10. Jennings, P. H., Singer, A. R. E., Pumphrey, W. I. Hot-Shortness of Some High-Purity Alloys in the System Aluminum-Copper-Silicon and Aluminum-Magnesium-Silicon. Journal of Institute of Metals, Vol. 74, pp. 227-248, 1948.
11. Spencer, D. B., Mehrabian, R. and Flemings, M.C. Rheological Behavior of Sn-15 Pct Pb in the Crystallization Range. ASME, Metallurgical Transactions, Vol. 3, pp. 1925-1932, July 1972.
12. Kou, S. Welding Metallurgy and Weldability of High-Strength Aluminum Alloys. Welding Research Council, New York, Bulletin 320, December 1986.
13. Matsuda, F. et al. Effect of Electromagnetic Stirring on Weld Solidification Structure of Aluminum Alloys (Report I) - Investigation of GTA Weld Metal of Thin Sheet. Transaction of JWRI, Vol. 7, pp. 111-127, 1978,
14. Matsuda, F. et al. Effects of Electromagnetic Stirring on the Weld Solidification Structure of Aluminum Alloy. Proceeding of the Conf. on Arc Physics and Weld Pool Behavior, Paper 10, The Welding Institute, Abington Hall, Abington, Cambridge, pp.

The guide rails of the carriage parking mechanisms should be made at least 3 in. longer to allow for wider distance between the Omni-guide sensor of the joint tracking device and the torch. At present, the tip of the sensor is located too close to the welding arc and is quickly overheated, if not protected. The stainless steel protector itself accumulates aluminum oxides and small spatter during welding of long panels which may fall into the weld.

Auxiliary equipment, developed by GARD on a mock-up level for supporting the experimental program, includes the loading/unloading structure, the support and guiding mechanisms for the communication lines, the pollution control and water circulating systems. Reliable performance of the auxiliary equipment proved GARD's conceptual ideas to be productive. These concepts are recommended for future design of production auxiliary equipment.

REFERENCES

1. Metal handbook, Properties and Selection: Nonferrous Alloys and Pure Metals. ASM, 9th Edition, Vol. 2, p. 54, 1979.
2. Ganaha, T., Pearce, B. P. and Kerr, H. W. Grain Structures in Aluminum Alloy GTA Welds. ASME, Metallurgical Transactions, Vol. 11A, pp. 1351-1359, August 1980.
3. Arata Y., et al. Trans. Japanese Research Welding Institute, Vol. 3, pp. 89-97, 1974.
4. Malin, V. Processes at the Base/Weld Metal Interface of Dissimilar Metal Welds During Welding and Post Weld Elevated Temperature Exposure. Presented at Dissimilar Metal Weld Task Group Meeting, Joint ASTM-ASME-MPC Committee, Chattanooga, TN, September 1983.
5. Brooks, J. A. and Allen, R. M. Microsegregation in Al-Cu Welds. Abstract of the paper, 1983 AWS Convention, Philadelphia, PA., p. 24.
6. Lanza fame, J. N. and Kattamis. T. Z. Solidification Structure and Tensile Properties of 2014 Aluminum Alloy Welds. Welding Journal, Vol. 52, pp. 226-232, May 1973.
7. Kou, S. and Le, Y. Three-Dimensional Heat Flow and Solidification during the Autogenous GTA Welding of Aluminum Plates. ASME, Metallurgical Transactions, Vol. 14A, pp. 2245-2253, November 1983.
8. Dudas, J. M. and Collins, F. R. Preventing Weld Cracks in High-Strength Aluminum Alloys. Welding Journal, Vol. 45, pp. 241-249, June 1986.
9. Lees, D. C. G. The Hot-Tearing Tendencies of Aluminum Casting Alloys. Journal of Institute of Metals, Vol. 72, p. 343, 1946.
10. Jennings, P. H., Singer, A. R. E., Pumphrey, W. I. Hot-Shortness of Some High-Purity Alloys in the System Aluminum-Copper-Silicon and Aluminum-Magnesium-Silicon. Journal of Institute of Metals, Vol. 74, pp. 227-248, 1948.
11. Spencer, D. B., Mehrabian, R. and Flemings, M.C. Rheological Behavior of Sn-15 Pct Pb in the Crystallization Range. ASME, Metallurgical Transactions, Vol. 3, pp. 1925-1932, July 1972.
12. Kou, S. Welding Metallurgy and Weldability of High-Strength Aluminum Alloys. Welding Research Council, New York, Bulletin 320, December 1986.
13. Matsuda, F. et al. Effect of Electromagnetic Stirring on Weld Solidification Structure of Aluminum Alloys (Report I) - Investigation of GTA Weld Metal of Thin Sheet. Transaction of JWRI, Vol. 7, pp. 111-127, 1978,
14. Matsuda, F. et al. Effects of Electromagnetic Stirring on the Weld Solidification Structure of Aluminum Alloy. Proceeding of the Conf. on Arc Physics and Weld Pool Behavior, Paper 10, The Welding Institute, Abington Hall, Abington, Cambridge, pp.

337-347, 1980.

15. Pearce, B. P. and Kerr, H. W. Grain Refinement in Magnetically Stirred GTA Welds of Aluminum Alloys. *Metallurgical Transactions*, Vol. 12B, pp. 479-486, September 1981.
16. Mironenko, V. N., et. al. Investigation of Chemical Non-Uniformity of Welded Joints on 1911 Aluminum Alloy. *Svarochnoye Proizvodstvo* (Welding Production), No. 8, pp. 5-6, August 1974.
17. Kou, S. and Le. Y. Improving Weld Quality by Low Frequency Arc Oscillation. *Welding Journal*, Vol. 64, pp. 51-55, March 1985.
18. Chihoski, R. A. Expansion and Stress Around Aluminum Weld Puddles. *Welding Journal*, Vol. 58, pp. 263-276, September 1979.
19. Gittos, N. F. and Scott, M. M. Heat-Affected Zone Cracking of Al-Mg-Si Alloys. *Welding Journal*, Vol. 60, pp. 95-103, June 1981.
20. Metzger, G. E. Some Mechanical Properties of Welds in 6061 Aluminum Alloy Sheet. *Welding Journal*, Vol. 46, pp. 457-469, October 1967.
21. Kelsey, R. A. Effect of Heat Input on Welds in Aluminum Alloy 7039. *Welding Journal*, Vol. 50, pp. 507-513, December 1971.
22. Makarov, V. P. Kinetics of Strengthening of Welded Joints of 1915 Alloy during Natural Aging. *Svarochnoye Proizvodstvo* (Welding Production), No. 6, pp. 32-33, June 1973.
23. Birman, Y. I., et al. Specifics of Welding of Aluminum Alloys with Forced Locally Directed Streams. *Svarochnoye Proizvodstvo* (Welding Production), No. 8, pp. 13-15, August 1983.
24. Nikiforov, G. D., Trusov, S. A., and Silant'eva, S. A. Redistribution of Hydrogen during Solidification of Aluminum. *Svarochnoye Proizvodstvo* (Welding Production), No. 9 pp. 34-37, September 1980.
25. Grigorenko, G. M. Formation of Pores in Welds. *Avtomaticheskaya Svarka* (Automatic Welding), No. 10, pp. 13-17, October 1970.
26. Devletian, J. H. and Wood, W. E. Factors Effecting Porosity in Aluminum Welds. *Welding Research Council, New York, Bulletin 290*, December 1983.
27. Strobelt, W. E. Inert Gas Weldment Effects Study. Phase I Report (July 1965-November 1965), Phase II Report (January 1966-June 1966), Final Report (January 1966-June 1966), under Contract NAS8-20168 from Aerospace Group, Quality Control Research Section, The Boeing Company, Boeing Reports Nos. D2-23647-4, D2-23647-5, and D2-23647-6.
28. Hassemeyer, E. A. Aluminum Welding for Space Vehicles and Welding in Outer Space. Report prepared by Welding Development Branch, Manufacturing Engineering

Laboratory, G. C. Marshall Space Flight Center, NASA, August 19, 1970.

29. Lyons, E. H. What is a Clean Surface? Trans. Electrochem. Soc., Vol. 88, p. 281, 1945.
30. Materials Preparation and Instrumentation for Welding S-IC Components. Final Report under Contract NAS-20363 from Illinois Institute of Technology Research Institute, September 1967.
31. Saperstein, Z. P., Prescott, G. R., and Monroe, F. H. Porosity in Aluminum Welds. Welding Journal, Vol. 43, pp. 443-453, October 1964.
32. Binger, W. W., Yande, G. P. and Michnuk, R. R. Internal Report, Alcoa Technical Center, 1975.
33. Woods, R. Porosity and Hydrogen Absorption in Aluminum Welds. Welding Journal, Vol. 53, pp. 97-108, March 1974.
34. Wroth, R. S. and Haryung, J. Effect of Welding Position on Porosity Formation in Aluminum Alloy Welds. NASA Report #SP-5918(02), pp. 21-23, 1972.
35. Miyazaki, M., et al. Quantitative Investigation of Heat-Affected Zone in Aluminum Alloy A6061. Welding Journal, Vol. 69, pp. 362-371, September 1990.
36. Masubuchi, K. Integration of NASA-sponsored Studies on Aluminum Welding. NASA Contractor Report, NASA CR-2064, prepared by MIT, Cambridge, MA for G. C. Marshall Space Flight Center, published by NASA, Washington D. C., pp. 5-64, June 1972.
37. Mondolfo, L. F. Aluminum Alloys: Structure and Properties. Butterworths, London, pp. 556-562, 1976.
38. Dumolt, S. D. An Investigation of the Microstructural Changes in the Heat-Affected Zone of Age-Hardenable Aluminum Alloys Using Transmission Electron Microscopy. Ph.D. Thesis, Carnegie-Mellon University, Pittsburgh, PA, 1983.
39. Panseri, C. and Federighi, T. A Resistometric Study of Precipitation in an Aluminum - 1.4% Mg₂Si Alloy. Journal of Institute of Metals, Vol. 94, pp. 99-107, 1966.
40. Lutts, A. Pre-precipitation in Al-Mg-Ge and Al-Mg-Si. ACTA Metallurgic, Vol. 9, pp. 577-586, June 1961.
41. Enjo, T. and Kuroda, T. Microstructure in Weld Heat-Affected Zone of Al-Mg-Si Alloy. Transaction of JWRI, Vol. 11, pp. 61-66, January 1982.
42. Thomas, G. The Ageing Characteristics of Aluminum Alloys. Journal of Institute of Metals, Vol. 90, pp. 57-63, 1961-1962.
43. Miyauchi, T., et al. Precipitation Process of Al-Mg-Si Alloys by Ageing. Journal of Japan Institute of Light Metals, 21-9, p. 595, 1971.

APPENDICES

APPENDICES A

SECTION 2

APPENDIX A1

The U.S. Army WES Drawings of the Access/Egress Mat Panel



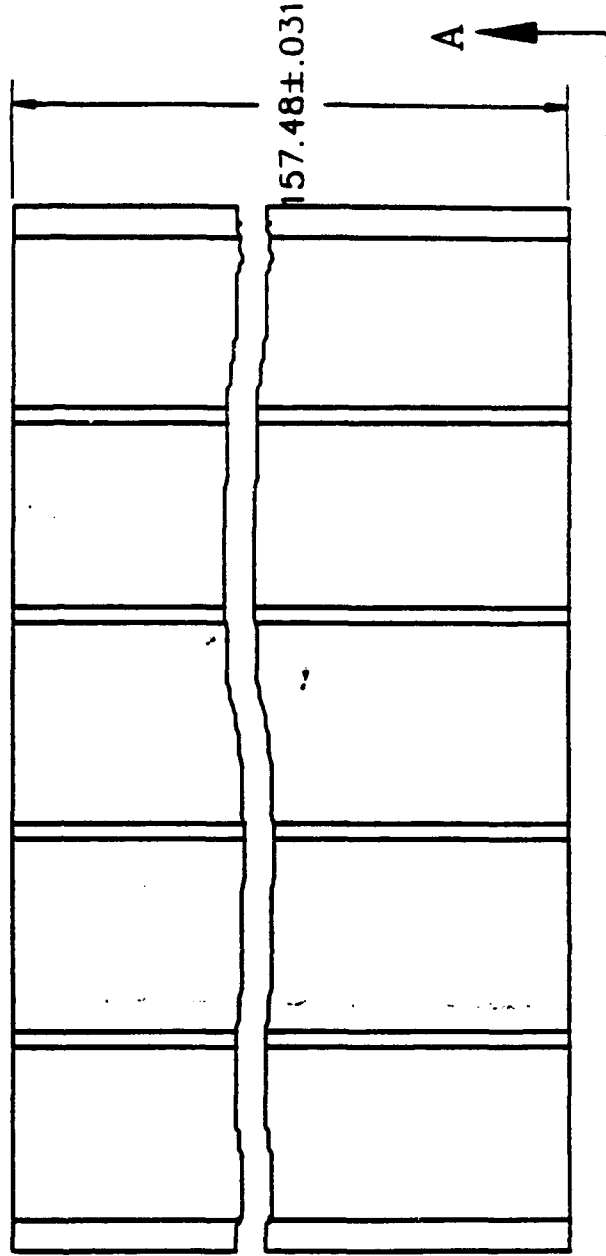
7E 7062

APPENDIX A2

**GARD's Drawings of the Extruded Mod. 1
Access/Egress Subpanels**

NOTES:

1. MATERIAL SHALL BE ALUMINUM
IN ACCORDANCE WITH ASTM B221,ALY 6061-T6
2. UNLESS OTHERWISE SPECIFIED ALL TOLERANCES
ON EXTRUDED SHAPE SHALL BE IN
ACCORDANCE WITH ANSI H35.2
3. TOLERANCES ON STRAIGHTNESS,
TWIST AND FLATNESS SHALL
BE ONE-HALF THE VALUES
AS SPECIFIED IN ANSI H35.2
4. THE BLENDING OF WEBS TO
SKINS SHALL BE SMOOTH
AND FREE OF DISCONTINUITIES,
THERE SHALL BE NO THINNING
OF WEBS OR SKINS AT BLEND
TANGENT POINTS OF RADII.



FRACTIONS : 1/8"		DIVISION		TITLE OR DESCRIPTION		1100	
2.00 : 1/8"		GARD		Division		Chamberlain	
2.00 : 1/8"		7448 North Matchez Avenue		Miles, IL 60648		(312) 947-8000	
ANGULAR : 90°		MIDDLE PANEL		001		001	
SP. 1/8"		CHECKED		BY		DATE	
TP 1/8"		BY		DATE		DATE	

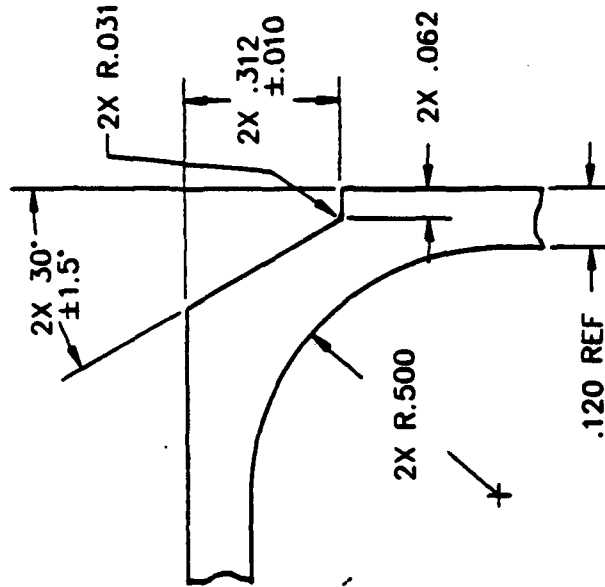
Technical drawing of a mechanical part, View A-A, showing a cross-section of a multi-ported cylindrical component. The drawing includes dimensions for overall length (8.412 ± .031), port spacing (1.623 ± .015), and port diameter (1.500 ± .010). It also specifies material properties (16X R .063, 16X 15 ± 1°, 16X .063, 8X .126) and a scale of 1/1.

VIEW A-A
SCALE: 1/1

[illegible]

[illegible]

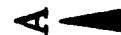
VIEW C
SCALE: 2/1



VIEW D
SCALE: 4/1

[illegible]

1. MATERIAL SHALL BE ALUMINUM
IN ACCORDANCE WITH ASTM B221,ALY 6061-T6
2. UNLESS OTHERWISE SPECIFIED ALL TOLERANCES
ON EXTRUDED SHAPE SHALL BE IN
ACCORDANCE WITH ANSI H35.2
3. TOLERANCES ON STRAIGHTNESS,
TWIST AND FLATNESS SHALL
BE ONE-HALF THE VALUES
AS SPECIFIED IN ANSI H35.2
4. THE BLENDING OF WEBS TO
SKINS SHALL BE SMOOTH
AND FREE OF DISCONTINUITIES,
THERE SHALL BE NO THINNING
OF WEBS OR SKINS AT BLEND
TANGENT POINTS OF RADII.

[illegible]

[illegible]

SCALE: 1/1

[illegible]

[illegible]

VIEW B
SCALE: 2/1

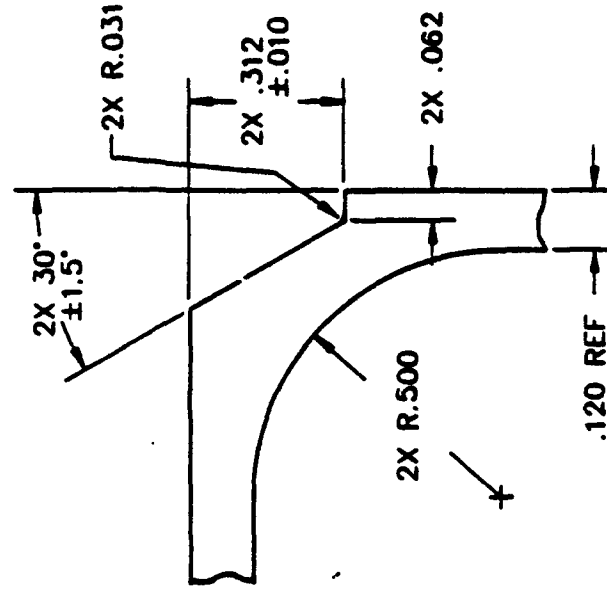
SCALE: 2/1

27 28 29 30 31 32 33 34 35										NO. ON PAGE NO.										TITLE OR DESCRIPTION										11922																																																																																									
FORMS										FRACTIONS : 1/2										GARD										Division										Chamberlain										Montreal																																																																					
										FINISHING										1/4 : 1/8										7449 North Sanchez Avenue										Miles, E. 90648 (312) 647-9000																																																																															
										PAVING										1/16 : 1/32																																																																																																			
																				ANGULAR : 15°																																																																																																			
																				23/24/25										7/12/13																																																																																									
																				26/27/28										8/14/15																																																																																									
																				29/30/31																																																																																																			
																				32/33/34																																																																																																			
																				35/36/37																																																																																																			
																				17										18																																																																																									
																				19										20																																																																																									
																				21										22																																																																																									
																				23										24																																																																																									
																				25										26																																																																																									
																				27										28																																																																																									
																				29										30																																																																																									
																				31										32																																																																																									
																				33										34																																																																																									
																				35										36																																																																																									
																				37										38																																																																																									
																				39										40																																																																																									
																				41										42																																																																																									
																				43										44																																																																																									
																				45										46																																																																																									
																				47										48																																																																																									
																				49										50																																																																																									
																				51										52																																																																																									
																				53										54																																																																																									
																				55										56																																																																																									
																				57										58																																																																																									
																				59										60																																																																																									
																				61										62																																																																																									
																				63										64																																																																																									
																				65										66																																																																																									
																				67										68																																																																																									
																				69										70																																																																																									
																				71										72																																																																																									
																				73										74																																																																																									
																				75										76																																																																																									
																				77										78																																																																																									
																				79										80																																																																																									
																				81										82																																																																																									
																				83										84																																																																																									
																				85										86																																																																																									
																				87										88																																																																																									
																				89										90																																																																																									
																				91										92																																																																																									
																				93										94																																																																																									
																				95										96																																																																																									
																				97										98																																																																																									
																				99										100																																																																																									
																				101										102																																																																																									
																				103										104																																																																																									
																				105										106																																																																																									
																				107										108																																																																																									
																				109										110																																																																																									
																				111										112																																																																																									
																				113										114																																																																																									
																				115										116																																																																																									
																				117										118																																																																																									
																				119										120																																																																																									
																				121										122																																																																																									
																				123										124																																																																																									
																				125										126																																																																																									
																				127										128																																																																																									
																				129										130																																																																																									
																				131										132																																																																																									
																				133										134																																																																																									
																				135										136																																																																																									
																				137										138																																																																																									
																				139										140																																																																																									
																				141										142																																																																																									
																				143										144																																																																																									
																				145										146																																																																																									
																				147										148																																																																																									
																				149										150																																																																																									
																				151										152																																																																																									
																				153										154																																																																																									
																				155										156																																																																																									
																				157										158																																																																																									
																				159										160																																																																																									
																				161										162																																																																																									
																				163										164																																																																																									
																				165										166																																																																																									
																				167										168																																																																																									
																				169										170																																																																																									
																				171										172																																																																																									
																				173										174																																																																																									
																				175										176																																																																																									
																				177										178																																																																																									
																				179										180																																																																																									
																				181										182																																																																																									
																				183										184																																																																																									
																				185										186																																																																																									
																				187										188																																																																																									
																				189										190																																																																																									
																				191										192																																																																																									
																				193										194																																																																																									
																				195										196																																																																																									
																				197										198																																																																																									
																				199										200																																																																																									
																				201										202																																																																																									
																				203										204																																																																																									
																				205										206																																																																																									
																				207										208																																																																																									
																				209										210																																																																																									
																				211										212																																																																																									
																				213										214																																																																																									
																				215										216																																																																																									
																				217										218																																																																																									
																				219										220																																																																																									
																				221										222																																																																																									
																				223										224																																																																																									
																				225										226																																																																																									
																				227										228																																																																																									
																				229										230																																																																																									
																				231										232																																																																																									

Technical drawing of a mechanical part, likely a bracket or flange, showing dimensions and tolerances. The drawing includes the following specifications:

- Overall width: 1.682 REF
- Overall height: 1.562 $\pm .024$
- Top flange thickness: 2X .420
- Top flange radius: 4X R.188
- Central hole diameter: \varnothing SYM
- Central hole radius: 2X R.938
- Central hole position: 2X .320
- Central hole tolerance: 2X .120 $+.025$ $-.015$
- Central hole reference: 1.260 REF
- Central hole radius: 2X R.938
- Central hole position: 2X R.938
- Central hole radius: 2X R.938

VIEW C
SCALE: 2/1



VIEW D
SCALE: 4/1

[illegible]

APPENDIX A3

GARD's Stress Analysis of Mat Panels

APPENDIX A3

PRELIMINARY ANALYSIS OF PANEL STRESSES

The panels, when in service, form a roadway supported on the ground which is loaded by vehicles from above. In essence this roadway is a plate on an elastic foundation. The foundation modulus for a California Bearing Ratio of 1.5 is estimated to be about 70 lbf/cu.in. For the macro analysis of this structure, it was assumed (conservatively) that the tire loads are concentrated. For analysis simplification, the panel was modeled as a beam on an elastic foundation.

The most significant bending stresses, with regard to the welds, are those corresponding to bending along the roadway (i.e. across the panel). It was first necessary to solve for the behavior along the panel (i.e. across the roadway) in order to determine a good estimate of the effective width of panel to be used for the 'beam'. This first analysis treated a single panel as a finite length beam on an elastic foundation loaded symmetrically by two concentrated loads (the wheels). The effective panel width (to be used in the cross panel analysis) was taken from these results as the width necessary to support the load at the peak beam deflection obtained. This result was 30.615 inches of effective panel width per tire.

For bending along the roadway (across the panel), the assembly was taken to be a three-span beam on an elastic foundation. The central span was a beam representing a single panel and this was hinged at each end to a semi-infinite beam (the other two 'spans'). The beam width was 30.615 inches and the bending moment of inertia of the 'beam' was based upon that width with two rectangles 0.120 inches thick and an overall height of 1.5 inches. The assembly was loaded by a concentrated 20,000 lbf load at the middle of the central span. The 20,000 lbf load here corresponds to the critical wheel load for an MLC 70 vehicle. The extremal bending moments in this 'beam' were used to calculate the algebraic maximum and minimum macro bending stresses in the panel.

Local bending stresses were analyzed as a uniform beam, built-in at both ends, with a uniform distributed load. The beam thickness is the cell thickness, 0.120 inches. At the upper surface of the panel, the distributed load was that corresponding to 160 psi load from the wheel. At the lower surface of the panel, which is in contact with the foundation, the distributed load corresponded to the foundation reaction at the peak downward deflection of the beam on elastic foundation. These local bending stresses were taken to be effective only at the middle of the central span (i.e. the middle of the panel supporting the wheel load). At the other extremal, where macro bending stresses are reversed (but diminished in magnitude), the local bending stresses were neglected (they are zero at the top since the wheel is not at that location, and they are quite small at the bottom).

RESULTS

The extremal macro bending stresses were found to be

- 16,670 psi and + 3,760 psi

at the top of the panel, and

+ 3,760 psi and -16,670 psi

at the bottom of the panel.

The local bending stresses, applicable at the location of the higher magnitude macro bending stress only, were evaluated as

Type I Weld: \pm 7,860 psi in the upper cell wall
 \pm 1,340 psi in the lower cell wall

Type II Weld: \pm 15,720 psi in the upper cell wall
 \pm 2,670 psi in the lower cell wall

Here the positive (tensile) stresses occur at the inside fibers of the cell walls and the negative (compressive) stresses apply to the outside fibers of the cell walls.

FATIGUE EVALUATION INPUTS

For purposes of preliminary fatigue evaluation of the panel welds, the macro stresses (magnified by a factor of 1.15 to account for impact) and local stresses are combined. We have essentially eight cases which should encompass the most severe stresses encountered for Type I and Type II welds.

- Case 1: Type I Weld, at the outside surface at top of panel
- Case 2: Type I Weld, at the inside surface at top of panel
- Case 3: Type II Weld, at the inside surface at top of panel
- Case 4: Type II Weld, at the outside surface at top of panel
- Case 5: Type I Weld, at the inside surface at bottom of panel
- Case 6: Type I Weld, at the outside surface at bottom of panel
- Case 7: Type II Weld, at the outside surface at bottom of panel
- Case 8: Type II Weld, at the inside surface at bottom of panel

The resultant extremal stresses for each cycle experienced in each of these eight cases are as follows.

Case 1:	- 27,000 psi --->	+ 4,300 psi
Case 2:	- 11,300 psi --->	+ 4,300 psi
Case 3:	- 35,000 psi --->	+ 4,300 psi
Case 4:	- 3,500 psi --->	+ 4,300 psi
Case 5:	- 4,300 psi --->	+ 20,500 psi
Case 6:	- 4,300 psi --->	+ 17,800 psi
Case 7:	- 4,300 psi --->	+ 21,900 psi
Case 8:	- 4,300 psi --->	+ 16,500 psi

These stresses were utilized for fatigue evaluation.

In addition, the peak stress along the weld was evaluated from the first (along the panel, across the roadway) macro analysis and amplified by the 1.15 factor to yield a cycle between -26,200 psi and 0 psi at the top of the panel and 0 psi and +26,200 psi at the bottom of the panel. These stresses, however were deemed ineffective for development of fatigue cracks because of their direction.

The information supplied to Prof. Lawrence for fatigue evaluation is attached as part of this Appendix.

APPENDIX A4

**U of I Report on Fatigue Analysis
of Weld Joints for Al Mat Panel**

University of Illinois at Urbana - Champaign
2129 Newmark Civil Engineering Laboratory • (217) 333-6928
205 North Mathews St. • Urbana • Illinois • 61801 • USA

June 18, 1988

Dr. Vladimir Malin
Senior Welding Engineer
Chamberlain Manufacturing Corp.
GARD Division
7449 North Natchez Avenue
Niles, Illinois 60648-3892

Regarding: **Fatigue Analysis of Weld Joints for Al Mat Panels**

Dear Vladimir,

As we discussed by telephone and as described in two mailings recently received from you, I have analyzed the fatigue life expected for the two candidate weldments for the fabrication of the aluminum mat panels. I wrote four programs to calculate the expected fatigue crack initiation (N_I) and fatigue crack propagation lives (N_p) expected of the two joints for the stresses estimated and supplied by Mr. Vaitys of GARD, Inc: see Attachments A and B. The programs were written for a Macintosh + running Turbo Pascal.

1. RESULTS

The results of my calculations are summarized in the tables below. Cases which seem most critical have been highlighted by printing their table entries in bold type.

1.1 Estimated Fatigue Strength for Crack Initiation at a Given Life.

Case	Joint	(GARD)	(GARD)	(GARD)	Fatigue Strength	
		ΔS (range) ksi.	S_a (amplitude) ksi.	R	S_a $N_I = 10,000$ ksi.	S_a $N_I = 100,000$ ksi.
1	I-top	31.3	15.6	-6.0	30.7	21.7
2	I-top	15.6	7.8	-2.6	27.8	20.3
3	II-top	39.7	20.0	-8.1	10.8	7.6
4	II-top	7.8	3.9	-0.8	8.0	6.1
5	I-bottom	24.8	12.4	-0.2	20.1	15.8
6	I-bottom	27.1	11.05	-0.24	20.4	16.0
7	II-bottom	26.2	13.1	-0.2	6.9	5.4
8	II-bottom	20.8	10.2	-0.26	7.0	5.5

1.2 Estimated Fatigue Crack Propagation Life for Stress Ranges Supplied by GARD

Case	Joint	(GARD)	(GARD)	Fatigue Crack Propagation Life
		ΔS (range) ksi.	(+) ΔS (positive range, only) ksi.	N_p cycles
1	I-top	31.3	4.3	1.9e+7
2	I-top	15.6	4.3	1.9e+7
3	II-top	39.7	4.3	5.0e+6
4	II-top	7.8	4.3	5.0e+6
5	I-bottom	24.8	20.5	1.7e+5
6	I-bottom	27.1	17.8	2.6e+5
7	II-bottom	26.2	22.0	3.8e+4
8	II-bottom	20.8	16.5	9.0e+4

2. ASSUMPTIONS

2.1 Material Properties:

I assumed "average" tensile and fatigue properties because of limited time. Actually the fatigue properties of aluminum alloys do not vary too much. The sources from which I drew my guesses for 6061 Al are included in Attachment C. The values I used in my calculations are given in the table below.

Average Aluminum Properties	Symbol	Code	Units	Value
Yield Strength (as-welded)	S_y	-	ksi.	20.0
(i. e., weld residual stresses)	σ_r	Sr	ksi.	20.0
Fatigue Strength Coefficient	σ'_f	Spf	ksi.	103.0
Fatigue Strength Exponent	b	b	-	-0.122
Peterson's "a" Parameter	a	ap	in.	0.005
Fatigue Crack Growth Coefficient	C	C	ksi $\sqrt{\text{in.}}$	1e-9
Fatigue Crack Growth Exponent	n	m	-	3.0

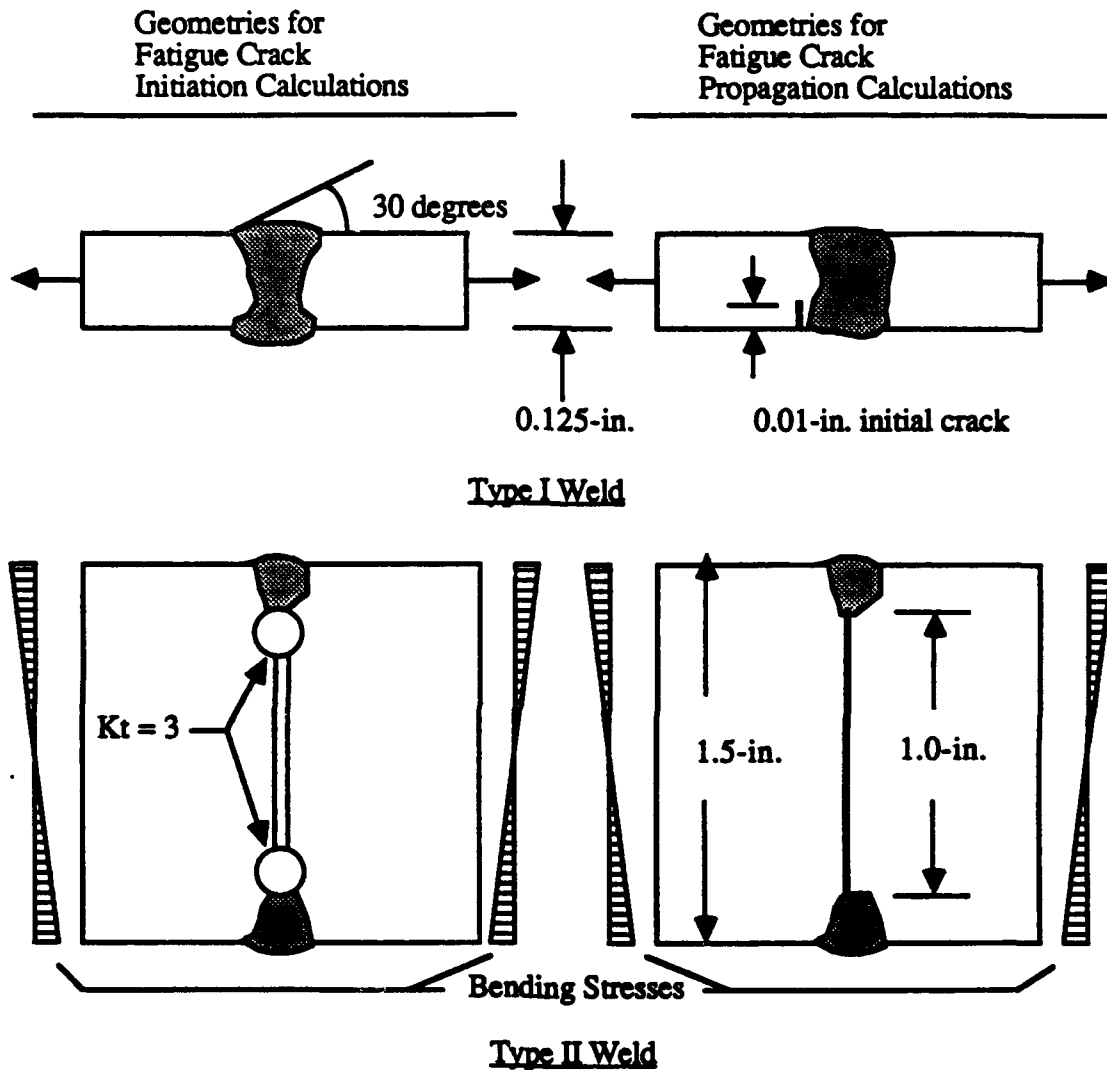
2.2 Local Geometries

The local geometries for the fatigue crack initiation (N_I) and fatigue crack propagation (N_P) calculations are shown below.

For N_I in Type I welds, I assumed a double-V butt weld geometry with a flank angle (theta) equal to 30 degrees. I assumed that the loading was purely axial ($x = 0$); that is, the worst case. Pure bending with the same extreme fiber stress gives longer fatigue lives and higher fatigue strengths. I assumed full tensile residual stresses, i.e. $S_r = S_y = 20.0$ ksi.

For N_I in Type II welds, I assumed the presence of a hole with a $K_t = 3$. This hole didn't help much because, by introducing it, large compressive excursions of stress become influential and damaging. I didn't analyze for N_I at the weld toes in this case because I

assumed that the LOP and fatigue crack propagation there will govern. I assumed full tensile residual stresses, i.e. $S_r = S_y = 20.0$ ksi.



For N_p in Type I welds, I assumed that the weld had very little crown and that there was a 0.01-in preexisting crack at the weld toe. Again I assumed pure axial loading and considered only the tensile portion of the load history recognizing that fatigue cracks are generally closed and do not propagate in compression. I used the LEFM model for a surface crack in a plate of finite width. Weld residual stresses were not considered; but if the residual stresses are large and tensile, the fatigue crack may be open for more of the load cycle than was here assumed.

LEFM MODEL USED FOR LOP IN TYPE II WELD

$$\sigma = \frac{3Ma}{2b^3}$$

$$\sigma_N = \frac{3Ma}{2(b^3-d^3)} = \frac{\sigma}{1-(a/b)^3}$$

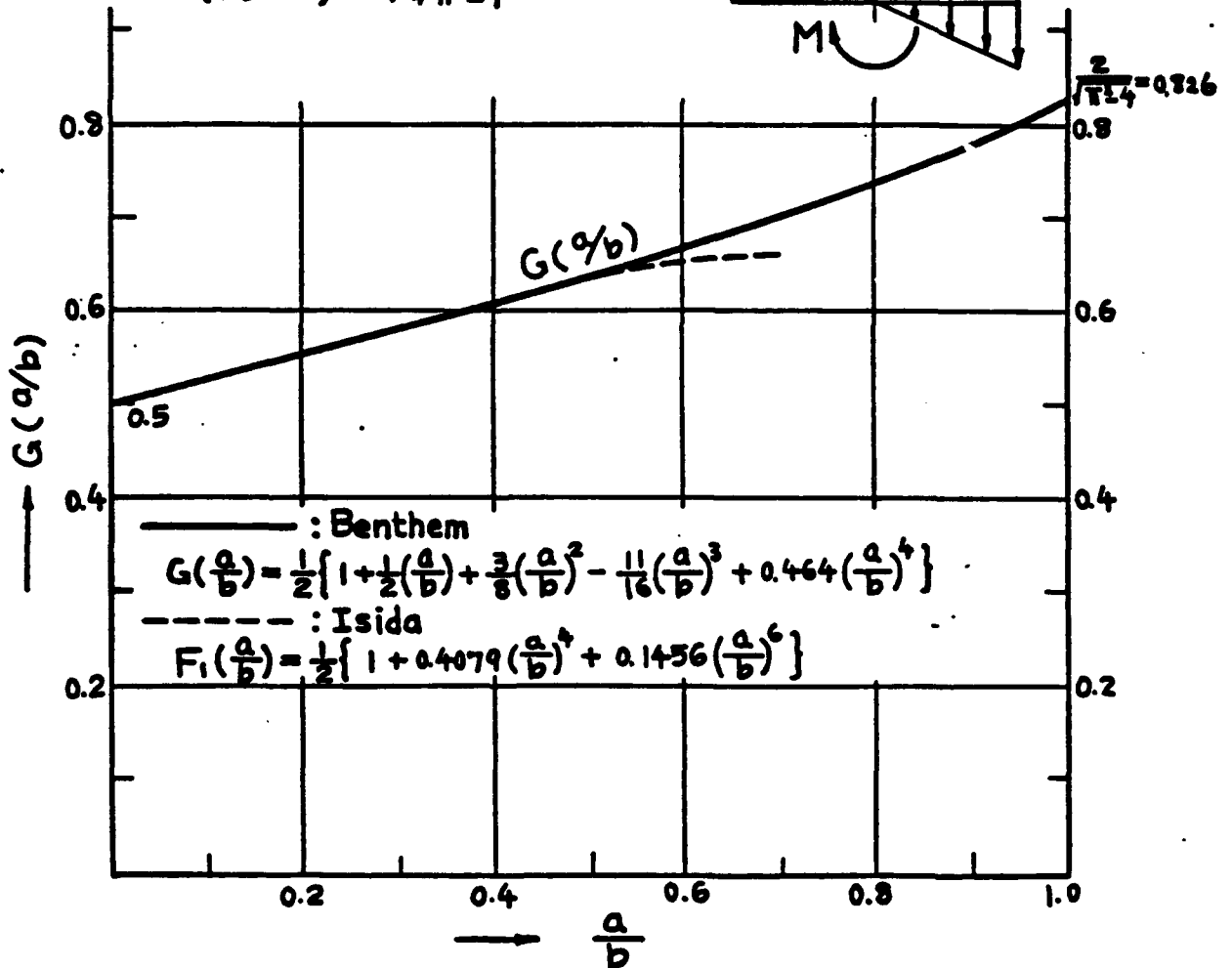
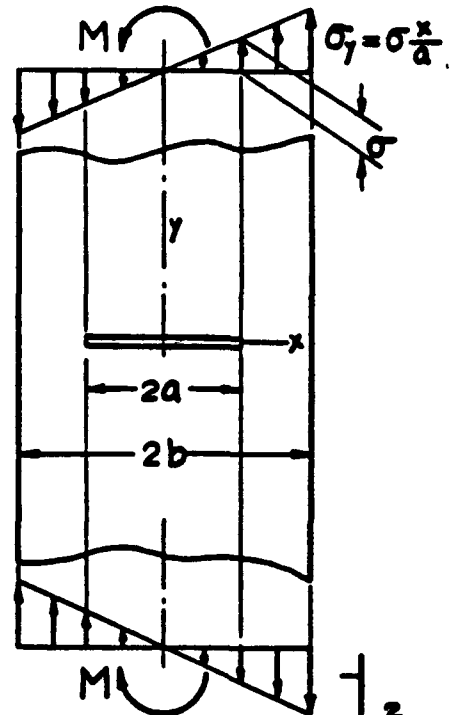
$$K_I = \sigma \sqrt{\pi a} \cdot F_1(a/b)$$

$$= \sigma_N \sqrt{\pi a} \cdot F_2(a/b)$$

$$G(a/b) = \frac{F_2(a/b)}{\sqrt{1-a/b}} = \frac{\{1-(a/b)^3\} F_1(a/b)}{\sqrt{1-a/b}}$$

$$G(a/b \rightarrow 0) = 1/2$$

$$G(a/b \rightarrow 1) = 2/\sqrt{\pi} \approx 1.107$$



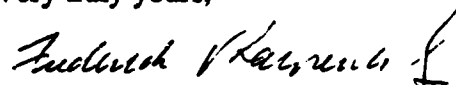
For N_p in Type II welds, I used the model shown above and the function $F1$ defined therein. The loading was assumed to be bending. Weld residual stresses were not considered; but if the residual stresses are large and tensile, the fatigue crack may be open for more of the load cycle than was here assumed.

In all cases above, I neglected the stresses (σ_x) perpendicular to the severe notch provided by the weld or the LOP since I believe they will not much influence events at these rather severe 2-dimensional notches. I think of 2-dimensional notches as being sensitive principally to the stresses normal to them (σ_y in this case). This is believed to be particularly the case for the Type II welds with their severe LOP. It is possible that weld ripple or some other fabrication induced defect could become critical and respond to the stresses longitudinal to the weld, but that case has not been considered. My notes are appended in Attachment D.

3. TENTATIVE CONCLUSIONS

1. Based on the stresses and weld geometries supplied by GARD, the most serious case seems to be Cases 7 and 8, that is, fatigue failure by fatigue crack propagation from the LOP at the bottom of the Type II weld. If the analysis is correct, even this life may be a factor of 2 larger than that required ($N_{reqd.} = 15,000$).
2. The fatigue life of the Type I weld would seem to be about 10 times larger than that of the Type II weld.
3. The critical cases for both the Type I and Type II welds appear to be the bottom weld.
4. For the Type II weld, no crack initiation life was assumed for the as-welded LOP. The addition of a circular hole at the root of the weld to blunt the LOP did not seem to add much of an initiation life because of the large stress range in this region caused by the large compressive stress excursions.

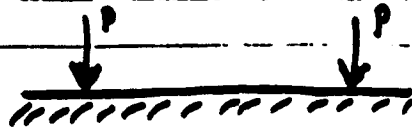
Very truly yours,



Dr. Frederick V. Lawrence, Jr.
Professor of Civil Engineering and
Metallurgy

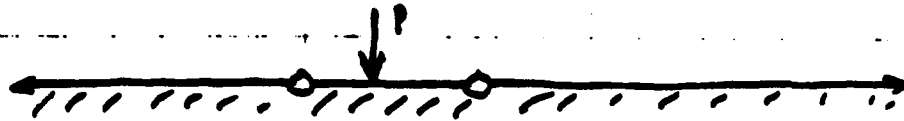
ATTACHMENT A
RESULTS OF GARD STRESS ANALYSIS

Macro σ_y stresses from finite beam on elastic foundation (full face width assumed)



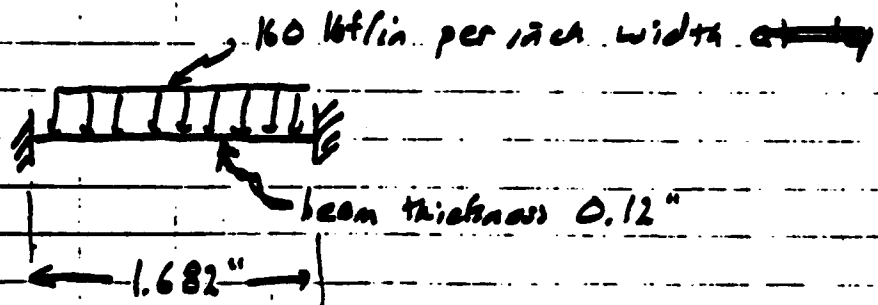
This analysis also used to determine effective width for macro bending in other direction.

Macro σ_x stresses from infinite, doubly-hinged beam on elastic foundation, using effective width from above.

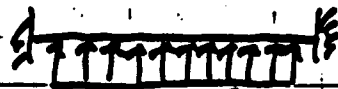


Local σ_x stresses from uniformly loaded beam, built-in at both ends.

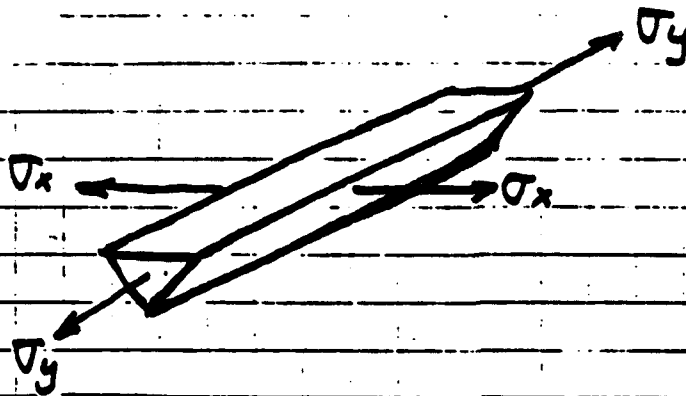
Top



Bottom

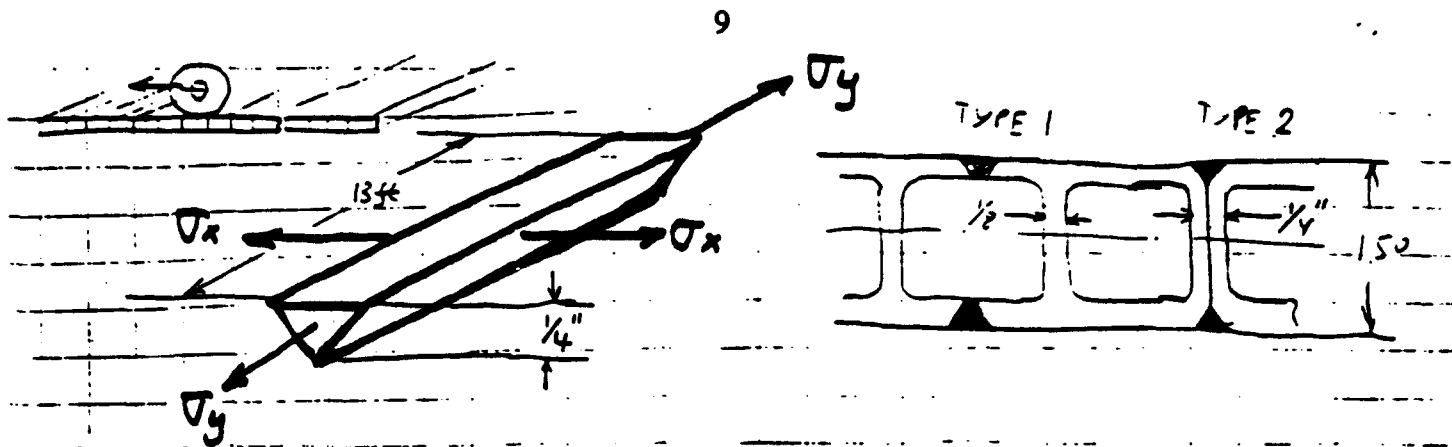


27.2 lbf/in per inch width
(based upon foundation modulus and
peak deflection from Macro σ_y analysis.)



Case #	σ_x	σ_y
1	$-27,000 \text{ psi} \rightarrow +4300 \text{ psi}$	$-26,200 \text{ psi} \rightarrow 0$
2	$-11,300 \text{ psi} \rightarrow +4300 \text{ psi}$	$-26,200 \text{ psi} \rightarrow 0$
3	$-35,000 \text{ psi} \rightarrow +4300 \text{ psi}$	$-26,200 \text{ psi} \rightarrow 0$
4	$-3500 \text{ psi} \rightarrow +4300 \text{ psi}$	$-26,200 \text{ psi} \rightarrow 0$
5	$-4300 \text{ psi} \rightarrow 20,500 \text{ psi}$	$0 \rightarrow 26,200 \text{ psi}$
6	$-4300 \text{ psi} \rightarrow +17,800 \text{ psi}$	$0 \rightarrow 26,200 \text{ psi}$
7	$-4300 \text{ psi} \rightarrow +21,900 \text{ psi}$	$0 \rightarrow 26,200 \text{ psi}$
8	$-4300 \text{ psi} \rightarrow +16,500 \text{ psi}$	$0 \rightarrow 26,200 \text{ psi}$

Note cases 1-4 are top weld
 5-8 are bottom weld
 1,2,5,6 are butt weld (Type 1)
 3,4,7,8 are box joint (Type 2)



Case	σ_x	σ_y
1	-27,000 psi \rightarrow +4300 psi	-26,200 psi \rightarrow 0
2	-11,300 psi \rightarrow +4300 psi	-26,200 psi \rightarrow 0
3	-35,000 psi \rightarrow +4300 psi	-26,200 psi \rightarrow 0
4	-3500 psi \rightarrow +4300 psi	-26,200 psi \rightarrow 0
5	-4300 psi \rightarrow +20,500 psi	0 \rightarrow 26,200 psi
6	-4300 psi \rightarrow +17,800 psi	0 \rightarrow 26,200 psi
7	-4300 psi \rightarrow +21,900 psi	0 \rightarrow 26,200 psi
8	-4300 psi \rightarrow +16,500 psi	0 \rightarrow 26,200 psi

Note cases 1-4 are top weld
 5-8 are bottom weld
 1,2,5,6 are butt weld (Type 1)
 3,4,7,8 are box joint (Type 2)

THESE FIGURES FOR THE HEAVIEST MLC 70 TRUCK. FOR MLC-24
 THE LOAD IS 60% OF THOSE.

LOAD: 2700 PASSES OF MLC 24 AND 300 PASSES OF MLC 70

ATTACHMENT B DEVELOPED COMPUTER PROGRAMS

```

PROGRAM Ni_Al_Butt;

USES  Memtypes, QuickDraw, OSIntf, ToolIntf, PackIntf, Sane;

var
  A, alphaA, alphaB, KfmA, KfmB, Kfeff : real;
  Sa : real;

const
  t      = 0.125;
  Theta  = 45;
  Ni     = 1e+5;
  R      = -6.0;
  x      = 0.0;
  Sfp    = 103;           {5083 data}
  Sr     = 20.0;
  b      = -0.122;
  ap     = 0.005;

PROCEDURE GetSa;
begin
  alphaA := 0.27 *XpwrY(Tan(pi*theta/180), 0.25);      {Butt Weld}
  alphaB := 0.165*XpwrY(Tan(pi*theta/180), 0.167);     {Butt Weld}

  KfmA := 1 + 0.5 * alphaA * sqrt(ap/t);
  KfmB := 1 + 0.5 * alphaB * sqrt(ap/t);
  Kfeff := (1 - x) * KfmA + x * KfmB;

  Sa := ((Sfp - Sr)*XpwrY((2*Ni),b))/(Kfeff*(1+((1+R)/(1-R))*XpwrY((2*Ni),b)));

end;

PROCEDURE PrintData;
begin
  WriteLn('alphaA      = ', alphaA:1:2);
  WriteLn('alphaB      = ', alphaB:1:2);
  WriteLn('KfmA        = ', KfmA:1:2);
  WriteLn('KfmB        = ', KfmB:1:2);
  WriteLn('Kfeff       = ', Kfeff:1:2);

  WriteLn('Sr (ksi)    = ', Sr:2:1);
  WriteLn('R           = ', R:1:1);
  WriteLn('Sa (ksi)     = ', Sa:2:1);
  WriteLn('Ni (cycles) = ', Ni:7:0);
end;

BEGIN                                     {Main Program}

  GetSa;
  PrintData;
  ReadLn;

END.

```

```

PROGRAM Ni_Al_Hole;

USES  Memtypes, QuickDraw, OSIntf, ToolIntf, PackIntf, Sane;

var
    A, alphaA, alphaB, Kf : real;
    Sa : real;

const
    Ni      = 1e+4;
    R        = -0.26;
    Sfp      = 103;           (5083 data)
    Sr        = 20.0;
    b         = -0.122;
    ap        = 0.005;

PROCEDURE GetSa;
begin
    Kf := 3;
    Sa := ((Sfp - Sr)*XpwrY((2*Ni),b))/(Kf*(1+((1+R)/(1-R))*XpwrY((2*Ni),b)));
end;

PROCEDURE PrintData;
begin
    WriteLn('Kf      = ',Kf:1:2);
    WriteLn('Sr      (ksi) = ',Sr:2:1);
    WriteLn('R        = ',R:1:1);
    WriteLn('Sa      (ksi) = ',Sa:2:1);
    WriteLn('Ni(cycles) = ',Ni:7:0);
end;

BEGIN                                     (Main Program)

    GetSa;
    PrintData;
    ReadLn;

END.

```

```

PROGRAM Np_Al_edge;

USES  Memtypes, QuickDraw, OSIntf, ToolIntf, PackIntf, Sane;

var   ai, da, Y, Fai, SUM, Np: real;
      i, J: Integer;

const  C      = 1e-9;
       m      = 3;
       n      = 200;
       ao     = 1e-2;
       af     = 0.125;
       S      = 4.3;
       t      = 0.125;

PROCEDURE getFai;                                {get  $\Delta K_{exp-m}$ }
begin
    Y := 1.12*sqrt(1/(cos(pi*ai/(2*t))));
    Fai := XpwrY(Y*S*sqrt(3.14159*ai), -m);
end;

BEGIN
    J := n*2;
    da := (af - ao)/J;
    ai := af;
    getFai;
    SUM := Fai;
    ai := ao;
    getFai;
    SUM := SUM + Fai;
    i := 1;
    repeat
        ai := ai + da;
        getFai;
        if odd(i) then SUM := SUM + 4*Fai;
        if odd(i+1) then SUM := SUM + 2*Fai;
        i := i + 1;
    until (i = J);
    Np := da/(3*C)*SUM;

    WriteLn('ao (in.)      = ', ao:2:2);
    WriteLn('af (in.)      = ', af:2:2);
    WriteLn('ai (in.)      = ', ai:2:2);
    WriteLn('da (in.)      = ', da:1:5);
    WriteLn('J              = ', J:4);
    WriteLn('S (ksi.)        = ', S:2:1);
    WriteLn('Fai             = ', Fai:5:9);
    WriteLn('SUM             = ', SUM:5:5);
    WriteLn('Np (cycles)     = ', Np:9:0);

    ReadLn;
END.

```

```

PROGRAM Np_Ai_LOP;

USES  Memtypes, QuickDraw, OSIntf, ToolIntf, PackIntf, Sane;

var   ai, da, Y, Fai, SUM, Np: real;
      i, J: Integer;

const  C      = 1e-9;
       m      = 3;
       n      = 200;
       ao     = 0.5;
       af     = 0.75;
       S      = 16.5;

PROCEDURE getFai;                                {get  $\Delta K_{exp-n}$ }
begin
    Y := 0.5*(1 + 0.4079*XpwrY((ai/af),4) + 0.1456*XpwrY((ai/af),6));
    Fai := XpwrY(Y*S*sqrt(3.14159*ai),-m);

end;

BEGIN
    J := n*2;
    da := (af - ao)/J;
    ai := af;
    getFai;
    SUM := Fai;
    ai := ao;
    getFai;
    SUM := SUM + Fai;
    i := 1;
    repeat
        ai := ai + da;
        getFai;
        if odd (i) then SUM := SUM + 4*Fai;
        if odd (i+1) then SUM := SUM + 2*Fai;
        i := i + 1;
    until (i = J);

    Np := da/(3*C)*SUM;

    WriteLn('ao (in.)      = ',ao:2:2);
    WriteLn('af (in.)      = ',af:2:2);
    WriteLn('ai (in.)      = ',ai:2:2);
    WriteLn('da (in.)      = ',da:1:5);
    WriteLn('J              = ',J:4);
    WriteLn('S (ksi.)        = ',S:2:1);
    WriteLn('Fai            = ',Fai:5:9);
    WriteLn('SUM            = ',SUM:5:5);
    WriteLn('Np (cycles)    = ',Np:9:0);

    ReadLn;

```

END.

ATTACHMENT C SOURCES OF AVERAGE ALUMINUM FATIGUE PROPERTIES

Steel	Monotonic Properties				Cyclic Properties					Ref.
	Young's Modulus E ksi	Yield Strength* S _y ksi	Ultimate Tensile Strength S _u ksi	True Fracture Strength σ _f ksi	True Fracture Ductility ε _f	Cyclic Strain Hardening Exponent n'	Fatigue Strength Coefficient σ' _f ksi	Exponent b	Threshold Stress Intensity Factor ΔK _{th} (at R = -1) ksi (in) ^{1/2}	
A-36	27.5 x 10 ³	36	75	---	---	0.14	125	-0.085	11	30, 35
HY-130	28.0 x 10 ³	147	160	224	0.92	0.100	216	-0.060	5.5 [†]	23, 36
2014-T6	10.0 x 10 ³	67	74	---	0.29	0.16	123	-0.106	2.75 [†]	37, 38
2024-T3	10.6 x 10 ³	55	68	---	0.28	0.065	160	-0.124	3.8	37, 49
7075-T651	10.1 x 10 ³	77.9	85.4	95.1	0.145	0.04	241.4	-0.149	2.5 [†]	23
7075-T6	10.3 x 10 ³	68	84	108	0.41	0.146	278.1	-0.176	3.5	23, 41
7075-T6	10.3 x 10 ³	68	84	108	0.41	0.146	191	-0.126	3.5	37, 41

* 0.2% offset

[†] Represent ΔK_{th} values at R = 0 condition. ΔK_{th} values at R = -1 condition have been calculated from ΔK_{th} values at R = 0 condition using ΔK_{th} = (1 - R) ΔK_{th(0)} (39).

Material	S _a (10 ⁷) ksi	ΔK _{th} ksi (in) ^{1/2}	a in.	Ref.
Mild steel	32	11	0.013	24, 30
BS L65	22	3.48	0.00313	25, 31
7075-T6	15 - 27.5	3.5	0.003	6, 40, 41
A-36	31	11	0.018	18, 30, 42
HY-130	55	10	0.0031	18, 23, 43
2024-T3	17 - 23	3.8	0.008	6, 4, 49

Table 9—Cyclic and Fatigue Properties of Base and Weld Materials for ASTM 5083-0/5183 Aluminum Welds

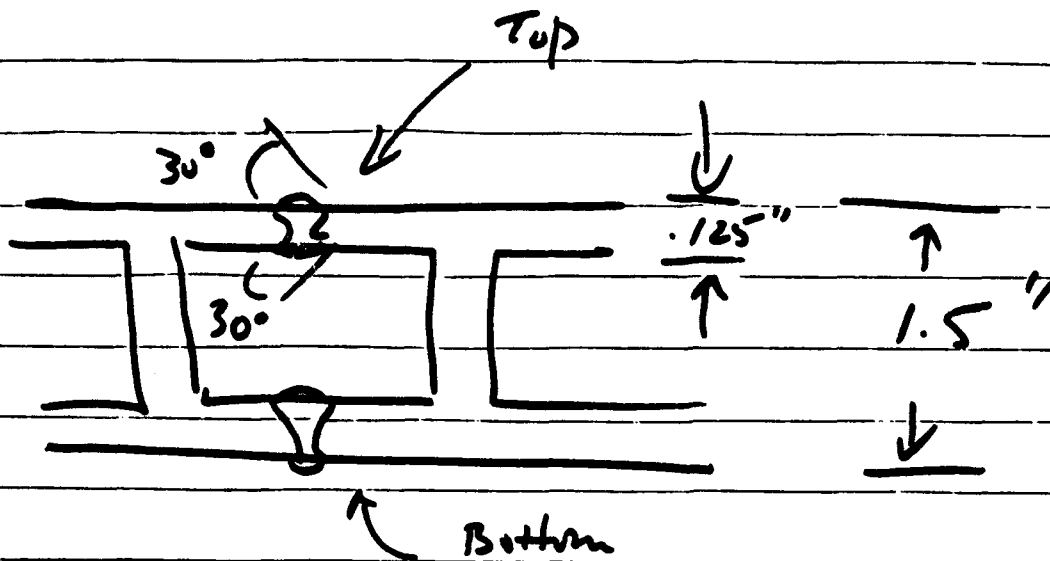
Material	5083-8M	5183-WM
Cyclic yield strength, 0.2% offset, ksi (MPa)	42 (290)	39 (269)
Cyclic strain hardening exponent, n'	0.114	0.072
Cyclic strength coefficient, K', ksi (MPa)	84 (580)	73.5 (507)
Fatigue strength coefficient, σ', ksi (MPa)	103 (711)	92.5 (638)
Fatigue ductility coefficient, ε'	0.405	0.581
Fatigue strength exponent, b	-0.122	-0.107
Fatigue ductility exponent, c	-0.692	-0.890
Transition fatigue life, 2N _{1/2} , reversals	640	205

ATTACHMENT D
CALCULATIONS AND NOTES

(N_I)

(16)

(1)



assume butt weld w/ 30° flange angle (N_I)
 assume edge notch w/ $r_o = 0.01"$ (N_p)
 assume residual stress = + 20 ksi (A_w)

at top:

Case #1

$-27 \rightarrow +4.5 \text{ ksi}$

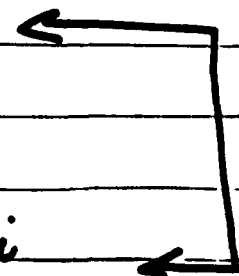
Range = 31.3 ksi

$S_{max} = 15.6 \text{ ksi}$

$R = \frac{S_{min}}{S_{max}} = -6$

$S_a \text{ for } 10,000 = 18.6 \text{ ksi}$

$S_a \text{ for } 100,000 = 14.9 \text{ ksi}$



(N_I)

(17)

(2)

Case #2 -11.3 → 4.3 ksi

$$\text{Range} = 15.6 \text{ ksi}$$

$$\text{Amp} = 7.8$$

$$R = \frac{-11.3}{4.3} = -2.6$$

$$S_a = 18.6 \text{ ksi for } 10,000$$

$$S_s = 14.9 \text{ ksi for } 100,000$$



Case #5 -4.3 to +20.5

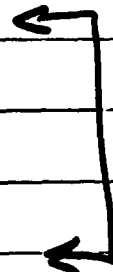
$$\text{Range} = 24.8 \text{ ksi}$$

$$\text{Amp} = 12.4 \text{ ksi}$$

$$R = -4.3 / 20.5 = -0.2$$

$$S_a = 18.6 \text{ ksi for } 10,000$$

$$S_a = 14.9 \text{ ksi for } 100,000$$



Case #6 -4.3 to 17.8 ksi

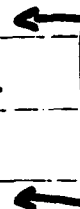
$$\text{Range} = 22.1 \text{ ksi}$$

$$\text{Amp} = 11.05 \text{ ksi}$$

$$R = -4.3 / 17.8 = -0.24$$

$$S_a = 18.6 \text{ ksi for } 10,000$$

$$S_a = 14.9 \text{ ksi for } 100,000$$



(18)

(3)

N_p

edge crack initially 0.01 - in
no effect of weld geometry.

in plate

finite plate

Case #1. -27,000 to 4300

$\Delta S \approx 4.3 \text{ ksi}$

$N_p = 22 \times 10^6 \text{ cycles}$

18,712,000

Case #2 -11,300 to 4300

$\Delta S \approx 4.30 \text{ ksi}$

$N_p = 22 \times 10^6 \text{ cycles}$

18,712,000

Case #5 -4300 psi to +20.500 ksi

$\Delta S \approx 20.5 \text{ ksi}$

$N_p = 211,000 \text{ cycles}$

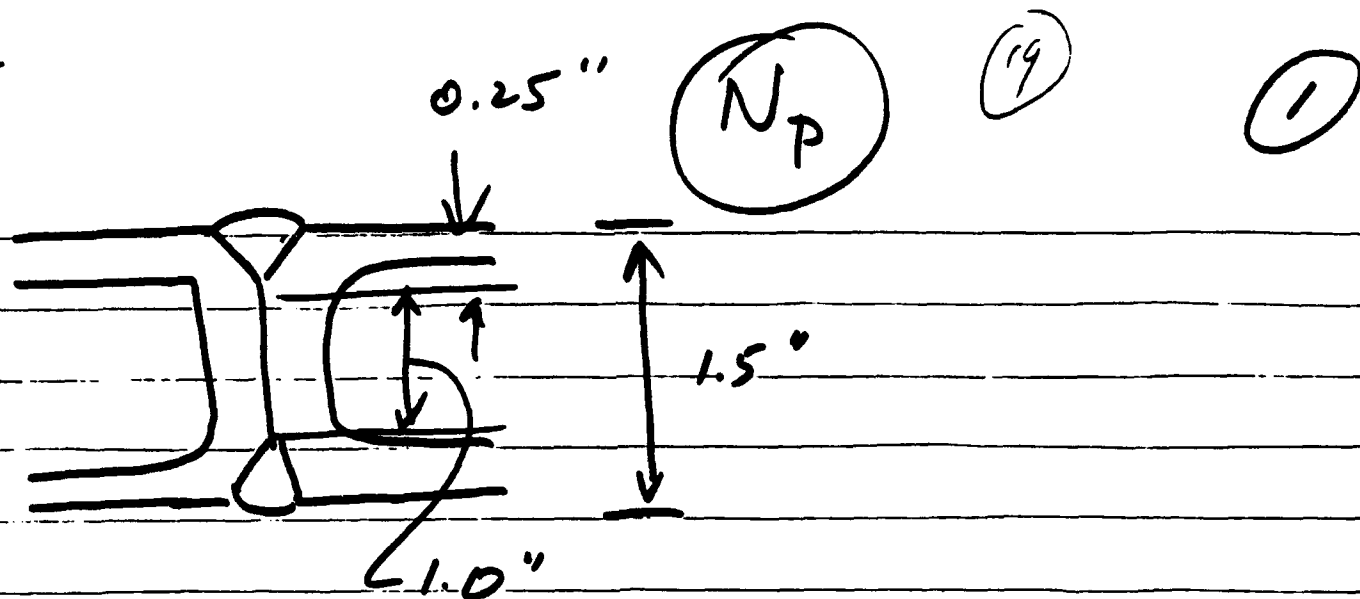
(172,693)

Case #6 -4.300 psi to 17.800 ksi

$\Delta S \approx 17.800 \text{ ksi}$

$N_p = 323,000 \text{ cycles}$

263,801



$$q_b = 0.5''$$

$$q_f = 0.75''$$

Case #3

$$-35 \rightarrow +4.3$$

$$\Delta S \approx 4.3 \text{ ksi}$$

$$N_p = 5 \times 10^6 \text{ cycles}$$

Case #4

$$-35 \rightarrow +4.3 \text{ ksi}$$

$$\Delta S \approx 4.3 \text{ ksi}$$

$$N_p \approx 5 \times 10^6 \text{ cycles}$$

Case #7

$$-4.3 \text{ to } +21.9 \text{ ksi}$$

$$\Delta S \approx 22 \text{ ksi}$$

$$N_p = 38,021 \text{ cycles}$$

Case #8

$$-4.3 \text{ to } 16.5$$

$$\Delta S = 16.5$$

$$N_p = 90,124 \text{ cycles}$$

NI

(20)

(2)

Case # 3 -35 to 4.3

$$\text{Range} = 39$$

$$\text{Comp} = 20$$

$$R = -8.1$$

$$S_a = 6.4 \text{ ksi for } 10, \text{ orv}$$

$$S_a = 5.1 \text{ ksi for } 100, \text{ orv}$$

Case # 4 - ~~35~~ to 4.3
(same)

Case #

Case # 4 -3.5 to 4.3

$$\text{Range} = 7.8$$

$$\text{Comp} = 3.9$$

$$R = -3.5/4.3 = -.8$$

$$S_a = 6.4 \text{ (10, orv)}$$

$$S_a = 5.1 \text{ (100, orv)}$$

Case # 17 -4.3 to 21.9 $R =$

$$\text{Range} = 26.2$$

$$\text{Comp} = 13.1$$

$$R = -4.3/21.9 = -0.2$$

(21)

(3)

$$S_a = 6.4 \text{ ksi} @ 10,000$$

$$S_a = 5.1 \text{ ksi} @ 100,000$$

Case # 8 $-4.3 \rightarrow +16.5 \text{ ksi}$ ✓

$$\text{Range} = 20.8$$

$$\text{Amp} = 10.4$$

$$R = -0.26$$

$$S_a = 6.4 @ 10,000 \text{ cycles}$$

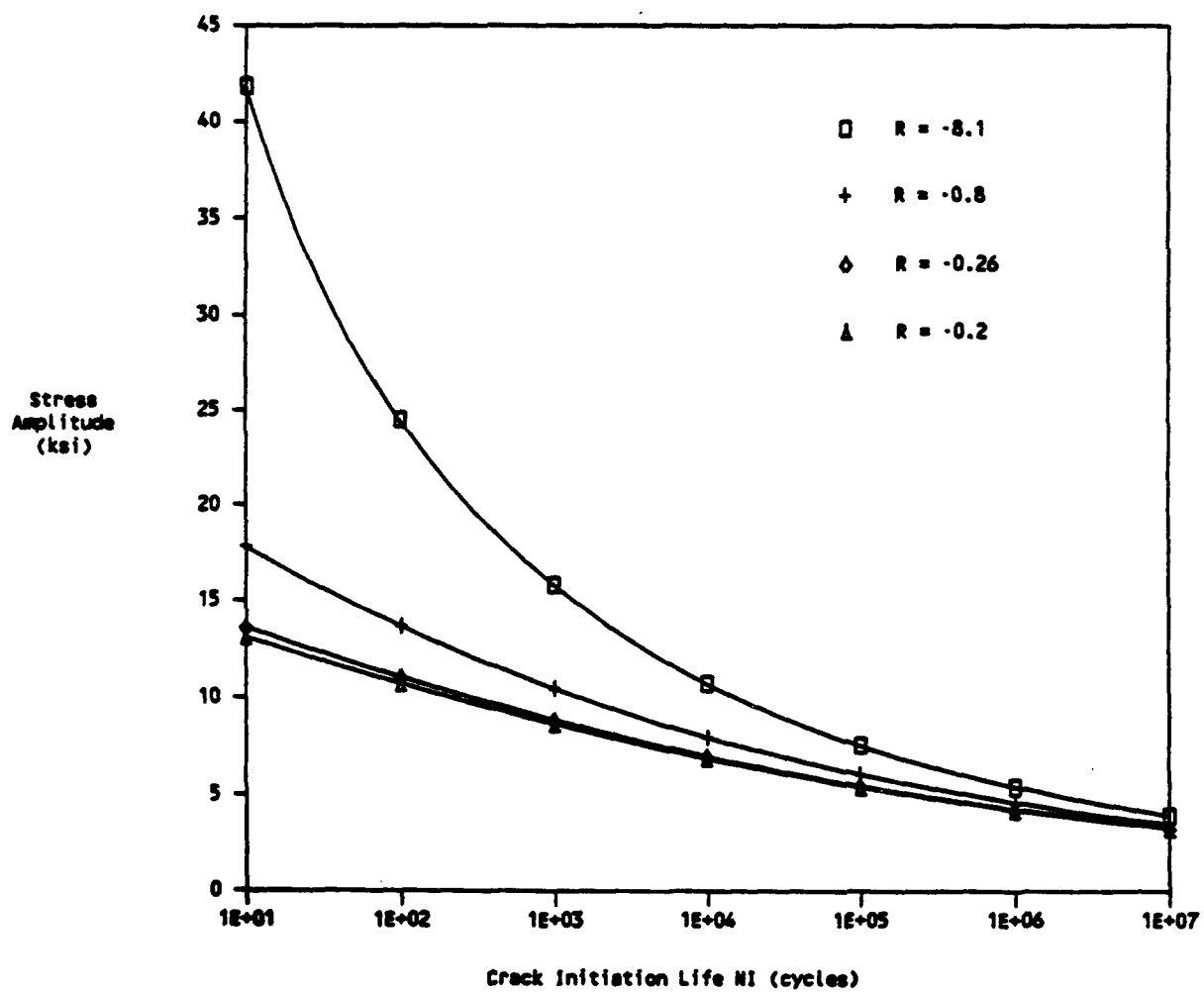
$$S_a = 5.1 \text{ ksi} @ 100,000 \text{ cycles}$$

APPENDIX A 5

**GARD's Evaluation of Fatigue Crack Initiation Life
for Type II Joints for Actual Mixed Load**

Crack Initiation Lives in Cycles

Case	Joint	S _a (ksi)		R	Crack Initiation Life (cycles)		
		high	low		high load	low load	mixed load
3	II-top	20.0	12.0	-8.1	281	5,145	1,882
4	II-top	3.9	2.3	-0.8	4,150,350	286,487,701	36,716,314
7	II-bottom	13.1	7.9	-0.2	10	2,703	99
8	II-bottom	10.2	6.1	-0.26	241	37,569	2,283



APPENDIX A6

Extended Analysis of Fatigue Crack Initiation Life of Type II Welds in Panels

APPENDIX A

EXTENDED ANALYSIS OF FATIGUE CRACK INITIATION LIFE OF TYPE II WELDS IN PANELS

The preliminary analysis of stresses and fatigue crack initiation and propagation lives for welds in the panels was reported last month. That analysis is very conservative as compared to reality. In most cases, this conservatism is tolerable, as the results show sufficient life to meet the panel's requirements. However, for Type II welds, the fatigue crack initiation lives following from the preliminary analysis are too low to substantiate acceptable panel behavior. For this reason, the analysis of these welds was extended to better represent the physical situation and, thereby, provide a less conservative (and more significant) measure of the fatigue crack initiation life of the Type II welds.

The principal improvement is the introduction of an FEM analysis to evaluate the stresses which develop at the tip of the weld root. The FEM model includes essentially one-quarter of a "cell" from the panel and is shown in Figure 1. This model was run on an IBM AT, using a commercially available FEM software package, Images 3-D. The load cases are shown schematically in Figure 2 and are described as follows:

- 1) A distributed load over the cut surface of the horizontal leg, apportioned to correspond to a macro bending stress of 1000 in-lbf/in on the panel.
- 2) A distributed load of 160 psi over the horizontal leg's outer surface, together with distributed loads over the cut surface of the leg, apportioned to correspond to the local bending moment that results from that distributed load.
- 3) A shear force of 100 lbf/in uniformly distributed over the cut surface of the horizontal leg.

The weld root stresses for these three load cases were recorded and later combined linearly to determine the peak stresses corresponding to the combined load cases that follow from the macro panel BOEF analysis superposed with the local analysis (as described in the last report).

Prof. Lawrence's algorithm for calculating Type II weld crack initiation life versus stress cycle was then used for each location (top and bottom of panel) and for each stress (normal X, normal Y, and both principal stresses) to compute the minimum crack initiation lives. This was done both for the 20,000 lbf tire load and for the 12,000 lbf tire load. These lives were then combined to get an effective life for the actual load history (90% at 12,000 lbf tire load and 10% at 20,000 lbf tire load).

The combined-load life to crack initiation results are as follows:

Weld at Upper Surface of Panel

Stress Component	Life in Cycles
Normal X	228,900
Normal Y	2, 012,800
First Principal	3, 094,800
Second Principal	187,000

Weld at Lower Surface of Panel

Stress Component	Life in Cycles
Normal X	2, 696,700
Normal Y	113, 275,000
First Principal	2, 479,000
Second Principal	99, 359,800

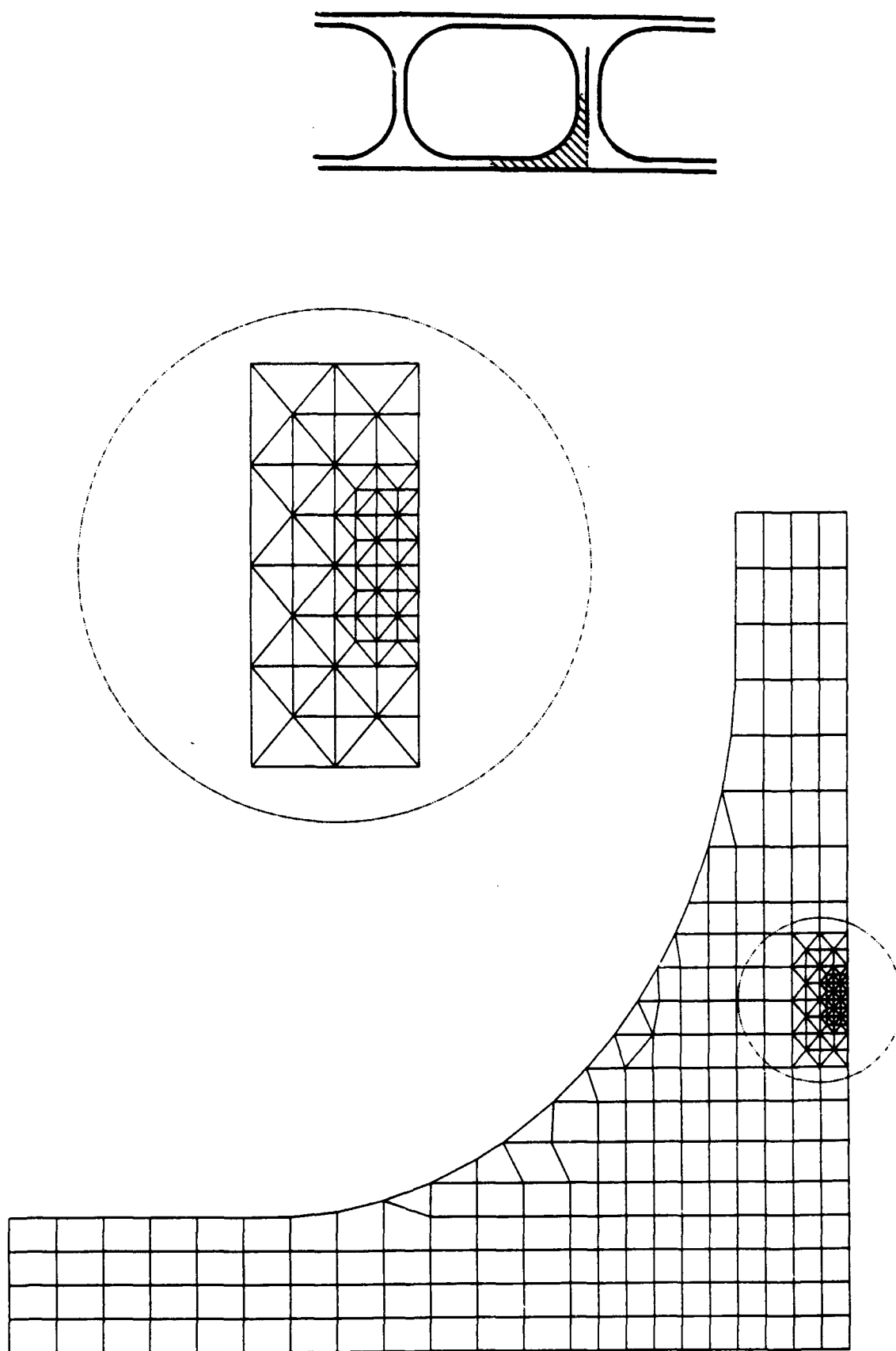
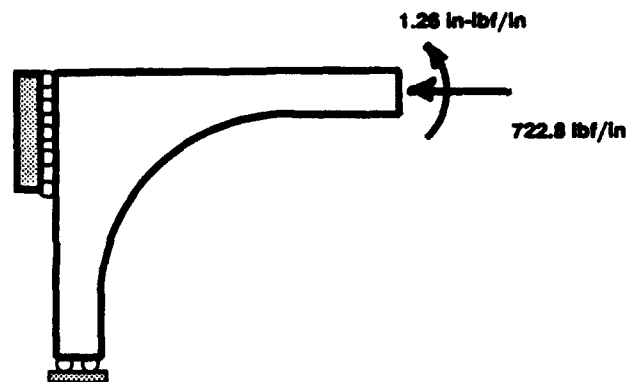
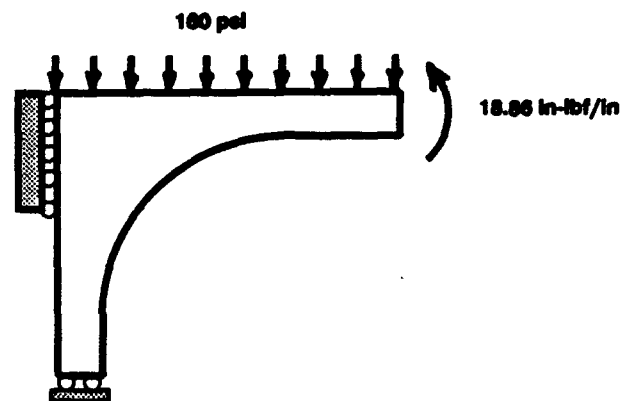


Figure 1 FEM Model of Panel Section

1000 in-lbf/in Bending Moment on Full Panel



160 psi Uniform Pressure on Surface of Panel



100 lbf/in Shear Force Across Horizontal Leg

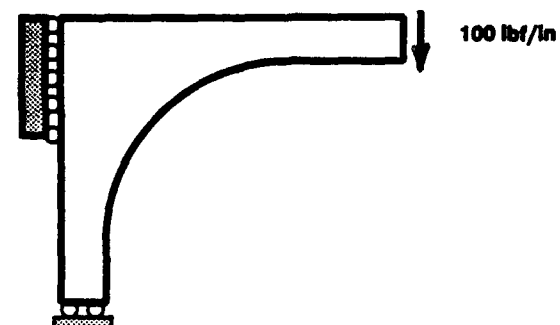


Figure 2 Basic Load Cases for FEM Model

APPENDIX A7

Revision to the Extended Analysis of Type II Welds

REVISION TO THE EXTENDED ANALYSIS OF TYPE II WELDS

Further discussions with Prof. Lawrence have revealed that the algorithm that he utilized for calculating Type II weld crack initiation life versus stress cycle should no be applied directly to GARD's extended analysis using weld root stresses computed from an FEM analysis. Prof. Lawrence's algorithm assumed the presence of a hole with factor 3 at the weld root. Current plans for the Type II welds suggest that no such hole will be provided and that the sections to be joined will be compressed against one another during the welding operation. The unjoined portion of the section boundaries then form what is, in effect, an incipient crack. For analysis purposes, in order to estimate the life before this "incipient crack" begins to propagate outward into the weld, Prof. Lawrence has suggested that the algorithm he had used should be altered to change the concentration factor from 3 to 11.

In addition to the modification noted above, Prof. Lawrence also suggested that the compressive portion of the stress cycle should not be included in the analysis using his algorithm, as the unjoined material between the upper and lower welds is now in contact (in contrast to his earlier assumption that these surfaces would be slightly separated).

Prof. Lawrence's algorithm was utilized in both revised forms to recalculate the crack initiation lives for Type II welds. The results of these calculations, along with the results of the earlier calculations (concentration factor 3, with compressive stresses included in the stress cycle), are tabulated in Table 1.

In either case (with or without the inclusion of the compressive portion of the stress cycle), the computed crack initiation lives are clearly insufficient. It is recognized, however, that the computation for the stresses at the weld root are based upon several assumptions which are clearly conservative. Rather than continue the analysis, at this point, to remove some of that conservatism, it will suffice to consider the fatigue crack propagation life for the Type II welds. Prof. Lawrence's algorithm for the propagation life was utilized with the computed stress cycle. Results, shown in Table 2, show that the propagation life is far in excess of that which is required.

TABLE 1
FATIGUE CRACK INITIATION LIFE FOR TYPE II WELDS

Weld Location	Stress Component	Initiation Life in Cycles		
		(K = 3)	(K = 11)	Tension Only (K = 11)
TOP	S _x	229,000	78	422,200
	S _y	2,013,000	433	23,668,000
	S ₁	3,095,000	268	78,243
	S ₂	187,000	117	407,339,000
BOTTOM	S _x	2,697,000	7	12
	S _y	113,275,000	854	3,900
	S ₁	2,479,000	1	1
	S ₂	99,360,000	2,332	70,700

TABLE 2
FATIGUE CRACK PROPAGATION LIFE FOR TYPE II WELDS

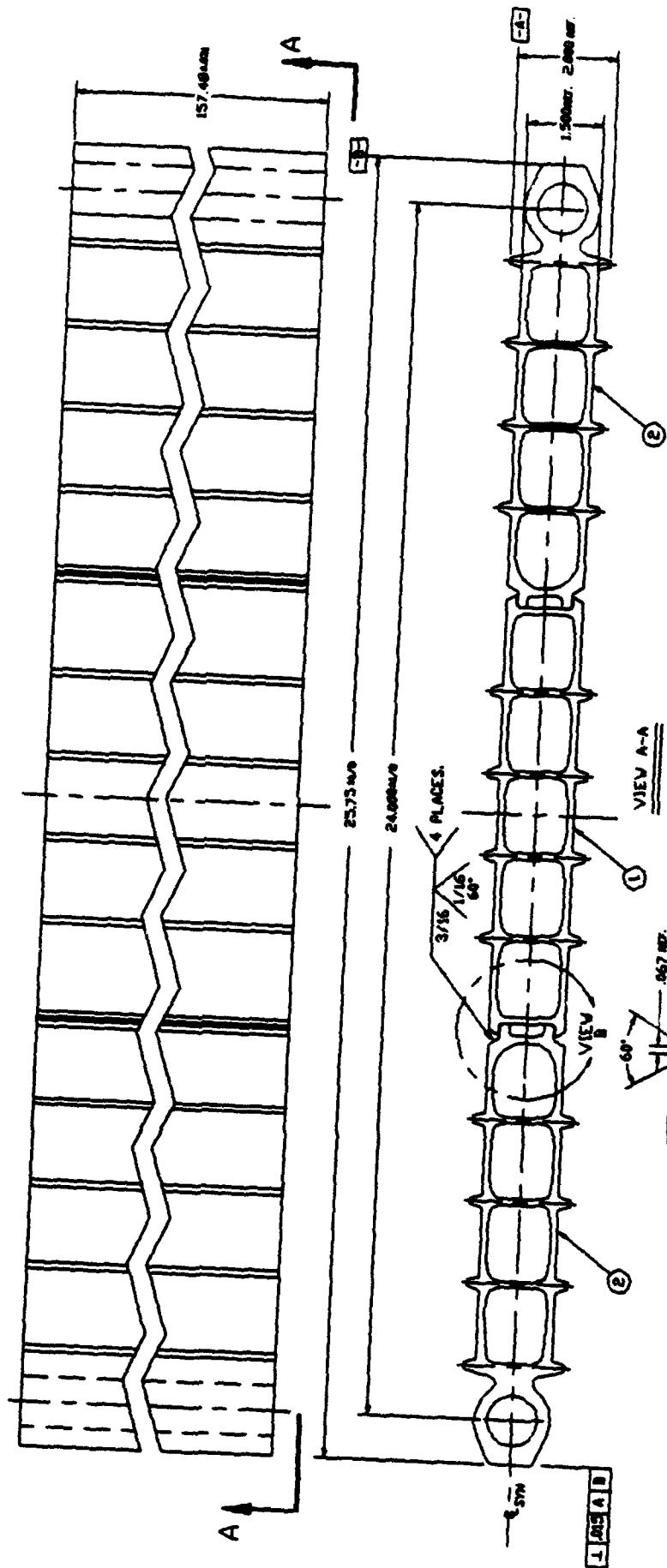
Weld Location	Stress Component	Propagation Life in Cycles
TOP	S _x	79,262,000
	S _y	273,155,000
	S ₁	48,706,000
	S ₂	692,780,000
BOTTOM	S _x	5,927,000
	S _y	21,753,000
	S ₁	3,819,000
	S ₂	49,391,000

APPENDIX A8

GARD's Drawings of Welded Mod. 2 Access/Egress Subpanels

NOTES

1. MATING SHALL BE ALIGNED IN ACCORDANCE WITH AREA 457 GRU-16.
2. VOLUMES SHALL BE IN ACCORDANCE WITH ONE AND TWO LATER CENTER.
3. VOLUMES SHALL BE CHARGED FOR AND OPERATIONS SHALL CENTER.
4. MATING OF THE MAT SHALL BE 60°.
5. VOLUMES SHALL BE 3/16" IN THICKNESS.
6. VOLUMES SHALL BE 1/16" IN THICKNESS.
7. VOLUMES SHALL BE 1/16" IN THICKNESS.
8. VOLUMES SHALL BE 1/16" IN THICKNESS.
9. VOLUMES SHALL BE 1/16" IN THICKNESS.
10. VOLUMES SHALL BE 1/16" IN THICKNESS.
11. VOLUMES SHALL BE 1/16" IN THICKNESS.
12. VOLUMES SHALL BE 1/16" IN THICKNESS.
13. VOLUMES SHALL BE 1/16" IN THICKNESS.
14. VOLUMES SHALL BE 1/16" IN THICKNESS.
15. VOLUMES SHALL BE 1/16" IN THICKNESS.
16. VOLUMES SHALL BE 1/16" IN THICKNESS.
17. VOLUMES SHALL BE 1/16" IN THICKNESS.
18. VOLUMES SHALL BE 1/16" IN THICKNESS.
19. VOLUMES SHALL BE 1/16" IN THICKNESS.
20. VOLUMES SHALL BE 1/16" IN THICKNESS.
21. VOLUMES SHALL BE 1/16" IN THICKNESS.
22. VOLUMES SHALL BE 1/16" IN THICKNESS.
23. VOLUMES SHALL BE 1/16" IN THICKNESS.
24. VOLUMES SHALL BE 1/16" IN THICKNESS.
25. VOLUMES SHALL BE 1/16" IN THICKNESS.
26. VOLUMES SHALL BE 1/16" IN THICKNESS.
27. VOLUMES SHALL BE 1/16" IN THICKNESS.
28. VOLUMES SHALL BE 1/16" IN THICKNESS.
29. VOLUMES SHALL BE 1/16" IN THICKNESS.
30. VOLUMES SHALL BE 1/16" IN THICKNESS.
31. VOLUMES SHALL BE 1/16" IN THICKNESS.
32. VOLUMES SHALL BE 1/16" IN THICKNESS.
33. VOLUMES SHALL BE 1/16" IN THICKNESS.
34. VOLUMES SHALL BE 1/16" IN THICKNESS.
35. VOLUMES SHALL BE 1/16" IN THICKNESS.
36. VOLUMES SHALL BE 1/16" IN THICKNESS.
37. VOLUMES SHALL BE 1/16" IN THICKNESS.
38. VOLUMES SHALL BE 1/16" IN THICKNESS.
39. VOLUMES SHALL BE 1/16" IN THICKNESS.
40. VOLUMES SHALL BE 1/16" IN THICKNESS.
41. VOLUMES SHALL BE 1/16" IN THICKNESS.
42. VOLUMES SHALL BE 1/16" IN THICKNESS.
43. VOLUMES SHALL BE 1/16" IN THICKNESS.
44. VOLUMES SHALL BE 1/16" IN THICKNESS.
45. VOLUMES SHALL BE 1/16" IN THICKNESS.
46. VOLUMES SHALL BE 1/16" IN THICKNESS.
47. VOLUMES SHALL BE 1/16" IN THICKNESS.
48. VOLUMES SHALL BE 1/16" IN THICKNESS.
49. VOLUMES SHALL BE 1/16" IN THICKNESS.
50. VOLUMES SHALL BE 1/16" IN THICKNESS.
51. VOLUMES SHALL BE 1/16" IN THICKNESS.
52. VOLUMES SHALL BE 1/16" IN THICKNESS.
53. VOLUMES SHALL BE 1/16" IN THICKNESS.
54. VOLUMES SHALL BE 1/16" IN THICKNESS.
55. VOLUMES SHALL BE 1/16" IN THICKNESS.
56. VOLUMES SHALL BE 1/16" IN THICKNESS.
57. VOLUMES SHALL BE 1/16" IN THICKNESS.
58. VOLUMES SHALL BE 1/16" IN THICKNESS.
59. VOLUMES SHALL BE 1/16" IN THICKNESS.
60. VOLUMES SHALL BE 1/16" IN THICKNESS.
61. VOLUMES SHALL BE 1/16" IN THICKNESS.
62. VOLUMES SHALL BE 1/16" IN THICKNESS.
63. VOLUMES SHALL BE 1/16" IN THICKNESS.
64. VOLUMES SHALL BE 1/16" IN THICKNESS.
65. VOLUMES SHALL BE 1/16" IN THICKNESS.
66. VOLUMES SHALL BE 1/16" IN THICKNESS.
67. VOLUMES SHALL BE 1/16" IN THICKNESS.
68. VOLUMES SHALL BE 1/16" IN THICKNESS.
69. VOLUMES SHALL BE 1/16" IN THICKNESS.
70. VOLUMES SHALL BE 1/16" IN THICKNESS.
71. VOLUMES SHALL BE 1/16" IN THICKNESS.
72. VOLUMES SHALL BE 1/16" IN THICKNESS.
73. VOLUMES SHALL BE 1/16" IN THICKNESS.
74. VOLUMES SHALL BE 1/16" IN THICKNESS.
75. VOLUMES SHALL BE 1/16" IN THICKNESS.
76. VOLUMES SHALL BE 1/16" IN THICKNESS.
77. VOLUMES SHALL BE 1/16" IN THICKNESS.
78. VOLUMES SHALL BE 1/16" IN THICKNESS.
79. VOLUMES SHALL BE 1/16" IN THICKNESS.
80. VOLUMES SHALL BE 1/16" IN THICKNESS.
81. VOLUMES SHALL BE 1/16" IN THICKNESS.
82. VOLUMES SHALL BE 1/16" IN THICKNESS.
83. VOLUMES SHALL BE 1/16" IN THICKNESS.
84. VOLUMES SHALL BE 1/16" IN THICKNESS.
85. VOLUMES SHALL BE 1/16" IN THICKNESS.
86. VOLUMES SHALL BE 1/16" IN THICKNESS.
87. VOLUMES SHALL BE 1/16" IN THICKNESS.
88. VOLUMES SHALL BE 1/16" IN THICKNESS.
89. VOLUMES SHALL BE 1/16" IN THICKNESS.
90. VOLUMES SHALL BE 1/16" IN THICKNESS.
91. VOLUMES SHALL BE 1/16" IN THICKNESS.
92. VOLUMES SHALL BE 1/16" IN THICKNESS.
93. VOLUMES SHALL BE 1/16" IN THICKNESS.
94. VOLUMES SHALL BE 1/16" IN THICKNESS.
95. VOLUMES SHALL BE 1/16" IN THICKNESS.
96. VOLUMES SHALL BE 1/16" IN THICKNESS.
97. VOLUMES SHALL BE 1/16" IN THICKNESS.
98. VOLUMES SHALL BE 1/16" IN THICKNESS.
99. VOLUMES SHALL BE 1/16" IN THICKNESS.
100. VOLUMES SHALL BE 1/16" IN THICKNESS.



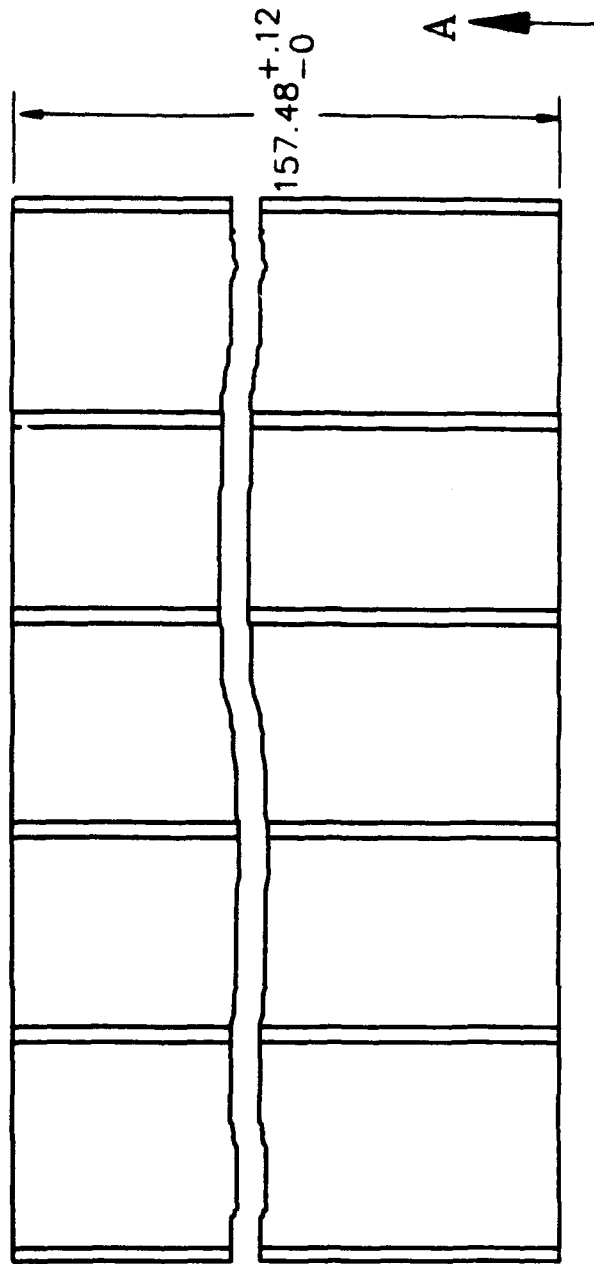
NO.	DESCRIPTION	QUANTITY	UNIT	REMARKS
1	WELDED MAT	157' 48"	LF	
2	WELDED MAT	25' 73"	WF	
3	WELDED MAT	1/16"	TH	
4	WELDED MAT	60°	ANG	
5	WELDED MAT	1/16"	TH	
6	WELDED MAT	60°	ANG	
7	WELDED MAT	1/16"	TH	
8	WELDED MAT	60°	ANG	
9	WELDED MAT	1/16"	TH	
10	WELDED MAT	60°	ANG	

WELDED MAT, ROADWAY,
ACCESS/EGRESS

VIEW B
(SCALE 1=2)

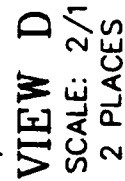
[illegible]

1. MATERIAL SHALL BE ALUMINUM
IN ACCORDANCE WITH ASTM B221,ALY 6061-T6
2. UNLESS OTHERWISE SPECIFIED ALL TOLERANCES
ON EXTRUDED SHAPE SHALL BE IN
ACCORDANCE WITH ANSI H35.2
3. TOLERANCES ON STRAIGHTNESS,
TWIST AND FLATNESS SHALL
BE ONE-HALF THE VALUES
AS SPECIFIED IN ANSI H35.2
4. THE BLENDING OF WEBS TO
SKINS SHALL BE SMOOTH
AND FREE OF DISCONTINUITIES,
THERE SHALL BE NO THINNING
OF WEBS OR SKINS AT BLEND
TANGENT POINTS OF RADII.

[illegible]

REVIEWS		
DATE	RECEPTION	APPROVAL
1/17		

[illegible]

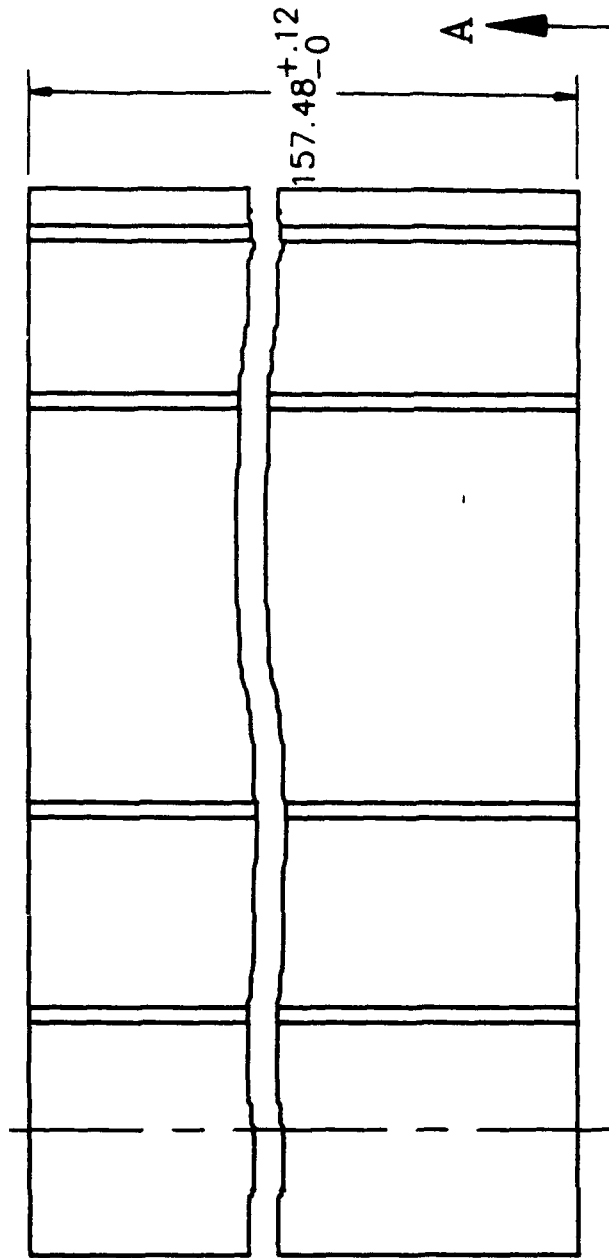
[illegible]

VIEW C
SCALE: 2/1
5 PLACES

[illegible]

NOTES:

1. MATERIAL SHALL BE ALUMINUM
IN ACCORDANCE WITH ASTM B221, ALY 6061-T6
2. UNLESS OTHERWISE SPECIFIED ALL TOLERANCES
ON EXTRUDED SHAPE SHALL BE IN
ACCORDANCE WITH ANSI H35.2
3. TOLERANCES ON STRAIGHTNESS,
TWIST AND FLATNESS SHALL
BE ONE-HALF THE VALUES
AS SPECIFIED IN ANSI H35.2
4. THE BLENDING OF WEBS TO
SKINS SHALL BE SMOOTH
AND FREE OF DISCONTINUITIES
THERE SHALL BE NO THINNING
OF WEBS OR SKINS AT BLEND
TANGENT POINTS OF RADII.



REVISIONS		DATE		APPROVAL	
LTD	DESCRIPTION	DATE	DATE	DATE	DATE

QTY REQD	DESCRIPTION OF DESCRIPTION	CODE REQD	PART OR IDENTIFIED NO	SPECIFICATION	REV NO

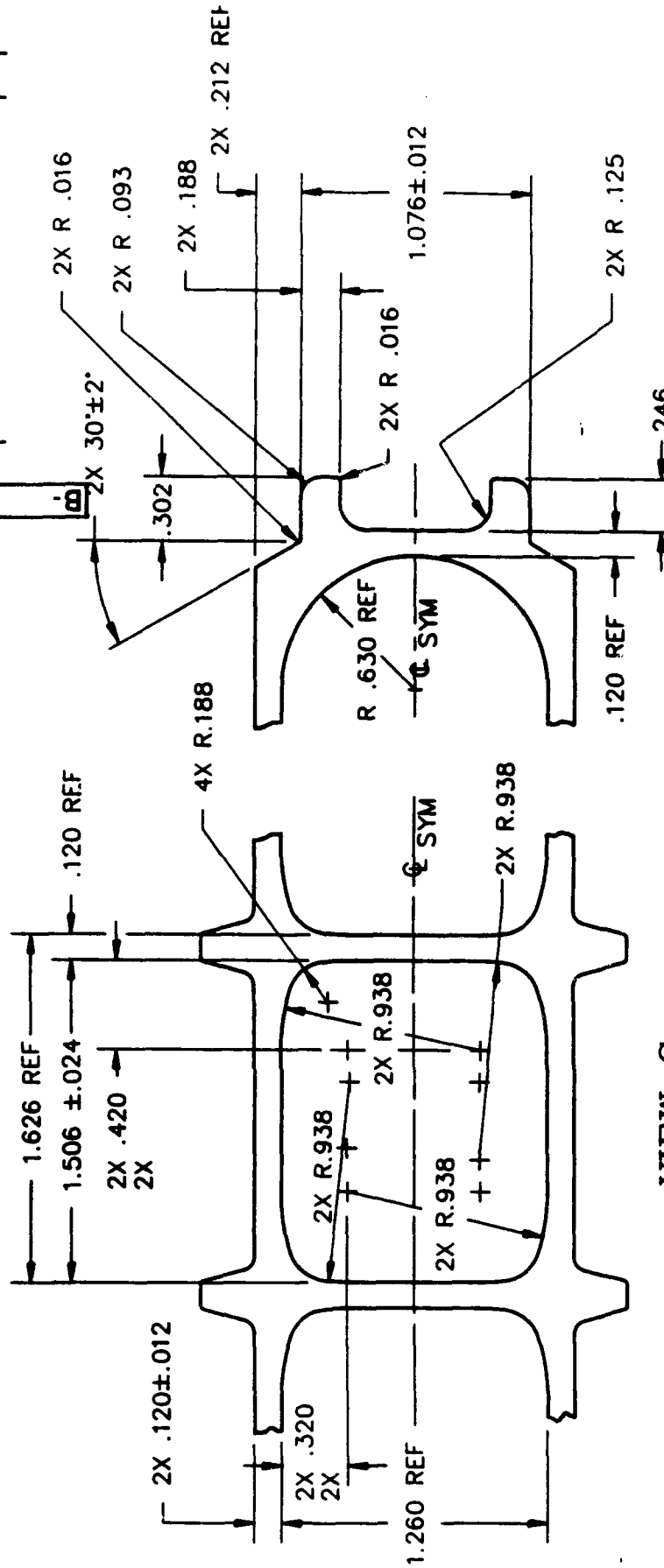
PARTS LIST	
SIGNATURE	DATE
APPROVED BY	
APPROVED BY	

END PANEL	
B	002

THREAT	DATE	DESCRIPTION	ATT
--------	------	-------------	-----

[illegible]

NOTES:



VIEW C
SCALE: 2/1
2 PLACES

VIEW D

REVISIONS		DATE		APPROVAL	
LYR	DESCRIPTION	DATE	APPROVAL	DATE	APPROVAL

QTY	DESCRIPTION OR DESCRIPTION	PART OR IDENTIFYING NO.	SPECIFICATION	ITEM NO.

PARTS LIST		DATE		BY	
QTY	DESCRIPTION	DATE	BY	DATE	BY

UNLESS OTHERWISE SPECIFIED ALL DIMENSIONS ARE IN INCHES		DATE		BY	
QTY	DESCRIPTION	DATE	BY	DATE	BY

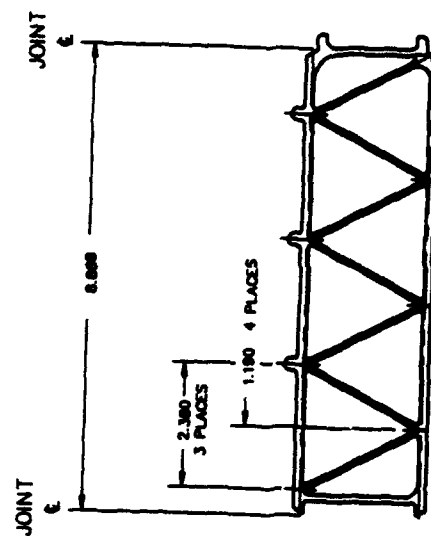
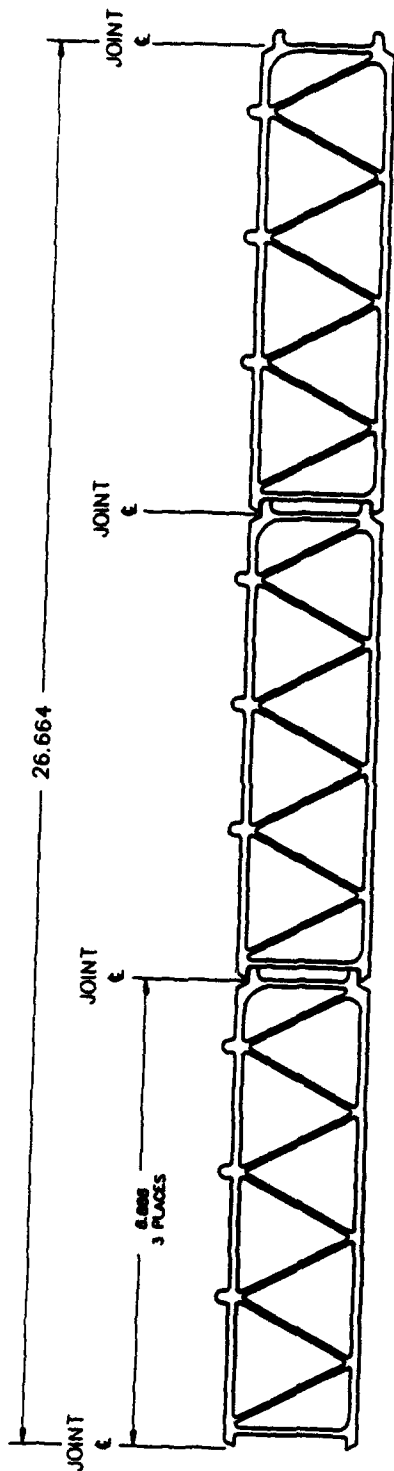
SIGNATURE		DATE		BY	
QTY	DESCRIPTION	DATE	BY	DATE	BY

MATERIAL		FINISH		APPLICATION	
QTY	DESCRIPTION	DATE	BY	DATE	BY

END PANEL		B		002	
QTY	DESCRIPTION	DATE	BY	DATE	BY

APPENDIX A9

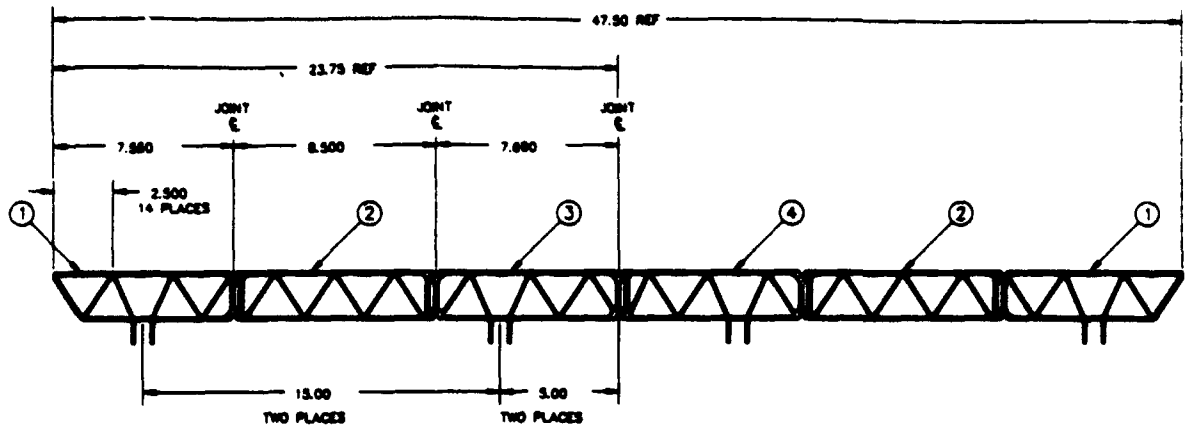
Conceptual Modification of the Ribbon Bridge Deck Panel



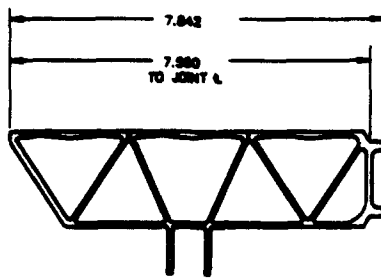
CONCEPT - RIBBON BRIDGE EXTRUSION

APPENDIX A10

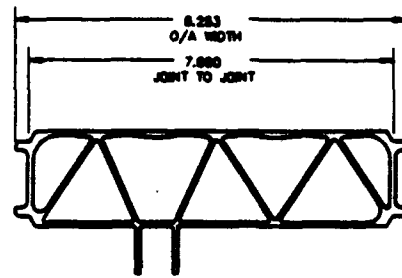
Conceptual Modification of the Light Assault Bridge Deck Panel



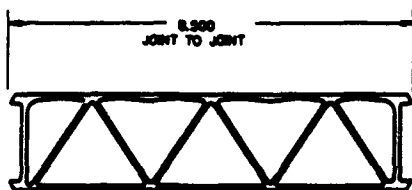
LAB ASSEMBLY
SCALE 1/2



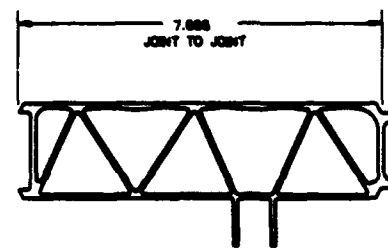
ITEM ①



ITEM ③



ITEM ②



ITEM ④

CONCEPT - L.A.B. EXTRUSION

APPENDIX A11

GARD's Report A1-161-30



1st Line - Inside Address

2nd

3rd

4th

Dear Sir:

GARD Division of Chamberlain Manufacturing Corporation is currently involved in a project which requires hollow extruded aluminum panels shown on the attached drawings and two dies. A limited number of such panels made of 6061-T6 alloy will be ordered for research purposes, namely:

Middle Panel	(Drwg. #001),	L = 180.00 in. - 32 panels
Middle Panel	(Drwg. #001),	L = 157.48 in. - 15 panels
End Panel	(Drwg. #002),	L = 157.48 in. - 30 panels

The total order is about 5,000 lbs. After completion of this research, annual panel requirement will be hundreds of thousands of pounds.

To participate in a bid for this work, it is necessary that you:

- 1) Confirm press availability to extrude hollow panels of the circle size required by the attached drawings. The drawings are proprietary to GARD and are not to be disclosed to a third party.
- 2) Evaluate tolerances specified on the drawings:
 - a) Mark up the drawings (under and above each specified tolerance) indicating tolerances specified by ANSI H35.2 (under) and those achievable at your facility (above).
- 3) Prepare cost quotations for the specified number of the extruded panels, including:
 - a) costs of the panels (\$/lb.) for tolerances specified by ANSI and those achievable at your facility,
 - b) cost of dies (\$/piece),
 - c) freight cost,
 - d) packaging cost (panels should be properly stacked and secured on wood bases, surfaces and edges of each panel should be properly protected from dirt, grease, inclement weather, scuffing or any other damage),
 - e) delivery schedule,
 - f) estimated cost of the panels in mass production.
- 4) Mail the marked drawings, the quotations and any information on your company capabilities to GARD as soon as possible. Evaluation of quotations will be performed during the last week of August 1988.

If you have problems with this schedule or any other questions do not hesitate to call the undersigned or Mr. Roy Schoon at 312-647-9000.

Truly yours,

V. Malin

Dr. Valdemar Malin
Project Manager

VM:mrn
Attachment

GARD'S REPORT A1-161-30

Bid Survey Among U.S. Extrusion Manufacturers **(Results and Analysis)**

1. Introduction

In August and September, 1988 GARD conducted a bid survey among U.S. extrusion manufacturers, members of the Aluminum Extruders Council. Among 150 members listed in the Directory of the Council, only 21 were prequalified to participate in the bid by their press capability (circle size of extruded products). The main objectives of the survey were to evaluate the manufacturing base for supplying extruded subpanels (the subpanels are to be joined by welding into the Waterways Experimental Station (WES) mat panels), and to determine realistic tolerances and costs of the extruded subpanels.

The survey has been viewed by GARD as very important since the results were expected to potentially affect the following aspects of the project:

- a) Fixture design might be affected since joint tracking devices might become necessary if industry does not meet the accuracy requirements for automatic welding of the extruded subpanels.
- b) Mat panel design might be affected as a result of industry inability to produce the subpanels technically and/or economically to the specified tolerances.
- c) Selection of 6061-T6 as a base material for the subpanels might be reviewed if extrudability of this material presents a serious problem. This, in turn, might affect the mat panel design as well.
- d) Many aspects of this project might be affected as a result of evaluation of the manufacturing base available in the U.S. for supplying the subpanels. If this base is limited, this might require review of the mat panel design also.

2. Results and Analysis of the Survey

2.1 Background

An introductory letter and a set of the draft drawings were submitted to each of the

21 potential bidders, in August 1988. A copy of the letter and the set of drawings are attached to this report.

The feedback from the manufacturers has not been as great as GARD had previously expected. It took more than two months for 19 bidders to respond. Among those who did respond, only a few met all the requirements specified in the introductory letter.

A summary of the answers is shown in the attached table. Analysis of the results of the survey shows how the required panel size, configuration, material and manufacturing tolerances affect both the number of extrusion manufacturers that are capable or willing to supply the mat panels and also the cost of the panels.

2.2 Effect of Panel Size and Configuration on Panel Extrudability

The size and configuration of the WES panel appeared to present a serious difficulty for the majority of the bidders. Only 8 of them have equipment to extrude panels of the required circle size (8.67 in.) with such an intricate and delicate multi-hollow configuration.

Some of the reasons for declining to bid are the following:

- a) Press capacity is not sufficient (most of the bidders).
- b) Wall thickness (0.120 in.) is too thin (Jarl Extrusions).
- c) Panel is too light and delicate for big presses (Taber Metals).

It turned out that multi-hollow panels require special expertise in addition to a press of sufficient capacity. For example, some manufacturers (Dolton, Cressona Aluminum, among others), which are normally capable of producing extrusions of a larger circle size than required, refused to bid because of the delicate panel configuration.

2.3 Effect of Panel Material on Panel Extrudability

Selection of 6061-T6 aluminum alloy as a base material for the mat panel reduced the number of the qualified bidders: only 4 of them are capable of handling this high-strength aluminum alloy.

The main reasons are the following:

- a) The material is too hard to produce it competitively (most of the bidders).
- b) Difficulties in metal flow are a concern (Aluminum Shapes).
- c) Non-uniformity of properties around the voids due to trapped heat is a matter of concern (Mid-America Extrusions).

The desirable substitute for 6061-T6, among the four companies which are not capable of handling this material, are 6063-T6 and 6005-T6 aluminum alloys. In the case of 6063-T6, the tensile strength of the alloy is 5 ksi lower than that of 6061-T6 (33 vs. 38 ksi).

2.4 Effect of Panel Tolerances on Panel Extrudability

All four companies which are capable of producing the subpanels using 6061-T6 aluminum alloy indicated that they would rather produce the extrusion with the tolerances specified by the ANSI Standard (Dimensional Tolerances for Aluminum Mill Products, ANSI-H35.2).

2.4.1 Effect of Panel Width Tolerance

According to this Standard, the width of the extruded subpanel has a tolerance of ± 0.064 in. GARD's attempt to reduce the tolerance to ± 0.031 in. disqualifies two manufacturers. Only two extruders, Mid-America Extrusions Corp. and Magnode Corp., are capable of producing subpanels with ± 0.031 in. tolerance. This is still not enough to meet the requirements for automatic welding (± 0.010 in.); however, to extrude the subpanels with such an accuracy is probably neither technically nor economically possible.

2.4.2 Effect of Panel Length Tolerances

The panel length tolerance (± 0.025 in.), specified by the Army, may present difficulties in automatic welding. Since 3 subpanels are lined up flush against one side of the fixture, the location of the other ends of the subpanels may vary by 0.5 in. or even 0.75 in. if they are made per the ANSI Standard ($\pm 3/8$ in.). This is not acceptable for automatic welding which will require ± 0.031 in. unless a special sensory device is developed to track the actual ends of the subpanels assembled in the fixture. A tolerance

of ± 0.031 in. is achievable only by additional cutting, as offered by Mid-America Extrusions.

2.4.3 Effect of Panel Straightness, Flatness and Twist

The ANSI Standard allows for 13-ft. long panels the following tolerances for straightness, flatness and twist: 0.0125 in./ft., 0.006 in./ft. of width and 1/4 deg./ft. (3 deg. max.). Only Magnode and Mid-America Extrusions met the Army requirement of 1/2 of the ANSI tolerances.

2.5 Effect of Panel Tolerances on Cost

Despite GARD's requirement, specified in the introductory letter, to show the cost of extrusions produced with both the ANSI and GARD tolerances, only one manufacturer (Magnode Corp.) responded.

According to Magnode's quotation, stricter tolerances on the width (8.67 in.) of the extruded subpanel (± 0.031 vs. ± 0.064 in.) increase the cost of the extrusion by 11% or \$0.21 per lb. (\$1.90 vs. \$2.11 per lb). Further tightening of the tolerance to ± 0.010 in. to meet the requirement for automatic welding (if technically possible) would probably increase the cost by 20-25% or roughly \$0.50 per lb.

The cost of cutting the panels to a specified length with ± 0.031 in. tolerance needed for automatic welding (indicated only in Mid-America Extrusions quotation) is \$1.23 per cut or approximately \$0.02 per lb.

The cost of die charges is not affected by the specified tolerances.

2.6 Ownership of Dies

Contrary to the Army requirement to procure the dies as "the property of the U.S. Government and stored by the contractors for a period of one year after completion of the contract," all the extrusion fabricators have the following typical provision in their quotations:

"Any equipment (including jigs, dies, tools, etc.) which Seller constructs or acquires solely for use in the production of products ordered hereunder shall be and remain Seller's property and in seller's sole possession and control. Any changes made by Seller hereto

shall be only for the use of such equipment and shall confer on Buyer no right of any kind with respect to such equipment. When Seller has not accepted orders from Buyer for products to be made with such equipment for a period of one year, then after 30 days written notice to Buyer, Seller may make such disposition of the equipment as it considers appropriate. Until the expiration of such one year period, Seller shall keep such equipment available for the production of products by Seller for Buyer."

A typical explanation for this provision is that dies require maintenance and do not typically fit other vendors' presses. However, in private conversations, both Magnode and Mid-America Extrusions showed flexibility about making arrangements satisfactory to the Army.

Conclusions

1. The extruded subpanel design (circle size and configuration), selected material and manufacturing accuracy resulted in a significant reduction of the manufacturing base in the U.S capable of supplying the subpanels.
2. Among 150 U.S. extruders listed in the Directory of the Aluminum Extruders Council, only 2 are capable or willing to meet all the requirements of the panel design, material and accuracy.

Recommendations

In GARD's opinion, there are some measures which could be considered in order to expand the manufacturing base for supplying the extruded subpanels. These are the following:

1. **Tolerances**

To relax the extruded subpanel tolerances, at least on the width of the panel, to an ANSI Standard level provided the existing design of the roadway dispenser system allows this. The problem of inconsistency in welded joint location resulting from this can be solved by using joint tracking devices during welding. This step will increase the number of qualified extruders from 2 to 4.

2. **Material**

To consider replacement of 6061-T6 aluminum alloy with 6063-T6. The resulting reduction of strength of the panel material can be compensated for by increasing the cross-sectional area of the panel. Some increase in weight and cost of the material will be a penalty in this case for further expansion of the manufacturing base from 4 to 8 qualified extruders.

3. **Configuration**

To increase the wall thickness of the subpanels at least to 0.156 in. This may make the extruders with big presses more willing to participate. This step may be made in conjunction with Step 2.

4. **Circle Size**

To decrease the width of the subpanels in order to reduce their circle size. However, this is not recommended since the manufacturing technology for welding of 3 joints on a 4-section mat panel would be significantly more complicated than that being developed for 2 joints on a 3-section mat panel.

RESULTS OF THE BID SURVEY AMONG U.S. EXTRUSION MANUFACTURERS

No.	C/Size, in.		Company Name and Address	Response	Quote	Alum. Alloy	Width Toler. in.	Panel Cost \$/lb.	Die Cost \$
	Hard Alloy	Soft Alloy							
1	31	31	Alcoa P.O. Box 7500 Lafayette, IN 47903	Y	Y	6061-T6	±.064 (ANSI)	2.60	6,000
2	-	14	Alcoa 515 th Alcoa Ave., P.O. Box 58407 Vernon, CA 90058	Y	N				
3	15	0	Aluminum Shapes Inc. 9000 River Road DeLair, NJ 08110	Y	Y	6063-T6 6005-T6	±.044	1.86 1.95	4,200
4	15	-	Cressona Aluminum Co. Pottsville St. Cressona, PA 17929	Y	N				
5	13	-	Dolton Extrusion Co. 14200 Cottage Grove Ave Dolton, IL 60419	Y	N				
6	13	13	Extrudex Aluminum Ltd. 45 Fenmar Dr. Weston, Ontario Canada, M92, 1M2	N					
7	12	12	Indal Aluminum 1900 34th St. Gulfport, MS 39501	Y	Y	6005-T6	±.054	1.82	3,700

No.	C/Size, in. Hard Alloy	Soft Alloy	Company Name and Address	Response	Quote	Alum. Alloy	Width Toler. in.	Panel Cost \$/lb.	Die Cost \$
8	16	-	Jarl Extrusions Inc. P.O. Box 871 Stateline Rd. Elizabethton, TN 37644	Y	Y	6063	±.064 (ANSI)	1.96	6,400
9	13	11	Kaiser Aluminum & Chemical Corp. 6250 E. Bandini Blvd. Los Angeles, CA 90040	Y	N				
10	14	12	Kaiser Aluminum & Chemical Corp. Highway 75 South Sherman, TX 75090	Y	N				
11	17	-	Magnode Corp. P.O. Box 292 Trenton, OH 45067-1599	Y	Y	6061-T6	±.031 ±.064	1.90 2.11	3,400
12	12	12	Mid-America Extrusions Corp 4925 Aluminum Dr. Indianapolis, IN 46218	Y	Y	6061-T6	±.031	1.68	2,685
13	13	12	Pimalco P.O. Box 5050 Chandler, AZ 85226	N					
14	10	-	Reynolds Metals Co. 401 Madrid Ave. Torrence, CA 90501	Y	N				
15	16	14	Reynolds Metals Co. 1701 Porter St. S.W. Grand Rapids, MI 49509	Y	N				

No.	C/Size, in.		Company Name and Address	Response	Quote	Alum. Alloy	Width Toler. in.	Panel Cost \$/lb.	Die Cost \$
	Hard Alloy	Soft Alloy							
16	14	-	Reynolds Metals Co. 1901 Reymont Road Richmond, VA 23227	Y	N				
17	28	28	Spectrulte Consortium Inc. College and Weaver Sts. Madison, IL 62060	Y	Y	6061-T6	±.064 (ANSI)	3.35	7,100
18	28	20	Taber Metals Inc. P.O. Box 1418 Russellville, AR 72801	Y	N				
19	10	10	Wells Aluminum Corp. 400 S. Main Street North Liberty, IN 46554	Y	Y	6063-T6	±.064 (ANSI)	2.18	3,150
20	12	12	Wells Aluminum Southeast, Inc. P.O. Box 627 Belton, SC 29627	Y	N				
21	14	-	The W. L. Bonnell Co. 25 Bornell Street Newnan, GA 30264	Y	N				

APPENDICES B

SECTION 4

22

APPENDIX B1

Specification for Inspection and Testing of Welded AE Panels

Specification for Inspection and Testing of Welded Mat Panels

1. Background

1.1 The test piece cut from the welded panel to be subjected to inspection and testing is shown in Fig. 1.

1.2. Panel material is 6061-T6 aluminum alloy.

1.3. Weld filler material is ER 4043 aluminum wire, per AWS A.5.10-latest edition.

1.4. Welding process is GMAW.

2. Inspection

2.1. A 17 in. long portion of the weld shall be radiographed to include one inch from both sides of centerline of weld upon completion of visual examination. Radiographic testing shall be performed and evaluated in accordance with the AWS D1.2 and the ASTM standards E94 and E142, latest editions. The results of the evaluation shall be reported in writing.

2.2. The radiographs shall be evaluated against applicable referenced radiographs in the ASTM E390 standard.

2.3. The referenced radiographs shall be graded according to the severity levels, 1 through 5 in order of increasing severity as indicated in Table 1 below.

2.4. The remainder of the discontinuities listed in Table 2 of ASTM E390 shall be ungraded and treated as unacceptable.

2.5. The acceptable radiographs of the test piece shall be interpreted as showing equal or less severity than indicated in Table 1 in a nine inch long test weld.

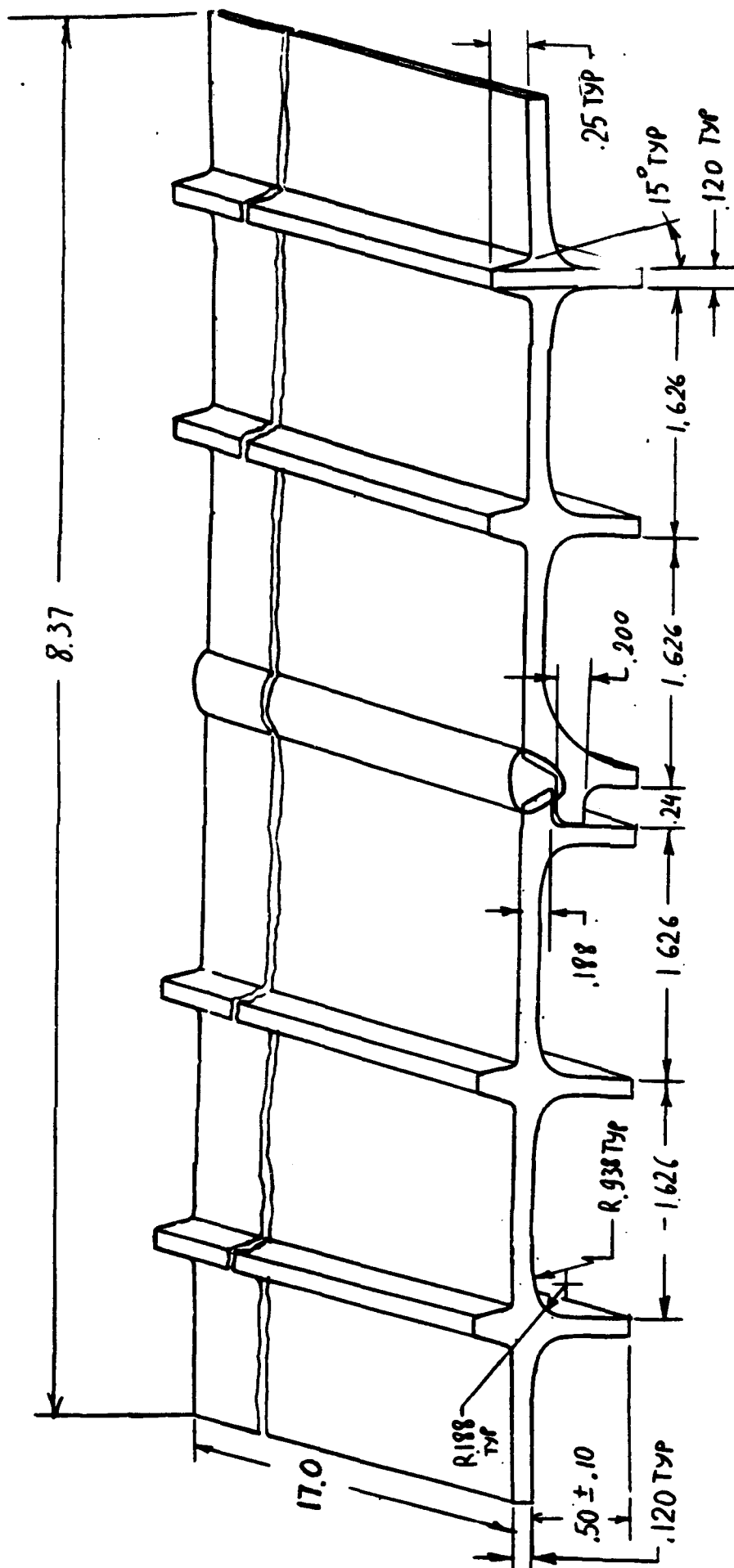


Figure 1 Test piece cut from welded mat panel

Table 1.

TYPES OF DISCONTINUITIES ACCEPTABLE FOR WELDS ON MAT PANEL	
Discontinuity Type	Severity Level Grading
Scattered Porosity	3
Fine Scattered Porosity	3
Coarse Scattered Porosity	2
Clustered Porosity	2
Linear Porosity	2
Slag Inclusions	2

3. Testing

3.1. Mechanical testing of the welded joint shall be conducted according to the AWS D1.2-83 Structural Welding Code, Aluminum and the ASME Boiler and Pressure Vessel Code, Section IX. If it is necessary the test specimens shall be machined to remove the stiffeners, tread risers, weld reinforcement and lock design details of the joint.

3.2. Tensile test shall be performed on two (2) transverse reduced-section specimens cut from the test piece transverse to the weld. Minimal tensile strength of 24 ksi shall be taken as an acceptance criterion in accordance with the AWS D1.2-83 Structural Code and the ASME Code. Yield strength, elongation and failure location shall be reported in writing as well.

3.3. Bend test shall be performed on transverse specimens. Two (2) root-bend and two (2) face-bend specimens shall be tested. The results shall be reported in writing.

3.4. Metallographic examination shall be conducted on three (3) samples.

- 1) A longitudinal sample (1 in. wide and 2 in. long) with weld reinforcement removed shall be prepared for grain structure macro examination. (Examination shall be done by GARD.)
- 2) A transverse sample with weld reinforcement intact shall be prepared and photographed with a metric scale as a background. (Macro examination of rate of dilution and weld geometry, including depth of penetration, width and height of reinforcement shall be performed by GARD.)
- 3) A transverse specimen shall be prepared for microstructure evaluation. The results of the evaluation shall be reported in writing.

3.5. Microhardness test shall be performed on the same specimen which was prepared for microstructure examination. Microhardness distribution shall be measured across the HAZ as shown in Fig. 2. The results shall be reported in writing.

C.161

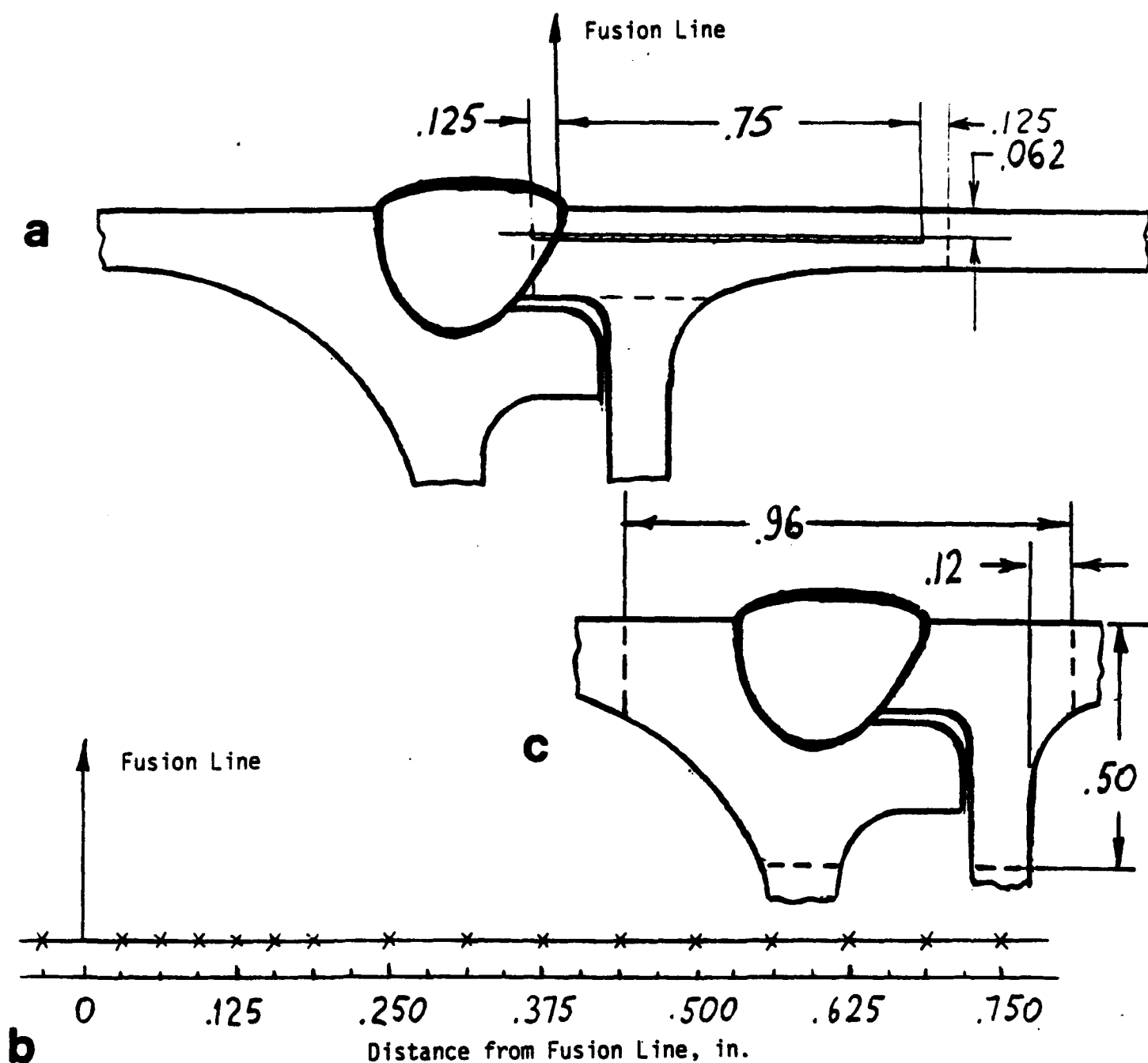
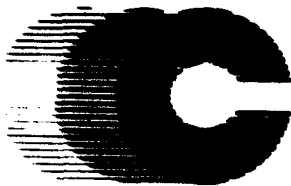


Figure 2 Transverse specimen for microstructure examination (a), Knoop (500g) hardness evaluation (hatched) area (a), hardness measurement layout (b), and transverse specimen for macro examination (c).

APPENDIX B2

Results of Radiographic Inspection of Experimental Welds of A, B & C Series



CERTIFICATE OF INSPECTION
CONAM INSPECTION

Page 1 of 1

1245 W. Norwood, Itasca, IL 60143
2090 E. 15th Avenue, Gary, IN 46402

Facilities In: Chicago, IL; Columbus, OH; Houston, TX; Philadelphia, PA; San Francisco, CA; Boston, MA; Gary, IN

Customer M.S.I. Dept. Q.C. Cust. P.O. 1075 Job No. 63571-
St. Address 1201 S 9TH AVE City & State Itasca, IL Spec. AMS D1 & ASTM A371-E 380
Job Location IAB-96 Contractor N/A E94 & 142
Dwg./Part No. SEE BELOW Part Description TEST PLATES

Description of Work RADIOGRAPHY Material Type ALUM. S.F.D. 38" KV 100 MA 5 Isotope & Curies 5
Size 14x17 5" Roll 10x12 8x10 70mm 4 1/2x17 5x7 4 1/2x10 E.R. No. Part Rec'd. No. Inspected No. Accepted No. Rej.
Type & No. 10 "M" 5 5 1 4

RAD. IDENT.	A C C T.	B R I L	LACK OF FUSION	LACK OF FUSION	FOR	SLAG	IN- CLU- SIONS	CRACKS	GAS	SHRINK	SEG- GA- TION	TEAR	SUB- FACE	UNDER- CUT	6- 8 M.	COMMENT SIZE, NUMBER, EXTENT, DESCRIPTION, ARTIFACT, ETC.
B-16																
1-2		X	X													LESS THAN .050" OF LACK OF FUSION
2-3																
B-17																
1-2		X		X												CL. 3 COARSE
2-3		X		X												CL. 3 COARSE
B-18																
1-2		X		X												CL. 3 COARSE & FINE CL. 1-2
2-3		X		X												CL. 3 COARSE
ALD REP.																
1-2																CL. 1 FINE & COARSE
2-3																CL. 1 FINE & COARSE
B-22 REP.																
1-2		X	X	X												CL. 2-3 COARSE
2-3		X	X	X												CL. 2 COARSE
R.N.																

INTERPRETER & DATE

OBSERVER

CUSTOMER

WE HEREBY CERTIFY THE PARTS LISTED HAVE BEEN TESTED IN CONFORMANCE WITH THE SPECIFICATIONS NOTED AND THAT WE ARE IN COMPLIANCE WITH THE PROVISIONS OF THE MERCURY CONTAMINATION CLAUSE. PARTS AND MATERIALS HAVE NOT BEEN SUBJECT TO MERCURY OR MERCURY CONTAMINANTS. THIS REPORT REPRESENTS CONAM INSPECTION INTERPRETATION OF THE RESULTS OBTAINED FROM THE TEST AND IS NOT TO BE CONSTRUED AS A GUARANTY OR WARRANTY OF THE CONDITION OF THE MATERIALS TESTED. CONAM INSPECTION SHALL NOT BE HELD LIABLE FOR MISINTERPRETATION OF CONDITIONS, LOSS, DAMAGE, INJURY, OR DEATH ARISING FROM OR ATTRIBUTED TO PERFORMANCE OF A TEST.



APPENDIX B3

Results of Mechanical Tests of Experimental Welds of A, B & C Series



Taussig
Associates Inc.

Metallurgical Engineers TEL: 708-676-2100 ■ FAX: 708-676-2101 ■ 708-676-2102 ■ 708-676-2103

Report No. 93844/August 13, 1990

CHAMBERLAIN GARD
Research & Development Division
7449 North Natchez Avenue
Niles, IL 60648

Attention: Mr. Vladimir Malin

S U B J E C T

Bend and Tension Testing of
Three (3) Groups of Welded Specimens

Submitted to our Laboratory 8/8/90

BACKGROUND

Three groups of welded test specimens were submitted to our laboratory for bend and tension testing in accordance with AWS D1.2-83. The three groups of specimens were identified as A4, A5, and A6. Each group consisted of four machined bend specimens, marked F1, F2, R1, and R2, along with two machined tensile specimens marked T1 and T2.

TEST RESULTS

Bend Testing

Each bend specimen was tested in accordance with Section 5.10. The specimens marked F1 and F2 were tested as face bends and the R1 and R2 specimens were tested as root bends. Bending was performed over a diameter of approximately 2-1/16" per Figure 5.10.2B. Bending was performed through 180°.

Visual examination of the bent test specimens revealed no significant defects in any of the four specimens from group A4. The face bends from groups A5 and A6 resulted in fracturing or evidence of cracks. No cracks or defects were identified in the root bends of groups A5 and A6. A summary of the test results is shown in the table below:

Bend Test Results

<u>Specimen Number</u>	<u>F1</u>	<u>F2</u>	<u>R1</u>	<u>R2</u>
Group A4	Pass	Pass	Pass	Pass
Group A5	FAIL*	FAIL*	Pass	Pass
Group A6	FAIL*	FAIL**	Pass	Pass

*Broke in two - porosity observed on fractured surface.

**Numerous fine cracks in weld, exceeding 1/8".
(Acceptance criteria per paragraph 5.10.3)

Tensile Testing

The six tension test specimens had been machined per Figure 5.9.1. A calibrated tension testing machine was used to apply and measure the loads required to fracture each specimen. The tests were performed in accordance with section 5.9. The results obtained from each test are shown in the table on page 2.

101

	<u>A4-T1</u>	<u>A4-T2</u>
Width, in.	1.503	1.504
Thickness, in.	.091	.091
Area, sq. in.	.1368	.1369
Tensile Load, lbs.	3,596	3,721
Tensile Strength, psi	26,300	27,200
Fracture Location	Weld	Weld
	<u>A5-T1</u>	<u>A5-T2</u>
Width, in.	1.502	1.504
Thickness, in.	.091	.100
Area, sq. in.	.1367	.1504
Tensile Load, lbs.	4,075	4,325
Tensile Strength, psi	29,800	28,800
Fracture Location	Weld	Weld
	<u>A6-T1</u>	<u>A6-T2</u>
Width, in.	1.504	1.503
Thickness, in.	.099	.105
Area, sq. in.	.1489	.1579
Tensile Load, lbs.	4,423	4,640
Tensile Strength, psi	29,700	29,400
Fracture Location	Weld	Weld

All of the tension test results meet the acceptance criteria of 24,000 psi minimum required by paragraph 5.9.3 and table 5.9.3 for 6061 base metal.

Respectfully submitted,

TAUSSIG ASSOCIATES, INC.

Mark A. Hineman

Mark A. Hineman
Senior Metallurgical Engineer

MAH/nb



Metallurgical Engineers 7530 Frontage Road ■ Skokie Illinois 60077 ■ 708 676-2100 ■ FAX 708 676-2132

Report No. 94076-2/August 29, 1990

CHAMBERLAIN GARD
Research & Development Division
7449 North Natchez Avenue
Niles, IL 60648

Attention: Mr. Vladimir Malin

S U B J E C T

Bend and Tension Testing of
a Group of Welded Specimens
Marked A10-REP

Submitted to our Laboratory 8/24/90

BACKGROUND

A group of welded test specimens was submitted to our laboratory for bend and tension testing in accordance with AWS D1.2-83. The group was identified as A10-REP. The group consisted of four machined bend specimens, marked F1, F2, R1, and R2, along with two machined tensile specimens marked T1 and T2.

TEST RESULTS

Bend Testing

Each bend specimen was tested in accordance with Section 5.10. The specimens marked F1 and F2 were tested as face bends and the R1 and R2 specimens were tested as root bends. Bending was performed through 180° and over a diameter of approximately 2-1/16" per Figure 5.10.2B.

Visual examination of the bent test specimens revealed no significant defects in any of the four specimens. These results meet the acceptance criteria of paragraph 5.10.3.

Tensile Testing

Both tension test specimens had been machined per Figure 5.9.1. A calibrated tension testing machine was used to apply and measure the loads required to fracture each specimen. The tests were performed in accordance with section 5.9. The results obtained from each test are shown in the table on page 2.

	<u>A10-T1</u>	<u>A10-T2</u>
Width, in.	1.504	1.504
Thickness, in.	.0949	.1034
Area, sq. in.	.1427	.1555
Tensile Load, lbs.	4,344	4,560
Tensile Strength, psi	30,400	29,300
Fracture Location	Base	Base

Both of the tension test results meet the acceptance criteria of 24,000 psi minimum required by paragraph 5.9.3 and table 5.9.3 for 6061 base metal.

Respectfully submitted,

TAUSSIG ASSOCIATES, INC.

Mark A. Hineman

Mark A. Hineman
Senior Metallurgical Engineer

MAH/nb



Metallurgical Engineers 7530 Frontage Road ■ Skokie Illinois 60077 ■ 708 676-2100 ■ FAX 708 676-2132

Report No. 94076/August 28, 1990

CHAMBERLAIN GARD
Research & Development Division
7449 North Natchez Avenue
Niles, IL 60648

Attention: Mr. Vladimir Malin

S U B J E C T

Bend and Tension Testing of
Three (3) Groups of Welded Specimens

Submitted to our Laboratory 8/24/90

BACKGROUND

Three groups of welded test specimens were submitted to our laboratory for bend and tension testing in accordance with AWS D1.2-83. The three groups of specimens were identified as B16, B17, and B18. Each group consisted of four machined bend specimens, marked F1, F2, R1, and R2, along with two machined tensile specimens marked T1 and T2.

TEST RESULTS

Bend Testing

Each bend specimen was tested in accordance with Section 5.10. The specimens marked F1 and F2 were tested as face bends and the R1 and R2 specimens were tested as root bends. Bending was performed through 180° and over a diameter of approximately 2-1/16" per Figure 5.10.2B.

Visual examination of the bent test specimens revealed no rejectionable defects in any of the twelve specimens. Minor defects, less than 1/16", were observed in the face bends of both B17 and B18. All twelve specimens conformed to the acceptance criteria of paragraph 5.10.3.

Tensile Testing

The six tension test specimens had been machined per Figure 5.9.1. A calibrated tension testing machine was used to apply and measure the loads required to fracture each specimen. The tests were performed in accordance with section 5.9. The results obtained from each test are shown in the table on page 2.

	<u>B16-T1</u>	<u>B16-T2</u>
Width, in.	1.500	1.500
Thickness, in.	.0984	.099
Area, sq. in.	.1476	.1485
Tensile Load, lbs.	3,906	3,788
Tensile Strength, psi	26,500	25,500
Fracture Location	Base	Base
	<u>B17-T1</u>	<u>B17-T2</u>
Width, in.	1.502	1.487
Thickness, in.	.0974	.0978
Area, sq. in.	.1463	.1454
Tensile Load, lbs.	4,606	4,319
Tensile Strength, psi	31,500	29,700
Fracture Location	Weld	Weld
	<u>B18-T1</u>	<u>18-T2</u>
Width, in.	1.497	1.500
Thickness, in.	.0888	.0900
Area, sq. in.	.1329	.1350
Tensile Load, lbs.	3,962	4,042
Tensile Strength, psi	29,800	30,000
Fracture Location	Base	Base

All of the tension test results meet the acceptance criteria of 24,000 psi minimum required by paragraph 5.9.3 and table 5.9.3 for 6061 base metal.

Respectfully submitted,

TAUSSIG ASSOCIATES, INC.

Mark A. Hineman

Mark A. Hineman
Senior Metallurgical Engineer

MAH/nb



Metallurgical Engineers 7530 Frontage Road ■ Skokie, Illinois 60077 ■ 708 676-2100 ■ FAX 708 676-2132

Report No. 94076-1/August 29, 1990

CHAMBERLAIN GARD
Research & Development Division
7449 North Natchez Avenue
Niles, IL 60648

Attention: Mr. Vladimir Malin

S U B J E C T

Bend and Tension Testing of
a Group of Welded Specimens
Marked B22-REP

Submitted to our Laboratory 8/24/90

BACKGROUND

A group of welded test specimens was submitted to our laboratory for bend and tension testing in accordance with AWS D1.2-83. The group was identified as B22-REP. The group consisted of four machined bend specimens, marked F1, F2, R1, and R2, along with two machined tensile specimens marked T1 and T2.

TEST RESULTS

Bend Testing

Each bend specimen was tested in accordance with Section 5.10. The specimens marked F1 and F2 were tested as face bends and the R1 and R2 specimens were tested as root bends. Bending was performed through 180° and over a diameter of approximately 2-1/16" per Figure 5.10.2B.

Visual examination of the bent test specimens revealed no significant defects in any of the four specimens. These results meet the acceptance criteria of paragraph 5.10.3.

Tensile Testing

Both tension test specimens had been machined per Figure 5.9.1. A calibrated tension testing machine was used to apply and measure the loads required to fracture each specimen. The tests were performed in accordance with section 5.9. The results obtained from each test are shown in the table on page 2.

	<u>B22-T1</u>	<u>B22-T2</u>
Width, in.	1.500	1.500
Thickness, in.	.101	.0966
Area, sq. in.	.1515	.1449
Tensile Load, lbs.	4,844	4,484
Tensile Strength, psi	31,800	31,000
Fracture Location	Weld	Base

Both of the tension test results meet the acceptance criteria of 24,000 psi minimum required by paragraph 5.9.3 and table 5.9.3 for 6061 base metal.

Respectfully submitted,

TAUSSIG ASSOCIATES, INC.

Mark A. Hineman

Mark A. Hineman
Senior Metallurgical Engineer

MAH/nb



Metallurgical Engineers 1531 Heritage Road ■ Brook Park, Ohio 44139 ■ Tel: 708 578-2100 ■ Fax: 708 578-0191

Report No. 94264/September 7, 1990

CHAMBERLAIN GARD
Research & Development Division
7449 North Natchez Avenue
Niles, IL 60648

Attention: **Mr. Vladimir Malin**

S U B J E C T

Bend and Tension Testing of
Four (4) Groups of Welded Specimens

Submitted to our Laboratory 9/7/90

BACKGROUND

Four groups of welded test specimens were submitted to our laboratory for bend and tension testing in accordance with AWS D1.2-83. The four groups of specimens were identified as C29, C30, C33, and C35. Each group consisted of four machined bend specimens, marked F1, F2, R1, and R2, along with two machined tensile specimens marked T1 and T2.

TEST RESULTS

Bend Testing

Each bend specimen was tested in accordance with Section 5.10. The specimens marked F1 and F2 were tested as face bends and the R1 and R2 specimens were tested as root bends. Bending was performed over a diameter of approximately 2-1/16" per Figure 5.10.2B. Each specimen was bent through 180°.

Visual examination of the bent test specimens revealed no significant defects in any of the four specimens from group C35. The R2 bends from groups C30 and C33 resulted in fracturing or evidence of cracks. No cracks or defects were identified in the root bends of groups C29 and C35. A summary of the test results is shown in the table below:

Bend Test Results

<u>Specimen Number</u>	<u>F1</u>	<u>F2</u>	<u>R1</u>	<u>R2</u>
Group C29	Pass	Pass	Pass	Pass
Group C30	Pass	Pass	Pass	FAIL
Group C33	Pass	Pass	FAIL	FAIL
Group C35	Pass	Pass	Pass	Pass

(Acceptance criteria per paragraph 5.10.3)

Tensile Testing

All eight tension test specimens had been machined per Figure 5.9.1. A calibrated tension testing machine was used to apply and measure the loads required to fracture each specimen. The tests were performed in accordance with section 5.9. The results obtained from each test are shown in the table on page 2.

	<u>C29-T1</u>	<u>C29-T2</u>
Width, in.	1.505	1.504
Thickness, in.	.1022	.101
Area, sq. in.	.1538	.1519
Tensile Load, lbs.	4,265	4,460
Tensile Strength, psi	27,700	29,400
Fracture Location	Weld	Weld
	<u>C30-T1</u>	<u>C30-T2</u>
Width, in.	1.500	1.500
Thickness, in.	.0977	.0906
Area, sq. in.	.1465	.1359
Tensile Load, lbs.	4,027	3,720
Tensile Strength, psi	27,500	27,400
Fracture Location	Base	Base
	<u>C33-T1</u>	<u>C33-T2</u>
Width, in.	1.500	1.501
Thickness, in.	.0777	.0869
Area, sq. in.	.1165	.1304
Tensile Load, lbs.	3,393	3,787
Tensile Strength, psi	29,100	29,000
Fracture Location	Base	Base
	<u>C35-T1</u>	<u>C35-T2</u>
Width, in.	1.498	1.499
Thickness, in.	.0938	.0748
Area, sq. in.	.1405	.1121
Tensile Load, lbs.	4,332	3,402
Tensile Strength, psi	30,800	30,400
Fracture Location	Base	Base

All of the tension test results meet the acceptance criteria of 24,000 psi minimum required by paragraph 5.9.3 and table 5.9.3 for 6061 base metal. Porosity was visually apparent on the fractured surfaces of both C29 specimens.

Respectfully submitted,

TAUSSIG ASSOCIATES, INC.

Mark A. Hineman

Mark A. Hineman
Senior Metallurgical Engineer

MAH/nb

APPENDICES C

SECTION 5

APPENDIX C1

Analysis of Temperature Control Requirements for Automatic Welding

Analysis of Temperature Control Requirements for Automatic Welding System

As a result of analyzing the requirements for welding process control for the automatic welding system which is now under development at CRC-Evans, GARD has concluded, from a technical standpoint, that temperature control is not necessary and offers little benefit for fabrication of aluminum mat panels. The reasons for this conclusion are the following:

1) Usefulness of Information Provided by Temperature

Information about the temperature of the heat-affected zone (HAZ) is useful if there is an established correlation between the temperature and properties of the HAZ. This correlation must be obtained experimentally by measuring the temperature at different areas across the welded joint and by testing the HAZ of the welded joint to determine the mechanical properties of these areas. Since the HAZ is relatively small and its properties change sharply across the joint, the experimental effort required to establish the correlation is very difficult.

While the theoretical usefulness of such temperature control is recognized in the literature, this approach has had limited practical application so far, for plates made of aluminum alloy of the 7000 series which are more sensitive to temperature. It is obvious that these results cannot be automatically transferred to the hollow panels made of 6061-T6 aluminum alloy. It would require a significant effort to establish a temperature-properties relationship in the HAZ for the mat panels, an effort which this project does not encompass. However, without such an investigation, temperature control can have very little meaning.

2) Redundancy of Information Provided by Temperature

Use of temperature control implies that by monitoring HAZ temperature it is possible to assess deviations in the HAZ properties. Leaving aside the validity of this statement (there are other factors which may affect the properties), it should be kept in mind that any deviation in the HAZ temperature will occur only as a result of fluctuations in welding parameters or heat input.

In the system being developed by GARD, welding parameters are accurately monitored and strictly controlled. This allows deviations in welding parameters to be

determined and restoration of parameters to preprogrammed values to occur before such deviations have caused changes in the HAZ temperature.

In this respect, when feedback control of welding parameters is utilized, temperature control of the HAZ provides secondary and redundant information.

3. Accuracy of Temperature Measurement

The temperature in aluminum is more difficult to measure than in steel due to its surface characteristics. Most of the common systems, including that considered in GARD's original proposal, pick up radiation over a wide wave length region from a spot on the surface of the metal and generate an integrated signal corresponding to some average temperature. The accuracy of this measurement is low even for a uniformly heated aluminum surface.

In order to improve the accuracy of the temperature control system, a few companies, such as Williamson Corp., Concord, Massachusetts, have developed a system which is capable of selecting radiation of a certain narrow wave length region. The system based on this principle is very sophisticated. It requires elaborate instrumentation and a great deal of effort to calibrate it. This would be impractical in a production environment.

4. Cost of Temperature Control

A simple common pyrometer system, as originally envisioned by GARD for temperature control, costs about \$700. The total cost of two systems, including integration, would probably run about \$2,000.

A more sophisticated pyrometer system such as described above will cost about \$7,000 and the overall cost of integration of two such systems may reach \$20,000.

Conclusion

The preceding discussion shows that temperature control for the GARD system designed with feedback control of welding parameters will provide redundant information which will be hard to obtain (in terms of necessary accuracy) and difficult to interpret intelligibly without additional costly experimental investigation.

2

In GARD's opinion, the Army requirement for temperature control should be dropped so that resources can be concentrated on more important aspects of the project. At the same time, the provisions necessary for later integration of a temperature control system can still be implemented in GARD's automatic system, so that this option can be added in the future if the Army should so desire.

APPENDIX C2

**Printouts of Welding Data
in Tabular and Graphic Formats**

G.A.R.D.

Operation:

File: B22

Station No. 0

Date 01/10/91 Time 11:05:15

ETM	GAS	TVS	WFS	VOLT	AMPS	HEAT
sec	cfh	ipm	ipm	vdc	adc	kj/in
0.1	44	36.0	114	16.6	66	1.83
0.2	44	36.0	143	17.0	52	1.47
0.4	45	36.0	164	16.7	72	2.00
0.5	44	36.0	194	17.2	92	2.64
0.7	45	36.0	218	18.2	103	3.12
0.8	45	36.0	239	19.0	116	3.67
1.0	45	36.0	270	18.6	144	4.46
1.1	45	26.3	296	19.6	156	6.98
1.3	45	20.3	315	20.6	168	10.23
1.4	44	17.5	332	21.6	179	13.26
1.6	44	14.8	338	22.2	184	16.56
1.7	44	14.4	337	22.2	186	17.21
1.9	44	14.2	344	22.1	187	17.46
2.0	45	14.3	347	22.2	186	17.33
2.2	45	14.9	345	22.2	185	16.54
2.4	45	14.4	340	21.9	188	17.16
2.5	45	14.7	347	22.3	184	16.75
2.7	45	14.4	348	22.1	187	17.22
2.8	45	14.8	348	21.9	188	16.69
3.0	44	15.8	343	22.1	186	15.61
3.1	44	15.4	343	22.0	185	15.86
3.3	46	15.3	345	21.7	190	16.17
3.4	45	15.0	342	22.1	187	16.53
3.6	45	14.3	340	22.0	188	17.35
3.7	45	13.8	346	22.0	187	17.89
3.9	45	14.1	341	21.8	189	17.53
4.0	45	14.5	343	21.8	189	17.05
4.2	45	14.6	345	21.8	189	16.93
4.3	45	15.2	340	21.8	190	16.35
4.5	45	15.4	339	21.8	191	16.22
4.7	45	14.4	338	21.8	191	17.35
4.8	45	14.5	343	21.7	191	17.15
5.0	45	14.7	340	21.9	190	16.98
5.2	45	14.4	345	21.8	192	17.44
5.3	44	14.4	350	21.8	191	17.35
5.4	44	14.4	347	21.8	191	17.35
5.6	44	14.7	345	21.7	192	17.01
5.8	44	14.9	345	21.7	191	16.69
5.9	45	14.6	343	21.4	196	17.24
6.0	45	14.7	336	21.6	192	16.93
6.2	45	14.0	337	21.7	192	17.86
6.3	44	14.4	339	21.7	192	17.36
6.5	44	14.2	338	21.7	192	17.60
6.7	45	13.6	344	21.7	192	18.38
6.8	45	14.5	352	20.8	202	17.39
7.1	45	15.1	349	21.4	195	16.58
7.3	45	15.1	344	21.8	191	16.54
7.4	45	14.7	340	21.8	192	17.08
7.6	45	13.7	345	22.0	189	18.21

ETM	GAS	TVS	WFS	VOLT	AMPS	HEAT
sec	cfh	ipm	ipm	vdc	adc	kj/in
7.7	45	14.4	342	21.8	190	17.26
7.9	45	15.3	339	21.8	190	16.24
8.0	45	15.3	344	21.8	190	16.24
8.2	46	15.6	422	21.8	190	15.93
8.3	48	15.5	384	21.6	193	16.14
8.5	45	14.4	365	21.8	191	17.35
8.6	45	14.2	353	21.7	190	17.42
8.8	48	14.8	344	21.7	191	16.80
8.9	46	15.2	341	21.7	190	16.28
9.1	45	15.2	341	21.5	193	16.38
9.2	45	14.7	342	21.7	193	17.09
9.5	45	14.7	341	21.5	193	16.94
9.6	44	14.5	347	21.8	192	17.32
9.8	45	14.4	350	21.5	193	17.29
9.9	45	14.1	355	21.6	193	17.74
10.1	46	15.1	332	21.6	192	16.48
10.2	47	15.3	337	21.6	192	16.26
10.4	45	15.2	335	21.7	193	16.53
10.5	45	14.9	338	21.5	194	16.80
10.7	45	14.4	339	21.6	193	17.37
10.8	46	15.3	342	21.6	192	16.26
11.0	46	14.5	333	20.6	204	17.39
11.1	45	14.8	340	21.4	197	17.99
11.3	45	14.8	339	21.5	193	16.82
11.4	45	14.6	344	21.4	193	16.97
11.6	45	15.1	344	21.4	195	16.58
11.8	45	14.7	343	21.6	193	17.02
11.9	45	15.0	340	21.5	193	16.60
12.1	46	16.4	346	21.7	192	15.24
12.2	46	14.5	346	21.6	191	17.07
12.4	45	14.6	344	21.6	193	17.13
12.5	45	14.9	343	21.6	192	16.70
12.7	45	15.2	340	21.5	193	16.38
12.8	45	14.2	342	21.5	193	17.53
13.0	46	14.8	348	21.6	192	16.81
13.2	45	14.9	340	21.5	194	16.80
13.3	45	15.0	343	21.6	192	16.59
13.5	45	14.5	339	21.4	195	17.27
13.6	45	14.5	339	21.1	200	17.46
13.8	46	14.6	343	21.4	196	17.24
13.9	45	15.1	341	21.4	193	16.41
14.1	45	14.7	346	21.5	194	17.02
14.3	45	14.4	347	21.5	194	17.38
14.4	45	14.4	347	21.5	193	17.29
14.6	46	14.8	346	21.6	192	16.81
14.7	45	14.6	344	21.6	193	17.13
14.9	45	14.6	346	21.6	193	17.13
15.0	44	16.0	347	21.6	192	15.55
15.2	45	15.0	345	21.4	195	16.69
15.3	45	15.0	345	21.5	193	16.60

ETM	GAS	TVS	WFS	VOLT	AMPS	HEAT
sec	cfh	ipm	ipm	vdc	adc	kj/in
15.5	44	15.0	351	21.6	192	16.59
15.6	45	15.1	349	21.6	193	16.56
15.8	45	14.5	349	21.5	193	17.17
15.9	48	14.7	343	21.5	193	16.94
16.1	45	14.8	345	21.5	194	16.91
16.2	45	15.3	342	21.5	193	16.27
16.5	45	14.8	345	21.6	192	16.81
16.6	45	14.7	345	21.4	193	16.86
16.8	45	14.8	341	21.5	194	16.91
16.9	45	15.1	334	21.4	195	16.58
17.1	45	14.8	338	21.4	196	17.00
17.2	45	15.6	340	21.6	193	16.03
17.4	45	15.4	340	21.6	193	16.24
17.5	46	15.2	338	21.5	194	16.46
17.7	45	14.8	342	21.4	194	16.83
17.8	45	14.5	346	21.4	195	17.27
18.0	45	14.4	341	21.5	193	17.29
18.1	45	15.0	338	21.4	193	16.52
18.3	45	14.1	339	21.6	193	17.74
18.4	45	14.5	338	21.6	192	17.16
18.6	45	15.5	344	21.5	193	16.06
18.8	45	14.6	342	21.6	192	17.04
18.9	45	15.4	343	21.6	192	16.16
19.1	45	15.4	345	21.5	193	16.17
19.2	45	15.1	346	21.6	192	16.48
19.4	45	15.0	348	21.6	192	16.59
19.5	45	14.7	345	21.5	192	16.85
19.7	45	14.8	345	21.6	192	16.81
19.8	45	14.8	344	21.5	193	16.82
20.0	45	15.0	343	21.6	192	16.59
20.1	45	15.0	349	21.4	193	16.52
20.3	45	14.6	344	20.6	204	17.27
20.4	45	15.0	342	21.1	198	16.71
20.6	44	15.7	351	21.4	196	16.03
20.7	43	15.7	343	21.4	195	15.95
20.9	45	14.8	340	21.4	193	16.74
21.1	44	14.5	341	21.4	193	17.09
21.3	44	14.7	338	21.7	192	17.01
21.4	45	13.6	341	21.7	192	18.38
21.6	45	14.6	343	21.6	192	17.04
21.7	45	14.7	342	21.6	192	16.93
21.9	44	14.2	341	21.6	193	17.61
22.0	44	14.6	345	21.5	194	17.14
22.2	45	14.9	340	21.6	192	16.70
22.3	45	14.7	341	21.5	193	16.94
22.5	45	14.7	346	21.5	193	16.94
22.6	45	15.4	339	21.6	192	16.16
22.8	44	14.7	338	21.5	193	16.94
22.9	45	14.9	339	21.5	193	16.71
23.1	45	14.5	338	21.7	190	17.06

ETM	GAS	TVS	WFS	VOLT	AMPS	HEAT
sec	cfh	ipm	ipm	vdc	adc	kj/in
23.2	44	14.5	345	21.6	192	17.16
23.5	45	14.2	345	21.6	192	17.52
23.6	45	15.3	348	21.6	192	16.26
23.8	45	14.8	345	21.6	192	16.81
23.9	45	14.5	339	21.7	191	17.15
24.1	45	14.4	338	21.7	190	17.18
24.2	45	14.5	341	21.6	190	16.98
24.4	45	14.3	339	21.8	189	17.29
24.5	46	14.9	341	21.8	191	16.77
24.7	46	14.2	333	21.6	190	17.34
24.8	45	13.7	336	21.9	188	18.03
25.0	45	14.4	338	21.9	188	17.16
25.1	45	14.4	335	21.7	189	17.09
25.3	45	14.8	336	21.7	190	16.71
25.4	46	15.2	336	21.8	190	16.35
25.6	46	15.4	335	21.8	189	16.05
25.8	46	15.2	342	21.8	190	16.35
25.9	44	14.6	341	21.8	189	16.93
26.1	45	14.7	342	21.8	189	16.82
26.2	45	15.2	341	21.6	192	16.37
26.4	45	15.0	341	21.6	193	16.68
26.5	45	14.1	339	21.5	194	17.75
26.7	45	14.5	344	21.5	193	17.17
26.8	45	14.7	396	21.6	192	16.93
27.0	46	13.9	368	21.5	193	17.91
27.1	45	14.7	360	21.4	195	17.03
27.3	45	14.6	348	21.4	196	17.24
27.4	46	14.4	345	21.4	195	17.39
27.6	46	14.4	348	21.5	193	17.29
27.8	45	14.1	347	21.6	192	17.65
27.9	45	14.4	352	21.6	192	17.28
28.1	45	14.8	348	21.5	194	16.91
28.3	46	15.4	342	21.5	194	16.25
28.4	45	15.0	340	21.4	195	16.69
28.6	45	15.6	343	21.5	193	15.96
28.7	45	14.7	341	21.6	193	17.02
28.9	45	14.6	341	21.4	195	17.15
29.0	45	14.7	348	21.4	193	16.86
29.2	45	14.6	346	21.8	190	17.02
29.3	45	14.5	340	21.7	191	17.15
29.5	48	15.7	340	21.7	191	15.84
29.6	46	14.1	340	21.8	190	17.63
29.8	45	14.3	341	21.7	191	17.39
29.9	45	14.0	344	21.8	190	17.75
30.1	45	13.9	336	21.5	193	17.91
30.2	45	14.2	343	21.8	190	17.50
30.5	46	15.3	343	21.6	192	16.26
30.6	45	14.8	347	21.6	192	16.81
30.8	45	14.5	342	21.4	193	17.09
30.9	45	14.9	341	21.4	193	16.63

ETM	GAS	TVS	WFS	VOLT	AMPS	HEAT
sec	cfh	ipm	ipm	vdc	adc	kj/in
31.1	45	14.9	341	21.5	194	16.80
31.2	45	14.0	341	21.5	193	17.78
31.4	45	13.3	341	21.5	194	18.82
31.5	45	14.7	341	21.7	192	17.01
31.7	45	15.8	343	21.1	195	15.62
31.8	45	14.4	340	21.4	193	17.21
32.0	45	14.0	338	21.6	192	17.77
32.1	45	14.7	345	21.8	190	16.91
32.3	45	15.2	342	21.6	192	16.37
32.4	45	15.2	344	20.6	199	16.18
32.6	45	14.8	340	21.2	199	17.10
32.8	45	14.7	344	21.1	198	17.05
33.0	45	15.1	345	21.0	200	16.69
33.1	45	15.1	341	21.1	199	16.68
33.2	45	15.3	339	21.1	200	16.55
33.4	45	15.2	339	21.2	198	16.57
33.5	45	14.9	340	21.1	197	16.74
33.7	45	14.9	342	21.2	198	16.90
33.9	45	14.6	345	21.4	197	17.33
34.0	45	14.7	346	21.4	196	17.12
34.2	45	14.8	341	21.4	196	17.00
34.3	45	14.8	340	20.9	201	17.03
34.4	44	15.1	338	21.0	200	16.69
34.6	44	15.4	341	20.8	203	16.45
34.8	45	14.8	331	20.6	206	17.20
34.9	45	14.6	341	20.6	206	17.44
35.1	45	14.9	347	21.0	200	16.91
35.3	45	14.9	341	21.4	193	16.63
35.4	45	14.8	343	22.8	183	16.92
35.6	45	14.0	343	22.0	184	17.35
35.7	45	14.3	344	23.4	176	17.28
35.9	45	14.2	343	24.4	174	17.94
36.0	44	14.0	345	24.1	175	18.08
36.2	44	13.4	338	24.2	168	18.20
36.3	43	14.6	340	23.7	174	16.95
36.5	44	15.6	336	21.5	190	15.71
36.6	45	15.2	337	20.6	206	16.75
36.8	45	14.7	340	20.4	207	17.24
36.9	45	13.5	345	20.6	206	18.86
37.1	44	14.9	344	20.6	207	17.17
37.2	44	15.1	346	20.4	210	17.02
37.5	45	14.2	351	20.3	207	17.76
37.6	45	14.9	346	20.4	208	17.09
37.8	45	14.8	341	20.6	207	17.29
37.9	46	15.0	337	20.6	206	16.97
38.1	48	15.2	339	20.6	206	16.75
38.2	45	15.7	338	20.7	204	16.14
38.4	46	15.5	340	20.6	206	16.43
38.5	46	15.0	346	20.6	206	16.97
38.7	45	15.4	348	20.6	206	16.53

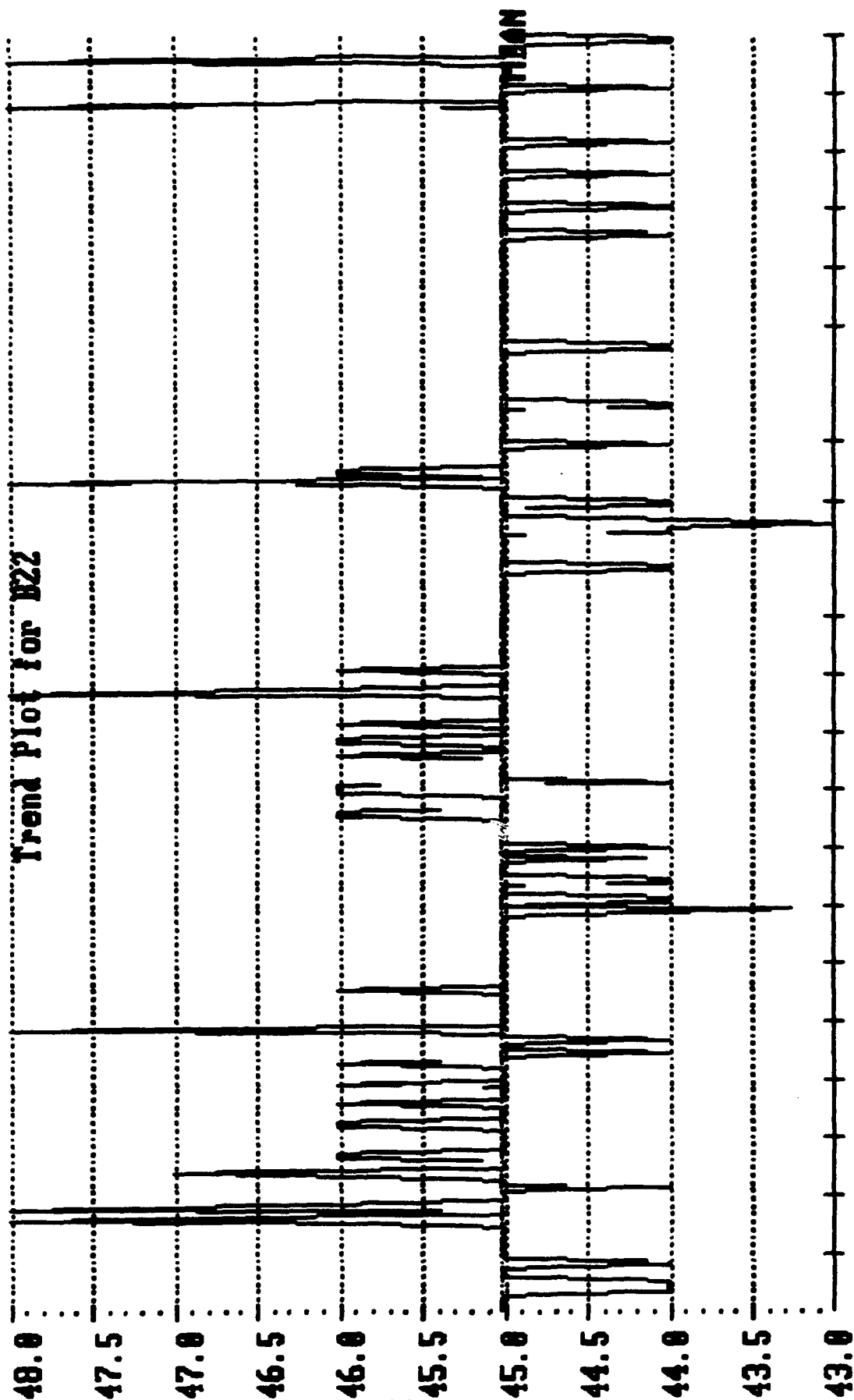
Page - 6

ETM	GAS	TVS	WFS	VOLT	AMPS	HEAT
sec	cfh	ipm	ipm	vdc	adc	kj/in
38.8	45	14.5	347	20.6	206	17.56
39.0	45	13.9	341	20.6	206	18.32
39.1	45	15.3	335	20.6	206	16.64
39.3	45	15.4	346	20.6	206	16.53
39.4	44	15.2	341	20.6	206	16.75
39.6	45	15.4	344	20.6	206	16.53
39.8	45	15.7	344	20.6	206	16.22
39.9	45	14.6	346	20.6	206	17.44
40.1	45	14.1	345	20.6	206	18.06
40.2	45	14.3	345	20.6	206	17.81
40.4	45	15.4	345	20.6	206	16.53
40.5	45	15.3	342	20.6	206	16.64
40.7	45	14.9	339	20.6	206	17.09
40.8	45	15.2	344	20.6	206	16.75
41.0	44	15.0	403	20.6	206	16.97
41.1	44	14.3	377	20.6	206	17.81
41.3	45	15.4	363	20.6	206	16.53
41.4	45	14.4	354	20.6	206	17.68
41.6	45	14.6	353	20.6	206	17.44
41.7	45	15.4	347	20.6	206	16.53
41.9	45	15.3	344	20.6	206	16.64
42.1	45	15.0	337	20.6	204	16.81
42.3	45	15.4	337	20.6	206	16.53
42.4	45	14.1	343	20.6	206	18.06
42.6	45	13.6	343	20.6	208	18.90
42.7	45	14.0	343	20.6	207	18.28
42.9	45	14.0	340	20.6	207	18.28
43.0	45	14.7	349	20.6	206	17.32
43.2	45	14.3	343	20.7	205	17.80
43.3	44	14.6	340	20.7	204	17.35
43.5	44	15.0	342	20.7	204	16.89
43.6	45	14.7	339	20.7	204	17.24
43.8	45	14.3	336	20.8	203	17.72
43.9	45	14.6	337	20.8	203	17.35
44.1	45	14.4	341	20.9	203	17.68
44.2	45	14.4	341	20.9	201	17.50
44.5	45	14.9	343	21.0	202	17.08
44.6	45	14.7	346	21.0	200	17.14
44.8	45	14.8	341	21.1	198	16.94
44.9	45	14.2	340	21.6	193	17.61
45.1	45	14.2	344	21.7	192	17.60
45.2	45	15.1	343	21.2	196	16.51
45.4	45	15.2	338	21.4	195	16.47
45.5	45	15.1	338	21.4	193	16.41
45.7	45	14.8	345	21.4	196	17.00
45.8	45	15.1	348	21.0	199	16.61
46.0	45	14.2	345	21.0	200	17.75
46.1	45	14.1	345	21.0	200	17.87
46.3	45	14.9	347	21.0	202	17.08
46.4	45	14.8	341	20.8	203	17.12

ETM	GAS	TVS	WFS	VOLT	AMPS	HEAT
sec	cfh	ipm	ipm	vdc	adc	kj/in
46.6	45	14.1	339	20.8	203	17.97
46.8	45	14.6	346	20.7	204	17.35
46.9	45	14.4	343	20.6	206	17.68
47.1	45	14.9	340	20.8	204	17.09
47.2	45	15.3	339	20.8	203	16.56
47.4	45	15.8	343	20.8	204	16.11
47.5	45	16.0	342	20.9	202	15.83
47.7	45	15.8	343	20.9	202	16.03
47.8	44	14.6	348	20.9	202	17.35
48.0	44	13.9	346	21.0	200	18.13
48.1	45	14.2	347	21.0	199	17.66
48.3	45	13.5	343	21.0	200	18.67
48.4	45	14.0	339	21.1	198	17.90
48.6	45	15.4	333	21.2	197	16.27
48.7	45	14.3	339	21.4	195	17.51
48.9	44	13.6	346	21.4	193	18.22
49.1	44	14.5	345	21.5	194	17.26
49.3	45	14.3	343	21.6	193	17.49
49.4	45	14.7	343	21.5	193	16.94
49.6	45	14.4	344	21.6	192	17.28
49.7	45	14.3	341	21.6	192	17.40
49.9	45	13.8	340	21.6	192	18.03
50.0	45	14.4	348	21.5	193	17.29
50.2	45	14.5	346	21.7	192	17.24
50.3	44	15.0	348	21.6	192	16.59
50.5	45	15.2	346	21.7	192	16.45
50.6	45	15.1	345	21.7	190	16.38
50.8	45	14.9	345	21.7	191	16.69
50.9	45	15.3	343	21.8	190	16.24
51.1	45	15.1	339	21.7	189	16.30
51.2	45	14.5	342	21.5	193	17.17
51.5	45	14.4	338	21.0	193	16.89
51.6	44	14.7	340	21.5	194	17.02
51.8	45	14.5	349	21.6	192	17.16
51.9	45	14.9	343	21.6	192	16.70
52.1	45	15.2	342	21.7	192	16.45
52.2	45	14.1	336	21.8	190	17.63
52.4	45	13.4	339	21.5	192	18.48
52.5	45	14.0	344	21.6	193	17.87
52.7	45	15.3	344	21.7	190	16.17
52.8	45	15.1	343	21.6	192	16.48
53.0	45	14.8	346	21.7	191	16.80
53.1	48	14.9	345	21.7	191	16.69
53.3	45	13.8	342	21.6	192	18.03
53.4	45	13.6	340	21.7	192	18.38
53.6	45	14.2	339	21.8	189	17.41
53.8	44	15.1	345	21.6	190	16.31
53.9	45	14.1	343	21.7	192	17.73
54.1	45	14.3	337	21.7	191	17.39
54.2	45	14.9	339	21.7	191	16.69

Page - 8

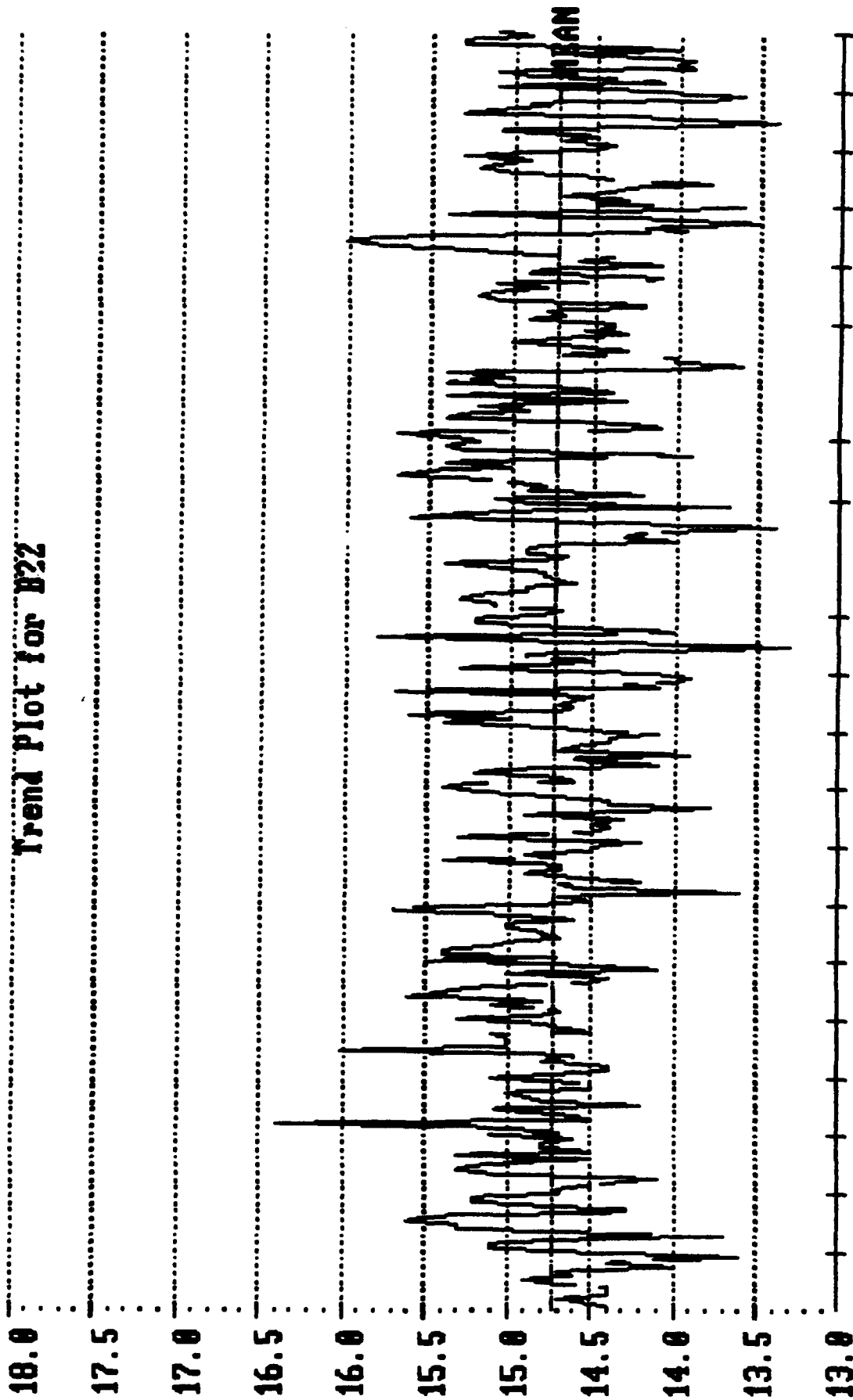
ETM	GAS	TVS	WFS	VOLT	AMPS	HEAT
sec	cfh	ipm	ipm	vdc	adc	kj/in
54.4	45	15.1	342	21.7	190	16.38
54.5	45	13.9	338	21.8	190	17.88
54.7	45	14.0	338	21.8	189	17.66
54.8	48	13.9	341	21.8	190	17.88
55.0	45	14.6	347	21.8	189	16.93
55.1	45	14.6	344	21.8	189	16.93
55.3	45	14.0	345	21.5	193	17.78
55.4	45	15.3	347	21.8	190	16.24
55.6	44	15.3	349	21.8	190	16.24
55.7	44	14.9	342	21.8	190	16.68
55.9	45	15.1	347	21.9	188	16.36
56.1	45	13.8	338	21.9	189	18.00
56.3	45	13.9	342	22.0	186	17.66
56.4	45	14.1	346	21.7	190	17.54
56.6	45	14.9	347	21.7	192	16.78
56.7	45	15.0	346	21.9	188	16.47
56.9	45	14.7	343	21.8	189	16.82
57.0	45	15.0	348	21.8	189	16.48
57.2	45	14.1	346	21.8	189	17.53
57.3	46	14.4	341	21.8	189	17.17
57.5	46	14.9	340	21.9	188	16.58
57.6	45	14.7	343	21.6	192	16.93
57.8	45	14.2	341	21.6	191	17.43
57.9	45	14.2	348	21.7	191	17.51
58.1	45	15.8	346	21.8	190	15.73
58.2	45	15.6	350	21.7	190	15.86
58.5	45	13.6	344	21.8	190	18.27
58.6	45	16.2	340	21.9	188	15.25
58.8	45	16.6	323	21.6	182	14.21
58.9	45	16.6	311	22.0	171	13.60
59.1	45	16.6	299	21.8	163	12.84
59.2	46	16.6	281	21.7	153	12.00
59.4	46	16.6	266	21.5	145	11.27
59.5	45	16.6	255	21.1	139	10.60
59.7	45	16.6	237	20.8	132	9.92
59.8	45	16.6	220	21.1	122	9.30
60.0	44	16.6	201	20.7	113	8.45
60.1	44	0.0	189	20.3	106	0.00
60.3	45	0.0	178	19.7	100	0.00
60.4	45	0.0	160	19.3	89	0.00
60.6	45	0.0	144	19.3	80	0.00
60.8	44	0.0	124	19.1	71	0.00
60.9	44	0.0	99	19.3	54	0.00
0.0	0	0.0	0	0.0	0	0.00
0.0	0	0.0	0	0.0	0	0.00
0.0	0	0.0	0	0.0	0	0.00
0.0	0	0.0	0	0.0	0	0.00
0.0	0	0.0	0	0.0	0	0.00
0.0	0	0.0	0	0.0	0	0.00
0.0	0	0.0	0	0.0	0	0.00
0.0	0	0.0	0	0.0	0	0.00



Record

GAS= 0.50 cfh/div File: B22
Operation: @
Total Records = 27
Mean Value = 45.02 cfh
Station = 0

Trend Plot for B22



Record

TUS= 0.50 ipm/div File: B22

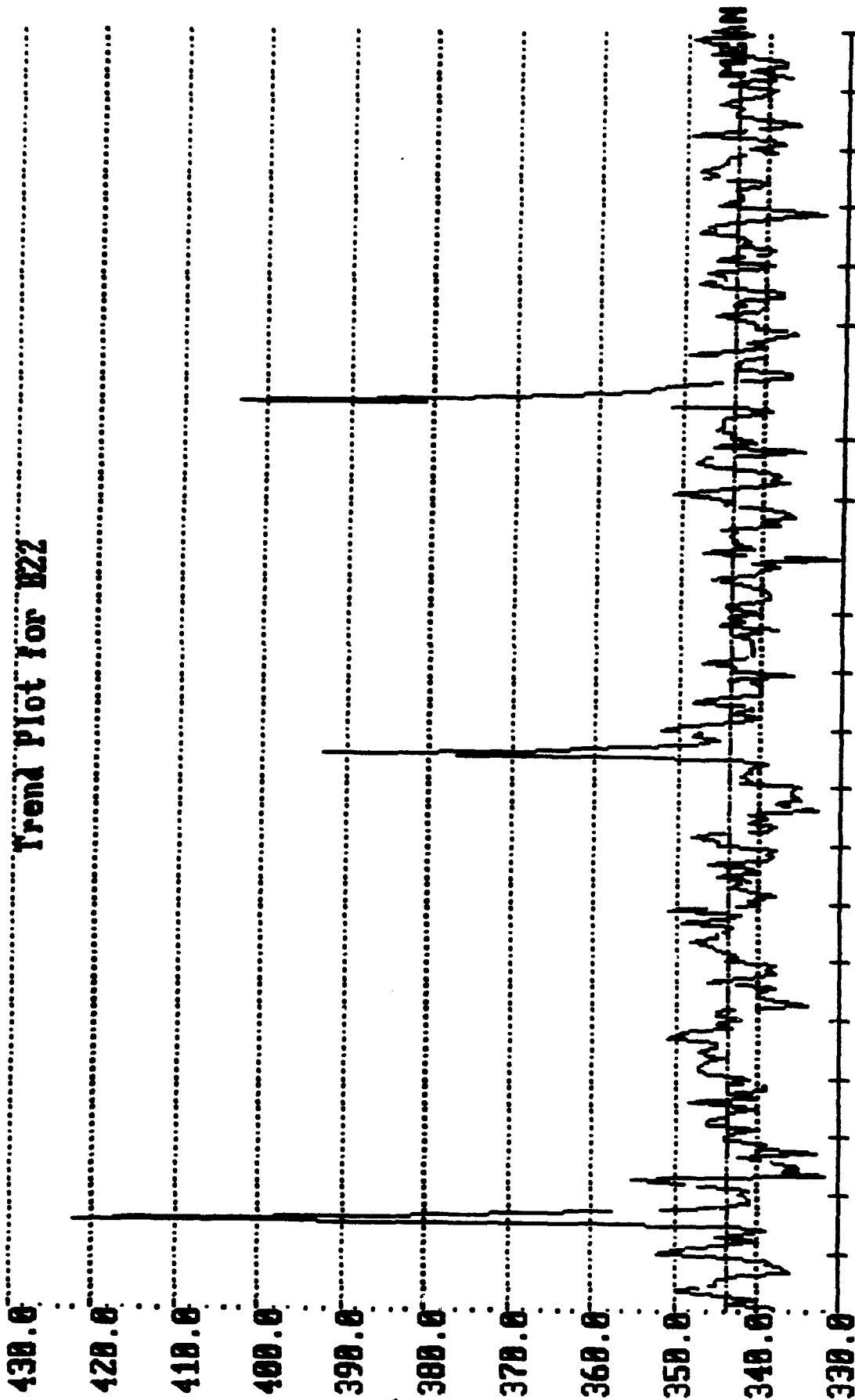
Operation: ③

Total Records = 27

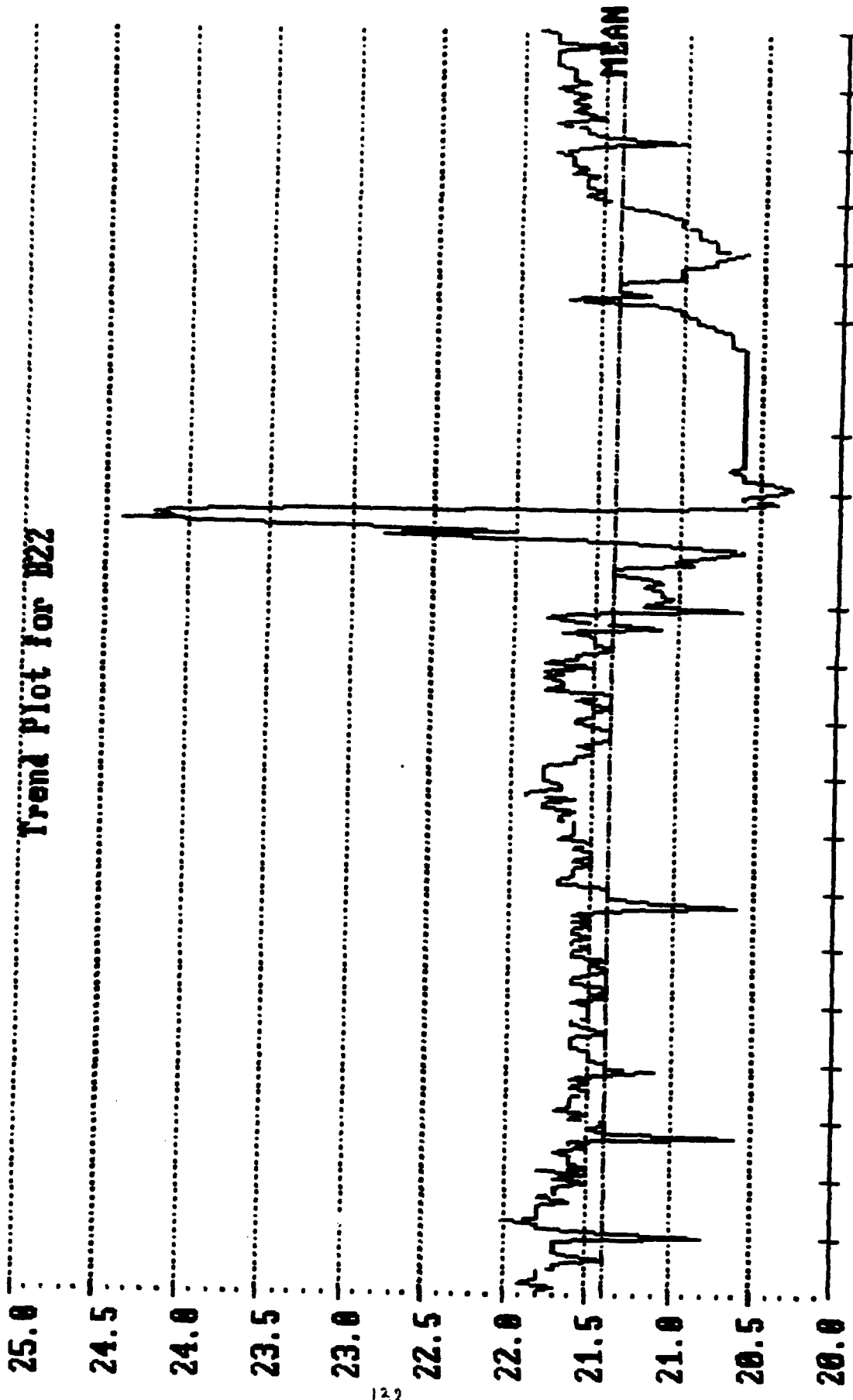
Mean Value = 14.72 ipm

Station = 0

Trend Plot for B22

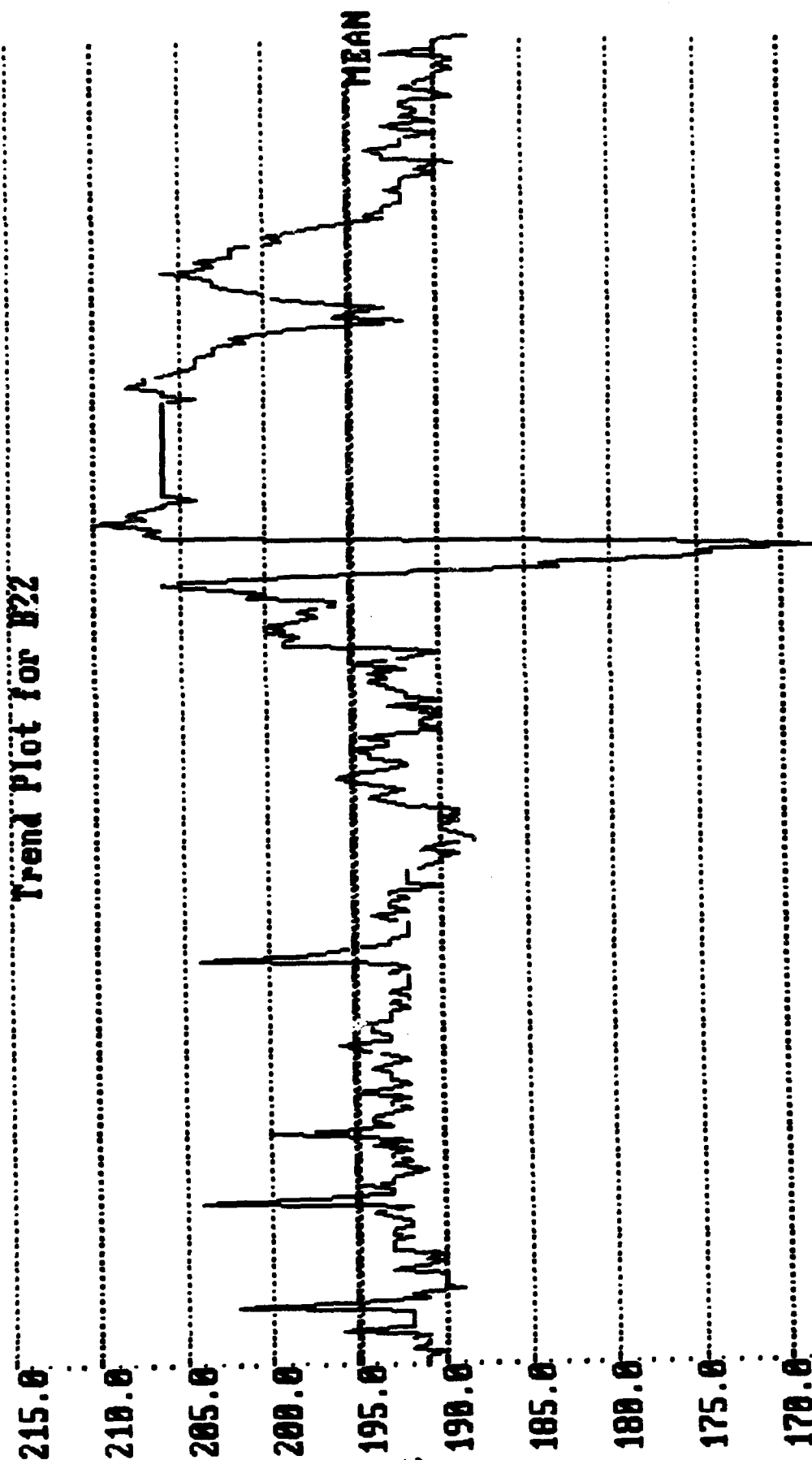


WFS=10.00 ips/div File: B22
 Total Records = 27
 Mean Value = 343.57 ips



VOLT= 0.50 vdc/div File: B22
 Operation: @
 Record
 Total Records = 27
 Mean Value = 21.48 vdc
 Station = 0

Trend Plot for B22



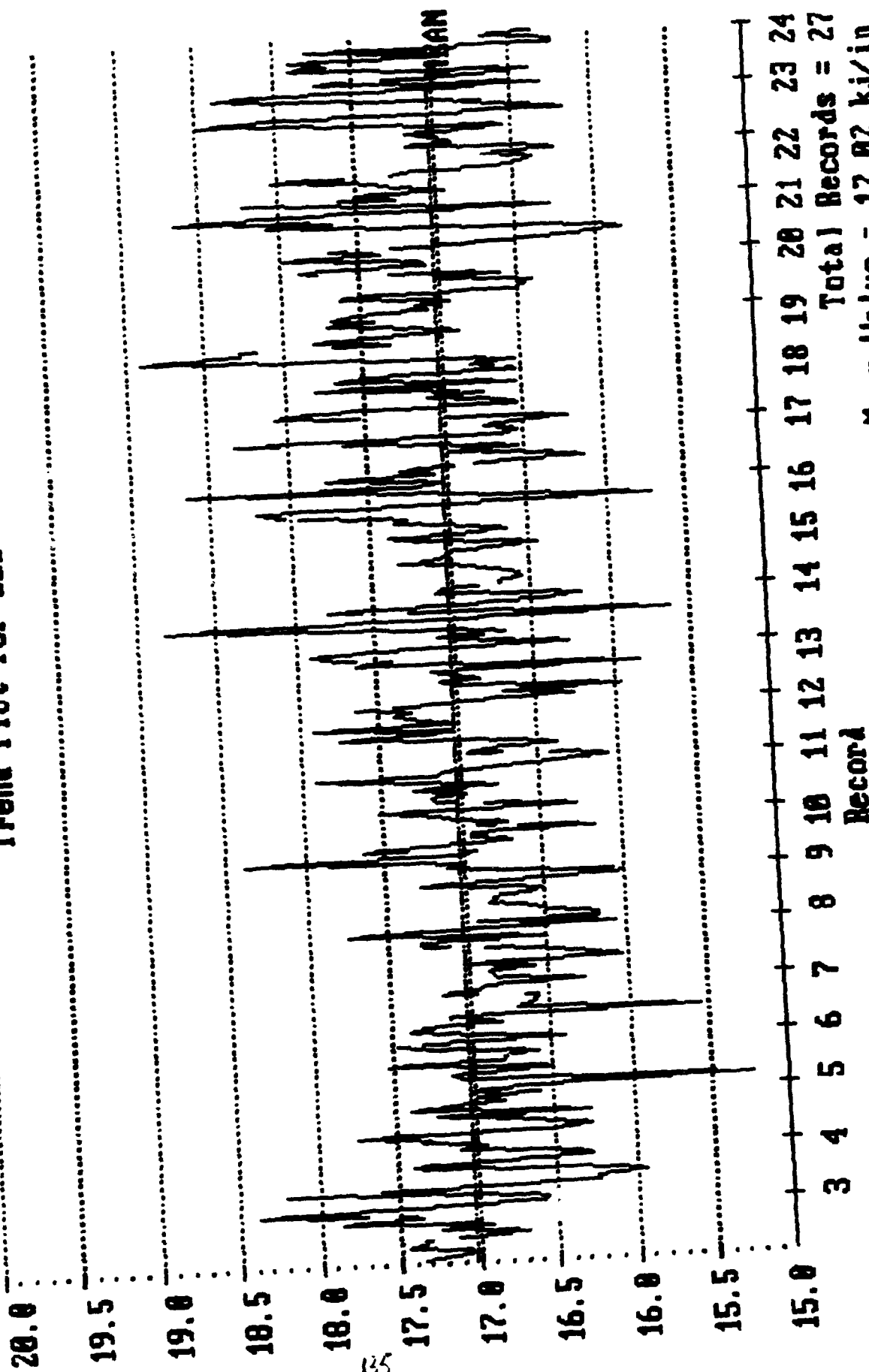
Record

Total Records = 27

AMPS= 5.00 adc/div File: B22

Mean Value = 195.07 adc

Trend Plot for B22



Total Records = 27
 Mean Value = 17.82 kJ/in
 Station = A

HEAT= 0.50 kJ/in/divFile: B22
 Operation: @

APPENDIX C3

GARD's Program Listing for Setting of Motion Parameters

```
Esc$ = CHR$(27)
```

Begin:

```
COLOR 14, 1, 1
CLS
```

GetFileName:

```
KeyIn$ = COMMAND$
FileName$ = KeyIn$
```

```
LOCATE 1, 5
PRINT "What filename would you like to use [SETUP]";
```

Retry:

```
LOCATE 2, 5

IF LEN(FileName$) > 0 THEN
    PRINT FileName$
ELSE
    LINE INPUT FileName$
END IF

IF LEN(FileName$) = 1 THEN END

IF LEN(FileName$) = 0 THEN
    FileName$ = "SETUP"
    LOCATE 2, 5
    PRINT FileName$
END IF

ON ERROR GOTO FileError
OPEN FileName$ FOR INPUT AS #1

ON ERROR GOTO 0

LOCATE 3, 5
PRINT SPACES(70)
```

SendLoop:

```
LOCATE 4, 45
PRINT YesNo$

OPEN "COM2:9600,N,8,1,CS,DS,CD" FOR RANDOM AS #2

VIEW PRINT 4 TO 24
```

GetFileData:

```
WHILE NOT EOF(1)
  LINE INPUT #1, FileData$

  IF LEFT$(FileData$, 1) <> ";" THEN
    PRINT #2, FileData$
    Now = TIMER
    DO UNTIL TIMER - Now >= .1
      LOOP
    DO UNTIL EOF(2)
      LINE INPUT #2, InData$
      PRINT InData$
    LOOP
  ELSE
    PRINT FileData$
    IF MID$(FileData$, 2, 1) = "*" THEN
      Now = TIMER
      DO UNTIL TIMER - Now >= .5
        LOOP
      END IF
    END IF
  END IF

WEND

Now = TIMER
DO UNTIL TIMER - Now >= 1
  LOOP

DO UNTIL EOF(2)
  InData$ = INPUT$(1, #2)
  PRINT InData$;
LOOP

PRINT #2, "1Z 2Z "

Now = TIMER
DO UNTIL TIMER - Now >= 1
  LOOP

DO UNTIL EOF(2)
  InData$ = INPUT$(1, #2)
  PRINT InData$;
LOOP

PRINT #2, "F "

CLOSE
```



```
Now = TIMER
DO UNTIL TIMER - Now >= 1
LOOP
```

```
END
```

FileError:

```
IF ERR = 53 THEN
    LOCATE 3, 5
    PRINT SPACES(70);
    LOCATE 3, 5
    PRINT UCASE$(FileName$); " cannot be found. Please re-enter
the filename.";
    LOCATE 2, 5
    PRINT SPACES(LEN(FileName$))
    FileName$ = ""
    RESUME Retry
ELSE
    LOCATE 3, 5
    PRINT "Unrecoverable error --"; ERR
    ON ERROR GOTO 0
END IF
```

Place Indexers On Line

E

* Pause .5 secs

; Set Normal Run Velocity for welding

TRAVEL SPEED

; A value of 1 = 36 inches per minute

TRAVEL SPEED

; Range is .001 to 20

TRAVEL SPEED

; Page 80

V.40

; Set START/STOP Velocity

; Page 80

VS.1

; Set distance and direction for move.

Gear Pitch Diameter = 2.125 inches

1 revolution = 6.675 inches

= 275000 steps

1 Inch = 41200 steps

1 Foot = 494500 steps

; Motor 1 goes in a clockwise direction to weld (use "+" in command).

; Motor 2 goes in a counterclockwise direction (use "-" in command).

; Page 79

1D+7417500

2D-7417500

; Set Acceleration to 10 rev/sec/sec. Range is 0.01 to 990.00 rev/sec/sec

; Page 80

A10

; Set Jog Acceleration to 37 rev/sec/sec. Range is .01 to 990.00 rev/sec/

; Page 80

JA37

; Set Jog Velocity to 9 rev/sec. Range is .001 to 20 rev/sec

; Page 80

JV9

; Enable Limit Switches

;LD0 Enables both CW and CCW limit switches.

;LD1 Enables CW limit switch.

;LD2 Enables CCW limit switch.

;LD3 Disables both CW and CCW limit switches.

; Page 81

1LD1

2LD2

; Set Encoder Resolution

; Page 83

ER363

; Set Encoder Deadband Width

; Page 83

1DW50

2DW50

; Set to input mode 1

; Page 120

IM1

; Set Normal Operation Mode

; Page 77

MN

; Set motor resolution to 25000 steps per revolution

; Page 81

MR10

; Set default Message level to full messages

; Page 120

MS1

; Set Option switches

; Page 118

; Power up off line

OSA1

; Set OffLine direction parameter to external

; Page 117

SSE1

; Ensure motors are energized

; Page 94

ST1

; Set Encoder Functions

; Page 84

; Motor Step Mode

FSB0

; Disable Stop on Stall

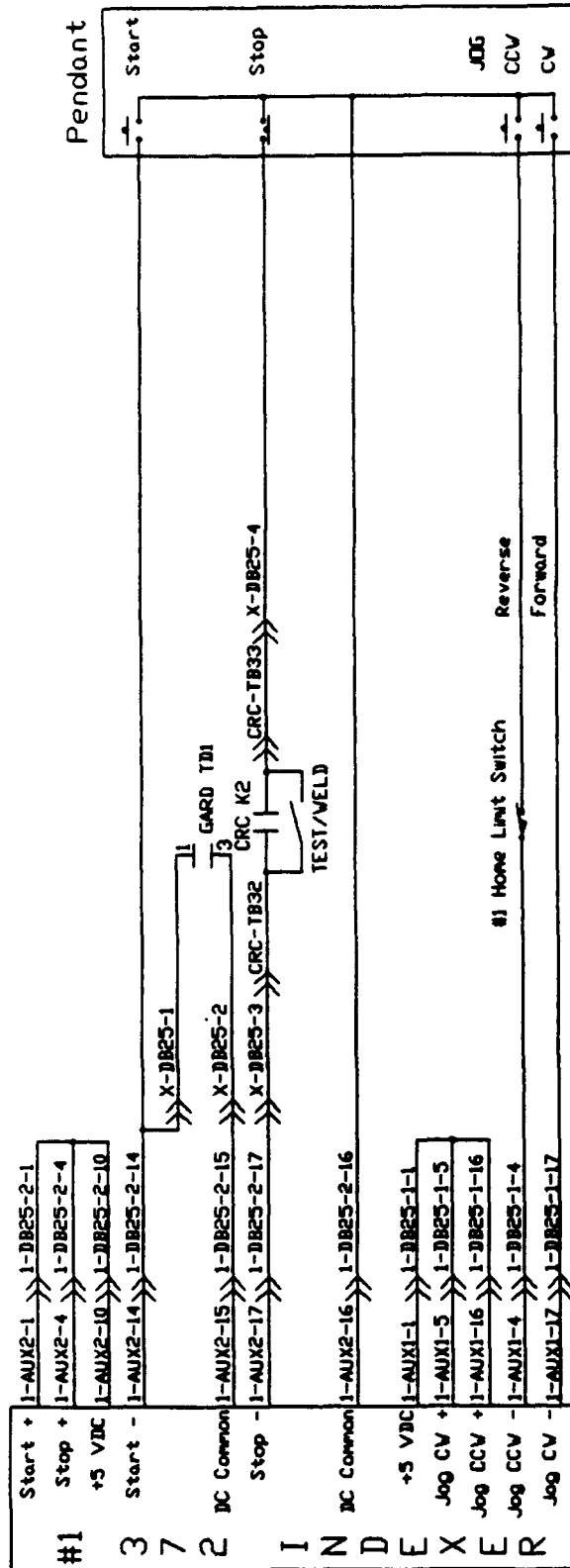
FSD0

; Save all default parameters

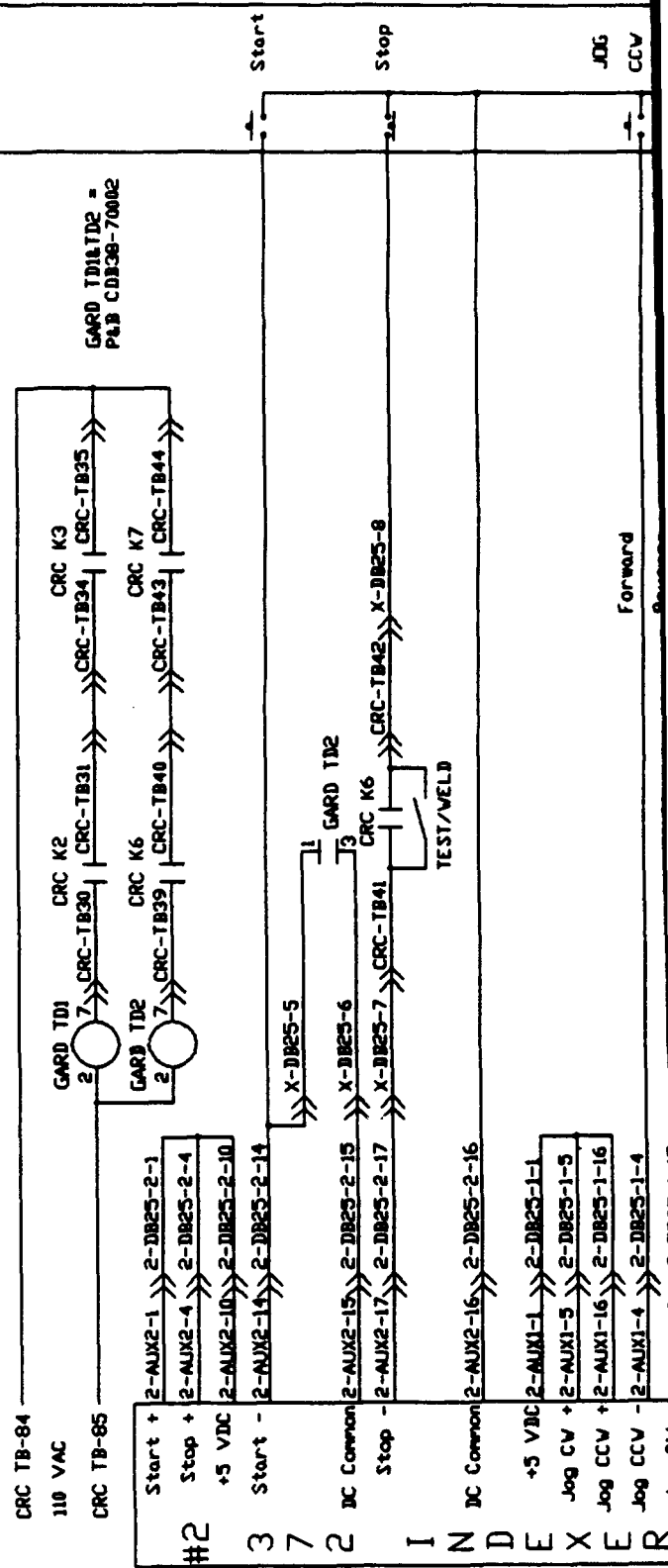
SA

APPENDIX C4

GARD's Schematic of Interface of the Welding and Motion Control Systems



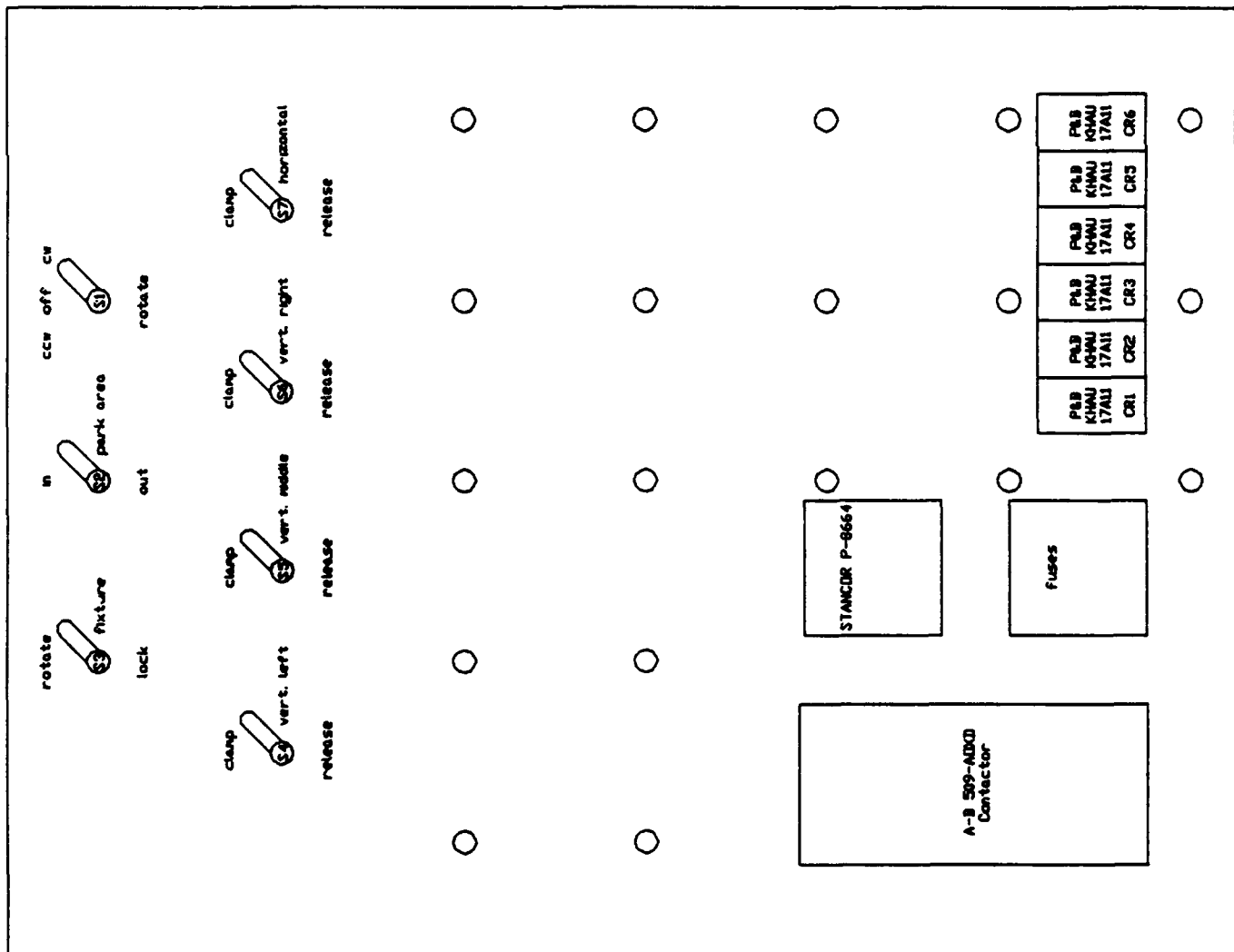
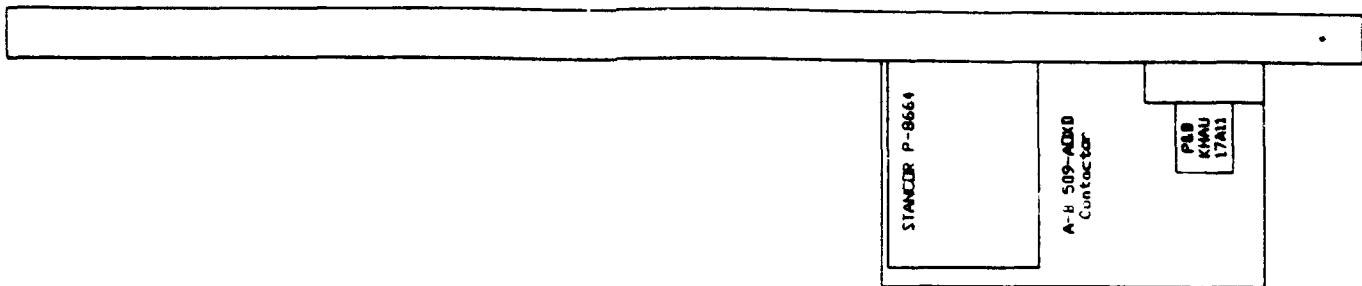
144



APPENDIX C5

**GARD's Drawings of
the Auxiliary Control Cabinet
of the Fixture Control (FC) System**

**Equipment Location
in the Auxiliary Control Cabinet**



**Cabling List
of the Auxiliary Control Cabinet**

Source	Cab.	Color	Destination	Description
	1	2		

I-AUX2-1	DB25-1		Start (+)	Wire to +5
I-AUX2-4	DB25-4		Stop (+)	Wire to +5
I-AUX2-10	DB25-10		+5 DC (+ Common)	
I-AUX2-13	DB25-13		Switch Common	DC Common
I-AUX2-14	DB25-14	Blk Brn	Start Sw. (-) (NO)	Start Signal
I-AUX2-16	DB25-16	Blk Red	Switch Common	DC Common to Pendant
I-AUX2-17	DB25-17	Blk Orn	Stop Sw. (-) (NC)	Stop Signal
I-AUX2-20	DB25-20		Switch Common	DC Common
I-AUX2-21	DB25-21		Switch Common	DC Common

Weld Carriage 1

I-AUX1-1	DB25-1		+5 DC (+ Common)	
I-AUX1-4	DB25-4	Blk	Jog CCW -	PB NO (Home Function).
I-AUX1-5	DB25-5		Jog CW +	Wire to +5
I-AUX1-16	DB25-16		Jog CCW +	Wire to +5
I-AUX1-17	DB25-17	Grn	Jog CW -	PB NO (Weld position.)

Weld Carriage 2

I-AUX1-1	DB25-1		+5 DC (+ Common)	
I-AUX1-4	DB25-4	Blk	Jog CCW -	PB NO (Weld position.)
I-AUX1-5	DB25-5		Jog CW +	Wire to +5
I-AUX1-16	DB25-16		Jog CCW +	Wire to +5
I-AUX1-17	DB25-17	Yel	Jog CW -	PB NO (Home Function).

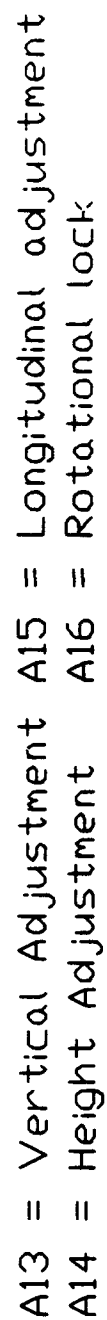
CRC - Computer Interface Connector

CRC-DB25-1	GARD-TD1-1		#1 Arc Active Contact (NO)
CRC-DB25-2	GARD-TD1-3		
CRC-DB25-3	CRC-TB32		#1 Stop Contact (NC)
CRC-DB25-4	CRC-TB33		
CRC-DB25-5	GARD-TD2-1		#2 Arc Active Contact (NO)
CRC-DB25-6	GARD-TD2-3		
CRC-DB25-7	CRC-TB41		#2 Stop Contact (NC)
CRC-DB25-8	CRC-TB42		
CRC-DB25-9	CRC-K4-3		#1 Weld Stop Contact (NC)
CRC-DB25-10	CRC-K4-2		
CRC-DB25-11	CRC-K8-6		#2 Weld Stop Contact (NC)
CRC-DB25-12	CRC-K8-7		

Source	Color	Cab.	Color	Park Area	Destination	Description
I-ENC-1	Green	D	Green	H	Encoder GREEN	Enc. Chan. B+
I-ENC-3	White	A	Brown	K	Encoder BROWN	Enc. Chan. A+
I-ENC-5	Blue	G	Blue	F	Encoder BLUE	Enc. Chan. 2R
I-ENC-14	Black	M	Black	M	Encoder BLACK	Enc. Gnd
I-ENC-23	Red	N	Red	J	Encoder RED	Enc. +5 VDC
Frame	Shield		Shield	N	Encoder Shield	
D-J2-1	Red	C	Red	D	Motor RED	Phase A+
D-J2-2	Black	F	Black	B	Motor BLACK	Phase A-
D-J2-3	Blue	H	Shield	A	Motor SHIELD	Gnd
D-J2-4	White	K	White	C	Motor WHITE	Phase B+
D-J2-5	Green	L	Green	E	Motor GREEN	Phase B-

I-XXXX-YY INDEXER D-XX-Y DRIVE

**Electric Schematic
of the Fixture Control (FC) System**



APPENDIX C6

The CDT Schedules



CRC-EVANS AUTOMATIC WELDING

INDUSTRIAL WELDING SYSTEMS

An Operation of CRC-Evans Pipeline International, Inc.

11801 NORTH HOUSTON-ROSELVY RD. • HOUSTON, TEXAS 77060 • (713) 689-6222 • TELEX 240714 CRC E

An **ESPEL** Corp.

CRC-Evans Part No. X5I5258

Version 2.4 - 183

10510

<u>SPC</u>	<u>GROUP A</u>	<u>WIRE DIAMETER</u>	<u>GAS</u>
0	1. Aluminum 4043 & 5356	.030"/0.8 mm	Ar
1	2. Aluminum 4043 & 5356	.035"/0.9 mm	Ar
2	3. Aluminum 4043	.045"/1.2 mm	Ar
3	4. Aluminum 4043	.062"/1.6 mm	Ar
4	5. Aluminum 5356	.045"/1.2 mm	Ar
5	6. Aluminum 5356	.062"/1.6 mm	Ar
 <u>GROUP B</u>			
6	1. Aluminum 4047	.040"/1.0 mm	Ar
7	2. Aluminum 4047	.045"/1.2 mm	Ar
8	3. Aluminum 5183	3/64"	Ar
9	4. Aluminum Bronze	.045"/1.2 mm	Ar
10	5. Aluminum Bronze	.035"/0.9 mm	Ar
11	6. Aluminum 5183	.062"/1.6 mm	Ar

APPENDIX C7

Procedures for Presetting Welding and Motion Parameters

To Program Welding Conditions

1. Turn on Power to computer using key switch.
2. Press reset buttons. SPC's will power up and self test. An error message will appear if the welding power suppliers are not turned on, it can be ignored.
3. Press A on SPC keyboard to enter alter limits program. Follow menu to make changes in welding parameters. Press 9 to step forward through menu, press C to step backward.

Example:

To change wire speed from 260 ipm to 350 ipm.

Press A

Press 1

Display reads:

Target speed

Run in speed

1

2

Press 1

Display reads:

Old target wire speed = 260

New target wire speed = 0000

Press 350 E

Display will read:

New target wire speed = 350

Press C to exit

Press A to exit

Travel Speed

To program travel speed:

1. Turn on computer
2. At prompt, type "CD \ WELD" "RET"
3. Type "Q" SETUP "RET"
4. Refer to Fig. 1

```
L 2      C 2      IAW      518k      *c:\weld\setup
```

Place Indexers On Line

E

```
; * Pause .5 secs
```

```
;-----  
; Set Normal Run Velocity for welding          TRAVEL SPEED  
; 11:1 ratio --- 1.0000 = 36 inches per minute TRAVEL SPEED  
;               .0278 = 1 inch per minute      TRAVEL SPEED  
; 29:1 ratio --- 2.6364 = 36 inches per minute TRAVEL SPEED  
;               .0733 = 1 inch per minute      TRAVEL SPEED  
; Range is .001 to 20                          TRAVEL SPEED
```

```
; Page 80
```

```
V.72
```

TRAVEL SPEED

```
;-----  
; Set START/STOP Velocity  
;               11:1 = .1  
;               29:1 = .26364
```

```
; Page 80
```

```
VS.1
```

```
;-----  
; Set distance and direction for move.  
;               Gear Pitch Diameter = 2.125 inches  
;               1 revolution = 6.6757 inches  
; *****
```

Figure 1

V. ← ## is travel speed

Range of ## is .001 to 20

if ## = 1.00

then speed is 36" per minute

Example:

To set a speed of 18" per minute

$$V = 18 / 36 = .5$$

Move cursor using arrow keys, change V ## to read V.50, use delete key to clear out any extra characters.

5. Simultaneously press Alt key and X

Prompt asks:

Save Changes

YES

NO

Press enter

6. Prompt C:\Weld> will be on screen.

Type "Send Setup" "RET"

at the end of this operation you should see:

* 1 ___ write operation successful

* 2 ___ write operation successful

◆ ◆

C:\Weld

To Record a Weld File

First create a directory to store the weld files in. As an example we will call it WELDFILE, the file name you select can have only eight or less characters.

1. Type "CD \ADM" "RET"

changes to ADM directory

2. Type "MD WELDFILE" "RET"

This command creates a subdirectory called WELDFILE. This is where you will store your recorded file.

3. Type "ADM61"

This brings up ADM program see Fig. 2

4. Press F2 function key, screen comes back as in Fig. 3

Press F2

GARD ADMNET(tm) MAIN MENU

```

%%%%%%%%%%%%%%%%%%%%%%%%%%%%%%%%%%%%%%%%%%%%%%%%%%%%%%%%%%%%%%%%%%%%%%%%%%%%%%
:           To Select Function Press [F]unction Key           :
%%%%%%%%%%%%%%%%%%%%%%%%%%%%%%%%%%%%%%%%%%%%%%%%%%%%%%%%%%%%%%%%%%%%%%%%%%%%%%
: [F1]      Help.                                             :
: [F2]      Collect Network Weld Data                        :
: [F3]      Display Stored Weld Data File                    :
: [F4]      Calculate ADM(tm) High/Low Limits                :
: [F5]      Graphical Display of Single Weld Data File      :
: [F6]      Graphical Display of Multiple Weld Data Files   :
: [F7]      Display Parameter Information                     :
: [F8]      Specify Limits of Process                        :
: [F9]      Configure Network Parameters                     :
: [F10]     Configure System Parameters                      :
: [ESC]     Return to Operating System                       :
%%%%%%%%%%%%%%%%%%%%%%%%%%%%%%%%%%%%%%%%%%%%%%%%%%%%%%%%%%%%%%%%%%%%%%%%%%%%%%
```

Figure 2

GARD
Collect Network Weld Data Menu

```

:
: To Select Function Press [Function Key]
:
: [F1] Collect Single Weld data file
: [F2] Collect Multiple Weld data files
: [F3] Statistical Process Control
: [ESC] Return to Main Menu
:

```

Figure 3

5. Program asks for # of welds to collect (see Fig. 4).

Type "100" "RET"

6. Program asks what # to call first file (see Fig. 5).

7. Program asks for a path for the file (see Fig. 6) type "\ADM\WELDFILE\" "RET"

8. Program asks for station # (see Fig. 7).

Type "100" for ADM 1, or

Type "200" for ADM 2

Screen displays blank weld file (see Fig. 8)

Computer is ready to record a file.

It will automatically record a new file each time the weld is turned on until it has recorded 100 files.

To display a recorded file

Press "ESC" "ESC" to return to main menu.

From Main Menu:

GARD
Multiple Weld Cycle Data Collection

[illegible]

Figure 4

```

#####;
:      Number of Welds to Collect (1-999) =   100
:      Start WELD###.DAT file with number (1-100)= 1
:
:
#####<

```

GARD
Multiple Weld Cycle Data Collection

[illegible]

162

```

#####
:      Station Number 200      :
#####

```

[illegible]

163

GARD
Pathname for Weld Data File

```

I
:      Input PATH Name [drive:\path\]      :
H
I
: \adm\weldfile\      :
H

```

Figure 9

CARD
Filename for Weld Data File

```

MMMMMMMMMMMMMMMMMMMMMMMMMMMMMMMMMMMMMMMMMMMMMMMMMMMMMMMMMMMMMMMMMMMM;
:      Input PATH Name [drive:\path\]      :
MMMMMMMMMMMMMMMMMMMMMMMMMMMMMMMMMMMMMMMMMMMMMMMMMMMMMMMMMMMMMMMMMMMM<

```

```

MMMMMMMMMMMMMMMMMMMMMMMMMMMMMMMMMMMMMMMMMMMMMMMMMMMMMMMMMMMMMMMMMMMM;
:      Input FILE Name name(.ext)]      :
MMMMMMMMMMMMMMMMMMMMMMMMMMMMMMMMMMMMMMMMMMMMMMMMMMMMMMMMMMMMMMMMMMMM<
MMMMMMMMMMMMMMMMMMMMMMMMMMMMMMMMMMMMMMMMMMMMMMMMMMMMMMMMMMMMMMMMMMMM;
: weld1.dat                               :
MMMMMMMMMMMMMMMMMMMMMMMMMMMMMMMMMMMMMMMMMMMMMMMMMMMMMMMMMMMMMMMMMMMM<

```

Figure 10

```

MMMMMMMMM ADM(tm) Station No. 200 MMMMMMMMM;
:ETM    GAS    TVS    WFS    VOLT    AMPS    HEAT  :
:sec    cfh    ipm    ipm    vdc    adc    kj/in  :
:.0      0      .0      0      .0      0      .0    :
:.0      0      .0      0      .0      0      .0    :
:.0      0      .0      0      .0      0      .0    :
:.0      0      .0      0      .0      0      .0    :
:.0      0      .0      0      .0      0      .0    :
:.0      0      .0      0      .0      0      .0    :
:.0      0      .0      0      .0      0      .0    :
:.0      0      .0      0      .0      0      .0    :
:.0      0      .0      0      .0      0      .0    :
:.0      0      .0      0      .0      0      .0    :
:.0      0      .0      0      .0      0      .0    :
:.0      0      .0      0      .0      0      .0    :
:.0      0      .0      0      .0      0      .0    :
:.0      0      .0      0      .0      0      .0    :
:.0      0      .0      0      .0      0      .0    :
MMMMMMMMMMMMMMMMMMMMMMMMMMMMMMMMMMMMMMMMMMMMMMMMMMMMMMMMMMMMMMMMMMMM<
Mean    0      .0      0      .0      0      .0
Sdev 0.00  0.00  0.00  0.00  0.00  0.00  0.00

```

```

MMMMMMMMMMMM Time MMMMMMMMMMMMMMMMMMMMMMMMMMMMMMMMMMMMMMMMMMMMMMMMMMMMMMMMMMMMMMMMMMM Current File MMMMM
:On: 11:42:16   Off: 00:00:00   No: 0      Tot Rec: 0      weld1.dat
MMMM F1 - Print MMM F2 - Next Rec. MMMM F3 - Last Rec. MMMM F10 - Exit MMMMMMMM

```

Figure 11

1. **Press Function key F3**

Prompt asks for the path to the file:

type "\ADM\WELDFILE\" "RET"

(see Fig. 9)

2. **Prompt asks for file name (.ext) (see Fig. 10)**

Type "WELD1.dat"

Remember, you must include the file extension (in this case, ".dat") for it to work.

3. **File will be displayed (see Fig. 11).**

To Program Welding Conditions

1. Turn on Power to computer using key switch.
2. Press reset buttons. SPC's will power up and self test. An error message will appear if the welding power suppliers are not turned on, it can be ignored.
3. Press A on SPC keyboard to enter alter limits program. Follow menu to make changes in welding parameters. Press 9 to step forward through menu, press C to step backward.

Example:

To change wire speed from 260 ipm to 350 ipm.

Press A

Press 1

Display reads:

Target speed

Run in speed

1

2

Press 1

Display reads:

Old target wire speed = 260

New target wire speed = 0000

Press 350 E

Display will read:

New target wire speed = 350

Press C to exit

Press A to exit